An Approach Towards Theragnostic Receptor Targeting with η^5-Cyclopentadienyl Derivatives of the *fac*-{$^{99m}Tc(CO)_3$}- and *fac*-{$Re(CO)_3$}-Core

Dissertation

zur

Erlangung der naturwissenschaftlichen Doktorwürde

(Dr. sc. nat.)

vorgelegt der

Mathematisch-naturwissenschaftlichen Fakultät

der

Universität Zürich

von

Daniel Can

von Auw AG

Promotionskomitee

Prof. Dr. Roger Alberto (Vorsitz)

Prof. Dr. Gilles Gasser

Zürich, 2013

dedicated to my family:

Aziz

Mirjam

Ibi

Haski

Beeti

Table of Contents

Summary

The chemical and biological evaluation of organometallic probes for nuclear medical applications in comparison to their purely organic analogs, or the study of the metal-mediated *retro*-Diels-Alder behaviour of derivatized cyclopentadienyl dimers is an overarching description of this thesis. Focussing on the synthesis of ^{99m}Tc-labelled radiopharmaceuticals and the corresponding cold rhenium-compounds, a variety of organic and inorganic cyclopentadienyl derivatives have been synthesized. Arylsulfonamides, -sulfamides and -sulfamates for the targeting of human carbonic anhydrase IX, hydroxamic acids acting as HDAC-inhibitors, organometallic antibiotics or catechol amine derivatives have been studied.

Organometallic complexes with bioactive ligands are nowadays interesting for both, the noninvasive imaging of biological features and the therapeutic treatment of diseases. While several transition metals across the periodic table are frequently used for therapy, ^{99m}Tc is the most prominent nuclide in nuclear medical diagnostics.[1, 2]
It would be desirable, in a *theragnostics* sense (therapy and diagnostics), to have identical compounds for combined therapy and non-invasive diagnosis.[3, 4] Among transition-metals, rhenium and technetium belong to the same triad. Therefore it is possible to use identical compounds for combined therapy and imaging.[3-5] While Re-based compounds can be used for therapy, the homologous compounds with ^{99m}Tc can serve as imaging agents for Single Photon Emission Computed Tomography (SPECT).[1, 2, 6]
[(CpR)M(CO)$_3$]-type compounds are considered as very stable complexes under various conditions and can synthetically be treated like aromatic organic molecules. Re-compounds are therefore usually synthesized starting from [(Cp)Re(CO)$_3$] and using standard organic synthesis procedures, whereas for the corresponding ^{99m}Tc-complexes, the uncoordinated HCp-ligand is prepared prior to complexation, either as a monomer or in its dimeric form.

Zusammenfassung

Die chemische und biologische Evaluation von organometallischen Stoffen für nuklearmedizinische Anwendungen, verglichen mit ihren rein organischen Analogas und die Untersuchung des Metall-vermittelten *retro*-Diels-Alder Verhaltens von derivatisierten Cyclopentadienyl-dimeren ist eine zusammenfassende Beschreibung dieser Dissertation. Mit einem Hauptaugenmerk auf die Synthese von ^{99m}Tc-markierten Radiopharmaka, wurde eine Vielfalt an organischen und anorganischen Cyclopentadienyl Derivaten hergestellt. Arylsulfonamide, -sulfamide und -sulfamate, die an die Carboanhydrase IX binden, Hydroxamsäuren, welche als HDAC-Inhibitoren dienen, organometallische Antibiotika oder Catecholamin Derivate wurden untersucht.

Organometallische Komplexe mit biologisch aktiven Liganden sind heute sowohl für die Anwendung der nicht-invasiven Bildgebung, als auch für therapeutische Behandlungen interessant. Während eine Vielzahl an Metallen quer durch das Periodensystem regelmässig für therapeutische Zwecke verwendet werden, ist ^{99m}Tc das meist verwendete Nuklid in der nuklear medizinischen Diagnostik.[1, 2] In einem *theragnostischen* (Therapie und Diagnostik) Kontext wäre es wünschenswert, identische Verbindungen für kombinierte Therapie und nicht-invasive Diagnose zu haben.[3, 4] Unter den Übergangsmetallen gehören Rhenium und Technetium zu derselben Triade. Daher ist es möglich, identische Verbindungen für kombinierte Zwecke der Therapie und der Diagnostik zu verwenden.[3-5] Während Rhenium-basierte Verbindungen für die Therapie eingesetzt werden, können die homologen Verbindungen mit Technetium-99m als Marker für die Photon Emission Computed Tomography (SPECT) dienen.[1, 2, 6]

Verbindungen vom Typ [(CpR)Re(CO)$_3$] werden allgemein unter den verschiedensten Bedingungen als sehr stabil angesehen und können synthetisch wie aromatische organische Moleküle behandelt werden. Re-Verbindungen werden daher üblicherweise ausgehend von [(Cp)Re(CO)$_3$] unter verwendung von standard organischer Synthesemethoden hergestellt, während für die entsprechenden ^{99m}Tc-Verbindungen der unkoordinierte HCp-Ligand, entweder als monomer oder in seiner dimeren Form vorgängig synthetisiert wird.

1. Introduction

1.1 Metals in Medicine

Medicinal inorganic chemistry is a relatively young field of research, which has emerged tremendously since the successful development of Cisplatin in the late 1960s. During the past 50 years, a multitude of metal containing anticancer, antirhumatismal, antiparasital, antimalarial and antibacterial compounds, enzyme inhibitors and MRI-contrast agents have been exploited and investigated.[7, 8] However, the vast majority of the pharmaceuticals on the market are based on organic agents, acting for example as inhibitors for receptors. Most of the organometallic or inorganic drugs act in a "Cisplatin manner", using the versatile reactivity of the metal center in biochemical environment. One reason for this might be the consequence of man's will to adopt to nature, where the rich redox chemistry and the relatively weak bonding interactions between metals and small molecules (the ligand binding energy in a typical coordination M-L bond is 50-150 kJ/mol) enables reversible binding, in contrast to the energetically stronger covalent bonds (energy of a single C-C bond is 300-400 kJ/mol) formed within organic molecules.[7] Structural changes imposed by metal cations such as Ca^{2+} or Zn^{2+} on proteins or nucleic acids are essential for the initiation of biological processes.[6] Binding sites in the binding pocket of proteins or receptors often contain metals as well. However, metal complexes are rarely found as structural recognition sites in receptor binding molecules, whereas this is exactly how most organic molecules and drugs tend to work. Covalent interactions of organic molecules with the biological environment only rarely take place.

Only recently inorganic compounds came into the scope of such applications. The structural complexity of metal containing compounds that are stable in biological systems was recognized to have an underestimated and unexplored potential for medicinal applications.[8] Ferrocene containing antimalarial[9, 10] or anticancer[11] compounds or chromium antibacterial agents[12] are recent examples for organometallic complexes acting via structural recognition (Figure 1).

In consequence to this development, metal containing compounds are nowadays found both, in the therapeutic treatment of diseases and in the noninvasive visualization of biological features. Comprising radioactive elements,

radiopharmaceuticals are known as small molecules or also as macromolecules like proteins or antibodies.[13] As a function of their biochemical behavior, they accumulate in particular regions of the body or in certain tissues. Depending on the radionuclides that are introduced, radiopharmaceuticals are designed for therapeutic treatment of diseases, for diagnosis or for combined clinical applications. Striking therapeutic elements are α- or β^--particle emitters, delivering a cytotoxic radiation dose to the target tissue. Incorporating β^+- (for Positron Emission Computed Tomography, PET) or γ- (for Single Photon Emission Computed Tomography, SPECT) emitting elements, radiopharmaceuticals follow a diagnostic purpose, providing detailed information of pathological structures or of physiological functions. Combining diagnostic radiopharmaceuticals with therapy, the effect and the progress of a treatment can be monitored in a noninvasive way. In the following course of this thesis, radiotherapeutic agents are not discussed but imaging agents with ^{99m}Tc will be in the scope. Combining such radiotracers with the corresponding cold Re-analogues, the "Theragnostic" (therapy and diagnostic) application of metal complexes will be discussed.

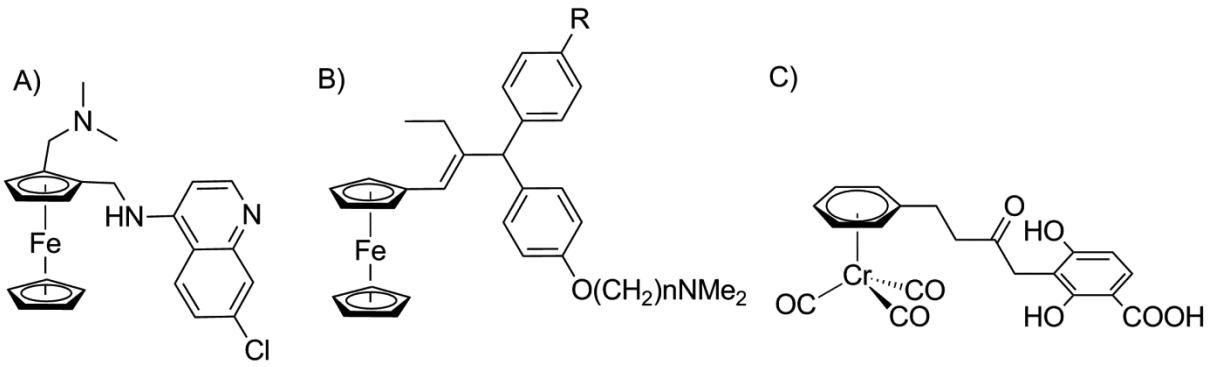

Figure 1: Organometallic complexes acting via structural recognition. A) Ferroquin – passed phase II clinical trials as an anti-malarial drug. B) Ferrocifen (R = H, n = 2-8) – anti-estrogens in MCF-7 breast cancer cell lines and against estrogen-dependent tumor xenografts in nude mice. C) Chromium based analogue of Platensimycin – inhibits the FabF enzyme in bacterial fatty acid biosynthesis.

1.2 ^{99m}Tc and Labeling

The eligibility criteria for radionuclides that are suitable for clinical use are demanding and versatile and confine therefore the assortment of possible nuclides dramatically. From a synthetic point of view, the preparation of a radiopharmaceutical must be fast in the timescale of the half life time of the radionuclide.[14] It should consist of one or at most of two steps in synthesis, which can be accomplished with a minimum of

complexity just before application and on-site. Beside synthetic strains, the half-life time of the radionuclide must match the pharmacology of the vector. It should be sufficiently long allowing dose preparation, administration to the patient, accumulation in the target tissue and collection of images. The energy of the emitted particles should be high enough to allow good quality images but as low as possible to minimize the radiation dose delivered to the patient. Commercial aspects like price and availability are other crucial points for routine clinical use.

Among transition metals, many different nuclides suit at least some of these demands. ^{94m}Tc, ^{99m}Tc, ^{111}In, ^{201}Tl, ^{60}Cu, ^{61}Cu, ^{64}Cu, ^{66}Ga, ^{67}Ga, ^{68}Ga, ^{44}Sc, ^{86}Y, ^{86}Zr and ^{89}Zr are examples of which some are more and others less studied and explored.[15-18] ^{99m}Tc is the most prominent nuclide in nuclear imaging.[2, 19-21] Roughly 85 % of the clinically administered radiopharmaceuticals consist of ^{99m}Tc complexes. With a half-life time of about 6h, the emission of pure γ-photons of 140 keV (accompanied by internal conversion and Auger electrons) and a few stable oxidation states it is suitable for versatile chemistry and for scintigraphy.[14] It is availabile as Na[^{99m}TcO$_4$] in low concentrations of 10^{-8} to 10^{-9} M in physiological saline from the ^{99}Mo/^{99m}Tc generator which simplifies clinical handling tremendously compared to nuclides that are generated by cyclotron. ^{99}Mo is produced from nuclear reactors, making it cheap.

Depending on the metal core fraction and on the ligand system which is coordinated, three different types of imaging agents are discriminated according to their mechanism of action *in vivo*.[14]

- Perfusion agents are chemically innocent coordination compounds, which do not contain a direct pharmaceutical function. They follow a certain biological pathway due to physico-chemical properties, which are predominantly defined by the ligand sphere surrounding the metal core.
- Biomimetics are organometallic complexes, comprising structural mimetics of biological or pharmaceutical lead structures. They bind to the same receptors or enzymes as the lead structures, and the metal contributes to the binding as an integrated part of the molecule.
- Targeting agents incorporate a targeting vector with a directly related biological function. This function is conjugated to, or integrated into a certain type of chelator, which coordinates to the metal center.

Introducing a metal complex into a biologically active function will change the structural- and also the biological properties of the vector. Keeping a radiochemically labeled agent biologically active is therefore challenging, especially for small molecules compared to labeled peptides, proteins or antibodies. A large number of techniques have been developed for ^{99m}Tc-labeling, which are classified into categories.[22] In the ***direct labeling approach*** the presence of disulfide bridges in peptides is used, for proteins and antibodies to incorporate a metal complex. By reduction with $SnCl_2$ free thiols are formed, which bind strongly to the Tc-core.

The formation of a ^{99m}Tc-chelate prior to coupling to the targeting function is called ***pre-labeling***, and prevents the targeting function from being exposed to the sometimes harsh labeling conditions. This strategy is often applied for the labeling of antibodies.[23]

In the ***post-labeling*** approach, a targeting vector is coupled via a linker to a chelator, which binds the metal center. The ***bifunctional chelator*** (BFC) is formed before complexation. Radiolabeling can be accomplished in the presence of the BFC. This strategy is often applied for the labeling of small molecules (Figure 2).

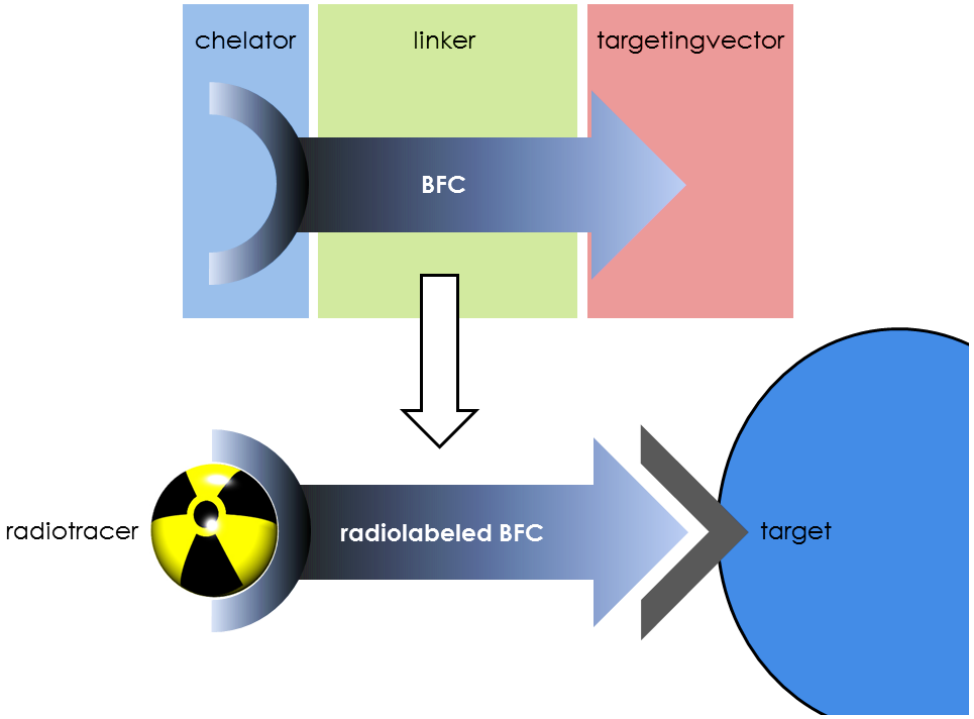

Figure 2: Schematic representation: imaging with the BFC-approach

Different core fractions with ^{99m}Tc comprising different oxidation states, chemistry, size and hydrophobicity are focused for applications in nuclear medicine. Clinically applied imaging agents frequently consist of a $[^{99m}Tc^{V}O]^{3+}$ or $[^{99m}Tc^{V}O_2]^{+}$ core, thermodynamically stabilized by tetradentate ligands with mixed N-, S- and O-donors.[19] Examples are diethylene-triamine-pentaacetic acid (DTPA), mercapto-acetyl-glycine-glycine-glycine (MAG3) or oxime-bridged hexamethyl-propylene amin oxime (HMPAO) (Figure 3). Currently extensively investigated ^{99m}Tc-fragments are the *fac*-$\{^{99m}Tc^{I}(CO)_3\}^{+}$-, the $\{^{99m}Tc^{V}N(PNP)\}^{2+}$- or the *fac*-$\{^{99m}Tc^{VII}O_3\}^{+}$-core (Figure 4).[24-26] Molecules labeled with these fragments often follow the concept of targeted imaging with the bifunctional chelator (BFC) approach.[14] Such complexes are often generated from a robust core fraction with a few coordination sites occupied by weakly bound substitution-labile ligands. These ligands correspond for example to the water molecules in $[^{99m}Tc(OH_2)_3(CO)_3]^{+}$[27, 28] or to the halides in $[^{99m}TcN(PNP)Cl_2]$[24] respectively. Tridentate σ- or π-donors, coupled to a targeting vector are popular ligand systems for *fac*-$\{^{99m}Tc^{I}(CO)_3\}^{+}$.[21, 29-31] $[^{99m}Tc(NS_3)L]$ containing targeting molecules are formed in a 4+1-approach from $[^{99m}Tc(EDTA)]^{-}$ in one pot together with the NS_3-chelator and an additional bifunctional ligand L.[32-36] *Fac*-$\{^{99m}TcO_3\}^{+}$-cores can be used as a derivatized $[^{99m}TcO_3(TACN)]^{+}$ moiety, where the biologically active functionality is either introduced with the 1,4,7-triazacyclononane (TACN) or, via 3+2 cyclo-addition, to two oxygen atoms.[37, 38]

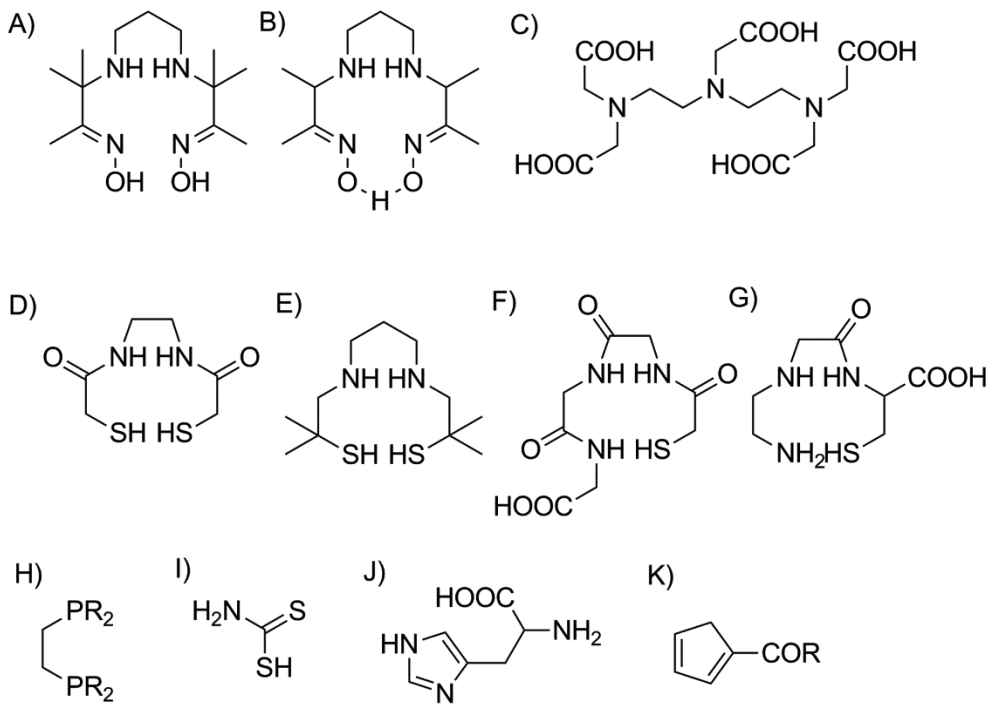

Figure 3: Preferred ligand systems for Re and Tc-chemistry in nuclear medicine. A) PnAO, B) HMPAO, C) DTPA, D) DADS, E) DADT, F) MAG3, G) MAMA, H) Diphos, I) DTC J) HIS, K) Cp.

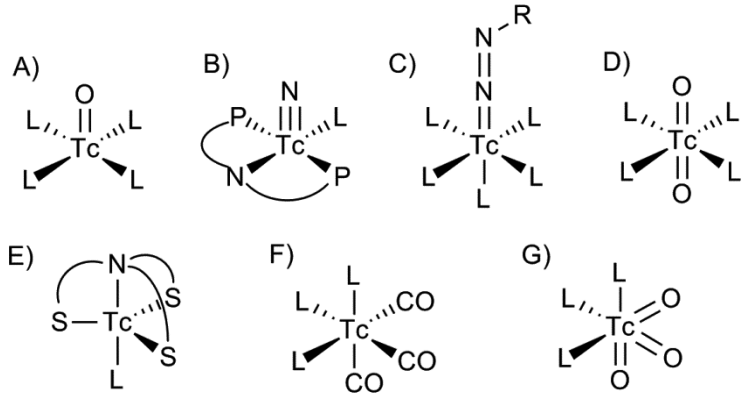

Figure 4: Investigated ^{99m}Tc-fragments. A) Square pyramidal Tc-oxo complexes ($[^{99m}Tc^{V}OL_4]^{3+}$) with tetradentate chelators, such as DADT, MAG3, DADS and MAMA. B) Square pyramidal Tc-nitrido complex of the form $[^{99m}Tc^{V}N(PNP)L]^{2+}$ with various chelators. PXP ligands are used for stabilisation of the $\{^{99m}Tc^{V}N\}$-core. C) $\{Tc^{V/III}\}$HYNIC-HYNIC can occupy one or two coordination sites (depending on R), which can influence the oxidation number of the metal. A coligand L, is needed to complete the coordination sphere. D) $[^{99m}Tc^{V}O_2]^{+}$, E) $[^{99m}Tc^{III}(NS_3)L]$, F) *fac*-$\{^{99m}Tc^{I}(CO)_3L_3\}^{+}$ with bidentate and tridentate chelators containing imidazoles, pyridines, amides, amines, carboxylic acids or others. G) *fac*-$\{^{99m}Tc^{VII}O_3L_3\}^{+}$.

Among transition-metals, rhenium and technetium belong to the same triade. Therefore it is possible to use identical compounds for combined therapy and imaging in a theragnostics approach.[3-5, 39] While Re-based compounds can be used for therapy, the homologous compounds with ^{99m}Tc can serve as imaging agents for single photon emission computed tomography (SPECT).[2, 4, 6, 19, 40] Following a BFC

approach with targeting agents, it is also possible to apply "cold" non-radioactive ^{185}Re for common chemo therapy, instead of the radiotherapy nuclides $^{186/188}$Re.

1.3 The Targeted Approach: Inhibitors and Selectivity

Within organometallic agents, several targets like DNA, mitochondria, cell membranes, receptors, enzymes or proteins are focused. The selection of an appropriate target is crucial for inducing the anticipated effect and strongly depends on the function or disease of interest.

Diagnosis and therapeutic treatment of many diseases requires molecules designed for binding to receptors and enzymes. Upon binding they interfere with biological processes related to these diseases, by acting as agonists or as antagonists. In this context, activators can induce the biosynthesis of compounds needed to overcome a malfunction. Leading to cell death on the other hand, inhibitors possess a competitively regulative aspect and are often studied in the treatment of cancer, where excessive proliferation can be opposed.

In contrast to healthy cells, metabolism is defective in diseased cells in many malfunctions. Therefore certain receptors or enzymes can be strongly overexpressed. Especially in cancer related tissues overexpression is frequently observed. Allowing selective accumulation of a targeting agent, these biomolecules are therefore of high interest for both, therapy or diagnosis. However, since nature has developed an enormous realm of functionally and structurally similar receptors and enzymes, selectivity for a specific target is a key criterion for the quality of an inhibitor.[41] As mentioned above, inhibitors are typically of organic nature but Meggers et al. recently showed that high selectivity does not only depend on intermolecular interactions but also on a versatile and directed three dimensional arrangement of different functionalities. As exemplified with organometallic protein kinase inhibitors,[42-44] chemically inert organometallic complexes offer the enhanced opportunity to populate biologically relevant chemical space compared to similar inhibitors with a purely organic scaffold. Therefore, bioorganometallic complexes exhibit a high potential as chemical probes.[42, 45-48]

1.4 Cp & Thiele's Acid

^{99m}Tc is available as Na[^{99m}TcO$_4$] in physiological saline. Any chemistry must therefore be performed in aqueous solution, which can be demanding and is not always straightforward for organometallic synthesis. Cyclopentadiene (HCp) is for imaging a conceptually and structurally uncommon ligand. It does not contain any heteroatoms, which renders the molecule hydrophobic and therefore in fact unsuitable for aqueous syntheses. Moreover HCp and many derivatives are unstable as a monomer and undergo Diels-Alder polymerization. However, *Hanzlik* et al. exemplified in the late 1970s with β-Ferrocenylalanine as an inhibitor of the phenylalanine decarboxylase, that organometallic Cp$^-$ sandwich-complexes can be tolerated in biological systems, when replacing phenyl rings.[49] Years later, *Jaouen* and coworkers confirmed this observation. They developed a variety of highly potent selective estrogen receptor inhibitors by replacing a phenyl ring in Tamoxifen with ferrocene or with [(Cp-R)Re(CO)$_3$]. The resulting molecules retained a high binding affinity for the estrogen receptor.[11, 50-55] With this example, beside ferrocene, Cp$^-$-complexes of the group 7 transition metal tricarbonyls became very popular for medicinal inorganic research. Bioorganometallic complexes containing ferrocene or [(Cp-R)M(CO)$_3$] (M = Re or ^{99m}Tc) exhibit a high potential as therapeutic agents or also as imaging agents as the Cp-complex can act as a structural analogue of phenyl rings. Additionally, [(Cp-R)M(CO)$_3$] (M = Re or ^{99m}Tc) is small in size and minimizes therefore steric interference with the biological environment in the binding site, which contributes to the retention of the function of the targeting vector. Another inherent advantage is the stability of these half sandwich complexes under physiological conditions. However, whereas ferrocene-based organometallic compounds have a high potential for therapy, their *in vivo* diagnostic use is limited since radionuclides such as ^{18}F or ^{11}C (PET) cannot easily be introduced or lead to substantial alteration of the chemical authenticity of the compound. As mentioned above, in a theragnostic sense, the bio-isosteric replacement of organic functionalities by group 7 transition metal complexes (Re or ^{99m}Tc) is interesting for both, therapy and diagnosis.

Drawbacks for the application of Cp$^-$-containing ^{99m}Tc-complexes for imaging arise from the synthetic properties of the HCp-ligand. Whereas macroscopic amounts of cold [(Cp-R)Re(CO)$_3$] complexes are accessible along classical organic and

organometallic methods, the ^{99m}Tc analogues must be prepared from aqueous buffer solutions and require the uncoordinated ligands to be synthesized in advance. HCp contains two conjugated double bonds and derivatives are therefore, in principle, easily accessible. But its tendency to undergo fast Diels-Alder di- or polymerization makes derivatization demanding. Beside this, η^5-coordination to *fac*-{Tc(CO)$_3$} requires deprotonation of HCp. A pK_a of roughly 14 of unsubstituted HCp is for pure hydrocarbons relatively low, but still too high for organometallic synthesis in water at physiological pH. In order to overcome these drawbacks, several multistep labelling procedures have been proposed.[56-59] But these syntheses include autoclave reactions in organic solvents and are therefore unacceptable for routine application.

However, electron withdrawing substituents have been shown to lower the pK_a of monomeric HCp-compounds, tremendously.[60-62] At a physiological pH of 7.4, the amount of deprotonated Cp$^-$ in solution is therefore increased and coordination to the *fac*-{Tc(CO)$_3$}-core is relieved. The pK_a of acetyl-HCp for example is 8.6, which is lower by 5 orders of magnitude relative to unsubstituted HCp. Also other α-keto substituted HCp-compounds have pK_a-values in the same range and are stable as deprotonated sodium salts in aqueous solutions for hours, even when exposed to air (Figure 5).[60]

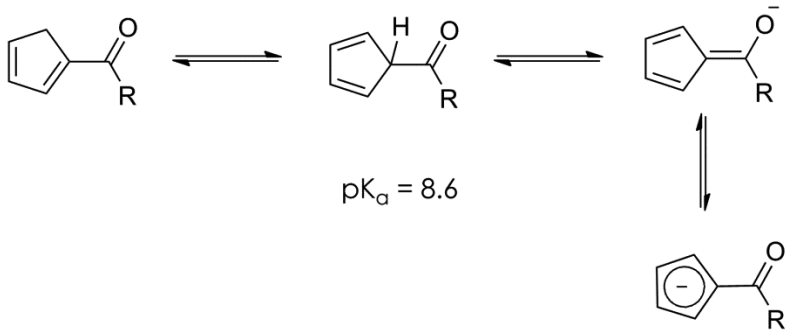

Figure 5: Deprotonation of Cp-derivatives. α-keto substitution of HCp lowers the pK_a by roughly 5 orders of magnitude – aqueous complexation with *fac*-{Tc(CO)$_3$} is now possible.

[(Cp-R)^{99m}Tc(CO)$_3$]-type complexes are therefore accessible in aqueous solution at temperatures below 100 °C with α-keto substituted HCp-compounds, which are stable as monomers for a sufficient long period. The same principle is true for the α-carboxylic acid HCp-COOH.[61] But unlike HCp-ketons, HCp-COOH tends to dimerize relatively fast and is not cracked at temperatures below 160 °C, making

derivatization of the acid with a targeting vector difficult. Stabilization as a ring-deprotonated sodium salt is not possible, due to the high acidity of the carboxylic acid function. However, the unexpected formation of [(CpCOOH)^{99m}Tc(CO)$_3$] using "Thiele's Acid", the Diels-Alder dimer of HCp-COOH, showed that the metal-mediated *retro* Diels-Alder reaction is a convenient synthesis, as Thiele's Acid can be regarded as a protected HCp-COOH. Based on this result, the general synthetic route to [(Cp-R)^{99m}Tc(CO)$_3$]-type complexes has been developed by derivatization of the acid function via amide coupling to biotargeting vectors. This procedure allows a fully aqueous preparation of a variety of bioactive compounds (Scheme 1).[61, 63] The metal mediated *retro* Diels-Alder reaction of (HCp-R)-dimers with [^{99m}Tc(OH$_2$)$_3$(CO)$_3$]$^+$ or directly with [^{99m}TcO$_4$]$^-$ permitted to transfer the principle of replacing phenyl rings in bioactive substances to ^{99m}Tc-labeled compounds as demonstrated with melanin targeting agents or with high affinity carbonic anhydrase inhibitors, which are part of this thesis.[5, 64]

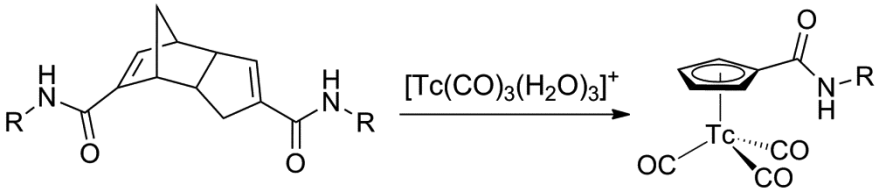

Scheme 1: Metal mediated *retro* Diels-Alder. Thiele's Acid derivatives do not cleave thermally below 160 °C. The *retro* Diels-Alder reaction with [^{99m}Tc(OH$_2$)$_3$(CO)$_3$]$^+$ or directly with [^{99m}TcO$_4$]$^-$ therefore must be metal mediated.

2. Results & Discussion

2.1 Index of Compounds

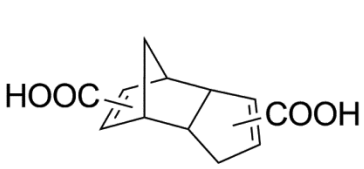

1

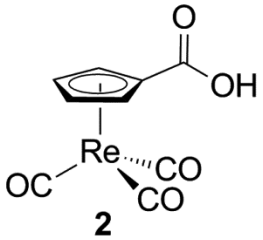

2

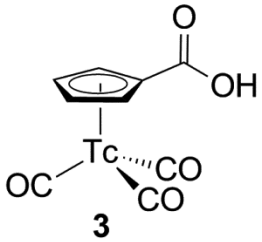

3

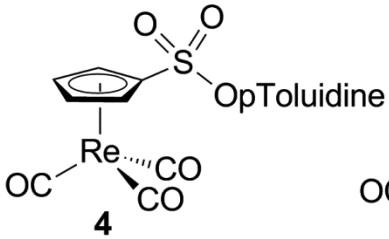

4

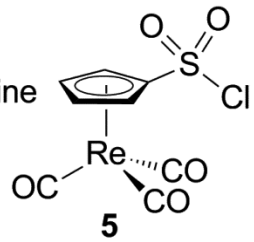

5

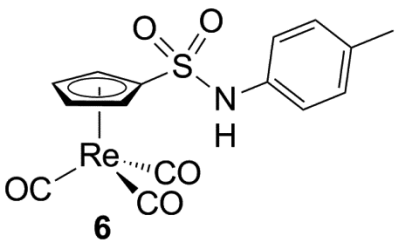

6

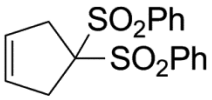

7

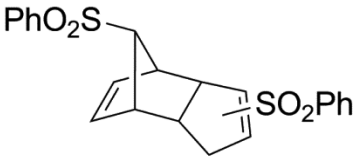

8

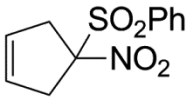

9

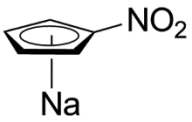

10

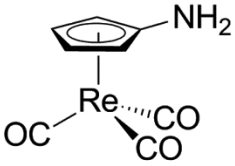

11

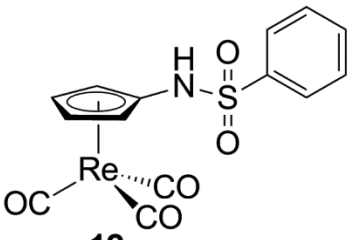

12

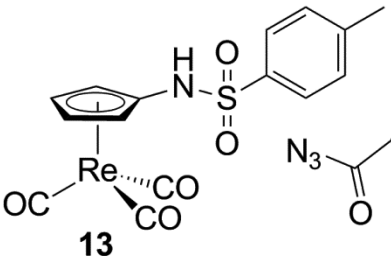

13

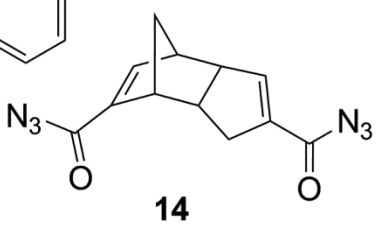

14

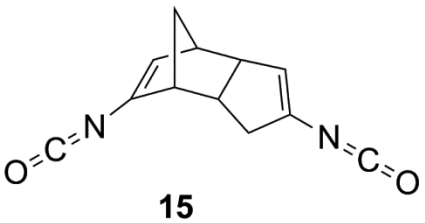

15

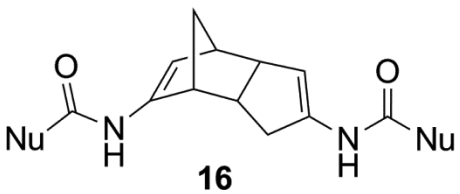

16

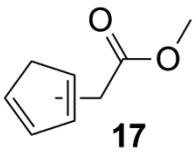

17

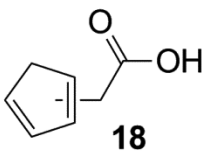

18

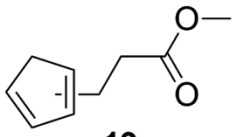

19

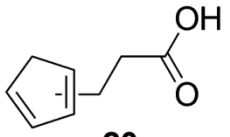

20

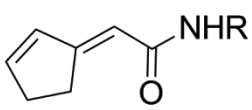

a R_1 = Bz
b R_2 = CH_2COOCH_3

21a/b

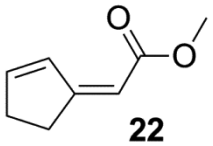

22

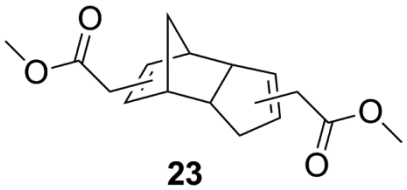

23

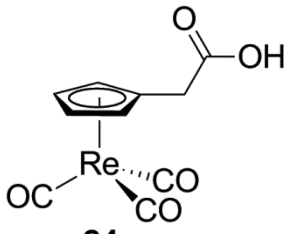

24a

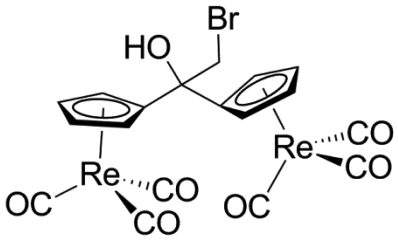

24b

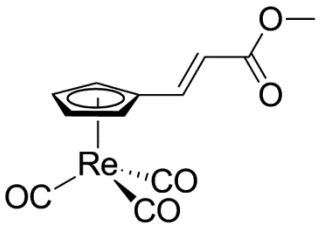

25

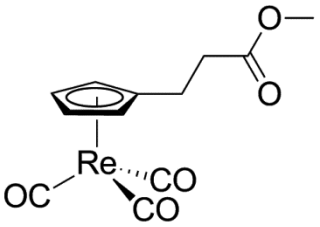

26

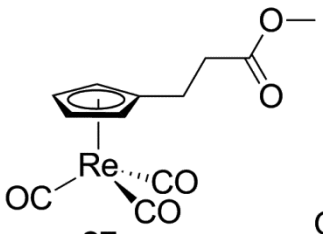

27

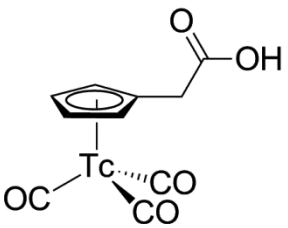

28

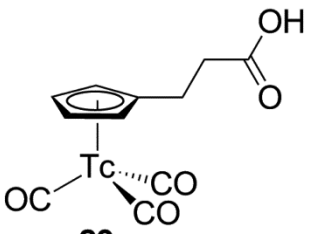

29

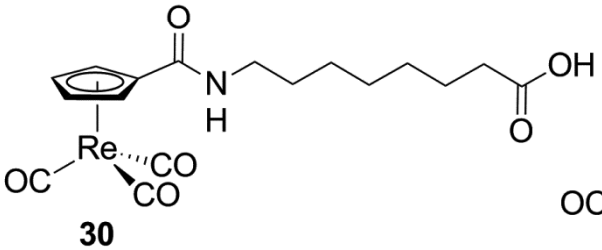

30

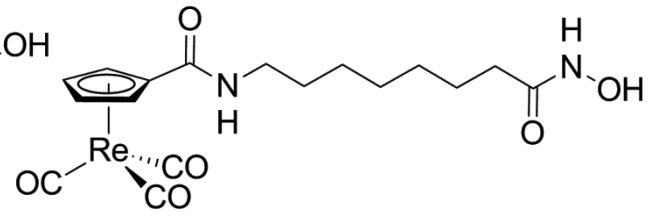

31

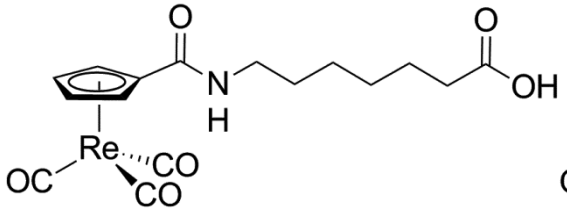

32

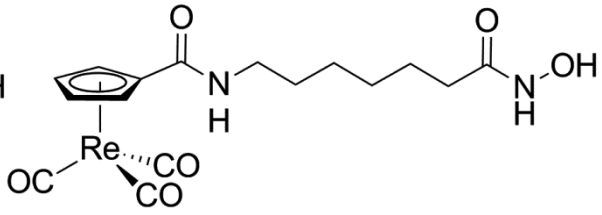

33

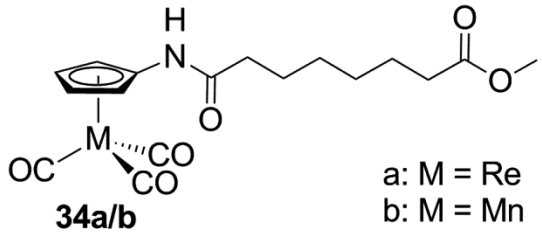

34a/b

a: M = Re
b: M = Mn

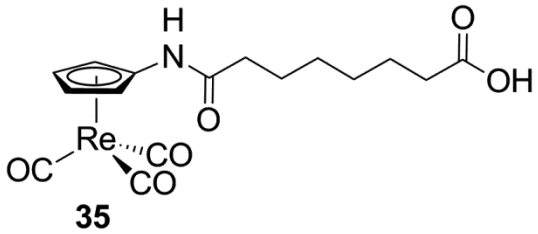

35

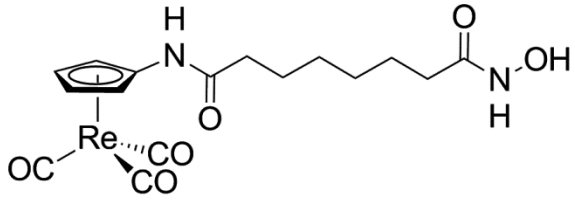

36

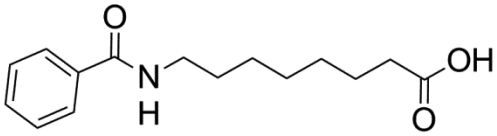

37

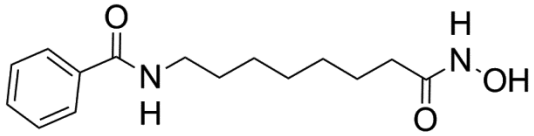

38

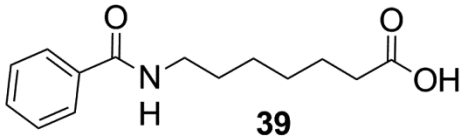

39

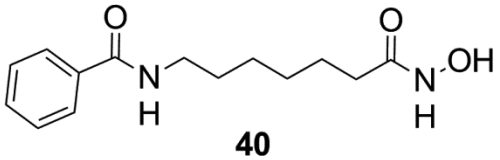

40

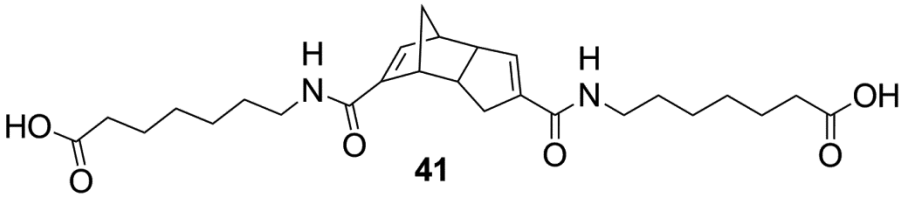

41

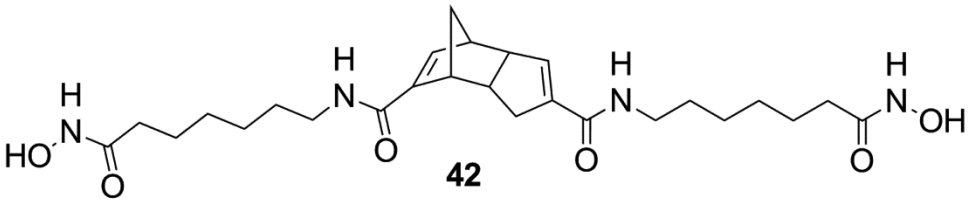

42

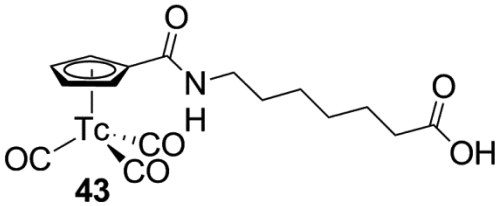

43

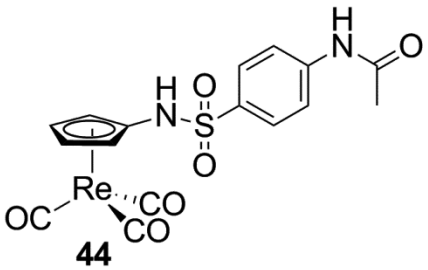

44

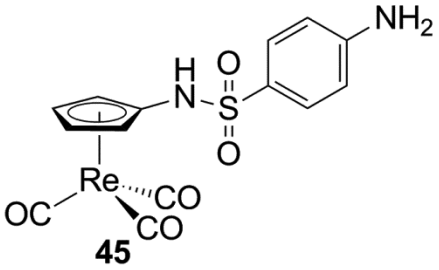

45

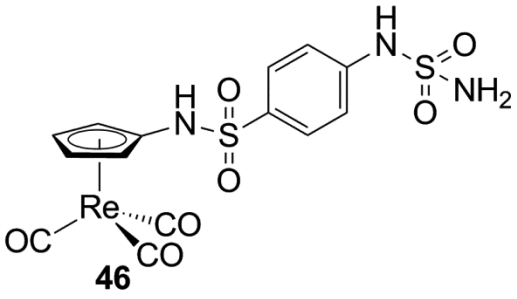

46

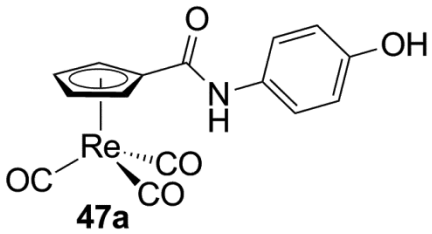

47a

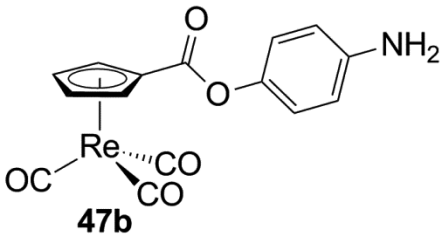

47b

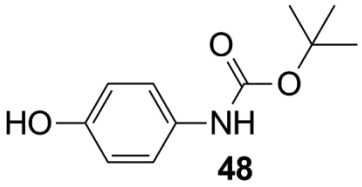

48

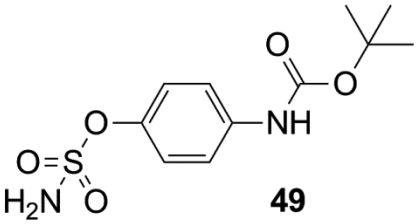

49

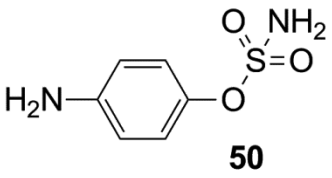

50

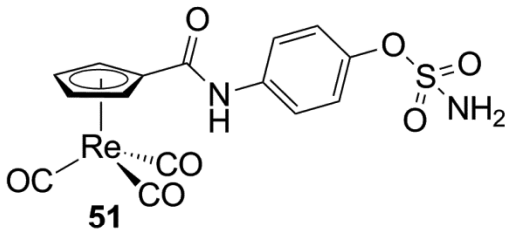

51

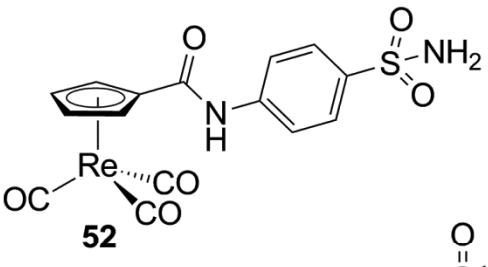

52

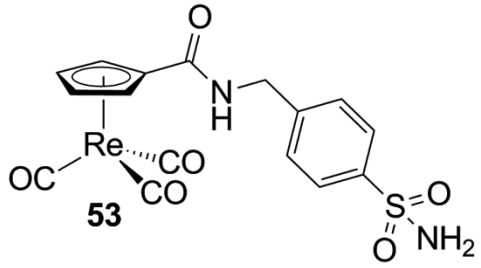

53

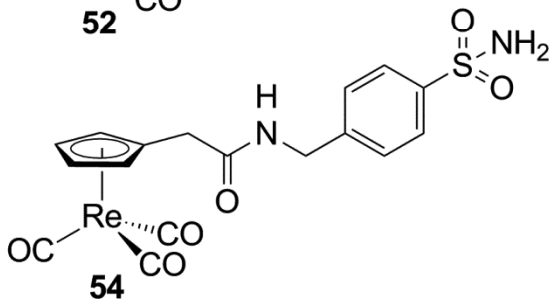

54

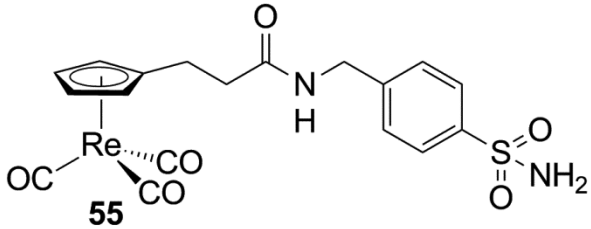

55

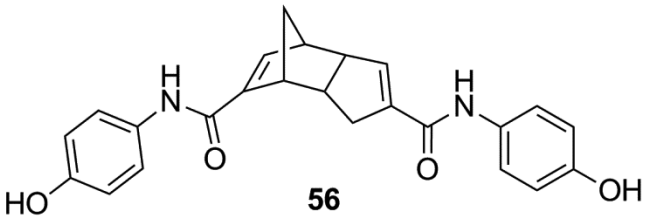

56

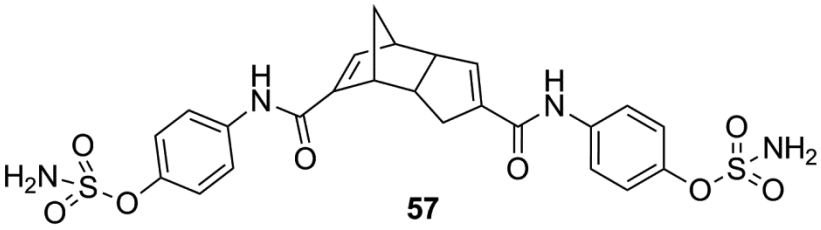

57

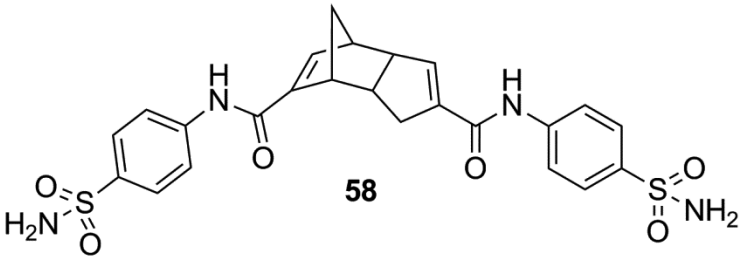

58

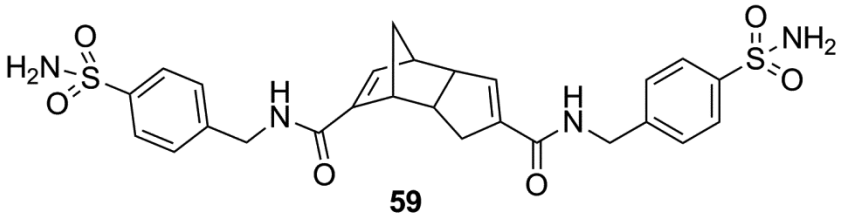

59

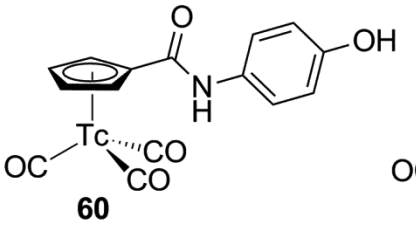

60

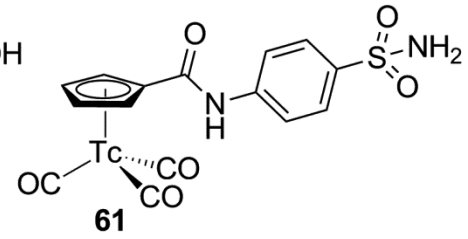

61

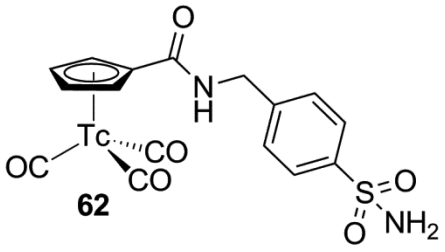

62

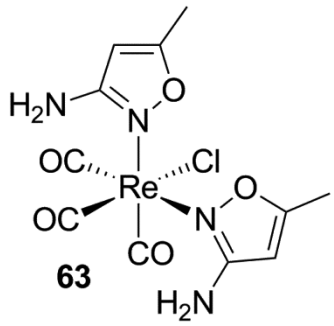

63

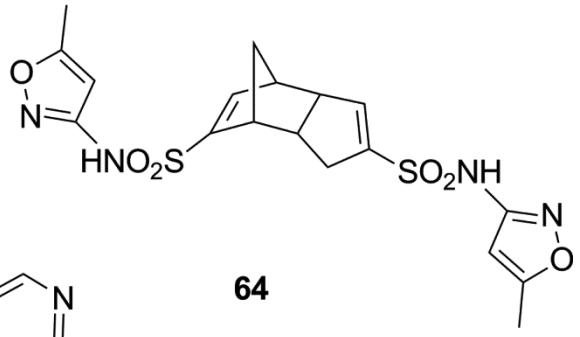

64

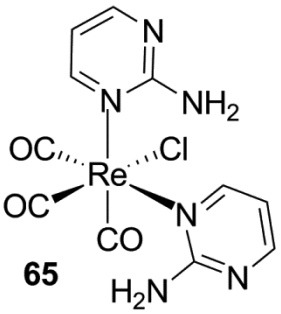

65

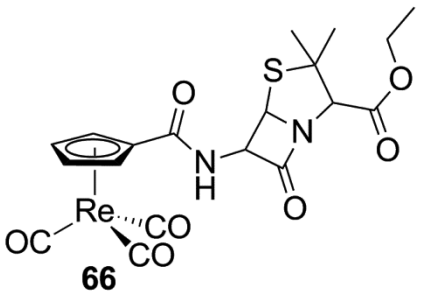

66

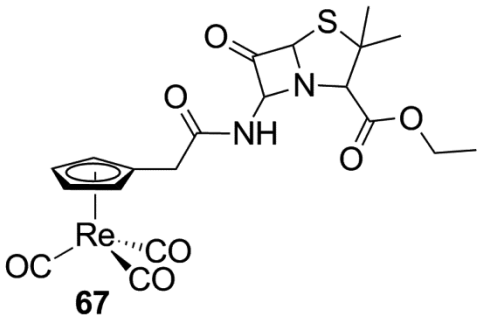

67

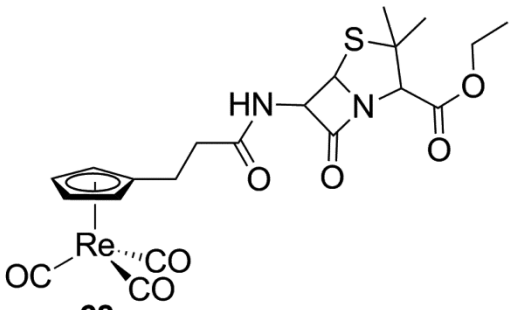

68

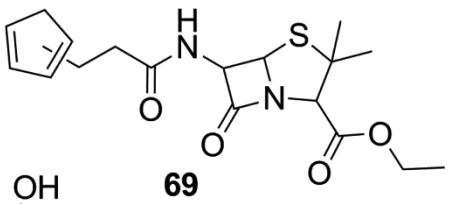

69

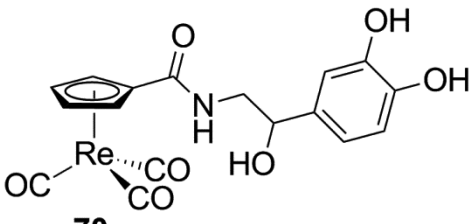

70

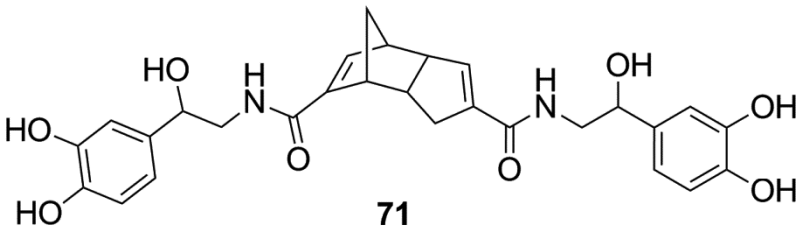

71

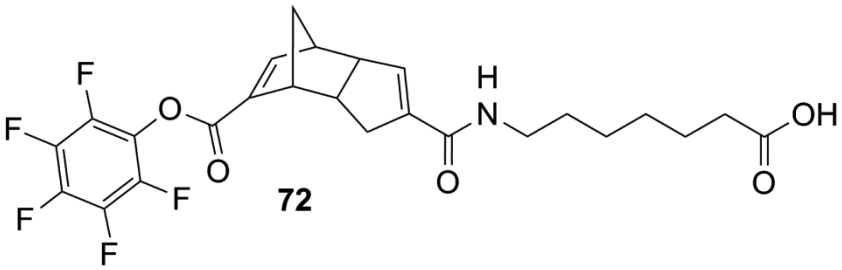
F
F
F
F
F
O
O
H
N
O
OH
O

72

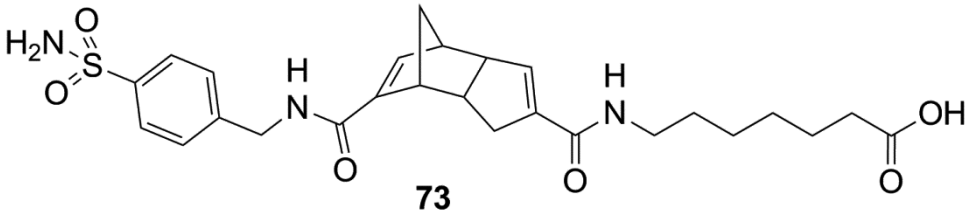
H2N
O
S
O
H
N
O
H
N
O
OH
O

73

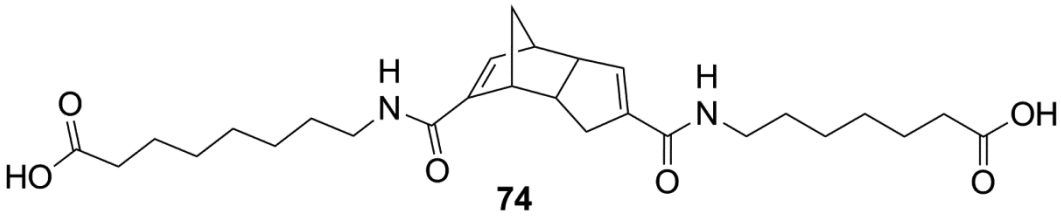
HO
O
H
N
O
H
N
O
OH
O

74

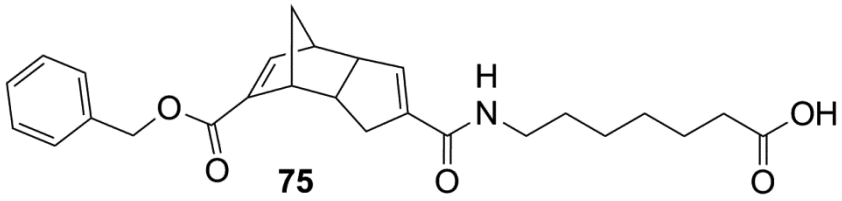
O
O
H
N
O
OH
O

75

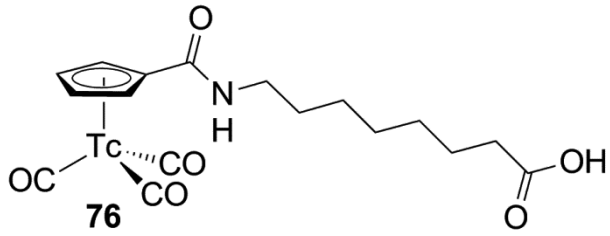
O
N
H
Tc
OC
CO
CO
OH
O

76

2.2 Cp-derivatization

The derivatization of cyclopentadiene or of complexes thereof has a long history in organic and organometallic chemistry. Many different substituents have been described in literature.[65-71] However, the number of reports, where these derivatives have been used to couple biologically active targeting vectors is comparably small.
Being part of the spacer between the chelator and the targeting vector, the functional group directly attached to the Cp is of high importance. This part of the bifunctional chelator (BFC) can influence interactions between the target and the targeting agent to a large extend. Beside physical properties, this functionality can influence also the chemical properties of the BFC. Depending on the electronic characteristics of the derivative, in uncoordinated HCp-compounds it can influence the electron density on the adjacent double bond and therefore also the bond lengths and electro- or nucleophilicity. This again has an influence on the monomer stability and dimerization rate, as well as on the acidity of the ring protons.
In the following chapter, the synthesis and the characteristics of different Cp-functionalities are discussed. In some cases, the free HCp-derivative was prepared along with the corresponding Re- and the ^{99m}Tc-complexes. Derivatives of some of these functional groups have been prepared as simple model compounds, and do not have any biological target.
Electron withdrawing substituents lower the electron density at the metal center. Therefore also the π-backdonation to the CO-ligands is diminished. This again has an impact on the C-O-bonding distance and on the IR-υCO-frequency.
Increased electron acceptance properties, means increased deshielding of neighbouring protons. This can be observed in the ^{1}H-NMR as a shift of the corresponding peaks towards lower field (higher ppm).
The electronic properties of the derivatives bound to the Cp influence therefore the electron density on neighbouring positions within the molecule. Therefore, the compounds can be classified by looking at the ^{1}H-NMR chemical shifts of proximate protons or at IR-υCO-bands.

2.2.1 Cp-COOH

A simple but at the same time very prominent and versatile way of introducing derivatives into organic molecules is the derivatization of carboxylic acids. Similar to aldehydes or ketones, the carbon atom of the carbonyl-group can be attacked by nucleophiles or by other chemical functions. However, the hydroxyl-part of the carboxy-group, which is substituted, is in fact a poor leaving group. Therefore, such reactions are usually either acid/base catalysed or require the activation by introduction of a better leaving group.
Besides the versatile chemical properties and opportunities that carboxylic acids offer, the physicochemical characteristics of this functional group can be of high importance as well, as they can influence the characteristics of the whole molecule.

The Ligand

The carboxylic acid of cyclopentadiene can be synthesized by addition of dry ice to a solution of NaCp in THF. The deprotonated Cp^- acts as a nucleophile and attacks the carbon atom of the solvated CO_2, to form after protonation HCp-COOH in three possible isomers **a**, **b** and **c** (Scheme 2).[70] These products undergo Diels-Alder dimerization or polymerization, to form 16 different isoforms of "Thiele's Acid" (**1**).[72-74] Purification by silica gel column chromatography yields selectively the main product, the 3'9'-endo-derivative, which is the only isoform used for further reactions in the course of this thesis. Similar to acetyl-Cp ($HCp\text{-}COCH_3$), the electron withdrawing carbonyl in HCp-COOH lowers the pK_a-value of the ring proton from 14 to a range of 8 to 9, which is of high importance from a synthetic point of view.[60-62]
The olefinic protons in the ^{1}H-NMR (MeOD) of Thiele's Acid are observed at 6.85 and at 6.52 ppm respectively. These shifts are reference values, with which derivatives will be compared.

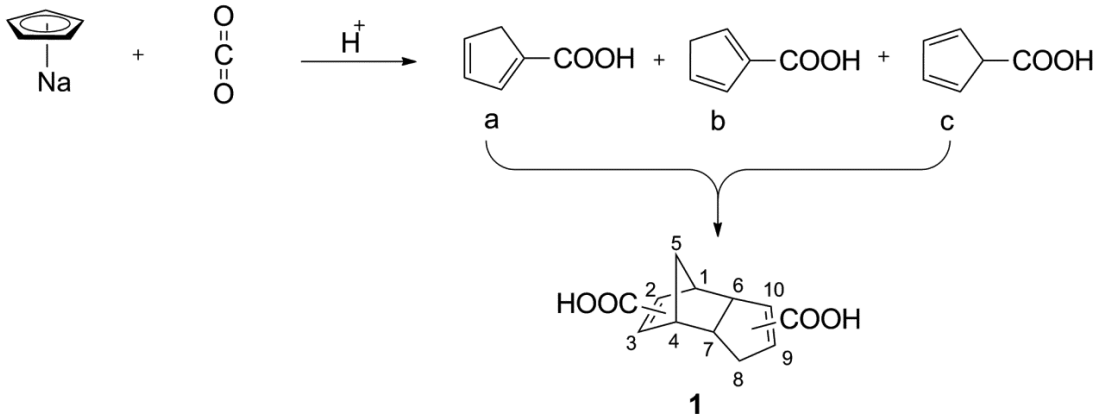

Scheme 2: Synthesis of Thiele's Acid. HCp-COOH undergoes quick Diels-Alder dimerization and forms 16 different isomers.

The Rhenium Complex

The classical method to prepare the carboxylic acid substituted cyclopentadienyl rhenium tricarbonyl half-sandwich complex [η^5-(CpCOOH)Re(CO)$_3$] is to add CO_2 in the form of dry ice to the deprotonated nucleophile [η^5-(CpLi)Re(CO)$_3$].[70] Newer approaches synthesized this complex from [$Re_2(CO)_{10}$] or from [$BrRe(CO)_5$] at temperatures around 165 °C, using the free ligand HCp-COOH as a monomer or as a dimer (**1**).[70] [(CpCOOH)Re(CO)$_3$] (**2**) is a remarkably stable compound and can synthetically be treated like an organic carboxylic acid. Therefore derivatives like amides or esters are accessible along common organic syntheses (Scheme 3). Considering the small size of [(Cp)Re(CO)$_3$], its stability and the possibility to replace phenyl rings in bioactive substances, **2** is very useful for the development of new targeting molecules along the BFC-approach.

The IR-υCO-bands (KBr) of **2** (2032 and 1916 cm^{-1}) are shifted towards higher frequencies compared to unsubstituted [(Cp)Re(CO)$_3$] (2018 and 1897 cm^{-1}), which indicates the electron accepting properties of the carboxylic acid portion.

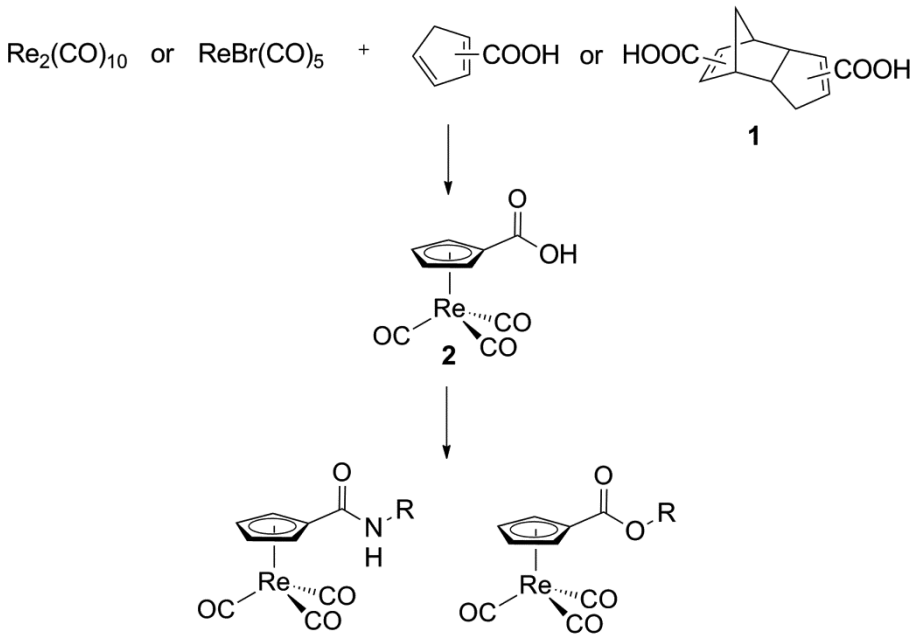

Scheme 3: Synthesis of [(CpCOOH)Re(CO)$_3$]. **2** can be treated like an organic carboxylic acid to form derivatives like esters or amides.

The Technetium Complex

[(CpCOOH)^{99m}Tc(CO)$_3$] (**3**) is accessible similar to the rhenium complex directly from the protonated free ligand HCp-COOH or from Thiele's Acid (**1**).[61] However in contrast to the rhenium synthesis, the quantitative preparation of the 99m-technetium analogue works at temperatures below 100 °C and does not require any organic solvents. As Thiele's Acid does not cleave thermally at these temperatures, the *retro* Diels-Alder reaction is suggested to be metal mediated. Mechanistically, the oxygens of the carbonyl groups serve as preliminar anchor groups, which bind to the metal center in a bidentate way (Scheme 4). The formation of an enolate, and therefore the generation of an intermediate carbo-cation, leads to the *retro* Diels-Alder rearrangement and to the separation of the two HCp-rings. Upon deprotonation, one of the two HCp-molecules coordinates η^5 to the metal center. Alternatively, instead of the oxygens of the carbonyl groups, preliminar coordination via the two double bonds of the HCp-dimer would also be a possible initial step.

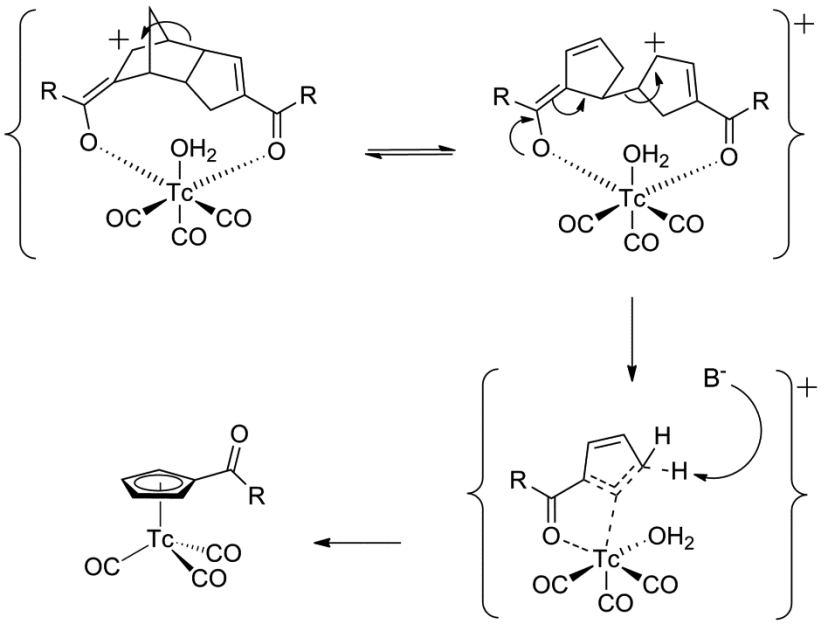

Scheme 4: Synthesis of [(CpCOR)^{99m}Tc(CO)$_3$] (R = OH or NHR'). [(CpCOOH)^{99m}Tc(CO)$_3$] (**3**) or derivatives are accessible from the protonated free ligands HCp-COR or from their dimers at temperatures below 100 °C in water.

Macroscopic amounts of the corresponding Re- or ^{99}Tc-complexes are synthetically not accessible along the same procedure. Though, except for the redox-properties, Re^{I} and Tc^{I} have very similar chemical characteristics. Suggesting the chelation of the metal center by the oxygen atoms of the HCp-dimer to be the rate determining step, then the low concentration of the metal compared to the ligand plays a crucial role for the kinetics of the reaction. Therefore, the study of the analogous reaction with microscopic amounts of Re or ^{99}Tc will be part of future mechanistic investigations.

In conclusion, carboxylic acid derived Cp-compounds have been described in literature in the form of the uncoordinated ligand (monomer or dimer **1**) and as η^5-coordinated Re- or ^{99m}Tc tricarbonyl complexes. The compounds are stable under ambient conditions and allow a wide range of synthetic manipulations at the carboxylic acid portion, even in aqueous solvents. Therefore they exhibit a high importance for synthetic or for biological radiopharmaceutical investigations. Synthetically, the Re- or ^{99m}Tc tricarbonyl complexes are accessible from Thiele's Acid **1**. But unlike the **metal mediated** *retro* Diel's-Alder synthesis of the ^{99m}Tc-complex, the corresponding Re-compound **2** is formed after **thermal** cleavage of the dimer **1** at high temperatures.

2.2.2 Cp-SO_3

In organic synthesis, sulfonates (RSO_3^-) are often used in substitution reactions. Their conjugated acids are considered as very strong, mainly due to resonance stabilisation of the deprotonated anions. For this reason, sulfonates are known as good leaving groups during substitution reactions. Moreover, Alkyl-sulfonic acids, similar to carboxylic acids can be derivatized by substitution of the hydroxyl-anion. Activation for example by halogenation is therefore indispensable. Sulfonic acids and derivatives (RSO_2R') are electron withdrawing substituents and are expected to have similar effects on the pk_a of a Cp-ring as carbonyls, which makes them interesting for organometallic chemistry.

From a biological point of view, sulfonic acids or derivatives like sulfonamides can form versatile hydrogen bond interactions with biomolecules. Sulfone derivatives can contribute to important parameters like selectivity or binding constants. Therefore, the -SO_2R-group is an interesting building block for the spacer part in a BFC.

As an example, the reaction of alkyl-sulfonyl chlorides (RSO_2Cl) with primary or secondary amines leads to the formation of internal sulfonamides, which have been used as antibiotics (see section 2.2.3). Their mechanism of action is related to the inhibition of bacterial enzymes, catalysing the folic acid synthesis. Terminal sulfonamides are nowadays extensively studied as carbonic anhydrase (CA) inhibitors, which are involved in many malignancies (see section 2.2.2).

The Rhenium Complexes

$[(CpSO_3)Re(CO)_3]^-$ is described as its *p*-toluidine-salt and was synthesized along literature procedure (Scheme 5).[71] Sulfuric acid serves as a source for sulfonation and is nucleophilically attacked by $[(Cp)Re(CO)_3]$. Precipitation from water by the addition of *p*-toluidine afforded compound **4**. In order to derivatize the sulfonate with a targeting vector, the sulfonyl chloride **5** was prepared by mixing **4** with PCl_5 without solvents. The two solids melted upon mixing and **5** was obtained by crystallization form CH_2Cl_2/hexane (Figure 6).[71]

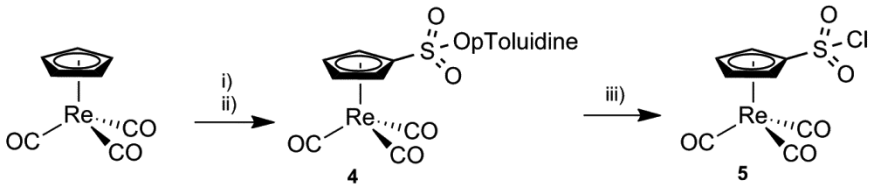

Scheme 5: Synthetic conditions: i) H_2SO_4, acetic anhydride. ii) ***p***-toluidine, H_2O, 90 %. iii) PCl_5, toluene, 70 %.

IR-υCO-bands (KBr) of **4** were observed at 2032 and at 1939 cm^{-1}. Compared to carbyxylic acid **2** (2032 and 1916 cm^{-1}), the asymmetric band is shifted towards higher frequencies, indicating even stronger electron acceptance of the sulfonic acid, compared to the carboxylic acid.

5 crystallized as light yellow plates in the triclinic crystal system P-1. The Cp^--ligand is η^5-coordinated to the central rhenium(I) tricarbonyl-core and the geometry around the metal is distorted octahedral. No unusual inter- or intramolecular contacts are observed. The overall geometry corresponds to a typical piano-stool complex.[75] The M-C (CO) and C-O bonds lengths are in the expected ranges of 1.91-2.15 and 1.10-1.15 Å for metal carbonyl groups.[75-79] Analyzing the individual M-C bond lengths to the Cp ligand reveals a small variation, from 2.261(2) to 2.324(3) Å. The longer M-C bonds are the ones opposite to the derivatized Cp-carbon, which forms the shortest bond. The bond length between C4 and S1 is 1.723(3) Å. The angle between C4-S1-Cl1 is 102.18(10)° referring to a distorted tetrahedral arrangement of the substituents around the sulfur atom. An Ortep-plot with important bond lengths and angles is given in figure 6.

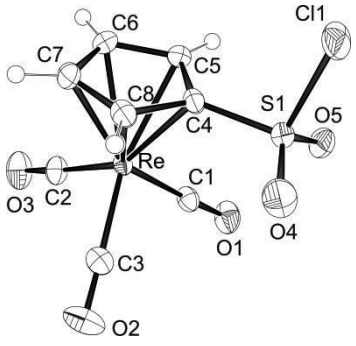

Figure 6: ORTEP representation of ***5***. Relevant bond lengths (Å) and angles (°): Re(1)-C(1) 1.911(3), Re(1)-C(2) 1.919(3), Re(1)-C(3) 1.919(3), Re(1)-C(4) 2.261(2), Re(1)-C(5) 2.306(2), Re(1)-C(6) 2.324(3), Re(1)-C(7) 2.323(3), Re(1)-C(8) 2.296(3), C(1)-O(1) 1.152(4), C(2)-O(2) 1.148(4), C(3)-O(3) 1.154(4), C(4)-S(1) 1.723(3), S(1)-O(4) 1.420(3), S(1)-O(5) 1.417(3), S(1)-Cl(1) 2.040(3), C(4)-S(1)-Cl(1) 102.18(10).

As a model for compound internal sulfonamides of the type [($CpSO_2NHR$)$Re(CO)_3$], compound **6** was prepared according to a literature procedure by refluxing a solution of **5** with ***p***-toluidine (Scheme 6).[71] Silica gel column chromatography afforded **6** in moderate yields. Using ethylene diamine and applying the same synthetic conditions did not form the desired compound (Scheme 6). Crystallization upon slow evaporation of the solvent, only revealed the hydrolysis product **4** (Figure 7). Unlike at room temperature, **5** is prone to hydrolysis at increased temperatures. However, the synthesis of the model compound was not optimized.

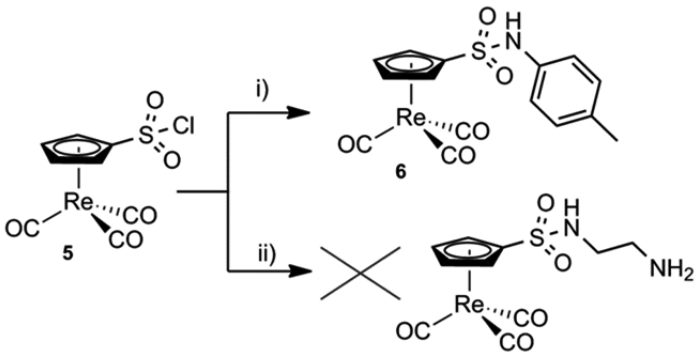

Scheme 6: Synthetic conditions: i) ***p***-toluidine, reflux, EtOH, 49 %. ii) ethylene diamine, reflux, EtOH.

An ORTEP presentation of the crystal structure of **4** is depicted in figure 7. The compound crystallized as a colourless block in the monoclinic crystal system P21/c as its ethylene diammonium salt, half of which belongs to the asymmetric unit. Cp-$(SO_3)^{2-}$ is η^5-coordinated to the ***fac***-{$Re^{I}(CO)_3$}-core and the geometry around the rhenium is distorted octahedral, showing a piano stool complex. The bond length C4-S1 is 1.774(5) Å and therefore very similar to **5**. The angles between C4-S1-O4 to -O6 are 105.1-105.6°, showing a distorted tetrahedral geometry around the sulfur. Comparable to **5**, a small variation from 2.279(4) to 2.319(5) Å is observed in the length of the individual M-C bonds to the Cp ligand. The longer bonds are the ones opposite to the derivatized Cp-carbon, which forms the shortest bond.

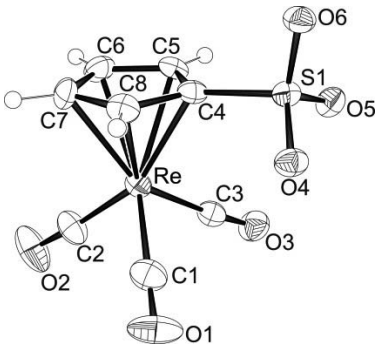

Figure 7: ORTEP representation of **4**. Relevant bond lengths (Å) and angles (°): Re(1)-C(1) 1.937(5), Re(1)-C(2) 1.934(7), Re(1)-C(3) 1.937(7), Re(1)-C(4) 2.279(4), Re(1)-C(5) 2.299(4), Re(1)-C(6) 2.319(5), Re(1)-C(7) 2.314(5), Re(1)-C(8) 2.298(5), C(1)-O(1) 1.131(7), C(2)-O(2) 1.137(10), C(3)-O(3) 1.144(8), C(4)-S(1) 1.774(5), S(1)-O(4) 1.462(3), S(1)-O(5) 1.458(4), S(1)-O(6) 1.445(4), C(3)-Re(1)-C(2) 90.5(3), C(3)- Re(1)-C(1) 89.7(2), C(2)- Re(1)-C(1) 90.9(2), O(6)- S(1)-O(5) 113.3(2), O(6)- S(1)-O(4) 112.9(2), O(6)- S(1)-O(4).

The Ligands

In order to introduce a variety of substituents or targeting vectors and to prepare the ^{99m}Tc imaging agents thereof, cyclopentadienyl sulfonic acid (HCp-SO_3H) is desired, which has been described in literature.[80] However, all attempts to reproduce the synthesis starting from the cyclopentadienyl monomer and refluxing with pyridine-SO_3-complex or with DMF-SO_3-complex respectively, failed. Therefore, alkyl-sulfone **8** was synthesized as an alternative model compound, in order to investigate the complexation behaviour of HCp-sulfones with *fac*-{^{99m}Tc(CO)$_3$}. **8** was described in literature and was prepared in a two-step synthesis.[68] The cycloalkylation of bis-phenylsulfonyl-methane with cis-1,4-dichloro-2-butene proceeded very slow but neat under basic conditions and at room temperature to form the di-substituted cyclopentene **7**. 1'2'-elimination of one phenylsulfinate upon treatment with KtBuO afforded HCp-SO_2Ph, which dimerized quickly to from compound **8** (Scheme 7).

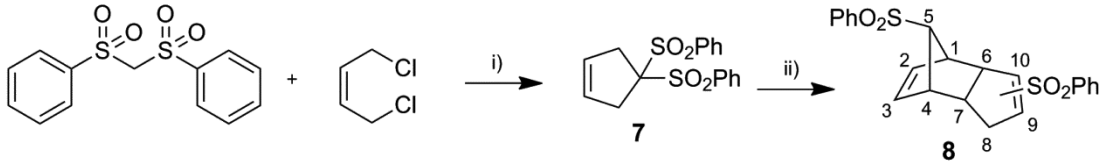

Scheme 7: Synthetic conditions: i) NaOH, catalytic amount of TBAF, Toluene, 90 %. ii) KtBuO, THF, 70 %.

The ^{1}H-NMR of **8** shows three protons in the olefinic range, whereas the signal for one proton on the bridged carbon is missing, in comparison to the Thiele's Acid isomer described above. This indicates therefore, that **8** is predominantly formed in the 5'9' or in the 5'10' substituted isoform as drawn in scheme 7.

The Technetium Complexes

In order to show that sulfones, besides carboxylic acids and their amides, can initiate a metal mediated *retro* Diels-Alder reaction, the usual labeling conditions for HCp-derivatives were applied to dimer **8**. Unfortunately no product formation was observed under these standard conditions, consisting of a self-made Isolink kit, a millimolar concentration of the HCp-ligand and heating of the basic aqueous solution at temperatures from 90 to 95 °C. The reason for the lack of product formation was not further investigated. However, whereas Thiele's Acid is usually isomerically purified, to obtain the 3'9'-substituted isoform, **8** is in the 5'9' or in the 5'10' substituted dimer present. Calculating the closest O-O distance of the two sulfone groups of **8**, a value of 4.734 to 5.797 Å was determined, depending on the isoform.[81] This distance is in the same range as measured for the methyl ester of Thiele's Acid, which revealed a value of 4.974 Å.[63] Therefore, the lack of product formation is not likely to be a consequence of an unsuitable distance of the donor atoms in the chelating group. However, 5' substituents do not contain a conjugated double bond with respect to the substituent. Therefore, the aforementioned mechanism (Scheme 4) is probably not adaptive to compound **8**.

Using the same quantities in a microwave synthesis at 130 °C, after 10 minutes one major new product was observed with 44 % yield (Scheme 8). 37 % of the activity was still unreacted $[^{99m}Tc(OH_2)_3(CO)_3]^+$, 2 % was identified as $[^{99m}TcO_4]^-$, and 17 % of unknown side products were formed. However, until today the corresponding rhenium reference compound has not been synthesized. Therefore, the structure of the observed major HPLC-peak still needs to be confirmed with the corresponding Re-compound.

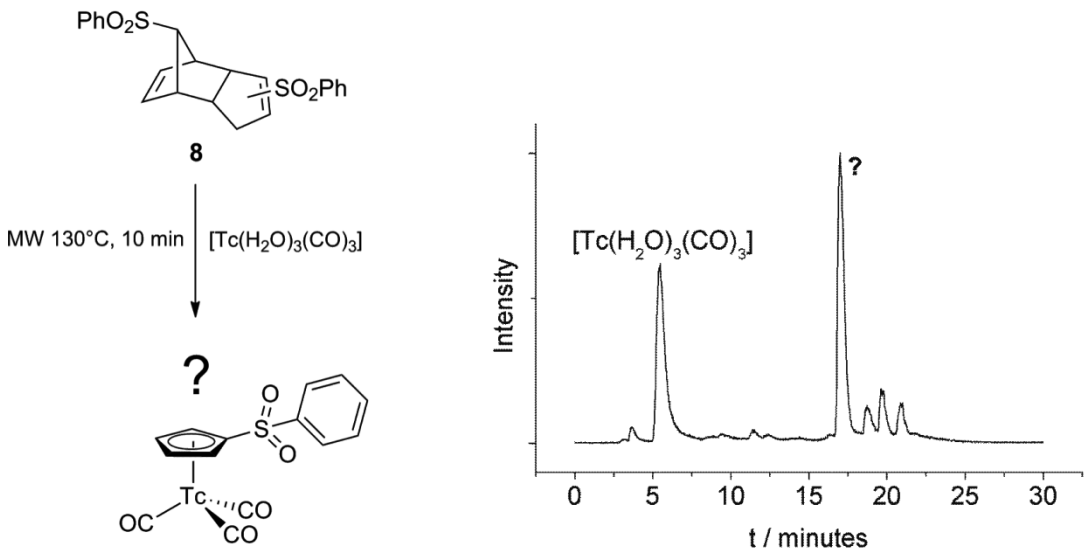

Scheme 8: Microwave assisted metal mediated retro Diels-Alder reaction of HCp-dimer sulfones.

In summary, the sulfonic acid of the [CpRe(CO)$_3$]-complex and some limited derivatives are available according to literature procedures. The obtained complexes are not sensitive to aqueous treatment and are acid/base resistant. However, even though the sulfonyl chloride is stable in aqueous solutions at low temperatures, it is prone to hydrolysis at increased temperatures.

The protonated uncoordinated HCp-sulfonic acid, which was described in literature,[80] was not accessible. Therefore, the corresponding ^{99m}Tc complexes were also not synthesized in the course of this thesis.

The sulfone-dimer **8** was prepared and its labeling behaviour with ^{99m}Tc was studied. Product formation was only observed in a microwave synthesis at 130 °C. However, the authenticity of the product must still be confirmed by comparison with the corresponding rhenium complex. As the temperature during the microwave synthesis was higher than the usually applied 90-95 °C, thermal cleavage of **8** instead of the metal mediated reaction can not be excluded and needs further investigation.

2.2.3 Cp-NO$_2$

One of the most electron withdrawing functional groups known in organic molecules is the nitro group.[82] Therefore, a tremendous impact on the pK_a value of neighbouring protons can be expected, which makes this functionality interesting for ^{99m}Tc-synthesis. Moreover, comparable to the enolate form of a ketone or to a carboxylic acid, the nitro group has a formal negative charge at one of the oxygen

atoms (Figure 8). Therefore, this group could serve as an initial anchor, which preliminary coordinates to the $[^{99m}Tc(OH_2)_3(CO)_3]^+$-precursor and initiates the formation of the η^5-coordinated compound under similar conditions used for other Cp-compounds.

However, unlike ketones, carboxylic acids or sulfonic acids, the nitro group does not offer the possibility of derivatization.

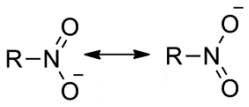

Figure 8: Resonance form of the nitro group.

Cp-NO_2 has been known since the early 1900 in the form of its ring deprotonated sodium salt.[73] The pK_a of the nitro derivative of HCp has been kinetically determined to be 3.25, which is a remarkable low value for a carbon acid.[62] The corresponding ^{99m}Tc-compound is still unknown.

The Ligand

As mentioned, Cp-NO_2 is known in the form of its ring deprotonated sodium salt.[65, 73] The compound was synthesized following the published procedures. **10** was isolated from a reaction mixture of isopropyl nitrate and *in situ* generated NaCp (Scheme 9). The ^{1}H-NMR of the orange solid was identical with the literature description.

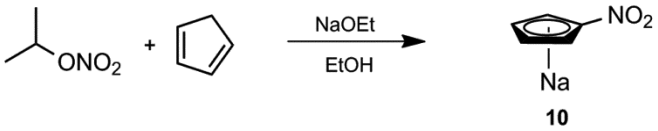

10

Scheme 9: Synthesis of **10**. Nitro-Cp has been known since the beginning of the 20th century.

Another approach for the preparation of **10** was assessed by using a similar setup as described for the synthesis of **8**. Phenylsulfonyl-nitromethane is commercially available. Cycloalkylation with cis-1,4-dichloro-2-butene formed the heterogeneously di-substituted cyclopentene ring **9**, analogously to the preparation of **7**. Crystals were grown by slow diffusion of hexane into a solution of **9** in a minimum of CH_2Cl_2 (Figure 9) and the molecule was characterized by ESI-MS, ^{1}H-NMR and elemental analysis.

The ^{1}H-NMR in $CDCl_3$ is very similar to **7.** But the signals for the olefinic and for the aliphatic protons of **9** sifted towards lower field (by 0.2 and 0.04 ppm respectively), due to the more electron withdrawing nitro group.

9 crystallized as a colourless plate in the monoclinic crystal system with space group P21/n. Two molecules are found in the asymmetric unit, upon only one is discussed, due to crystallographic identity. The bond between C3 and C4 is 1.309(3) Å, which is in the range of a common C=C double bond, in contrast to the C-C single bonds between the other carbons in the five-membered ring (1.492(3) to 1.541(2) Å).[79] Other bond lengths and angles are given along with an ORTEP-plot in figure 9.

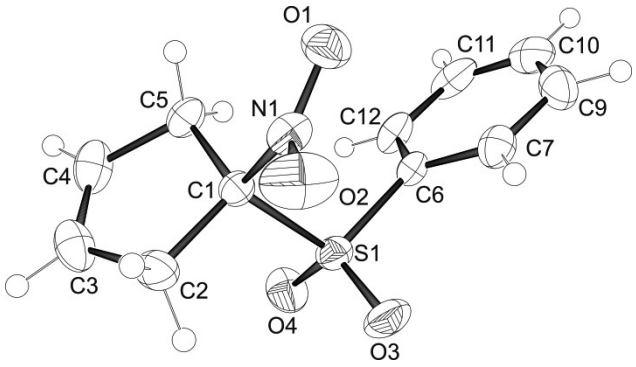

Figure 9: ORTEP representation of **9** (two molecules were present in the asymmetric unit, upon only one is shown here, due to crystallographic identity). Relevant bond lengths (Å) and angles (°): C(1)-N(1) 1.512(2), C(1)-S(1) 1.8453(16), C(3)-C(4) 1.309(3), C(2)-C(3) 1.492(3), C(4)-C(5) 1.496(3), C(1)-C(5) 1.535(2), C(1)-C(2) 1.541(2), N(1)-O(2) 1.2145(19), N(1)-O(1) 1.2259(19), O(3)-S(1) 1.4370(13), O(4)-S(1) 1.4295(13), O(2)-N(1)-O(1) 123.56(16), O(4)-S(1)-O(3) 120.04(9), N(1)-C(1)-C(5) 112.31(14), N(1)-C(1)-C(2) 112.28(14), N(1)-C(1)-S(1) 105.09(10).

Upon elimination the nitro group proved to be a better leaving group than the phenylsulfinate and the isolated product corresponded to **8** (Scheme 10). **10** was therefore not obtained with this method.

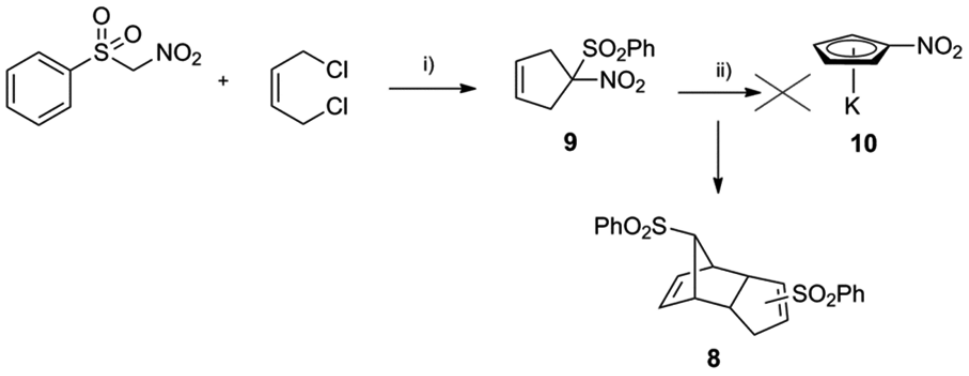

Scheme 10: Synthetic conditions: i) NaH, DMF, 80 %. ii) KtBuO, THF, 65 %.

The Technetium Complex

Sodium complex **10** was added to a saline solution of [^{99m}Tc(OH$_2$)$_3$(CO)$_3$] at a physiological pH value. Heating at temperatures of 90-95 °C did not lead to the formation of the desired product and only starting compounds were recovered. Variations in the pH (3-7) did not improve the result. The lack of product formation was not further investigated.

With a pK_a of 3.25,[62] under labeling conditions at a physiological pH of about 7.4 nitro-Cp is present in its deprotonated form to a large extend. Additionally, as known from its resonance structures, similar to carbonyl derivatized HCp-compounds it offers the possibility of an anchoring group, which can be useful for the formation of the {^{99m}Tc(CO)$_3$}-complex. The sodium salt **10** was prepared along literature procedure and is readily soluble and stable in water.[65, 73] Nonetheless, the transmetallation reaction of **10** to the ^{99m}Tc-core was not observed.

The alternative synthesis of **10** via preparation of the heterogeneously di-substituted cyclopentene ring **9** followed by elimination of phenylsulfinate failed, as the nitro group proved to be a better leaving group. The corresponding Re-complex was not prepared.

2.2.4 Cp-NH$_2$

In contrast to the functional groups discussed before, the amino group has electron donating properties. For this reason, HCp-amino-compounds might not have suitable pk_a values for organometallic synthesis as discussed before. However, many pharmacological active compounds and natural substances are aniline derivatives and contain the amino group in the form of amides or as internal sulfonamides, coupled to sulfones. Replacement of such anilines by the organometallic congener [(CpNH$_2$)M(CO)$_3$] (M = Re or ^{99m}Tc) would therefore increase the field of application and the possibilities for these compounds in therapy and in diagnostics tremendously.

Coupling of a hypothetic HCp-NH$_2$ to carboxylic acids has the advantage of a carbonyl group in close proximity to the HCp-ring. As shown with ketones and carboxylic acids, the carbonyl group in α-position to the HCp can serve as an anchoring group, binding to [^{99m}Tc(OH$_2$)$_3$(CO)$_3$]$^+$ as an initial step for the *retro* Diels-

Alder reaction and the formation of η^5-coordinated Cp^--complexes. Using HCp-NH_2 as a building block, the carbonyl group would be in the β-position, which might still be close enough, to fulfil the task as an anchoring group.

The Rhenium Complexes

The rhenium complex [$(CpNH_2)Re(CO)_3$] has been described in literature.[69] Activation of [$(Cp)Re(CO)_3$] with nBuLi, followed by nucleophilic attack of ***p***-toluene sulfonyl azide, and reduction with $NaBH_4$, formed the desired compound (Scheme 11). **11** is stable under ambient conditions and in water.

IR-measurement (KBr) revealed the υCO-bands of the amine **11** at 1995 and 1874 cm^{-1}, compared to 2018 and 1897 cm-1 for unsubstituted [$(Cp)Re(CO)_3$]. The shift towards lower frequencies indicates higher electron density on the metal center and a longer C-O bonding distance of the carbonyl ligands. This is in accordance with the assumption of electron donating properties of the NH_2-group.

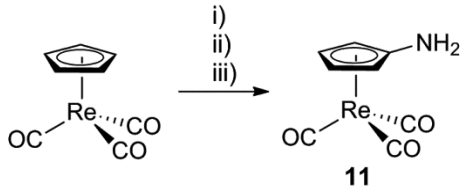

11

Scheme 11: Synthetic conditions: i) nBuLi, THF, -78 °C. ii) $ToSN_3$, THF. iii) NaBH4, EtOH, 69 %

Compounds **12** and **13** were synthesized as model compounds, to explore the synthesis and the physical properties of complexes containing an internal sulfonamide function (Scheme 12). Inverting the sulfonamide moiety, **12** corresponds to the model compound **6**. Analogous structural variations for biologically active derivatives could give interesting information about binding modes, when the biological data are compared.

12 and **13** both were synthesized by stirring a solution of **11** and the appropriate sulfonyl chloride. Unlike **12**, **13** required refluxing temperature.

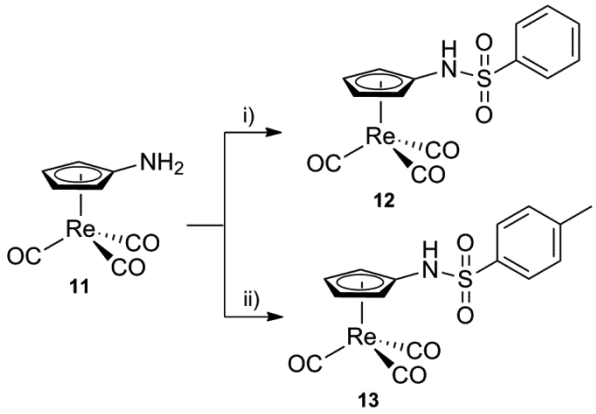

Scheme 12: Synthetic conditions: i) benzenesulfonyl chloride, CH_2Cl_2, RT, 95 %. ii) *p*-Toluenesulfonyl chloride, CH_2Cl_2, reflux, 95 %.

The ^{1}H-NMR-spectrum of **12** and **13** ($CDCl_3$) clearly indicated the presence of the internal sulfonamide bond adjacent to the Cp^- with two sets of ***pseudo*** triplets at 5.23 and at 5.03 ppm for **12** and at 5.32 and at 5.11 ppm for **13** respectively, in comparison to the starting compound **11** (4.53 and 4.28 ppm). The shifts of the characteristic Cp^--protons towards lower field show, that the introduction of the SO_2-Ar-substituent has an impact on the Cp^--ring, as it decreases electron density.

The Ligands

Unlike the rhenium complex, the corresponding free $HCpNH_2$-ligand has not been prepared before. It is arguable, if such a compound could exist, considering the possibility of the formation of the imine-form of the compound (Figure 10). It is also not known, how stable the monomer would be and how fast polymerization would occur.

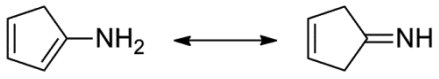

Figure 10: $HCp\text{-}NH_2$ can form the corresponding imine.

Therefore the amine in the form $HCp\text{-}NH_2$ was not synthesized in during this thesis, even though this would be the most comfortable form for derivatization with targeting vectors or others. Synthetic access to *in situ* derivatized amines in their dimeric form was aimed in order to prevent side reactions. With this strategy, the uncontrolled formation of a diversity of polymers is excluded. Moreover, introducing

electron withdrawing derivatives at the amine could prevent the molecule from forming the imine.

Starting from the defined structure of Thiele's Acid, the target compound was synthesized by Curtius Rearrangement. The Curtius Rearrangement is the thermal decomposition of carboxylic azides to form isocyanates. These intermediates can be treated with a nucleophile, like alcohols or amines, to form the corresponding urea or, if hydrolysed with water, the corresponding carbamic acids (Scheme 13).[83]

The Curtius Rearrangement is nowadays widely used and investigated.[84-88]

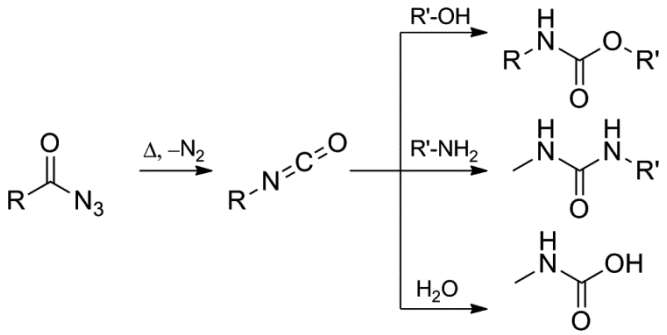

Scheme 13: Schematic overview of the Curtius Rearrangement.

Using diphenylphosphoryl azide, Thiele's Acid was converted to the corresponding acid azide **14**, which was isolated, purified by silica gel column chromatography and analysed by ESI-MS, ^{1}H-NMR and IR. Upon heating, the rearrangement occurred and the isonitrile **15** was formed. **15** was not isolated, due to decomposition of the compound, but the isonitrile group was identified by liquid IR-measurement. Addition of the nucleophiles **a** to **f**, *in situ* generated the final products (Scheme 14). Compounds **16a**-**b** were characterized by ESI-MS, IR and ^{1}H-NMR analysis. However, no evidence for the formation of **16c**-**f** was found, as characterization was not conclusive.

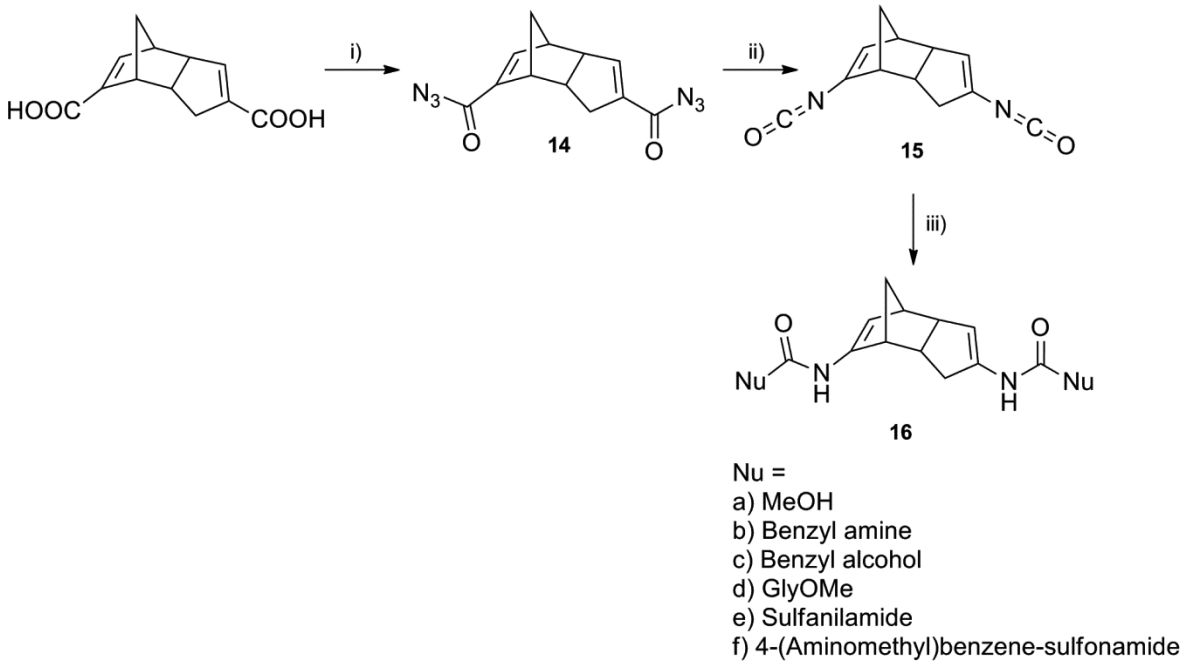

Scheme 14: Synthetic conditions: i) Diphenylphosphoryl azide (DPPA), NEt_3, toluene 80 %. ii) Heated to 80 °C, toluene. iii) addition of the nucleophiles **a-f**, toluene.

The progress of the reaction was followed by time resolved IR-measurement and by ^{1}H-NMR (Figure 11-13). Therefore, **14** was dissolved in toluene for the IR-experiment or in deuterated toluene-d^8 for the ^{1}H-NMR-experiment respectively. The measurement was started, when the reaction temperature of 80 °C was reached. IR-spectra were recorded every 2 minutes and ^{1}H-NMR were measured every 10 minutes during the reaction process and directly from the reaction mixture. ^{1}H-NMR measurement is more sensitive compared to IR-measurement. Therefore, reaction times in the two experiments can differ.

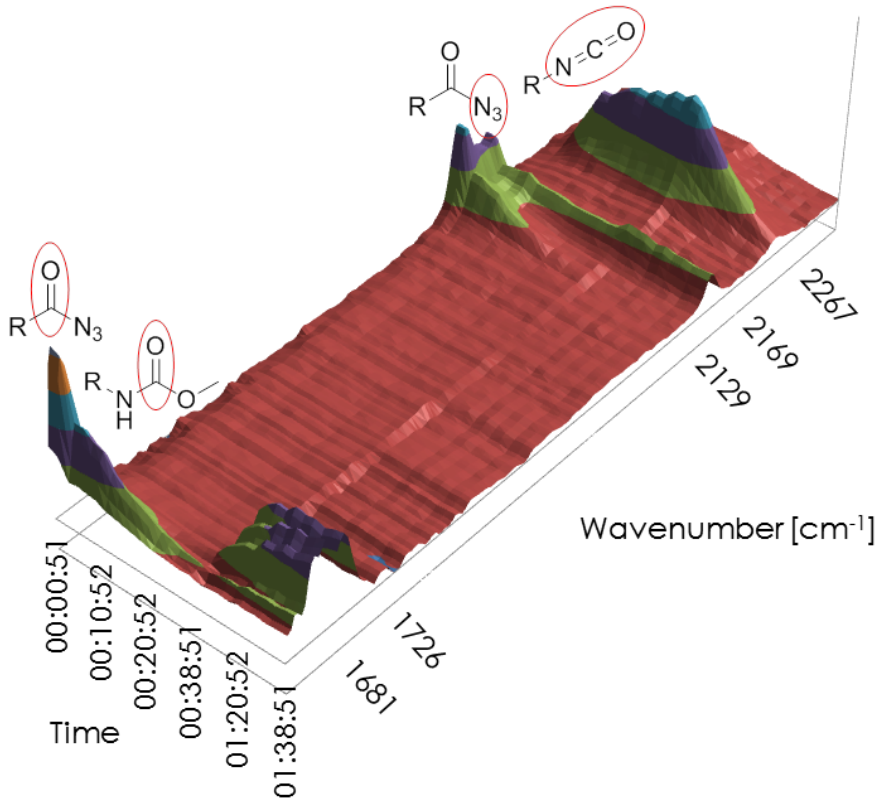

Figure 11: Time resolved IR-measurement of the curtius rearrangement of **14** to **15** and the following nucleophilic addition of MeOH to form **16a**.

Time resolved IR clearly showed the disappearance of the CO and the N_3 IR-bands of the acid azide at 1681 cm^{-1} and at 2130 cm^{-1} respectively. At the same time, a new band was growing in intensity at 2267 cm^{-1}, indicating the formation of the isonitrile. Nearly full conversion was reached after 20 minutes. 25 minutes after the beginning of the measurement methanol was added, whereupon the isonitrile band decreased rapidly and a new, broad signal in the range of 1726 appeared. This was interpreted as the stretching frequency of the urea-carbonyl, which was formed (Figure 11 and 12).

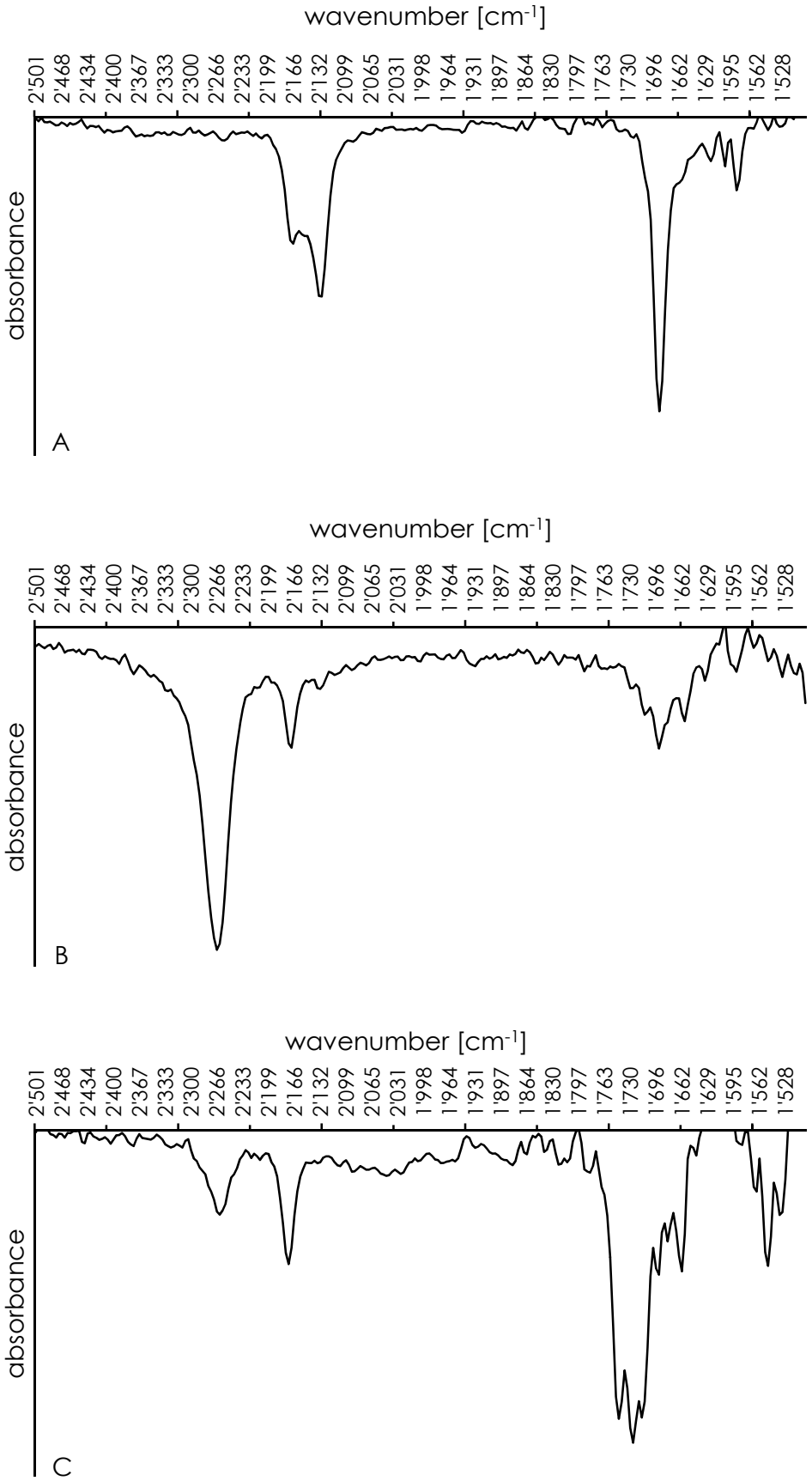

Figure 12: IR spectrum of **14** (A), **15** (B) and **16a** (C) in toluene.

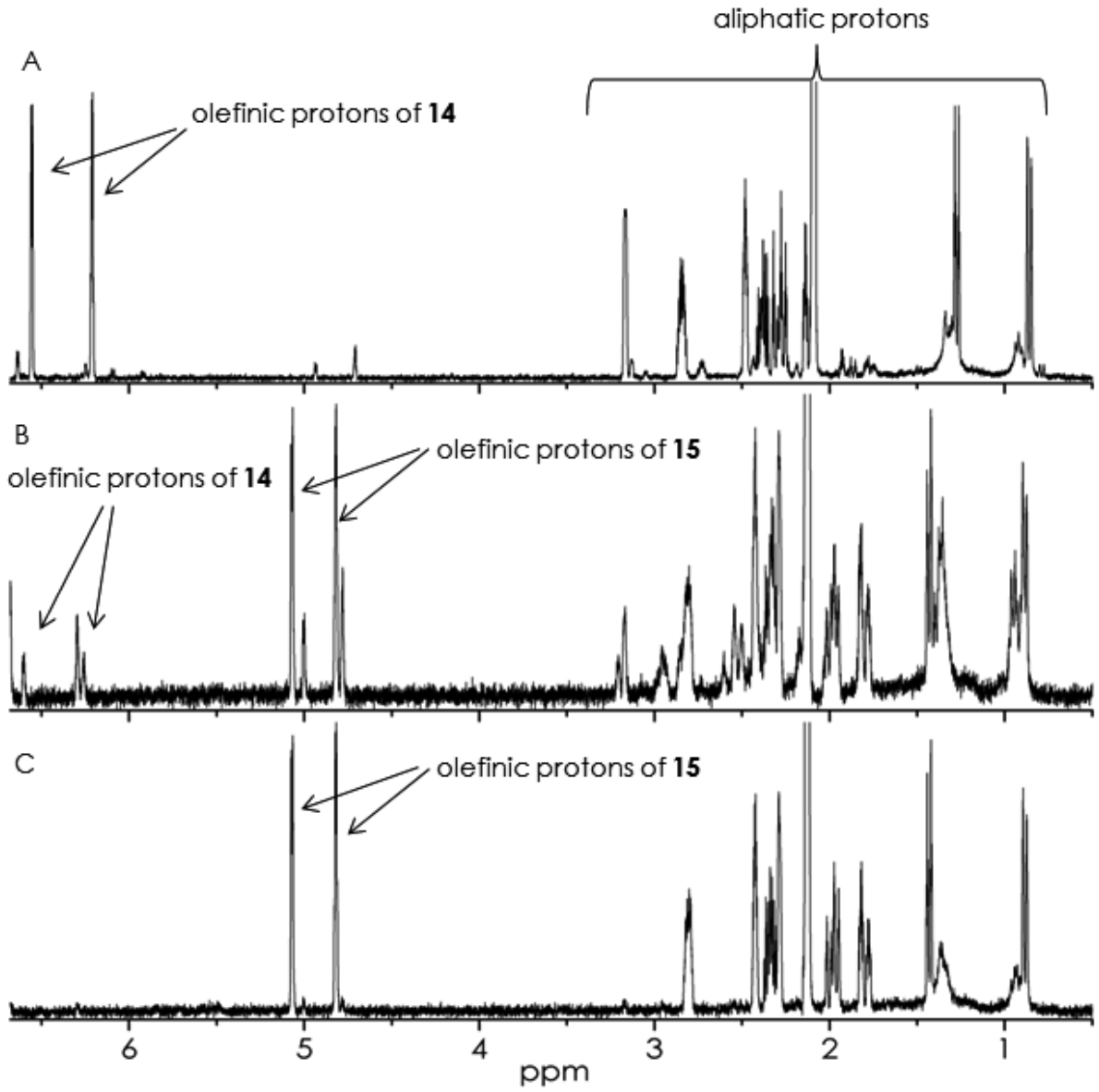

Figure 13: ^{1}H-NMR-spectra (toluene-d^{8}): A) no isonitrile formed yet, t=0 minutes B) partially formed isonitrile, t=33minutes C)full conversion of **14** to **15** after 41 minutes

A similar behaviour was observed, when the reaction was recorded in the ^{1}H-NMR. The process can be followed by looking at the chemical shifts of the olefinic protons, which are in close proximity to the reaction centers (Figure 13). The signals for **14** disappeared completely after roughly 40 minutes (higher sensitivity compared to the IR-measurement) and the formation of two new signals in the olefinic region indicated the formation of the isonitrile **15**. Upon addition of MeOH, these peaks decrease again and the formation of two new peaks shows the formation of **16** (Figure 14).

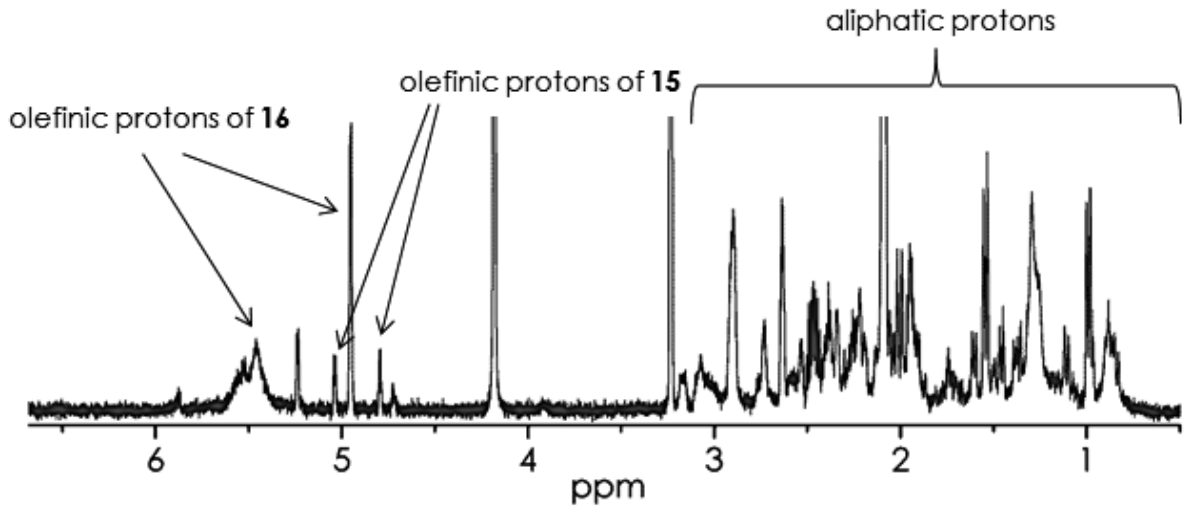

Figure 14: ^{1}H-NMR-spectra (toluene-d^{8}): The signals for **15** disappear upon MeOH addition and two new signals for **16** are rising in the olefinic region.

The aniline analogue **11** was prepared according to literature.[69] The complex is stable under ambient or aqueous conditions and is also not prone to decomposition at increased temperatures or under acidic and basic treatment. Synthetically, it can be treated like aniline and nucleophilic coupling reactions are suitable methods for derivatization.

In situ derivatized HCp-amines in their dimeric form were prepared from Thiele's Acid applying the Curtius Rearrangement. The reaction progress was investigated by time resolved IR-measurement and by ^{1}H-NMR. Using diphenylphosphoryl azide, Thiele's Acid was converted to the corresponding acid azide **14**, which is stable under ambient conditions. Stability towards aqueous solutions was not assessed. Upon heating, the rearrangement occurred and the isonitrile **15** was formed. **15** was not isolated, due to decomposition of the compound, but the isonitrile group was identified by liquid IR-measurement. Addition of nucleophiles like alcohols or amines, *in situ* generated the compounds **16a-b.** No evidence for the formation of **16c-f** was found, as characterization was not conclusive. The 99mTc-labeling behaviour of **16a-b** is subject of on-going investigations.

2.2.5 Cp-CH_2COOH & Cp-CH_2CH_2COOH

Similar to amines, alkyl substituents on the HCp-ring are electron donating derivatives. Due to hyper conjugation, electron density can be transferred from σ-orbitals of the alkyl substituent into free or partially filled antibonding π-orbitals of the conjugated double bond of the HCp. Coupled to a carboxylic acid function, such Cp-compounds are interesting for organometallic syntheses. The possibility of an anchoring group for the preparation of η^5-coordinated Cp^--complexes of the *fac*-{$^{99m}Tc(CO)_3$}-core is retained. Using HCp-$(CH_2)_n$-COOH with n = 1 or 2 as a building block, the carbonyl group is in β- or in γ-position to the HCp-ring. This might still be close enough, to serve as an anchoring group for complexation, in terms of bringing the HCp-moiety in close proximity to the metal. Similar to Thiele's Acid, such compounds could be easily and versatile derivatized with bioactive components.
From a biological point of view, with methylene groups between the HCp and the carboxylic acid, a new way of altering the spacer in a BFC is introduced; before *and* after the coupling function. This way of variation represents a new factor for interesting structure activity relationships (SARs).
In general, the scaffold Ar-$(CH_2)_n$-CONHR is very common in biological systems and in pharmaceuticals. Organometallic analogues of this moiety represent therefore potential building blocks in the development of new pharmaceuticals or imaging agents.

The Ligands

The uncoordinated HCp-compounds **17** and **19** have both been prepared before.[66, 89] Using bromoacetic acid methylester or methyl-3-brompropionate respectively, the two compounds were synthesized along a similar route (Scheme 15). Both ligands were obtained as the methyl esters after distillation under reduced pressure. The compounds were characterized by NMR and were identified as an isomeric mixture. **17** and **18** were not observed in the ESI-MS measurement, alluding to insufficient ionizing properties of the compounds. Hydrolysis was performed with a solution of LiOH in a solvent mixture of MeOH, THF and H_2O to form the carboxylic acids **18** and **20**.

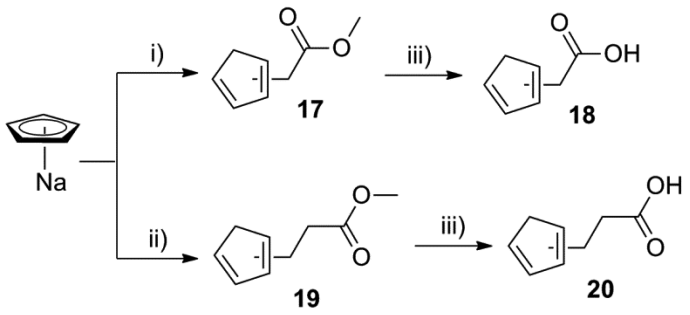

Scheme 15: Synthetic conditions: i) bromoacetic acid, THF, 30-50 %. ii) methyl-3-brompropionate, THF, 30-50 %. iii) LiOH, THF/MeOH/H_2O 69-74 %.

18 was coupled to a benzyl amine or to glycine methyl ester respectively, to form amides **21a**-**b** as model compounds for derivatized HCp-CH_2CONHR-type of ligands. Therefore, **18** was activated with O-(7-Azabenzotriazol-1-yl)-N,N,N',N'-tetramethyluronium hexafluorophosphate (HATU) in DMF *in situ*, and was then mixed with the appropriate amine (Scheme 16). Products were formed in moderate yields of 20 and 55 % respectively. **21a**-**b** were characterized by ESI-MS and ^{1}H-NMR. **21a** was crystallized from CH_2Cl_2/Hexane and the structure was analysed by x-ray diffraction.

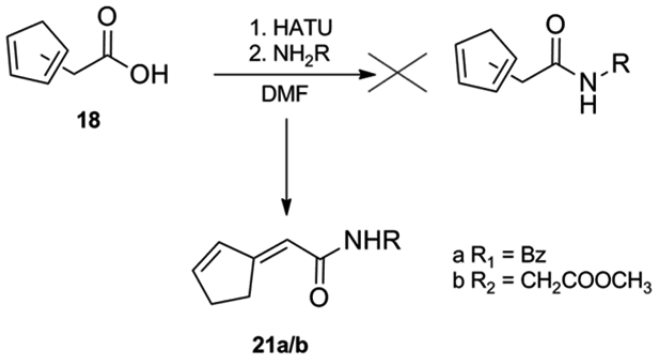

Scheme 16: Synthetic conditions: i) HATU, DMF. ii) NH_2R, DMF, 20-55 %

The ^{1}H-NMR revealed three sets of multiplets in the olefinic region and two sets of multiplets in the aliphatic region. This speaks for the formation of an isomerically pure product, which is not in accordance with the utilization of an isomerically mixed starting compound. Taking the acidity of the α-proton of the methylene group into account, a rearrangement of the cyclopentadiene double bond could be an explanation for this observation. This assumption was confirmed by the crystal structure of **21a** (Figure 15). Two molecules were present in the asymmetric unit, upon only one is discussed here, as they are crystallographically identical. The C1-C2 bond

length in compound **21a** is 1.338(2) Å and is therefore in the range of an usual C=C double bond.[79] All the other bonds in the HCp-ring are within 1.4583(17) and 1.5337(19) Å in lengths and correspond therefore to carbon-carbon single bonds. In agreement with the suggested isomerisation is the bond distance between C5 and C6 with 1.3401(17) Å, revealing a C=C double bond. As compound **21b** shows the same pattern in the ^{1}H-NMR, a similar rearrangement of the structure can be assumed. Due to this isomerisation, amides of the form of HCp-CH_2CONHR were not observed. **21a** crystallized in the triclinic crystal system P-1. Important bond lengths and angles are given in figure 15.

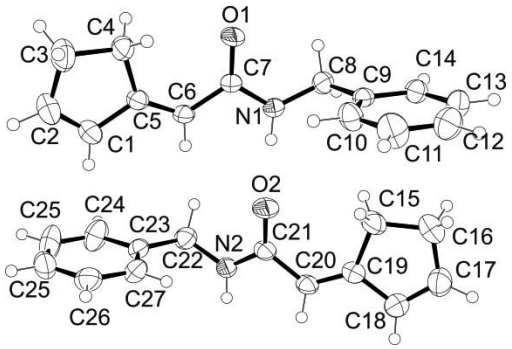

Figure 15: ORTEP representation of **21a**. Relevant bond lengths (Å) and angles (°) (of only one molecule, due to crystallographic identity): C(1)-C(2) 1.338(2), C(1)-C(5) 1.4583(17), C(2)-C(3) 1.485(2), C(3)-C(4) 1.5337(19), C(4)-C(5) 1.5078(17), C(5)-C(6) 1.3401(17), C(6)-C(7) 1.4684(16), C(2)-C(1)-C(5) 110.99(13), C(1)-C(2)-C(3) 112.31(13), C(2)-C(3)-C(4) 104.11(12), C(5)-C(4)-C(3) 105.66(11), C(5)-C(6)-C(7) 123.98(10), O(1)-C(7)-N(1) 121.42(11).

HCp-COOH undergoes rapid Diels-Alder dimerization to form Thiele's Acid. This dimer or amides thereof react via metal mediated *retro* Diels-Alder reaction with $[^{99m}Tc(OH_2)_3(CO)_3]^+$ and can form $[(Cp\text{-}COR)^{99m}Tc(CO)_3]$-type complexes. They are therefore of high value for aqueous organometallic chemistry and for the development of new BFCs. In this context, it woud be utterly interesting, if the dimers of the carboxylic acids **18** and **20** would behave in a similar way, when reacted with $[^{99m}Tc(OH_2)_3(CO)_3]^+$. Containing methylene groups directly attached to the HCp-ring, dimerization of the compounds **18** and **20** does not occur with the same rate as for HCp-COOH. The reaction products, which were formed by keeping the ester **17** without additives at temperatures from 4-25 °C or at -20 °C respectively were analysed (Scheme 17). ^{1}H-NMR revealed that at -20 °C a mixture of the rearrangement product **22** and dimer **23** was formed after roughly two months, whereas at temperatures from 4 to 25 °C, almost exclusively the dimeric form **23** was obtained in a comparable timescale (Figure 16).

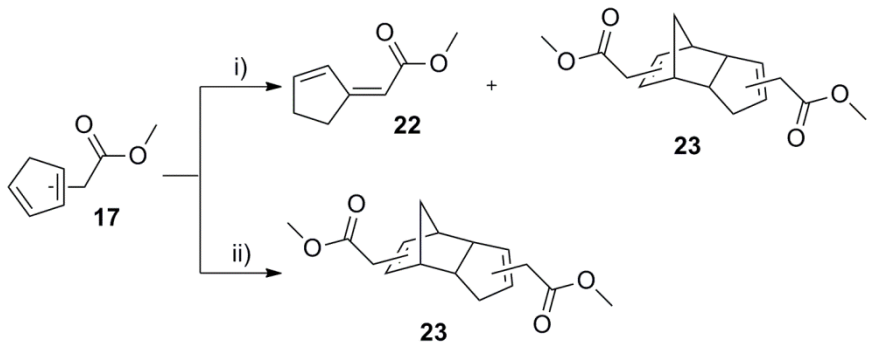

Scheme 17: Synthetic conditions: i) -20 °C. ii) 4-25 °C

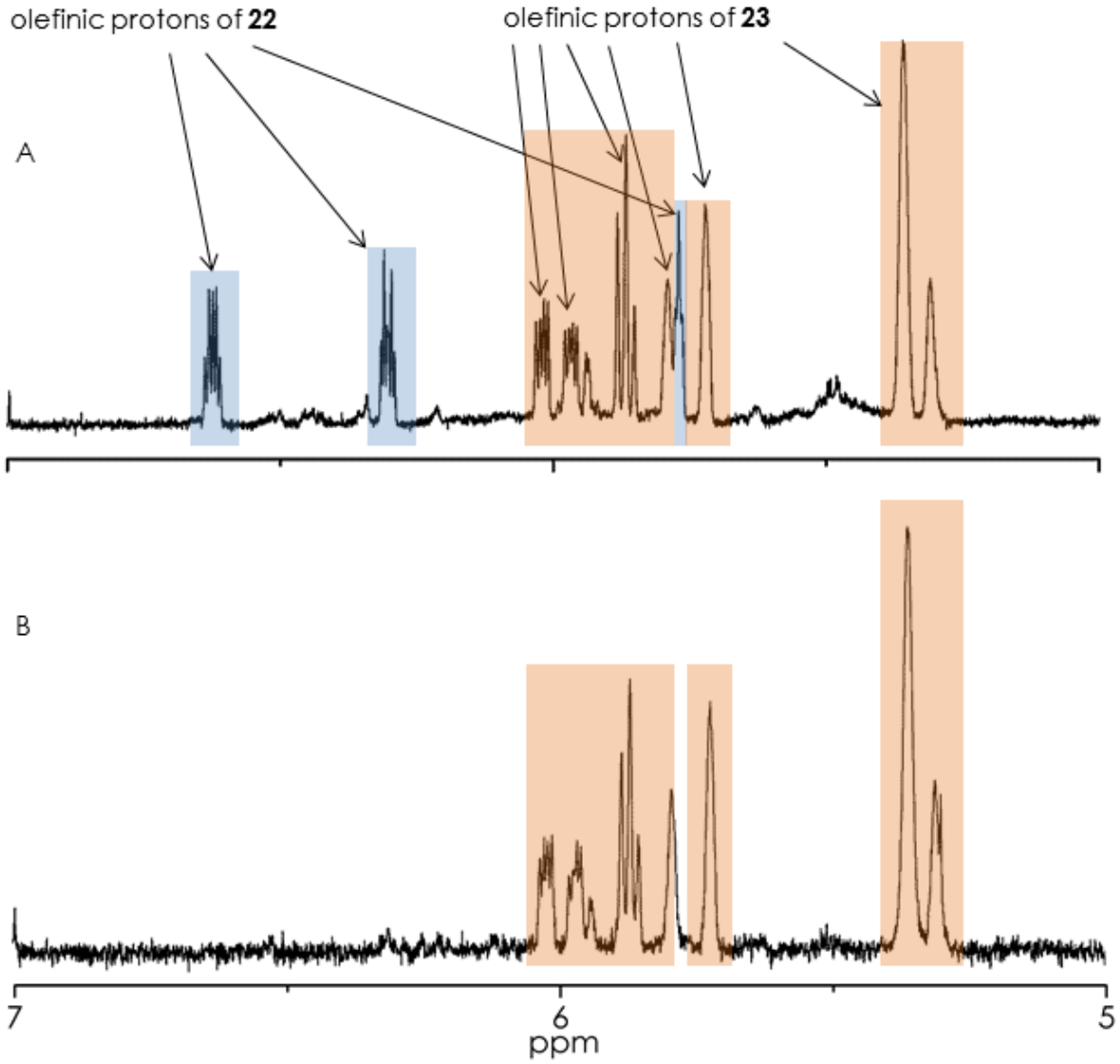

Figure 16: ^{1}H-NMR-spectra ($CDCl_3$). A) **17** stored at -20 °C forms a mixture of rearrangement product **22** and an isomeric mixture of dimer **23**. B) **17** stored at 4-25 °C forms an isomeric mixture of dimer **23** and no **22**.

The Rhenium complexes

Using [(Cp)Re(CO)$_3$], the synthesis of the Re-complex **24a** with bromoacetic acid failed (Scheme 18). The nucleophilic attack by the nBuLi-deprotonated Cp$^-$ occurred unexpectedly at the carbonyl of the ester, instead of the brominated α-carbon. The methoxy group was therefore substituted by [(Cp)Re(CO)$_3$]. Moreover, another nucleophilic attack occurred at the same carbonyl to finally form a binuclear complex. **24b** was purified by silica gel column chromatography, analysed by ^{1}H-NMR and IR and was crystallized from CH_2Cl_2/Hexane (Figure 17).

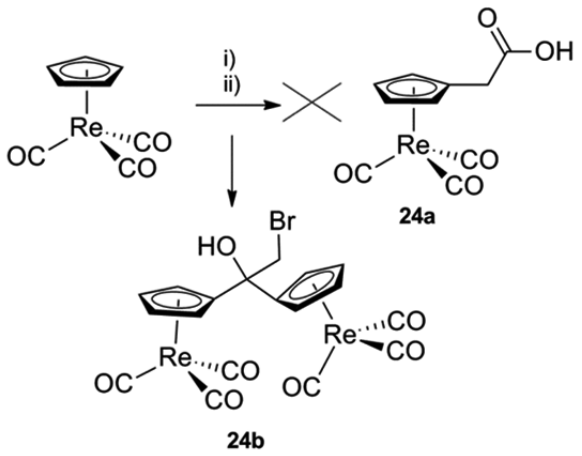

Scheme 18: Synthetic conditions: i) nBuLi, THF, -78 °C. ii) methyl bromoacetate, THF, 50 %

The ^{1}H-NMR ($CDCl_3$) of **24b** shows three sets of Cp-signals, each as a multiplet, at 5.71 ppm, at 5.56 ppm and at 5.30 ppm respectively, corresponding to 8 protons in total. The methylene singlet was observed at 3.72 ppm and the singlet of the hydroxyl proton can be found at 2.41 ppm. Characteristic IR-υCO-bands were observed at 2018 and at 1921 cm^{-1} (KBr). In comparison to unsubstituted [(Cp)Re(CO)$_3$] (2018 and 1897 cm^{-1}), only the frequencies of the asymmetric motion of the carbonyls shifted towards higher frequencies, which is related to the substituents on the α-carbon of **24b**.

The binuclear complex **24b** crystallized in the monoclinic crystal system with space group P21/c as a colourless plate. The central rhenium(I) atoms are η^5-coordinated by the Cp$^-$-ligands. The coordination geometry around the metal centers are distorted octahedrons. The overall geometry corresponds to typical piano-stool complexes.[75] C-O bond lengths of the carbonyl ligands are for both complexes very similar and are within 1.146(5) and 1.152(4) Å.[75-79] They are therefore comparable to those found for compound **4**. Unlike **4** and **5**, the individual M-C bond lengths to the

Cp ligand do not show a significant variation and range from 2.295(3) to 2.314(4) Å. Selected bond lengths and angles are given in figure 17.

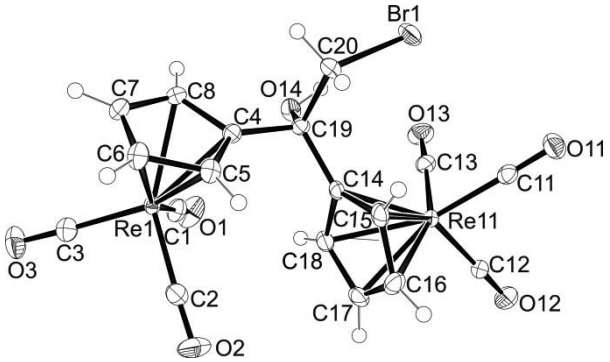

Figure 17: ORTEP representation of **24b**. Relevant bond lengths (Å) and angles (°): Re(1)-C(1) 1.908(4), Re(1)-C(2) 1.914(4), Re(1)-C(3) 1.922(4), Re(1)-C(5) 2.295(3), Re(1)-C(6) 2.299(4), Re(1)-C(7) 2.303(4), Re(1)-C(4) 2.306(3), Re(1)-C(8) 2.314(4), Re(11)-C(11) 1.912(4), Re(11)-C(13) 1.914(4), Re(11)-C(12) 1.924(4), Re(11)-C(18) 2.308(3), Re(11)-C(17) 2.308(4), Re(11)-C(15) 2.313(4), Re(11)-C(14) 2.317(3), Re(11)-C(16) 2.317(4), C(1)-O(1) 1.152(4), C(2)-O(2) 1.147(5), C(3)-O(3) 1.151(4), C(4)-C(5) 1.427(5), C(4)-C(8) 1.446(5), C(4)-C(19) 1.513(5), C(5)-C(6) 1.424(5), C(6)-C(7) 1.408(5), C(7)-C(8) 1.426(5), C(11)-O(11) 1.150(4), C(12)-O(12) 1.151(4), C(13)-O(13) 1.146(5), C(14)-C(15) 1.420(5), C(14)-C(18) 1.438(5), C(14)-C(19) 1.516(5), C(15)-C(16) 1.424(5), C(16)-C(17) 1.435(6), C(17)-C(18) 1.420(5), C(19)-O(14) 1.427(4), C(19)-C(20) 1.537(5), C(20)-Br(1) 1.964(4), C(1)-Re(1)-C(2) 90.29(17), C(1)-Re(1)-C(3) 88.86(16), C(2)-Re(1)-C(3) 91.59(16), C(11)-Re(11)-C(13) 88.57(16), C(11)-Re(11)-C(12) 89.62(15), C(13)-Re(11)-C(12) 86.93(16), O(14)-C(19)-C(4) 105.4(3), O(14)-C(19)-C(14) 111.3(3), C(4)-C(19)-C(14) 109.7(3), O(14)-C(19)-C(20) 111.7(3), C(4)-C(19)-C(20) 103.1(3), C(14)-C(19)-C(20) 114.9(3), C(19)-C(20)-Br(1) 113.3(2).

The desired compound **24a** was synthesized in a rather uncommon way for organometallic complexes. Similar to the ^{99m}Tc-labeling of HCp-compounds, ligand **18** was reacted with $(NEt_4)_2[Re(Br)_3(CO)_3]$ in water, in presence of Borax ($Na_2B_4O_7$*$10H_2O$) at 95 °C. This reaction represents therefore one of the rare examples, of aqueous synthesis of a $[(CpR)Re(CO)_3]$ complex, where the Re-complex is prepared analogously to the ^{99m}Tc-complex (Scheme 19). However, yields were low (20 %), as $[Re(Br)_3(CO)_3]^{2-}$ is known for its cluster formation under basic aqueous conditions.[90]

24a was analysed by IR (KBr), NMR ($CDCl_3$), ESI-MS (CH_3OH) and elemental analysis. Crystals were grown from CH_2Cl_2/Hexane and the structure was elucidated (Figure 18).

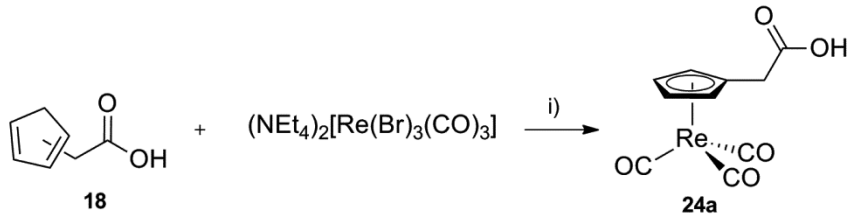

Scheme 19: Synthetic conditions: i) $Na_2B_4O_7*10H_2O$ (Borax), H_2O, 95 °C, 20 %.

Characteristic IR-υCO-bands were observed at 2020 and at 1911 cm^{-1} (KBr). In comparison, carboxylic acid **2** revealed higher frequencies (2032 and 1916 cm^{-1}), which is in accordance with the assumption of the electron donation by the methylene spacer in **24a**. However, comparing **24a** to [(Cp)Re(CO)$_3$] (2018 and 1897 cm^{-1}) the IR-υCO-bands are not shifted towards lower frequencies, but are found higher. The electron acceptance by the carboxylic acid affects therefore the electron density on the metal to a larger extend than the donating nature of the methylene group, despite of the larger distance of the carboxylic acid function.

The compound crystallized as colourless block in the triclinic crystal system P-1. The structure shows a η^5-coordinated Cp^--ligand, bound to the rhenium(I) atom, therefore the geometry around the metal center is distorted octahedral, exhibiting a typical piano-stool complex.[75] The carboxylic acid function is with a torsion angle of 78.9(3)° between C5-C4-C9-C10 close to perpendicular to the plane of the Cp^--ring. In accordance with the lower IR-υCO-frequencies, the C-O bond lengths of the carbonyl ligands of **24a** (1.149(3)-1.152(3) Å) are longer than those found for compound **4** (1.131(7)-1.144(8) Å), but compare well to those of **24b** (1.146(5)-1.152(4) Å). Other important bond lengths and angles are given in figure 18.

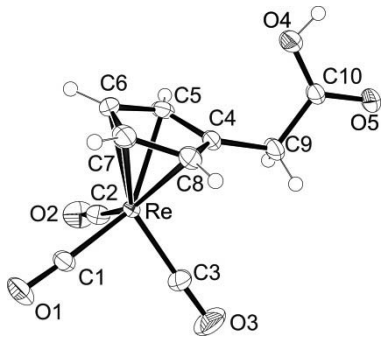

Figure 18: ORTEP representation of **24a**. Relevant bond lengths (Å) and angles (°): Re(1)-C(1) 1.912(2), Re(1)-C(3) 1.913(2), Re(1)-C(2) 1.917(2), Re(1)-C(7) 2.299(2), Re(1)-C(6) 2.3002(19), Re(1)-C(5) 2.301(2), Re(1)-C(4) 2.3053(19), Re(1)-C(8) 2.308(2), C(1)-O(1) 1.152(3), C(2)-O(2) 1.149(3), C(3)-O(3) 1.151(3), C(4)-C(5) 1.419(3), C(4)-C(8) 1.436(3), C(4)-C(9) 1.499(3), C(5)-C(6) 1.423(3), C(6)-C(7) 1.425(3), C(7)-C(8) 1.419(3), C(9)-C(10) 1.508(3), C(10)-O(5) 1.246(3), C(10)-O(4) 1.270(3), C(1)-Re(1)-C(3) 89.86(10), C(1)-

Re(1)-C(2) 88.55(9), C(3)-Re(1)-C(2) 91.13(10), C(4)-C(9)-C(10) 114.63(18), O(5)-C(10)-O(4) 124.0(2), O(5)-C(10)-C(9) 118.6(2), O(4)-C(10)-C(9) 117.28(18).

Surprisingly, carboxylic acid complex **27** was not accessible by the same synthetic pathway using its uncoordinated ligand **20**. However, the corresponding ferrocene-complex has been synthesized by Horner-Wardsworth-Emmons olefination.[91] The same synthetic strategy was applied to $[(Cp)Re(CO)_3]$ and carboxylic acid **27** was obtained. $[(CpCOH)Re(CO)_3]$ was prepared according to literature from $[(Cp)Re(CO)_3]$.[92] Treatment with triethyl phosphonoacetate in methanol gave olefin **25** in 80 % yield. Hydrogenation of the double bond with H_2 on Pd under an atmosphere of H_2, followed by ester hydrolysis with LiOH gave the desired complex **27** (Scheme 20). The compounds were analysed by IR (KBr), NMR ($CDCl_3$), ESI-MS (CH_3OH) and elemental analysis. Crystals were grown from CH_2Cl_2/Hexane and the structure was elucidated (Figure 19).

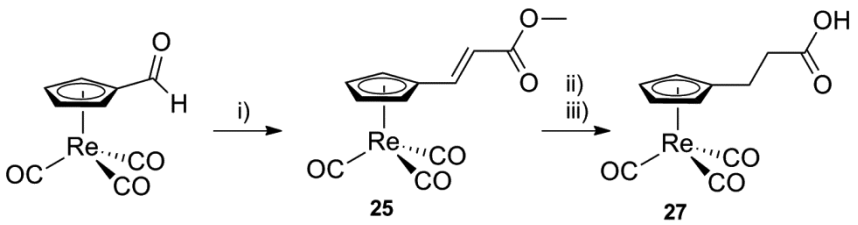

Scheme 20: Synthetic conditions: i) Triethyl phosphonoacetate, MeOH, 80 %. ii) H_2/Pd/C, EtOAc. iii)LiOH, H_2O/MeOH/THF

In the ^{1}H-NMR ($CDCl_3$) the *pseudo* triplets of the aromatic Cp-protons were detected at 5.31 and at 5.26 ppm respectively. In comparison to **24a** (5.46 and 5.31 ppm), these signals are shifted towards higher field, which is in accordance with the increased distance to the deshielding carboxylic acid function. IR-υCO-bands were observed at 2023 and at 1912 cm^{-1}, and are thus about the same as for **24a**.

27 crystallized in the triclinic crystal system P-1 as a colourless block. The bond distances between the first methylene group C9 and the Cp-ring carbon C4 is 1.504(4) Å and the bond length between the methylene carbons C9 and C10 is 1.515(4) Å. The distance from C10 to the carbonyl C11 is slightly shorter with 1.492(4) Å. These values compare well to those found in structure **24a**. Other bonding distances and angles are given in figure 19.

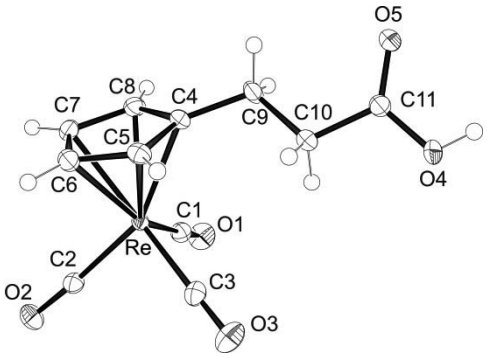

Figure 19: ORTEP representation of **27**. Relevant bond lengths (Å) and angles (°): Re(1)-C(2) 1.910(3), Re(1)-C(3) 1.919(3), Re(1)-C(1) 1.919(3), Re(1)-C(6) 2.287(3), Re(1)-C(5) 2.291(3), Re(1)-C(7) 2.304(3), Re(1)-C(8) 2.311(3), Re(1)-C(4) 2.324(2), C(1)-O(1) 1.154(4), C(2)-O(2) 1.148(4), C(3)-O(3) 1.148(4), C(4)-C(9) 1.504(4), C(9)-C(10) 1.515(4), C(10)-C(11) 1.492(4), C(11)-O(5) 1.224(3), C(11)-O(4) 1.301(3), C(2)-Re(1)-C(3) 1.33(12), C(2)-Re(1)-C(1) 90.10(12), C(3)-Re(1)-C(1) 90.61(12), O(5)-C(11)-O(4) 123.5(3), O(5)-C(11)-C(10) 123.2(3), O(4)-C(11)-C(10) 113.3(2).

The Technetium Complexes

As discussed above, HCp-compounds with a carboxylic acid function can be labelled as monomers or as dimers with ^{99m}Tc. The deprotonated hydroxyl part can serve as a preliminary anchoring group for the metal center.[61] With the ligands **18** and **20** this anchoring group is retained. However, the carbonyl group is in β- or in γ-position relative to the HCp-ring. Therefore their distance to the HCp-chelator is larger than in the compounds discussed above, but might still be close enough, to serve as an anchoring group and to initiate complex formation. Similar to Thiele's Acid, such compounds could be easily and versatile derivatized with bioactive targeting functions. Unfortunately, a rearrangement of the double bonds in the HCp-ring was observed upon amide coupling of compound **18**. Therefore, the desired ^{99m}Tc-complexes with these ligands were not accessible along the classical route.

However, carboxylic acids **18** and **20** were used under the general reaction conditions for the labeling of HCp-derivatives, in order to investigate their complexation properties. Ligands were present in their monomeric form and in millimolar concentrations. The reactions were studied in a one-pot procedure, where the ligand and the self-made Isolink Kit were sealed in a vial and $[^{99m}TcO_4]^-$ was injected, and in a two-step reaction, where $[^{99m}Tc(OH_2)_3(CO)_3]^+$ was synthesized before and added to the ligand in a separate step. Both procedures resulted in the neat formation of the desired ^{99m}Tc-complexes **28** and **29** respectively (Scheme 21 and 22). No substantial side products were observed in all cases. The products were analysed by coinjection with the corresponding Re-complexes. Esters are usually

hydrolysed during the labeling, thus the same results were observed when the methyl esters **17** and **19** were used instead of the acids **18** and **20**.

However, conversion rates of the ^{99m}Tc starting compounds were very different for the ligand **18** compared to **20**. Whereas **18** caused quantitative product formation after 30 minutes (Scheme 21), the reaction with **20** reached only 7 % conversion after the same time and 62 % after 5 hours. Much higher rates were observed, when the labeling with **20** was performed in a microwave reactor. At temperatures of 130 °C, 65 % conversion to **29** was observed after 30 minutes. 16 % of the $[^{99m}Tc(OH_2)_3(CO)_3]^+$ was oxidized to $[^{99m}TcO_4]^-$ and 19 % was still unreacted starting compound (Scheme 22).

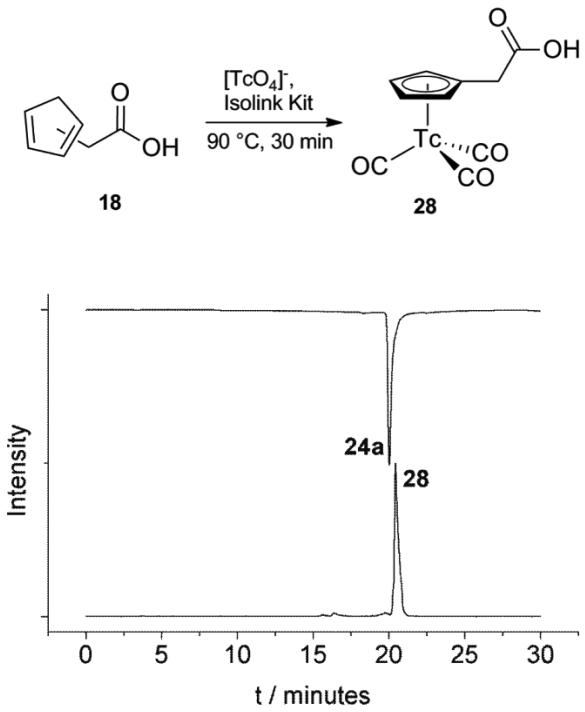

Scheme 21: Bottom-up trace: γ-trace of the one-pot labeling of **18** with $[^{99m}TcO_4]^-$ and Isolink Kit. Top-down trace: UV-trace of Re-compound **24**. Quantitative and radiochemically pure conversion of $[^{99m}TcO_4]^-$ to complex **28**.

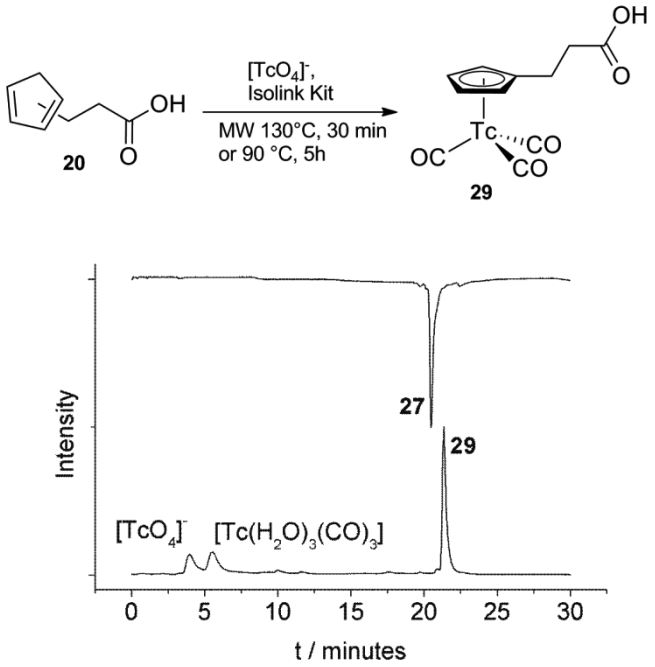

Scheme 22: Bottom-up trace: γ-trace of the one-pot labeling of **20** with $[^{99m}TcO_4]^-$ and Isolink Kit. Top-down trace: UV-trace of Re-compound **27**.

The labeling behaviour of **23**, the dimeric form of **18**, was also assessed. As seen with the monomer **18**, the carboxylic acid group in β-position to the Cp is close enough to serve as an anchoring group towards the metal core, in order to initiate complexation of the Cp-ring. In that case, the metal mediated *retro* Diels-Alder reaction, similar to Thiele's Acid, might be possible for dimer **23** as well. Therefore, the same set-up as used for the labeling of **18** was applied and **23** was added. Product formation was observed. The conversion rate with the dimer was significantly lower than with the monomer. After 40 minutes at 90 °C, only 34 % of the starting compound was converted. However, using microwave synthesis at temperatures of 130 °C, 67 % conversion to the ^{99m}Tc-complex **28** was observed after 40 minutes. 21 % of the ^{99m}Tc was oxidized to $[^{99m}TcO_4]^-$, and 12 % was still unreacted starting compound (Scheme 23).

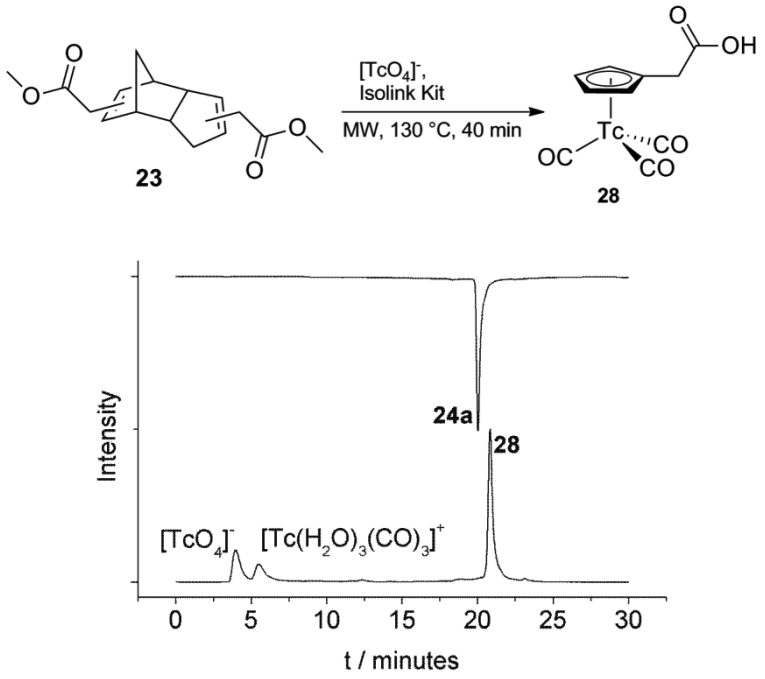

Scheme 23: Bottom-up trace: γ-trace of the one-pot labeling of **23** with $[^{99m}TcO_4]^-$ and Isolink Kit. Top-down trace: UV-trace of Re-compound **24**.

With the synthesis of the uncoordinated and protonated HCp-compounds **17** and **19**, containing methylene groups between the HCp and the carboxylic acid, a new way of altering the spacer in a BFC has been introduced; before *and* after the coupling function. Apart from ester hydrolysis, the two compounds are water and air-stable. **17** undergoes slow Diels-Alder dimerization at room temperature. Keeping **17** at -20 °C, beside the dimer **23**, the rearrangement product **22** is formed. The dimerization behaviour of **19** was not investigated. Derivatisation of the carboxylic acid **18** by amide coupling with primary amines leads to rearrangement of the double bonds and the formation of a cyclopentene ring, as observed with compounds **21a/b**. Therefore cyclopentadienyl amides of **18** are not accessible.

18 and **20** contain a carboxylic acid function in β- or in γ-position, with respect to the HCp-ring. Labelling experiments with $[^{99m}Tc(OH_2)_3(CO)_3]^+$ proved that these positions are still close enough, to allow anchoring of the metal center by the carboxylic acid portion. Therefore, bringing the metal in close proximity, η^5-coordination of the HCp-portion is simplified. However, conversion rates of the ^{99m}Tc starting compounds were very different for the ligand **18** compared to **20**, which is in accordance with the increasing distance of the anchoring group to the HCp-moiety. Similar to Thiele's Acid, the dimer **23** can undergo metal mediated *retro* Diels-Alder reaction and form

the same product as obtained with the monomer **18**. The mechanism however is unclear.

Using [(Cp)Re(CO)$_3$], the synthesis of the corresponding Re-complex **24a** with bromacetic acid failed and the binuclear compound **24b** was obtained instead. However, **24a** was synthesized similar to the ^{99m}Tc-compound **28** using ligand **18** with [Re(Br)$_3$(CO)$_3$]$^{2-}$ in water.

Using a Horner-Wardsworth-Emmons olefination, the Re-complex **27** was synthesized.

2.3 Biologically Relevant Vectors

The aforementioned functionalities at the Cp-chelator can be derivatized with biologically active vectors, to finally form the BFC. These vectors usually consist of a certain functional group, which is connected to a spacer, which again can be bound to the Cp-derivative. The vector for a target is usually kept constant, while the spacer can be altered, in order to explore possible structure activity relationships (SARs) and to reach the best possible interaction between the host and the targeting molecule. In the following chapter, the synthesis of different targeting functionalities with different spacers and for different targets will be discussed. Syntheses included the Re-complexes, the free ligands and the ^{99m}Tc-complexes (Figure 20). Some of the examples were also biologically investigated.

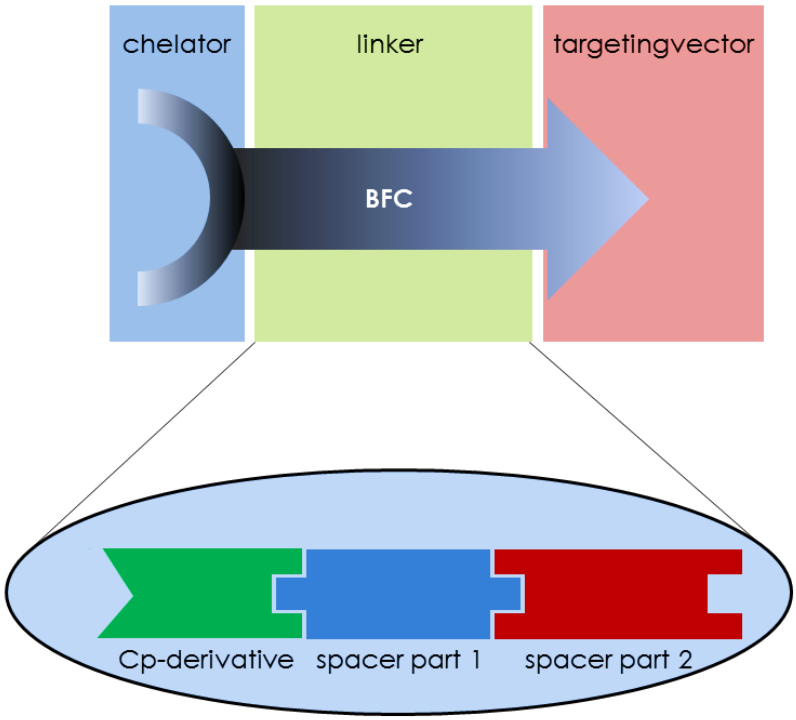

Figure 20: The linker is built of different parts, including the Cp-derivative, which can be altered.

2.3.1 HDAC-Inhibitors

Histone deacetylases (HDACs) catalyze the removal of acetyl groups of ε-lysine tails on histone proteins, causing condensed chromatin and therefore transcriptional silencing. Hence cancer cells escape apoptosis.[93] As HDAC inhibitors can counter cancer progression, they contribute to apoptosis and the formation of growth arrest proteins.[94, 95] Since these enzymes are highly overexpressed in cancer tissues, they are targets for both, cancer diagnosis and therapy. Vectors, which target HDACs often incorporate terminal hydroxamic acids. Suberoylanilide hydroxamic acid (SAHA, Figure 21) is a clinically approved inhibitor. It is administered for the treatment of a number of hematological and solid tumors.[96] While different organometallic SAHA-analogues containing ferrocene or *cis*-platin respectively have been investigated for therapeutic application,[97-99] such bioinorganic SAHA-analogues for radiopharmaceutical application are still unknown.[93]

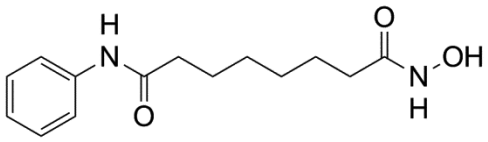

Figure 21: Lewis structure of Suberoylanilide hydroxamic acid (SAHA)

The Rhenium Complexes.

[(Cp)Re(CO)$_3$] structurally can be introduced into bioactive substances by replacing phenyl rings. Following this strategy, slightly modified organometallic SAHA-analogues **31**, **33** and **36** were synthesized (Figure 22).[93] Compounds **31** and **33** are carboxylic acid-conjugates, whereas the native SAHA is an amino-conjugate. Additionally, in order to tune interactions with the binding pocket, compound **31** contains one methylene spacer more than the lead compound between the amide group and the terminal hydroxamic acid portion. In addition to these compounds, **36** was synthesized, the exact structural analogue of SAHA. The position of the amide linker and the length of the aliphatic spacer correspond to the native SAHA and the only difference to the lead structure is the replacement of the phenyl ring with [(Cp)Re(CO)$_3$].

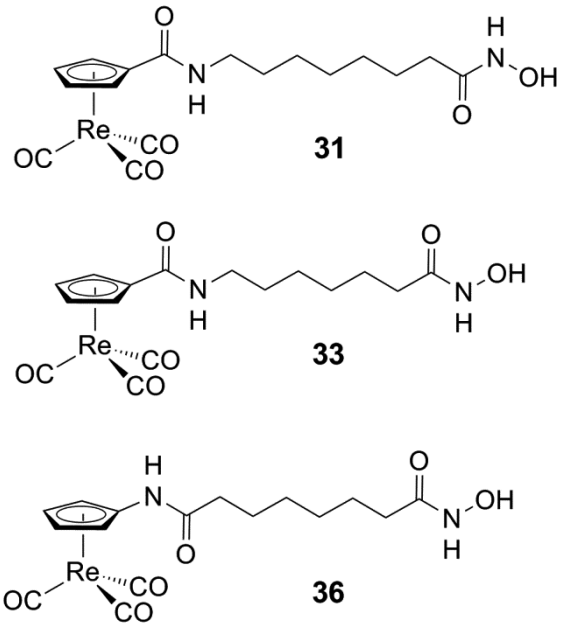

Figure 22: Overview: Compounds **31**, **33** and **36** differ in the length of the methylene-chain. Moreover, **31** and **33** are Cp-acid-conjugates, whereas **36** is a Cp-amino-conjugate. **36** is the exact structural analogue of SAHA.

[(Cp-COOH)Re(CO)$_3$] (**2**) was activated with pentafluorophenyl trifluoroacetate (PFPTFA) and coupled to the appropriate amine to form complexes **30** and **32**. Activation of the terminal carboxylic acids with ethyl chloroformate and treatment with hydroxylamine gave the final products **31** and **33** (Scheme 24).

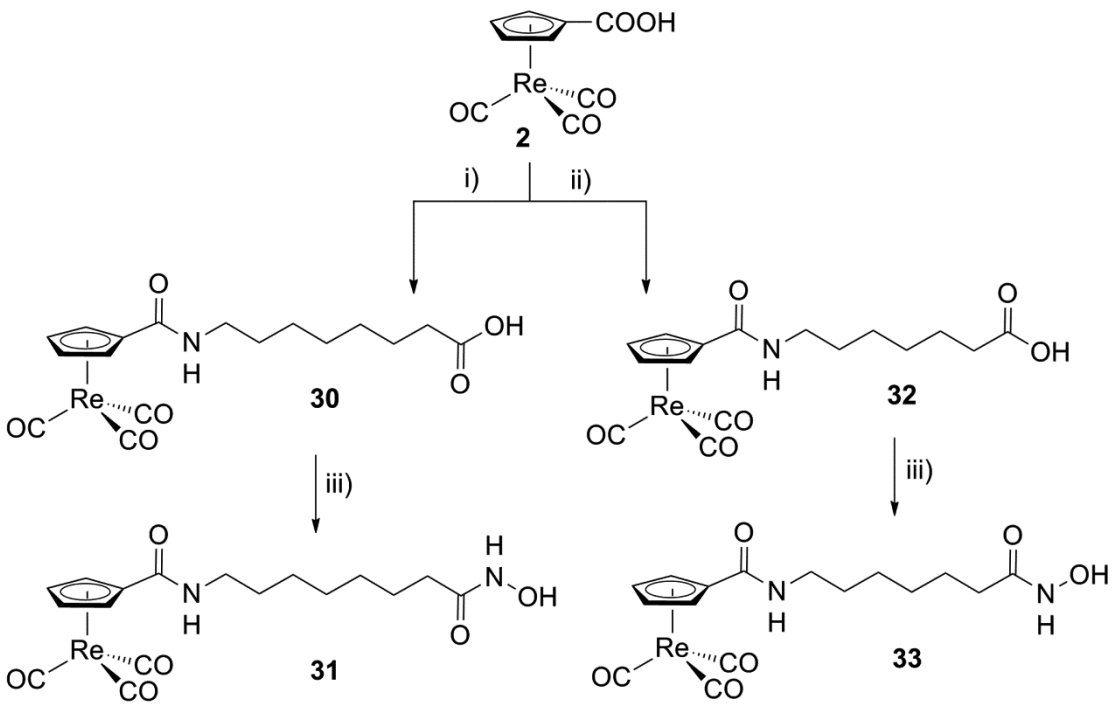

Scheme 24: Synthetic conditions: i) Pentafluorophenyl trifluoroacetate, 8-aminocaprylic acid, DMF, 88 %. ii) Pentafluorophenyl trifluoroacetate, 7-aminoheptanoic acid, DMF, 86 %. iii) Ethyl chloroformate, NH_2OH, THF 80 – 86 %.

The ^{1}H-NMR spectrum of **30** and **32** in DMSO-d_6 shows the two aromatic Cp-signals at 6.26 and at 5.70 ppm respectively. In comparison to **2** (DMSO-d_6, 6.21 and 5.74 ppm), the signals did not move significantly. The multiplets of the methylene groups can be found from 3.13 to 1.25 ppm. However, IR-υCO-frequencies (KBr) indicate increased C-O bond lengths of the carbonyl ligands (2022 and 1907 cm^{-1}), caused by increased electron density on the metal compared to the starting compound **2** (2032 and 1916 cm^{-1}).

Upon coupling to hydroxylamine, the chemical shift of the methylene multiplets shifted. The metal core and functionalities in close proximity were hardly influenced.

[(Cp-NHCO$(CH_2)_6$COOMe)M$(CO)_3$] (**34a/b**) (a: M = Re, b: M = Mn) was synthesized by activation of suberic acid monomethyl ester with isobutyl chloroformate and coupling with [(Cp-NH_2)M$(CO)_3$] (**11**). The obtained ester **34a** was hydrolyzed with aqueous LiOH. Activation of the terminal carboxylic acid with ethyl chloroformate and treatment with hydroxylamine gave the final product **36** (Scheme 25). Compound **36** corresponds structurally to native SAHA.

The Mn-complex **34b** was synthesized exclusively for crystallographic purposes and was not exploited further. Crystals were grown by dissolving in a minimum of CH_2Cl_2

and slow addition of hexane as a precipitant. An Ortep-plot with important bond lengths and angles is given in figure 23. **34b** crystallized in the monoclinic crystal system P21/c and the central manganese is η^5-coordinated to the Cp^--ligand. The geometry around the manganese is distorted octahedral and the amide group is almost coplanar with the Cp^--ring, showing a torsion angle of -2.5(4)° between O4-C9-N1-C4. The Mn-C (CO) bond lengths range from 1.776(3) to 1.784(3) and are substantially shorter than those found for the Re-complexes discussed above. As a consequence of the smaller radius of the metal center, the individual Mn-C bond lengths to the Cp ligand are shorter as well in comparison to the Re-complexes **4**, **5**, **24a/b** and **27**. They also reveal variations, from 2.194(2) (Mn1-C4) to 2.102(3) Å (Mn1-C6), similar to **4** and **5**. However in contrast to compounds **4** and **5**, the shortest M-C bonds (Mn1-C6 and Mn1-C7) are the ones opposite to the derivatized Cp-carbon, which forms the longest bond (Mn1-C4).

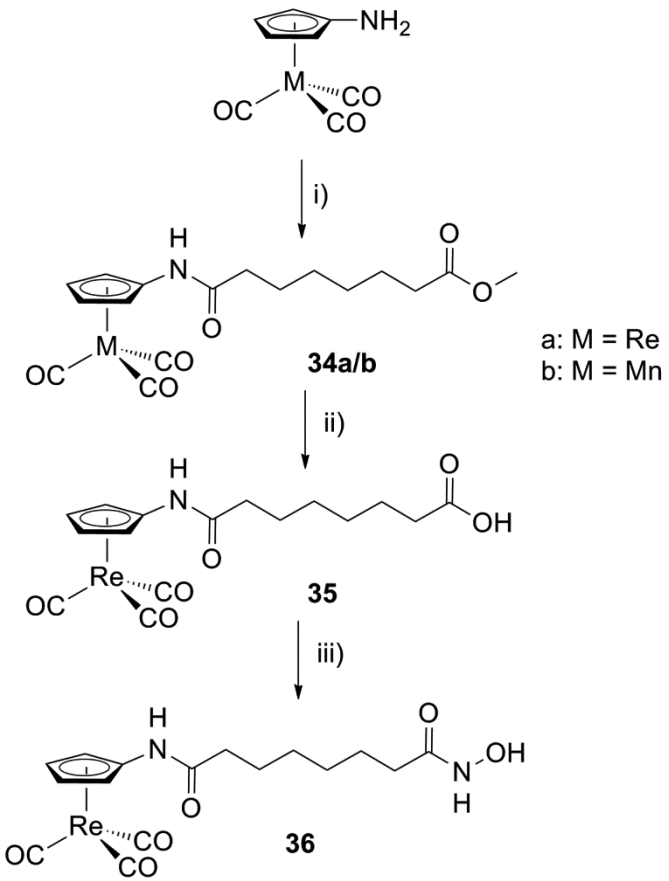

Scheme 25: Synthetic conditions: i) Suberic acid monomethyl ester activated with isobutyl chloroformate, THF, 98 %. ii) LiOH, H_2O, MeOH, THF, 98 %. iii) Ethyl chloroformate, NH_2OH, THF 80 – 86 %.

Upon amide coupling of **11** to suberic acid monomethyl ester, the characteristic IR-υCO-bands of **34a** were observed at 2019 and at 1913 cm^{-1} (KBr). Compared to the starting compound **11** (1995 and 1874 cm^{-1}), these values indicate a tremendous change in the electronic conditions around the metal, caused by the electron withdrawing nature of the carbonyl.

Alterations at the pendent functional group caused shifts of the neighbouring methylene multiplets. The metal core and functionalities in close proximity were hardly influenced.

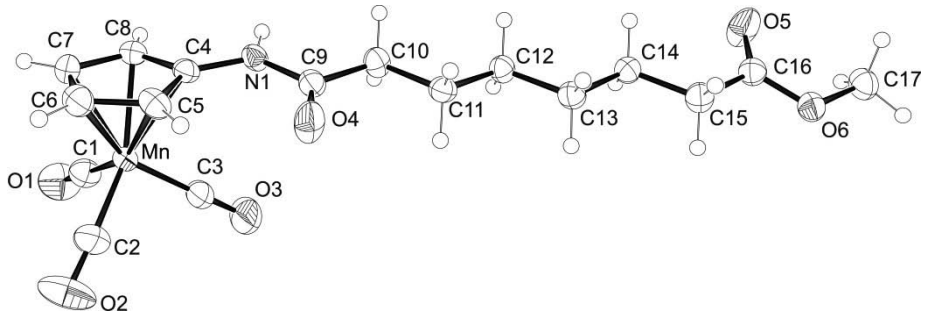

Figure 23: ORTEP representation of **34b**. Relevant bond lengths (Å) and angles (°): Mn(1)-C(1) 1.784(3), Mn(1)-C(2) 1.784(3), Mn(1)-C(3) 1.776(3), Mn(1)-C(4) 2.194(2), Mn(1)-C(5) 2.146(2), Mn(1)-C(6) 2.102(3), Mn(1)-C(7) 2.105(3), Mn(1)-C(8) 2.133(3), C(1)-O(1) 1.147(4), C(2)-O(2) 1.138(4), C(3)-O(3) 1.143(4), C(4)-N(1) 1.400(3), C(9)-O(4) 1.212(3), C(16)-O(5) 1.192(3), C(16)-O(6) 1.325(3), C(3)-Mn(1)-C(2) 93.72(15), C(3)-Mn(1)-C(1) 92.19(15), C(2)-Mn(1)-C(1) 90.54(14), O(4)-C(9)-N(1) 121.7(3), O(4)-C(9)-C(10) 123.6(3), O(5)-C(16)-O(6) 122.9(3), O(5)-C(16)-C(15) 124.8(3), C(16)-O(6)-C(17) 116.0(2).

The Organic SAHA-Analogues

For the direct comparison of the biological activity of organic and inorganic inhibitors, the organic congeners of compounds **31** and **33**, namely **38** and **40** were prepared. As mentioned before, **36** corresponds to the native SAHA. Syntheses were performed analogously to the organometallic compounds, as described above (Scheme 26).[93] The inhibitors were purified by silica gel chromatography and analysed by NMR, ESI-MS, and CHN-analysis. Characterization will not be discussed here.

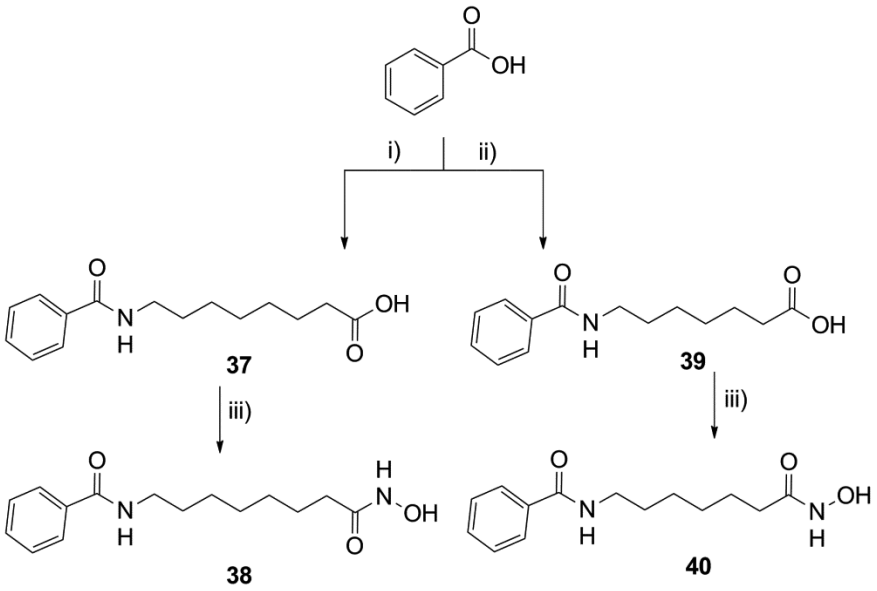

Scheme 26: Synthetic conditions: i) Pentafluorophenyl trifluoroacetate, 8-aminocaprylic acid, DMF, 90 %. ii) Pentafluorophenyl trifluoroacetate, 7-aminoheptanoic acid, DMF, 89 %. iii) Ethyl chloroformate, NH_2OH, THF 90-92 %.

The Ligands

As mentioned in section 2.1.4, the synthesis of an uncoordinated HCp-NH_2 molecule was not achieved. Therefore, the preparation of the non-coordinated ligand of SAHA analogue **36** was not possible. However, as a chemical proof of concept for the ^{99m}Tc-labeling of HDAC-inhibitors with pendent hydroxamic acids, **42** was synthesized, a dimeric form of the protonated ligand of compound **33**.[93]

Thilele's Acid was activated with PFPTFA in DMF in quantitative yield.[63] The obtained PFP-ester was isolated and did not hydrolyse during the aqueous work-up, which proves, that PFP-esters cause only weak activation of carboxylic acids. However, primary amines are nucleophilic enough to form amide bonds with PFP-activated Thiele's Acid. The addition of two equivalents of 7-aminoheptanoic acid together with an excess of NEt_3 led to the formation of compound **41**. Activation of the terminal carboxylic acids with O-(7-Azabenzotriazol-1-yl)-N,N,N',N'-tetramethyluronium hexafluorophosphate (HATU) and treatment with O-(*tert*-Butyldimethylsilyl)- hydroxylamine gave hydroxamic acid **42**, after aqueous work-up (Scheme 27).

Two triplets at 7.81 and at 7.52 ppm respectively for the NH-protons in the ^{1}H-NMR spectrum of **41** (MeOD) indicated the formation of an amide bond. The signal for the olefinic protons shifted from 6.86 ppm for Thiele's Acid to 6.63 ppm and from 6.51 to 6.30 ppm due to increased shielding of the olefinic protons. The same effect of

increased electron donation to the Cp upon amide coupling was observed in the IR-measurement of complexes **30** and **32** (see above).

After coupling of the two terminal carboxylic acids functions to hydroxylamine, the ^{1}H-NMR-signals of the methylene groups adjacent to the terminal carbonyl shifted clearly from 2.12 to 2.27 ppm but did not have any effect on the HCp-protons.

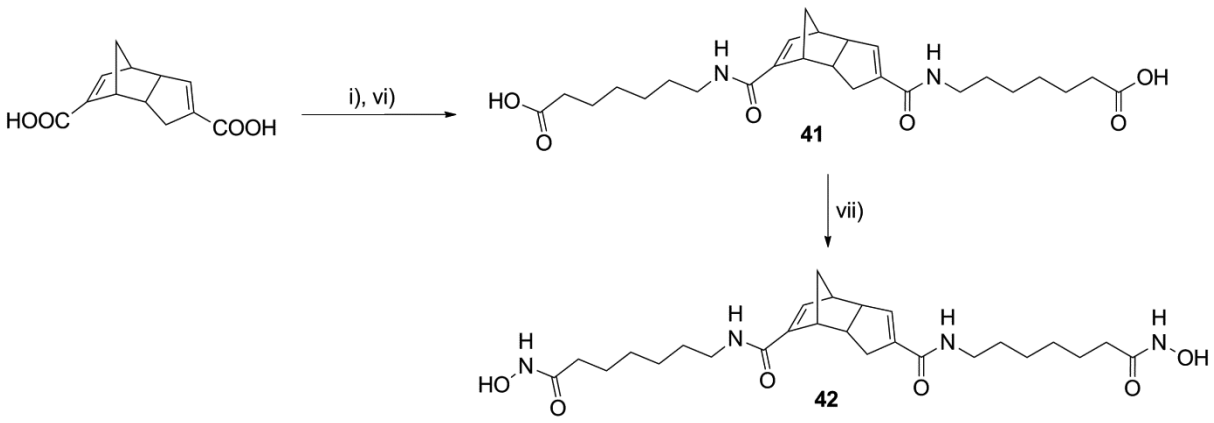

Scheme 27: Synthetic conditions: i) Pentafluorophenyl trifluoroacetate, DMF, quantitative. vi) 7-aminoheptanoic acid, triethylamine, DMF, 54 %. vii) HATU, O-(tert-Butyldimethylsilyl)hydroxylamine, H_2O, DMF, 70 %.

The Technetium Complexes

Acording to the theragnostic concept, the Re-HDACIs **31**, **33** and **36** could be applied in combination with the corresponding ^{99m}Tc-labelled compounds; macroscopic amounts of Re for therapy and microscopic amounts of the ^{99m}Tc-analogues for diagnosis. Therefore, attempts were made to label **42** with $[^{99m}Tc(OH_2)_3(CO)_3]^+$. But heating of a millimolar solution of **42** with $[^{99m}Tc(OH_2)_3(CO)_3]^+$ at 90 °C resulted only in the quantitative formation of $[^{99m}TcO_4]^-$ (Scheme 28). Hydroxamic acids are oxidants towards $[^{99m}Tc(OH_2)_3(CO)_3]^+$. The same behavior was observed, when $[Re(Br)_3(CO)_3]^{2-}$ was mixed with **42** or with other hydroxamic acids. However, oxidation only occurred, when the metal core contained weakly bound and substitution labile ligands, like the water molecules in $[^{99m}Tc(OH_2)_3(CO)_3]^+$ or the bromides in $[Re(Br)_3(CO)_3]^{2-}$. Preliminary formed $[(Cp\text{-}R)M(CO)_3]$ complexes did not show any decomposition under the same conditions. This leads to the assumption, that coordination of the hydroxamic acid function to the metal core is a key-step of this side reaction. Therefore the hydroxamic acids were protected by acetylation at the hydroxyl position. But esters are usually cleaved off under the basic labeling conditions, thus the desired labeling product was not obtained.

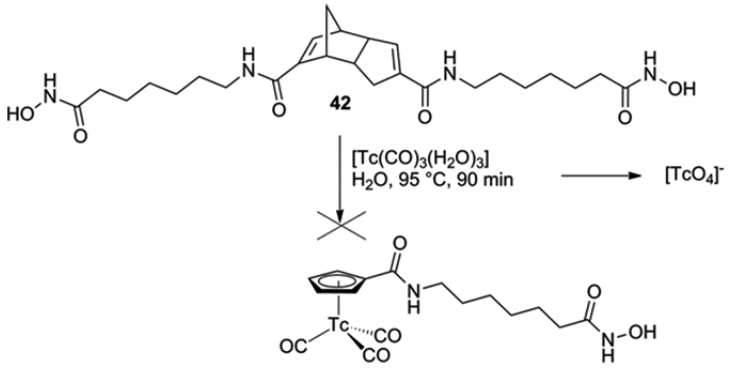

Scheme 28: Hydroxamic acids oxidize the metal in $[^{99m}Tc(OH_2)_3(CO)_3]^+$ or in $[Re(Br)_3(CO)_3]^{2-}$ to $[TcO_4]^-$ or $[ReO_4]^-$ respectively.

However, the one-pot labeling of **41** with $[^{99m}TcO_4]^-$ in presence of an Isolink Kit showed after 80 minutes at 90 °C the expected product **43** in 87 % yield and high radio chemical purity (Scheme 29).[93] Two-step procedures, where The $[^{99m}Tc(OH_2)_3(CO)_3]^+$ precursor is prepared in advance, works equally well. The nature of the ^{99m}Tc-compound was confirmed by co-injection with the corresponding Re-complex **32**.

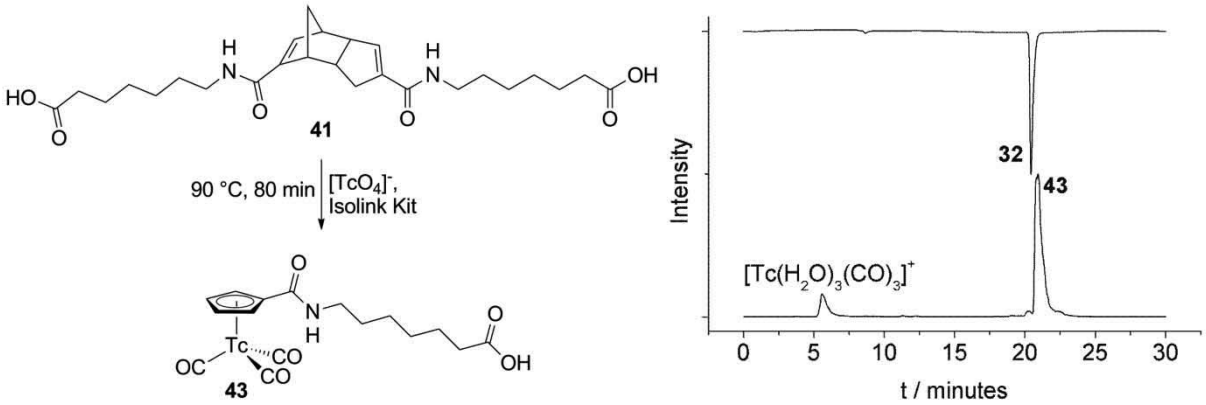

Scheme 29: Bottom-up trace: γ-trace of the one-pot labeling of **41** with $[^{99m}TcO_4]^-$ and Isolink Kit. Top-down trace: UV-trace of Re-compound **32**.

In Vitro Cytotoxicity

Analyzing the anti-tumor activity of organometallic HDAC-inhibitors **31, 33** and **36**, cytotoxicity towards five carcinoma cell lines was evaluated.[93] In order to have a direct comparison, the corresponding organic congeners SAHA, **38** and **50** were tested the same way. The cancer cell lines were exposed to increasing concentrations of the different compounds for 72 h and the cellular viability was determined by MTT assay. The viability of cells in the presence of the tested

compounds was compared to that observed in control cultures and the percentage of growth inhibition was calculated. The dose-response curves demonstrate the antiproliferative effects of all compounds, exemplified in Figure 24 for human cervical carcinoma HeLa and vulva epidermal carcinoma A431 cells. The IC_{50} (*i.e.*, the concentration producing 50 % inhibition of growth) was determined for five cells lines and is expressed in micromolar concentration (Table 1).

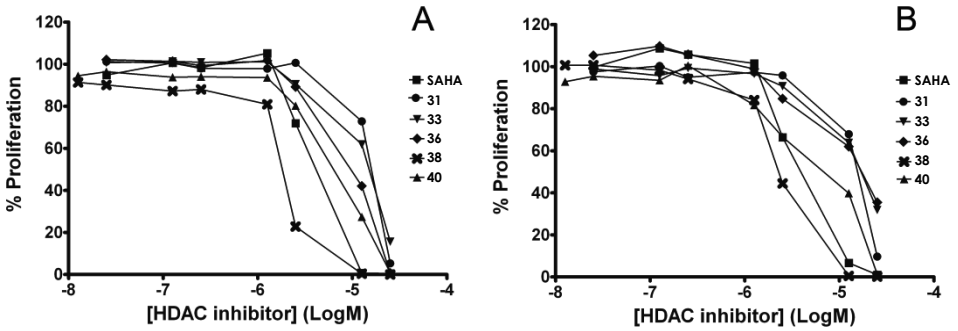

Figure 24: Cytotoxicity on human cervical carcinoma HeLa cells (A) and vulva epidermal carcinoma A431 cells (B).

Table 1: Cytotoxicity profile of compounds **31**, **33**, **36**, **38** and **40** and of the reference HDAC inhibitor SAHA for 72 h (37 °C/5 % CO_2) continuous treatment of five different tumor cell lines (MCF-7 Human breast carcinoma, A431 Human vulva epidermal carcinoma, A375 Human melanoma, B16F1 Murine melanoma).

Compound	IC_{50} (µM)					Mean ± SD
	MCF-7	A431	HeLa	A375	B16F1	
31	9.47	13.7	14.4	14.7	9.82	12.4 ± 2.6
33	15.2	17.1	13.3	23.3	12.6	16.3 ± 4.3
36	11.4	17.3	8.34	12.5	15.2	12.9 ± 3.4
38	1.71	2.51	1.65	2.63	3.10	2.32 ± 0.62
40	7.19	5.22	5.83	4.85	8.88	6.39 ± 1.65
SAHA	3.74	4.44	4.45	4.58	3.67	4.18 ± 0.43

The analysis of the data presented in table 1 allows to understand how the position of the amide linker and the length of the alkyl chain, attached to the $[(Cp)Re(CO)_3]$-framework, may affect the anti-tumoral capacity of organometallic HDCA inhibitors. Moreover, it allows to evidence if the replacement of phenyl rings by $[(Cp)Re(CO)_3]$ is tolerated in the investigated examples.

Table 1 shows, that after a drug administration period of 72 h, SAHA displayed a broad cytotoxicity across cell lines from different tumor entities with a mean IC_{50} value of 4.2 ± 0.4 µM. This value, obtained from the MTT assay, is in agreement with

the antiproliferative activity of SAHA previously reported by using the Alamar Blue cell viability assay (IC_{50} = 3.3 μM, a mean value for several tumor cell lines).[100]

Among the new compounds reported here, the organic SAHA-analogue **38** showed the lowest IC_{50} values for all tested cell lines. This indicates a superior potency for HDCA-inhibition in vitro, even higher than the one described for the native SAHA. In fact, the mean IC_{50} value for compound **38** (2.32 ± 0.62 μM) (**38** contains a longer aliphatic chain and inverted amide linker as compared to SAHA) was about 2 or 3 times lower than the one obtained for SAHA or compound **5** respectively (4.2 ± 0.4 and 6.39 ± 1.65 μM), both containing the shorter hexyl alkyl chain. These results suggest that cytotoxicity of HDAC inhibitors of the class of benzamide derivatives may depend on the length of the methylene chain attached to the benzamide framework.

The organometallic HDACis **31, 33** and **36,** are less active in each case as compared to the respective organic congeners SAHA, **38** and **40**. The mean IC_{50} for **31** was 12.4 μM, compared to 2.3 μM for **38**. Re-complex **33** and the corresponding molecule **40** displayed values of 16.3 μM and 6.4 μM, respectively and while SAHA presented a value of 4.2 μM, Re-complex **36** displayed a higher IC_{50} of 12.9 μM. This slight decrease of antiproliferative capacity of the Re-complexes indicates the more bulky [(Cp)Re(CO)$_3$] to be disfavored over a simple planar phenyl ring and might be caused by reduced ability of cellular penetration. Nevertheless, the Re-complexes still retain a high cytotoxic activity, comparable to their organic congeners. No significant effect on cytotoxicity was observed by altering the position of the amide linker at the Cp. Similar mean values of IC_{50} were obtained for **33** and **36** (16.3 ± 4.3 vs 12.9 ± 3.4 μM). All biological experiments were performed by using methanol as co-solvent (to a final concentration of ≤ 0.1 %). Although this solvent is known to be toxic to cells, here due to its low concentration, the cell viability in the control experiments was higher than 90 %.

In summary, a series of new organometallic HDAC-inhibitors with pendend hydroxamic acids, as well as their organic congeners were synthesized and characterized. The preparation of the ^{99m}Tc analogues using the uncoordinated HCp-dimer failed under standard labeling conditions (millimolar concentration of the ligand, [^{99m}Tc(OH$_2$)$_3$(CO)$_3$]$^+$, 90-95 °C). Oxidation of [^{99m}Tc(OH$_2$)$_3$(CO)$_3$]$^+$ to [^{99m}TcO$_4$]$^-$ was caused by the hydroxamic acid portion prior to η^5 complex formation. However,

the same labeling conditions applied to terminal carboxylic acids formed the desired product. [(CpR)^{99m}Tc(CO)$_3$]-complexes, where R is a HDAC-targeting hydroxamic acid, are therefore not accessible via metal mediated *retro* Diels-Alder reaction.
Cytotoxic evaluation of the Re-complexes revealed low micromolar IC_{50}-values on different tumor cell lines. The values are in the same range as found for SAHA and prove the concept of replacing phenyl rings by [(CpR)Re(CO)$_3$] to be applicable in the case of organometallic HDAC-inhibitors. Slight alterations in the length of the aliphatic spacer as compared to the hexyl alkyl chain in SAHA do affect the activity of the HDACis. Increasing the number by one methylene group shows increased cytotoxic capacity. No significant effect was observed when the position of the amide linker at the Cp-ring was altered.

2.3.2 CA-Inhibitors

Carbonic anhydrases (CAs) are zinc metalloenzymes, found in both, prokaryotes and eukaryotes.[101] They catalyze the essential formation of carbonic acid from CO_2 and water, and are involved in many different physiological and pathological processes. In mammals, 16 different isozymes are known, which are either membrane bound, expressed in the cytosol or in mitochondria.[101, 102] One feature that attracts interest in CAs from a pharmaceutical point of view is the hypoxia induced overexpression of hCAIX and hCAXII in many malignancies, including cancer.[101, 103-106] Therefore, CAs are a potential target for both cancer diagnosis and therapy and specific inhibitors will allow for targeted imaging of cancer tissue or growth inhibition, respectively. However, the large number of isozymes combined with the diffuse localization of CAs makes selective accumulation of inhibitors difficult.[102] Whereas several fluorescent sulfonamide-based CAIs or radio-iodinated monoclonal antibodies are exploited for diagnostic application,[107-110] only one report of ^{99m}Tc-labeled inhibitors has been published.[111] CAs have also been used as host for artificial metalloenzymes. Ruthenium based piano-stool complexes with pendent sulfonamide groups displayed moderate binding affinities for hCAII.[112]

The Rhenium Complexes

Meggers et al. recently showed that high selectivity does not only depend on intermolecular interactions but also on a directed 3D arrangement of different

functionalities as exemplified with organometallic protein kinase inhibitors.[42-44] Inert organometallic complexes offer the opportunity to populate biologically relevant space. Thus, bioorganometallic complexes are versatile chemical probes.[42, 45-48] Retaining the concept of extended three dimensional space population by organometallic complexes, new arylsulfonamide, -sulfamide or -sulfamate based CAIs containing the small [(Cp-R)M(CO)$_3$]-motif (M = Re or ^{99m}Tc) were synthesized.
The structures of complexes **46** and **51**-**55** differ in the spacer in terms of length and functionality adjacent to the Cp, as well as in the pendent terminal group (Figure 25). Compound **46**, similar to model compounds **12** and **13**, contains an internal sulfonamide group, which is coupled at the nitrogen atom to the Cp and via sulfur atom to the *para*-arylsulfamide. **51**-**53** have an amide group in the spacer, which is bound via a carbonyl group to the Cp. The amide-nitrogen in **51** is attached directly to the *para*-arylsulfamate and in **52** to the *para*-arylsulfonamide. Unlike compound **53**, which contains an additional methylene group between the amide nitrogen and the terminal *para*-arylsulfonamide. Complexes **54** and **55** follow this scaffold and contain a methylene group between the amide nitrogen and the terminal *para*-arylsulfonamide moiety too. In contrast to **53**, **54** and **55** contain also methylene spacers between the carbonyl and the Cp-chelator: **54** contains one and **55** contains two methylene-groups, displacing the metal complex further away from the actual targeting vector.

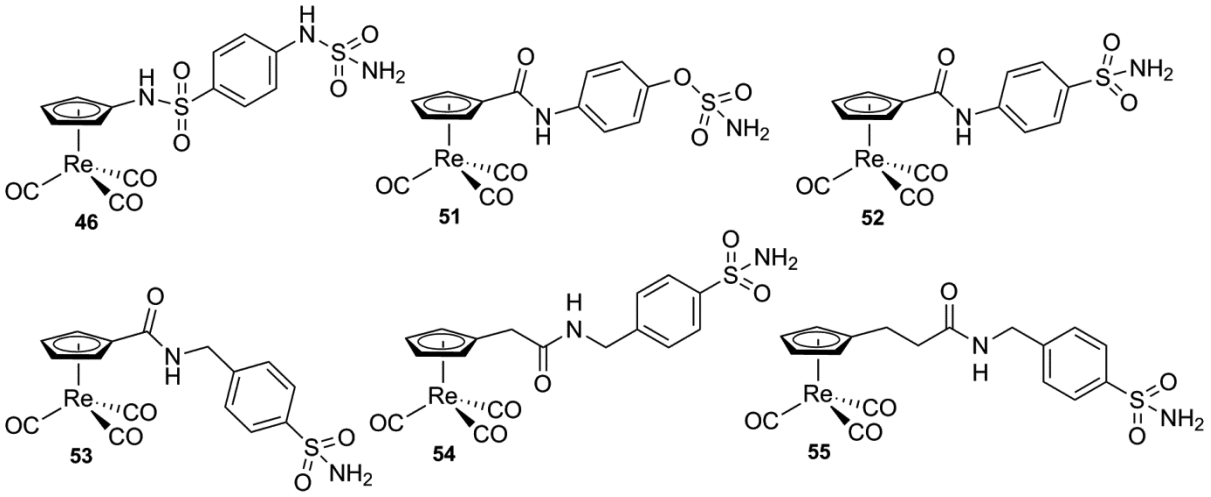

Figure 25: Overview: **46** and **51**-**55** differ in the spacer, as well as in the pendent terminal group.

[(Cp-NH$_2$)Re(CO)$_3$] (**11**) was coupled to acetamidobenzolsulfonylchloride in refluxing CH_2Cl_2. The resulting product **44** was filtered off and purified by silica gel column

chromatography. Acidic hydrolysis of the pendent acetyl group followed by sulfamoylation afforded compound **46** (Scheme 30).

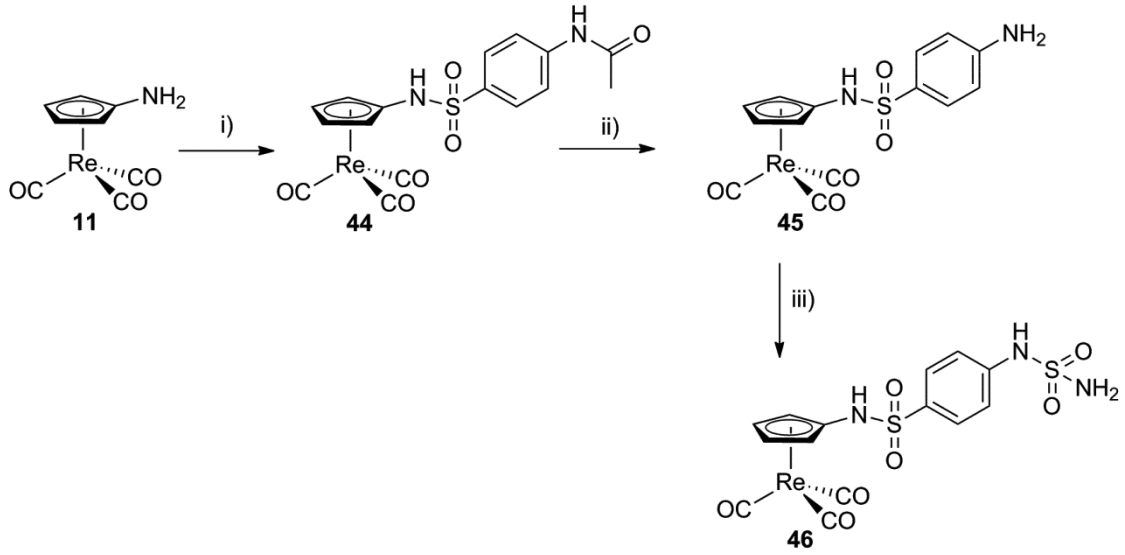

Scheme 30: Synthetic conditions: i) Acetamidobenzolsulfonyl chloride, CH_2Cl_2, 80 %. ii)HCl, H_2O, EtOH, 98 %. iii) Sulfamoylchloride, DMA, 68 %.

In the ^{1}H-NMR-spectrum of **44** (MeOD), the four phenyl-protons were observed isochronically and show a singlet at 7.82 ppm. Characteristic IR-υCO-bands for sulfonamide **44** (amino conjugate) were detected at 2020 and at 1915 cm^{-1} (KBr) and are thus similar to amides of the form of **34a** (also amino conjugate, 2024 and 1910 cm^{-1}). Amide substitution of **11** causes therefore a comparable change in the electronic environment around the metal as sulfonation. However, inversion of the internal sulfonamide group as seen for example in compound **6,** decreases electron density on the metal and the IR-υCO-bands shift towards higher frequencies (2036 and 1957 cm^{-1} for **6**).

Upon deacetylation, the isochronicity of the phenyl-protons is lifted in compound **45** and two multiplets are observed at 7.55 and at 6.72 ppm respectively.

45 was crystallized from CH_2Cl_2 by slow addition of hexane as a percipitant. The structure was elucidated and an ORTEP-plot is shown in figure 26. The compound crystallized in the orthorhombic crystal system Pbcn. The Re-atom shows η^5-coordination by the Cp^--ligand. The M-C (CO) bond lengths range from 1.908(3) to 1.920(3). The C-O bond lengths of the carbonyl ligands of **45** (1.140(4)-1.154(3) Å) are longer than those found for compound **4** (1.131(7)-1.144(8) Å), but compare well to

those of **24a**/**b** (1.146(5)-1.152(4) Å). Other important bond lengths and angles are given in figure 26.

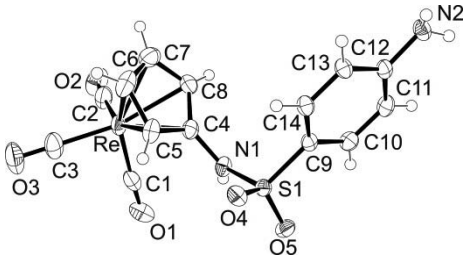

Figure 26: ORTEP plot of **45**: Important bond lengths (Å) and angles (°): Re(1)-C(1) 1.920(3), Re(1)-C(2) 1.908(3), Re(1)-C(3) 1.917(3), Re(1)-C(4) 2.319(2), Re(1)-C(5) 2.304(3), Re(1)-C(6) 2.302(3), Re(1)-C(7) 2.290(3), Re(1)-C(8) 2.319(3), C(1)-O(1) 1.140(4), C(2)-O(2) 1.154(3), C(3)-O(3) 1.144(3), C(9)-S(1) 1.749(2), O(4)-S(1) 1.4311(17), O(5)-S(1) 1.4281(18), N(1)-S(1) 1.6337(19), C(2)-Re(1)-C(3) 90.18(12), C(2)-Re(1)-C(1) 88.32(13), C(3)-Re(1)-C(1) 89.31(13), N(1)-S(1)-C(9) 108.52(11)

For the synthesis of **51**, two different strategies were considered. Coupling of 4-aminophenol to [(Cp-COOH)Re(CO)$_3$] (**2**), followed by sulfamoylation of the pendent hydroxyl group, or sulfamoylation of 4-aminophenol prior to coupling to **2** would, both lead to the formation of **51**.

However, activation of **2** with PFPTFA and addition of 4-aminophenol lead to the mixed formation of 39 % of the amide **47a** and 24 % of the ester **47b**. Separation of the two compounds was achieved by silica gel column chromatography. Only small amounts of **51** were obtained upon sulfamoylation of **47a**, therefore this strategy was not further pursued (Scheme 31).

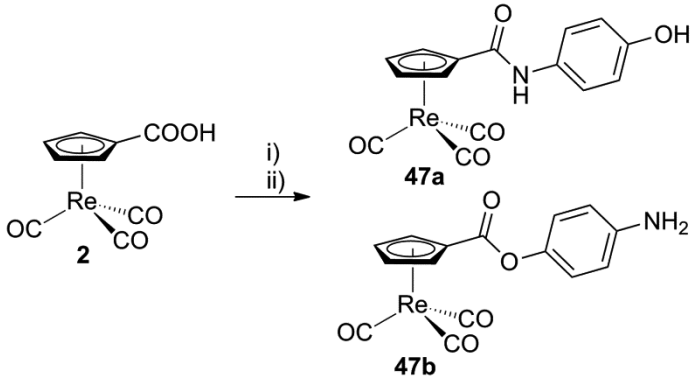

Scheme 31: Synthetic conditions: i) Pentafluorophenyl trifluoroacetate, DMF, 80 %. ii)4-aminophenol, DMF, 39 % and 24 %.

For a different synthetic approach to **51**, 4-aminophenol was boc-protected at the nitrogen site and sulfamoylated at the pendend hydroxyl-group to form the intermediate **49** in good yields (85 %). Acidic deprotection using TFA in CH_2Cl_2 formed

compound **50**, which was then coupled to HATU-activated [(Cp-COOH)Re(CO)$_3$] (**2**), to form **51** in acceptable yields (Scheme 32 and 33).

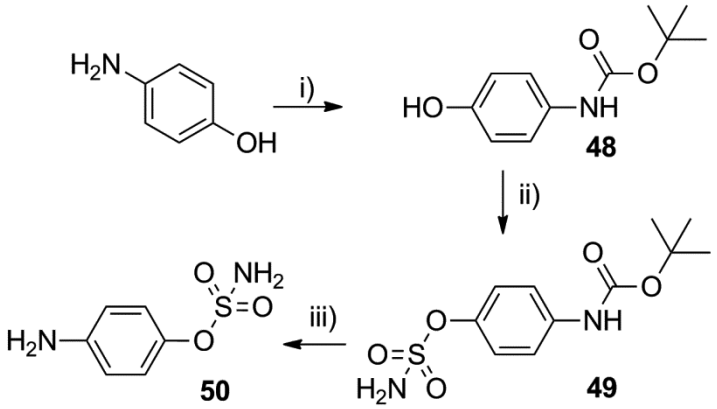

Scheme 32: Synthetic conditions: i) Boc_2O, CH_2Cl_2, 78 %. ii) Sulfamoylchloride, DMA, 85 %. iii) TFA, CH_2Cl_2, 98 %.

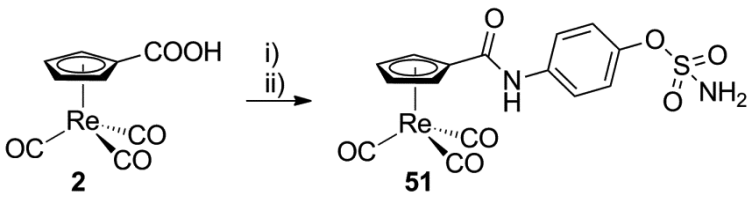

Scheme 33: Synthetic conditions: i) HATU, DMF. ii) **50**, DMF, 66 %.

The ^{1}H-NMR of **51** in DMSO-d_6 exhibited a shift of the two sets of aromatic Cp$^-$-*pseudo* triplets of 0.28 and of 0.07 ppm respectively, compared to unsubstituted carboxylic acid **2**. The IR-υCO-bands were observed at 2030 and at 1941 cm^{-1} (KBr). Especially the asymmetric frequency is shifted towards higher frequencies, compared to the starting compound **2** (1916 cm^{-1}).

Crystals were grown from a concentrated methanol solution of **51** by slow evaporation of the solvent. The compound crystallized in the triclinic crystal system P-1. Similar to complex **34b**, the carbonyl group is almost coplanar with the Cp$^-$-ring and shows a torsion angle between C6-C7-C9-O4 of -4.1(10)°. The geometry around the rhenium is distorted octahedral (Figure 27). The M-C (CO) bond lengths range from 1.897(13) to 1.949(8).

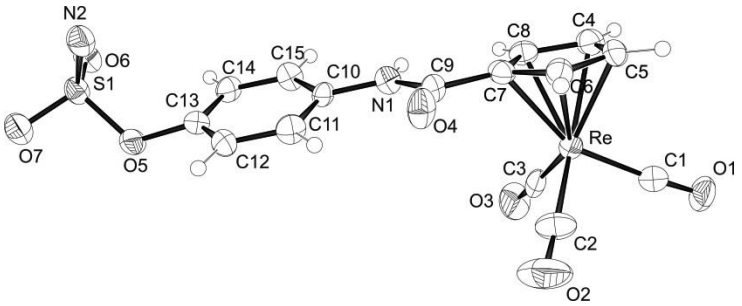

Figure 27: ORTEP plot of **51**: Important bond lengths (Å) and angles (°): Re(1)-C(1) 1.926(10), Re(1)-C(2) 1.949(8), Re(1)-C(3) 1.897(13), Re(1)-C(4) 2.287(7), Re(1)-C(5) 2.297(7), Re(1)-C(6) 2.280(8), Re(1)-C(7) 2.281(7), Re(1)-C(8) 2.282(8), C(1)-O(1) 1.130(12), C(2)-O(2) 1.115(12), C(3)-O(3) 1.175(15), O(6)-S(1) 1.425(7), O(7)-S(1) 1.433(6), O(9)-S(1) 1.585(6), N(2)-S(1) 1.565(8), C(3)-Re(1)-C(1) 90.1(4), C(3)-Re(1)-C(2) 90.4(5), C(1)-Re(1)-C(2) 89.5(4), O(6)-S(1)-O(7) 119.0(4), O(6)-S(1)-N(2) 108.3(4), O(7)-S(1)-N(2) 109.7(4), O(6)-S(1)-O(9) 108.7(4), O(7)-S(1)-O(9) 101.8(3), N(2)-S(1)-O(9) 108.9(4)

Activation of [(Cp-COOH)Re(CO)$_3$] (**2**) with PFPTFA, isobutyl chloroformate or with oxalyl chloride followed by the addition of sulfanilamide did not lead to desired product formation. Aniline-type of amines like sulfanilamide are not nucleophilic enough to form amide bonds using these activation methods with carboxylic acid **2**. However, the benzotriazole-ester which is formed when carboxylic acids are reacted with HATU, is very reactive. Therefore, similar to the synthesis of **51**, **2** was activated *in situ* using HATU, where upon the coupling worked smoothly (Scheme 34). Purification by silica gel column chromatography gave **52** in 80 % yield. Crystals were obtained by slow evaporation of a concentrated methanol solution.

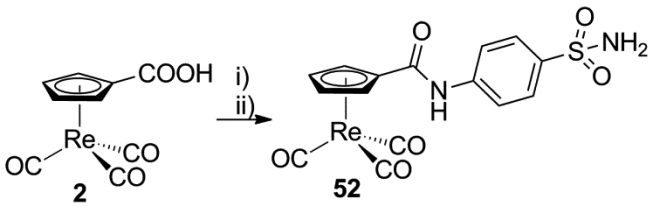

Scheme 34: Synthetic conditions: i) HATU, DMF. ii) Sulfanilamide, DMF, 80 %.

Structurally, **52** is very similar to **51** around the metal center. The sulfamate group in **51** is too far away from the Cp$^-$-chelator to cause significant differences in the properties of the metal complex. IR-υCO-frequencies (KBr) for **52** (2034 and at 1941 cm^{-1}) are thus similar to **51** (2030 and at 1941 cm^{-1}). Especially the asymmetric vibration is energetically higher than found for starting compound **2** (2032 and 1916 cm^{-1}) and confirms therefore the trend, that amide formation affects predominantly the asymmetric vibration frequencies.

The ^{1}H-NMR in DMSO-d_6 exhibited the typical two sets of *pseudo* triplets at a comparable range (6.51 and at 5.82 ppm) as **51**. However, unlike in **51**, the Phenyl protons in **52** were recorded isochronically at 7.80 ppm.

52 crystallized in the triclinic system with space group P-1. The amide group is almost coplanar with the η^5-coordinated Cp$^-$-ring (torsion angle C5-C4-C9-O4 of -0.1(4)°), whereas the phenyl ring is slightly twisted out of the plane (torsion angle C15-C10-N1-C9 of 18.1(4)°). The geometry around the rhenium(I) is distorted octahedral (Figure 28). The M-C (CO) bond lengths are in average shorter than the ones found for complexes **24a**/**b**, **27**, **45** and **51** and range from 1.900(4) to 1.906(4).

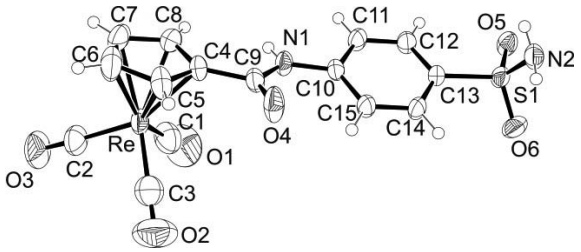

Figure 28: ORTEP plot of **52**: Important bond lengths (Å) and angles (°): Re(1)-C(1) 1.900(4), Re(1)-C(2) 1.901(4), Re(1)-C(3) 1.906(4), Re(1)-C(4) 2.291(3), Re(1)-C(5) 2.287(3), Re(1)-C(6) 2.299(3), Re(1)-C(7) 2.290(3), Re(1)-C(8) 2.293(3), C(1)-O(1) 1.139(4), C(2)-O(2) 1.138(4), C(3)-O(3) 1.148(4), C(13)-S(1) 1.766(3), N(2)-S(1) 1.605(3), O(5)-S(1) 1.4388(17), O(6)-S(1) 1.430(2), C(1)-Re(1)-C(2) 88.69(15), C(1)-Re(1)-C(3) 90.29(16), C(2)-Re(1)-C(3) 88.89(16), O(6)-S(1)-O(5) 118.09(11), O(6)-S(1)-N(2) 106.40(13), O(5)-S(1)-N(2) 107.25(12)

Mafenide, in contrast to sulfanilamide contains a methylene spacer between the aromatic moiety and the primary amine. It is not an aniline-type of amine and is more nucleophilic and reactive towards activated carboxylic acids. Therefore, the activation of **2** as a pentafluoro phenyl-ester, using PFPTFA, was chosen to form a mildly activated precursor.[63] Addition of mafenide, in presence of sufficient amount of triethylamine, resulted in the quantitative formation of sulfonmide **53**, which was purified by silica gel column chromatography (Scheme 35).

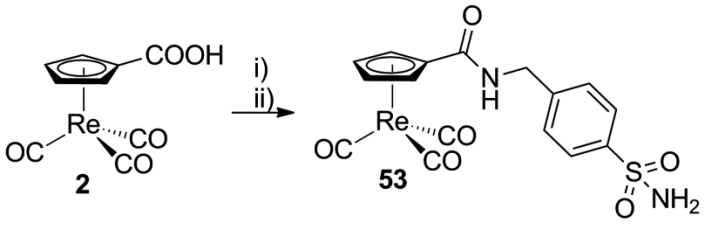

Scheme 35: Synthetic conditions: i) Pentafluorophenyl trifluoroacetate, DMF, 80 %. ii) Mafenide, DMF, 78 %.

The more electron donating nature of the methylene spacer in mafenide have an impact on the IR-υCO-frequencies of **53**, when compared to **51** or **52**. υCO-frequencies were observed at 2025 and at 1918 cm^{-1} (KBr), in contrast to **51** (2030 and 1941 cm^{-1}) or **52** (2034 and 1941 cm^{-1}). The same effect is observed in the ^{1}H-NMR (DMSO-d_6). The Cp$^-$-*pseudo* triplets of **53** were detected at 6.34 and at 5.75 ppm. This corresponds to a shift of 0.15 or 0.06 ppm (compared to **51**) and of 0.17 or 0.07 ppm (compared to **52**) towards higher field. In contrast to **52**, phenyl protons were not recorded isochronically.

In contrast to the CAIs discussed above, where the coupling function is directly bound to the Cp, a new way of altering the spacer in a BFC is introduced, when the building blocks **24a** or **27** respectively are used. With methylene groups between the Cp and the amide, variations before *and* after the coupling function are generated. This variation represents a new factor for interesting structure activity relationships (SARs).

54 and **55** both were synthesized along an analogous procedure to the preparation of **53** (Scheme 36). Product **54** was worked up by aqueous extraction and did not require further purification. Arylsulfonamide **55** needed additional purification by silica gel column chromatography. Both complexes were analysed by IR (KBr), NMR, ESI-MS and elemental analysis.

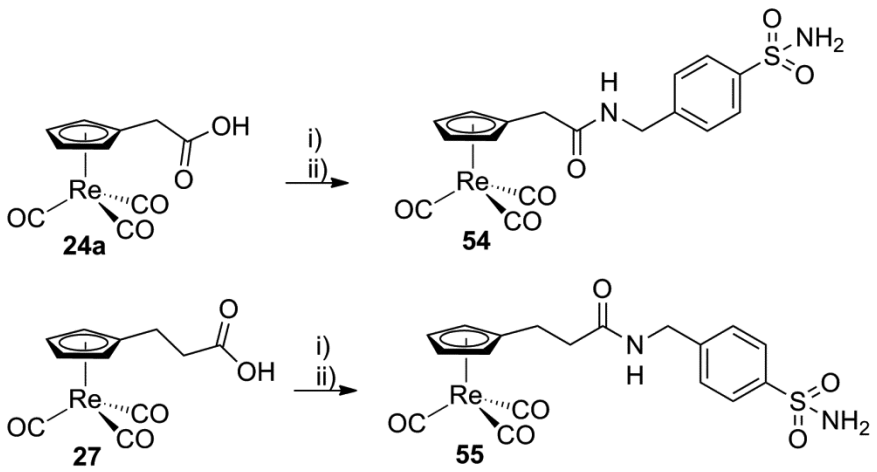

Scheme 36: Synthetic conditions: i) Pentafluorophenyl trifluoroacetate, DMF, 70-80 %. ii) Mafenide, DMF, 66-78 %.

Upon amide coupling, the asymmetric IR-υCO-band of **54** (1930 cm^{-1}) shifted towards higher frequencies, whereas the symmetric number did not change (2020 cm^{-1}), when compared to starting compound **24a** (2020 and 1911 cm^{-1}). In **55**, the distance between the metal center and the position of the amide coupling is larger than in **54**. Therefore, IR-υCO-frequencies do not shift substantially (2017 and 1911 cm^{-1} for **55** compared to 2023 and 1912 cm^{-1} for **27**).

The Ligands

As described above, the synthesis of a free HCp-NH_2 molecule was not achieved in the course of this thesis. Therefore, the synthesis of the uncoordinated ligand of **46** was not possible. However, the protonated dimers of the free ligands of the synthesized CAIs **51**-**53** were prepared. Depending on whether the nucleophile was an aniline-type of amine or not, Thiele's Acid was activated with oxalyl chloride (for **56** and **58**) or with PFPTFA (for **59**) (Scheme 37-39). In presence of triethylamine, the appropriate amine was added and the reaction progress was monitored by HPLC. **56** was purified by silica gel column chromatography. After treatment with sulfamoylchloride, **57** was isolated. **58** percipitated from the reaction mixture and was washed on a filter with fresh THF and a small portion of MeOH.

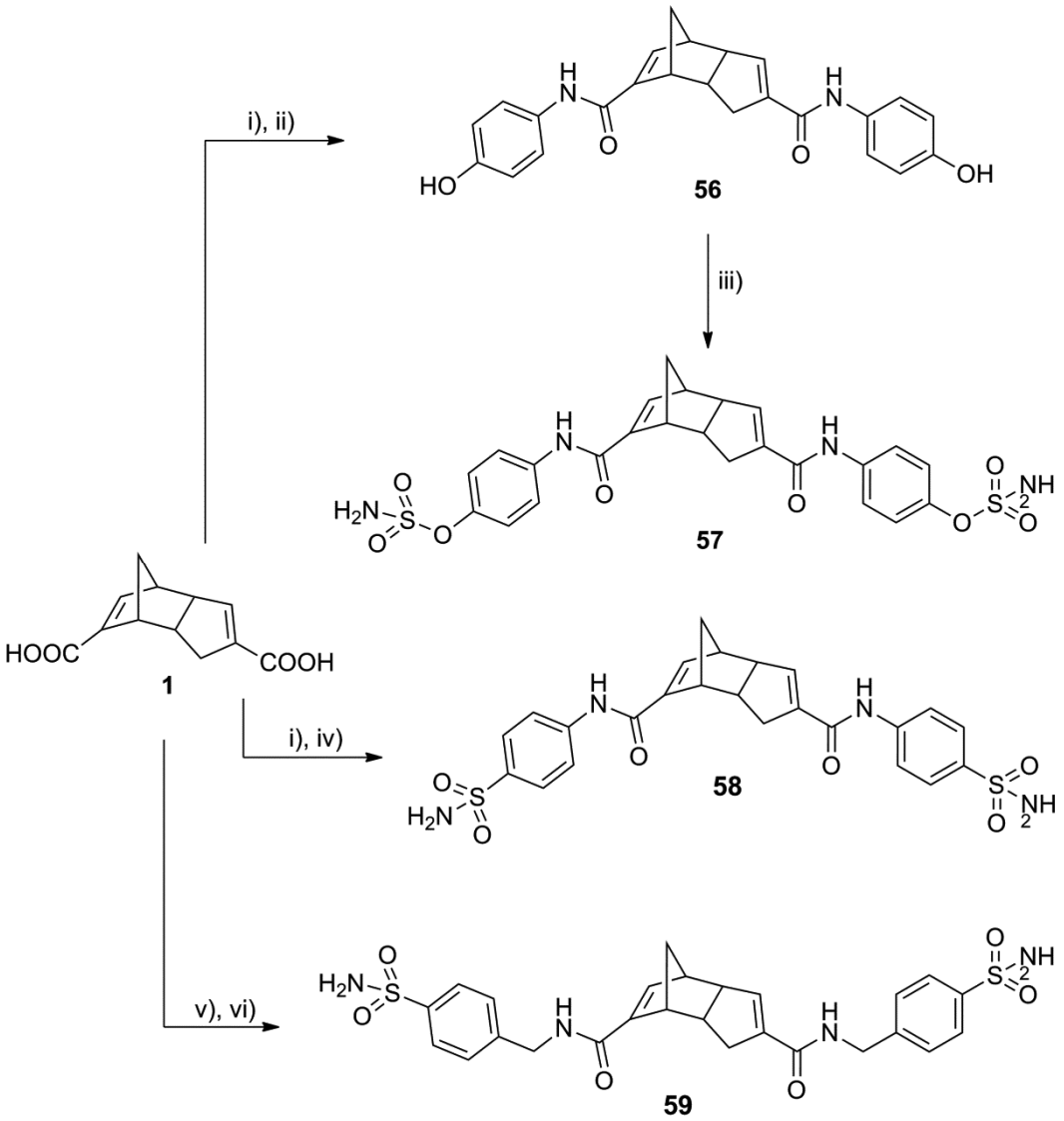

Scheme 37: Synthetic conditions: i) Oxalylchloride, CH_2Cl_2. ii) 4-Aminophenol, THF, 63 %. iii) Sulfamoylchloride, CH_2Cl_2, 89 %. iv) Sulfanilamide, THF, 43 %. v) Pentafluorophenyl trifluoroacetate, DMF, 88 %. vi) Mafenide, DMF, 90 %.

The Technetium Complexes

Surprisingly, **57** did not give the desired product, when reacted with $[^{99m}Tc(OH_2)_3(CO)_3]^+$ under our labeling conditions. The arylsulfamate-function is unstable under these reaction conditions, which leads to the degradation of the ligand. However, labeling with precursor **56** formed the corresponding product **60** in 72 % yield (Scheme 38).

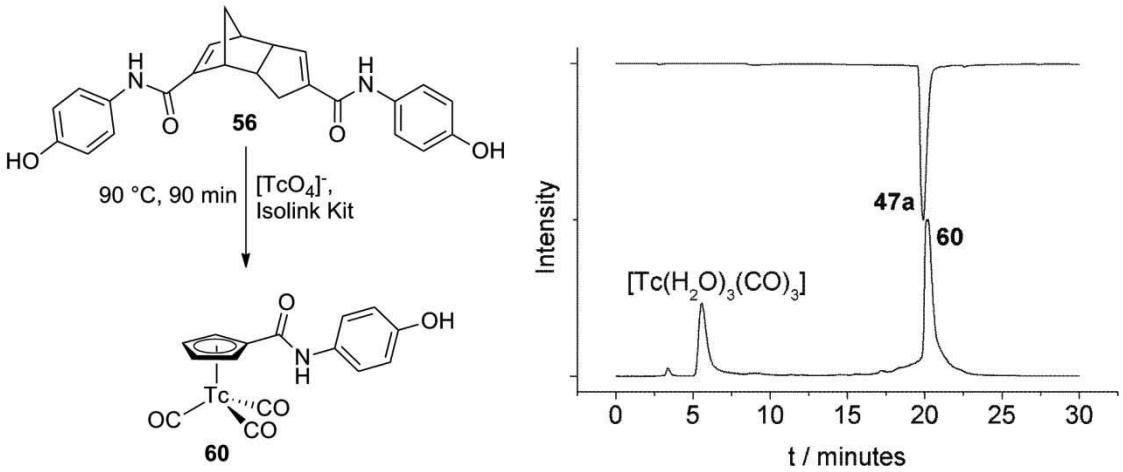

Scheme 38: Bottom-up trace: γ-trace of the one-pot labeling of **56** with $[^{99m}TcO_4]^-$ and Isolink Kit. Top-down trace: UV-trace of Re-compound **47a**. 27 % of the activity was observed as unreacted $[Tc(CO)_3(OH_2)_3]^+$ and 1 % as $[TcO_4]^-$.

In contrast to the arylsulfamate-functionality, the arylsulfonamide-group was stable under labeling conditions. The ^{99m}Tc analogues of **52** and **53**, namely **61** and **62** were prepared. No degradation was observed. The authenticity of the products was assessed by comparing the HPLC retention times of **52** with **61** and **53** with **62** (Scheme 39 and 40).

The one-pot reactions with $[^{99m}TcO_4]^-$ gave nearly quantitative yields at 90 °C after 60-90 minutes. Two-step procedures, where The $[^{99m}Tc(OH_2)_3(CO)_3]^+$ precursor is prepared in advance, works equally well. Ligands **58** and **59** were present in millimolar concentrations. No sideproducts were observed during the labeling procedure.

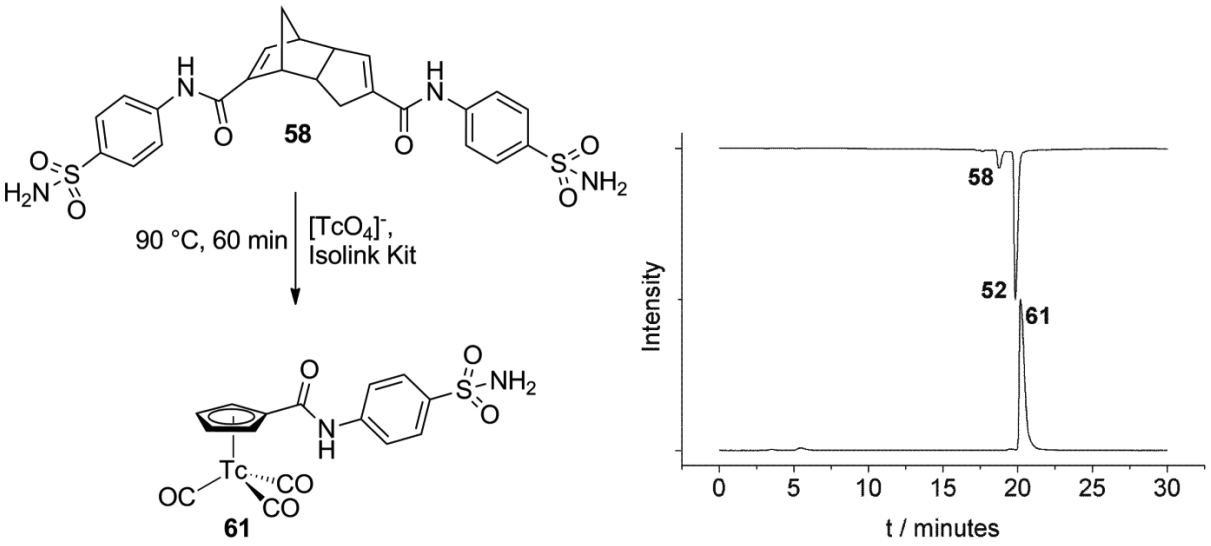

Scheme 39: Bottom-up trace: γ-trace of the one-pot labeling of **58** with $[^{99m}TcO_4]^-$ and Isolink Kit. Top-down trace: UV-trace of Re-compound **52**.

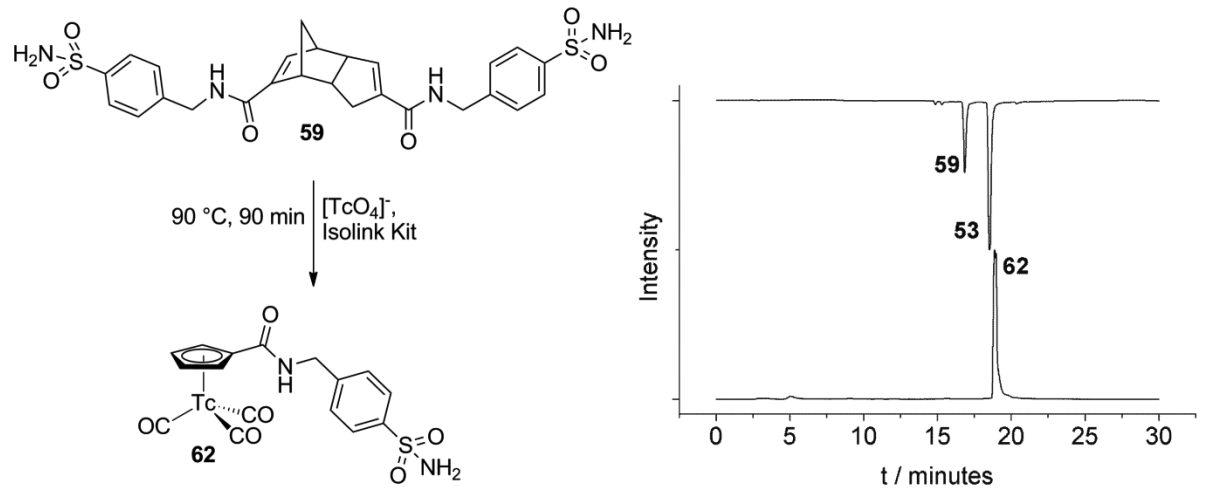

Scheme 40: Bottom-up trace: γ-trace of the one-pot labeling of **59** with $[^{99m}TcO_4]^-$ and Isolink Kit. Top-down trace: UV-trace of Re-compound **53**.

In Vitro Binding Affinities

Binding studies of complexes **46** and **51**-**55** with 12 CA isozymes showed inhibition constants in the low nanomolar range for some of the isoforms (Table 2).

Such low K_i values are uncommon for bioorganometallic compounds or radiopharmaceuticals.[113] The hCA II, VI, VII, IX, XII and XIII are considered as sulfonamide- and sulfamate-avid isoforms[101] which is consistent with the observed values for inhibitors **46** and **51**-**55**. It should be noted that the K_i values reported here for the various isoforms compare well to those of the AZA standard and are for some isoforms even better. In addition, distinct selectivity for hCA IX, XII and XIV over the other isoforms was observed. The K_i ratios (hCA II/hCA IX) of 4.0 (for **53**) or 7.0,

respectively (for **51** and **52**), indicate a clear preference for hCA IX, overexpressed in certain tumors, over the physiologically dominant hCA II. In contrast, **54** and **55** do not show a preference of hCA IX over hCA II. Compound **46** showed the most pronounced selectivity pattern (solid line in Figure 29) and strongly favors hCA II, IX, XIV. Compounds **51**-**53** all behave similarly, K_i values of the standard acetazolamide (AZA) do not show such a distinct preference pattern for any of the isoforms. It has only a slightly higher affinity for hCA II over hCA IX (hCA II/hCA IX = 0.5).

Inhibition constants found for **46** and **51**-**53** are, thus, in the same range as found for organic inhibitors[101] but much better than those reported for the aforementioned two organometallic CA inhibitors,[111, 112] indicating smaller and more compact [(Cp-R)M(CO)$_3$] (M = Re or ^{99m}Tc) to be favored over more bulky metal complexes.

Table 2: Inhibition data of complexes **46** and **51**-**53** against selected CA isozymes in comparison with acetazolamide (AZA). [a] Data was determined by the CA-catalyzed hydration of CO_2.

	K_i (nM)[a]						
Compound	**46**	**51**	**52**	**53**	**54**	**55**	**AZA**
CAI	39	2570	4590	2775	288	246	250
CAII	15.1	27.4	35.5	25.3	4.5	6.2	12
CAIV	467	32.9	41.1	33.8			74
CAVA	481	113	124	109			63
CAVB	305	105	104	102			54
CAVI	497	10.6	22.1	14.5			11
CAVII	360	7.6	21.3	10.1			2.5
CAIX	43	3.7	5.2	7	3.8	4.7	25
CAXII	6.7	4.5	6.9	4.4	42.7	59.8	5.7
CAXIII	482	62.1	78.5	56.8			17
CAXIV	20.1	4.1	7.9	5.4			41
CAXV	313	28.4	36.8	12.5			72

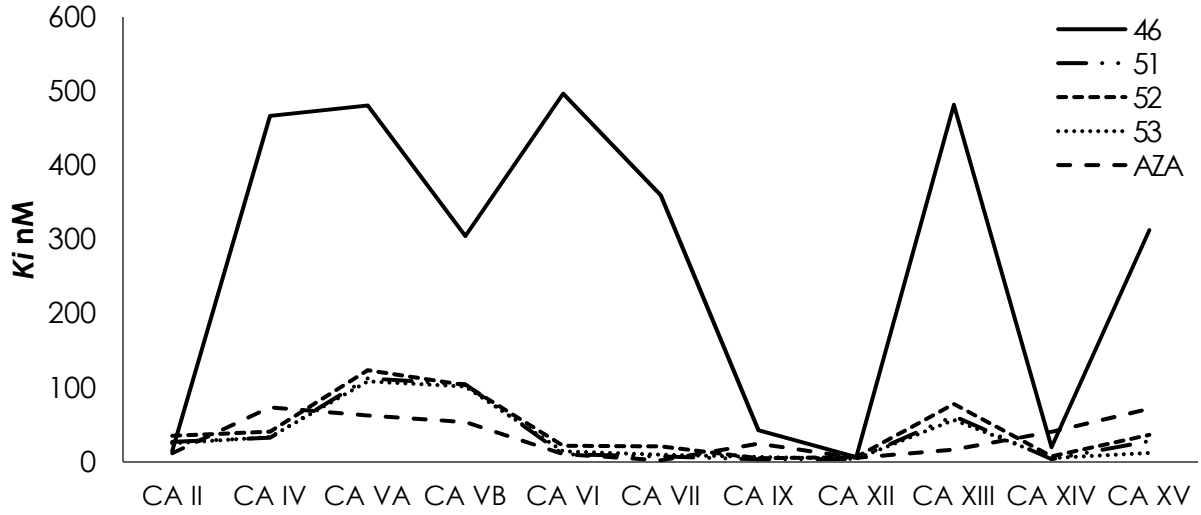

Figure 29: Graphical representation of K_i values of compounds **46** and **51**-**53** for selected isozymes of hCAs.

In Vitro pH-Studies

CAs are amongst the most effective catalysts known in biological systems (k_{cat}/K_M > 10^8 M^{-1}).[102] Due to increased carbonic acid formation, the high activity of hypoxia-induced, overexpressed CAs leads to a remarkable extracellular pH drop in tumor tissue (to ≈ 6 as compared to 7.4 in normal tissues).[101, 111, 114, 115] Consequently, strong CA inhibition will reduce acidification. To confirm this hypothesis, hCA IX-induced extracellular acidification was quantified before and after exposure to the inhibitors ***52*** and ***53.*** The three different human carcinoma cell models cervical adenocarcinoma HeLa, breast adenocarcinoma MDA MB 231 and colon adenocarcinoma HT29 were studied. This panel of cell lines was assessed by western blot for the levels of hCA IX expression under normoxic and hypoxic conditions (Figure 30). The HeLa and HT29 carcinoma cells showed elevated levels of hCA IX under hypoxic conditions while MDA MB 231 did not. Only HT29 cells expressed hCA IX under normoxic conditions, albeit at a lower amount than under reduced oxygen levels. This basal expression in HT29 cells is not surprising, and might be caused by the cluster shaped growth of these cells.

In order to minimize potential cytotoxicity of the complexes, extracellular acidification experiments were performed at a 0.5 mM concentration of the Re complexes ***52*** and ***53***. Hypoxic incubation of HeLa and HT29 cells led to the expected extracellular acidification by about 0.5 to 0.7 pH units, caused by

overexpression of hCA IX. Under normoxic conditions, a pH drop of only about 0.1 for HeLa (no overexpression) and 0.2 for HT29 (slight expression) was found.

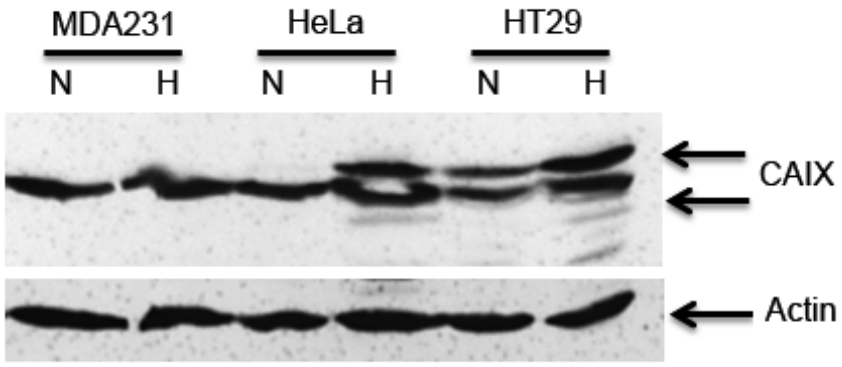

Figure 30: Western blot analysis of hCA IX expression in normoxic N (21 % O_2, 24 h) and hypoxic H (1 % O_2, 24 h) MDA MB 231, HeLa and HT29 carcinoma cells using a polyclonal hCA IX antibody. Actin was used as loading control.

The presence of the reference inhibitors mafenide and sulfanilamide under hypoxia caused a significant reduction of extracellular acidification; more pronounced for HeLa than for HT29 cells (Figure 31A compare with 31C). The Re complexes **52** and **53** showed a distinct reduction of extracellular acidification, in hypoxia comparable or even better than the organic compounds, confirming CA IX inhibition. The normoxic extracellular pH was not significantly affected by incubation with either compound, indicating a specific interaction with hCA IX. In agreement with the lack of hCA IX expression, MDA MB 231 cells did not show a pH difference for cells grown under normoxic or hypoxic conditions.

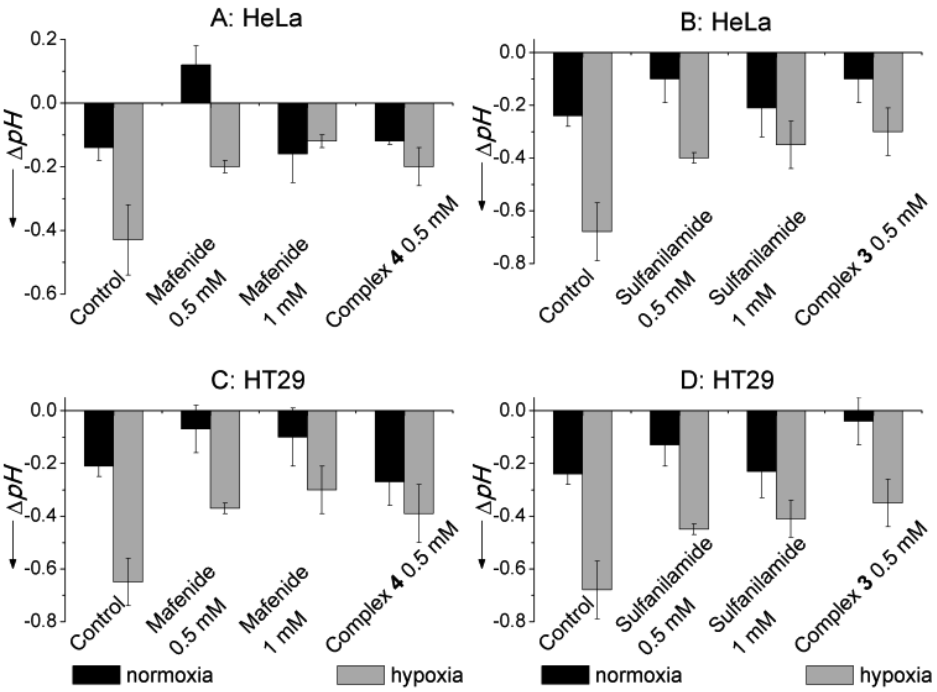

Figure 31: Effect of the reference sulfonamides and compounds **52** and **53** on the reduction of extracellular acidification in HeLa and HT29 cell lines. Cells were incubated for 24h. Data show the mean ± S.D. of 4 replicates and are plotted as difference between pH_e values (delta pH = $pH_{after\ incubation}$ − $pH_{before\ incubation}$) measured in absence (control) or in presence of the sulfonamides.

Protein Crystallization

In order to assess the binding mode of the Re-based CAIs with proteins, crystals of hCA II were grown by "hanging drop" vapor diffusion. The crystals were then soaked with the respective inhibitor and gave diffraction data until 1.2 Å resolutions. The electron density of the complete complex **53** could be traced, confirming its localization in the binding pocket of hCA II. An electron density map of the binding pocket is shown in Figure 32A. The binding mode is reminiscent to the arrangement as seen in other hCA II structures.[116, 117] Avvaru et al. defined two binding pockets I and II for elongate hCA II inhibitors.[118] Complex **53** binds in the hydrophobic pocket II (SI). The deprotonated nitrogen of the arylsulfonamide terminus coordinates to the Zn-atom of the active site (Figure 32B). The major conformation of the [(Cp)Re(CO)$_3$] unit, including the amide linker, does not interact with either the protein or water molecules. However, there is a hydrophobic interaction between the [(Cp)Re(CO)$_3$]-moiety and the hydrophobic part of Phe131, Leu198 and Pro202. Further details are given in the supporting material.

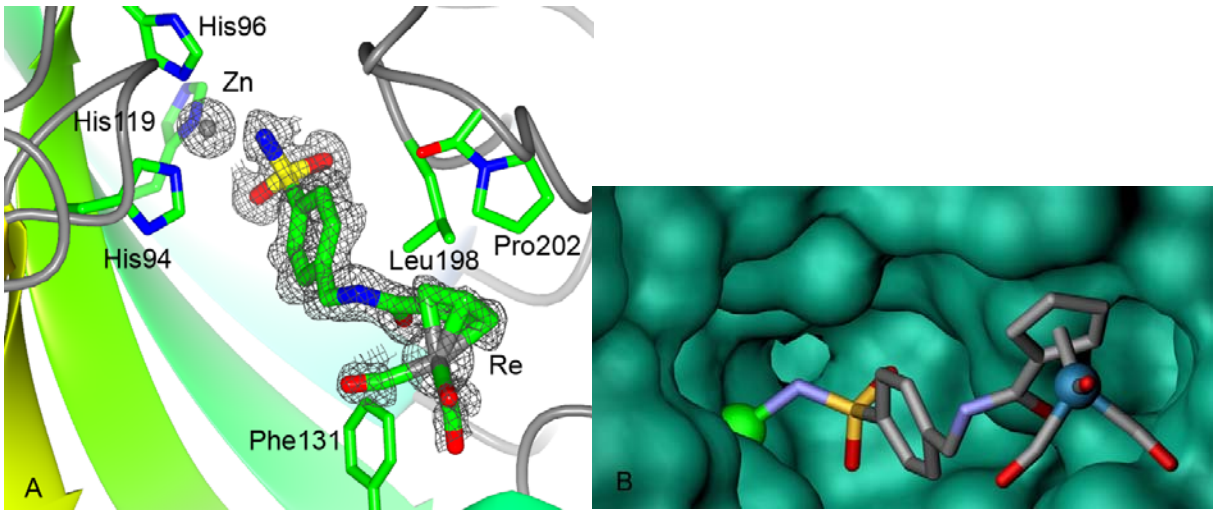

Figure 32: A: Crystal structure of **53** bound to hCA II (only major conformation of **53** shown) A: Electron density map of **53**, superimposed with the stick-model of the inhibitor bound to the active site of hCA II. Hydrophobic interactions can be observed between the [(Cp)Re(CO)$_3$]-moiety and Phe131, Leu198, and Pro202. B: Detail of the binding cavity of hCA II with **53**. The Zn atom is shown as a green sphere.

In Vivo Biodistribution

In vivo accumulation of **61** and **62** in HT-29 tumors was evaluated at 1h and 4h *post* injection (Table 3 and 4).

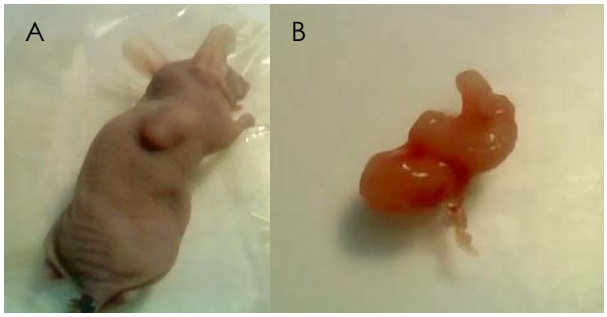

Figure 33: A) Balb/C nude mouse bearing HT-29 colorectal tumor after 14 days of inoculation. Animals were previously s.c inoculated with 107 HT-29 colon carcinoma cells ressuspended in 50 % Matrigel. B) HT29 tumor removed from mouse of image A).

Table 3: Biodistribution of **61** in BaLb/C nude mice with human HT-29 colon carcinoma (n = 3).

Tissue/organ	% ID/g ± SD	
	1h	**4h**
Tumor	**0,70± 0,12**	**0,36 ± 0,12**
Blood	25,54 ± 12,05	7,39 ± 6,82
Liver	23,59 ± 3,19	55,84 ± 4,92
Intestine	3,08 ± 0,25	10,39± 6,17
Spleen	9,51 ± 2,69	7,03 ± 5,63
Heart	9,02 ± 4,54	0,99 ± 0,74

Lung	6,36± 2,67	3,11 ± 2,55
Kidney	13,13 ± 0,90	5,57 ± 4,19
Muscle	1,23 ± 0,10	0,50 ± 0,41
Bone	2,06 ± 0,13	1,26 ± 0,88
Stomach	5,18 ± 1,99	6,51 ± 2,92
Pancreas	1,71± 0,00	0,97 ± 0,79
Total excretion	**4,9 ± 0,1**	**3,5 ± 1,0**

Table 4: Biodistribution of **62** in BaLb/C nude mice with human HT-29 colon carcinoma (n = 3).

Tissue/organ	% ID/g ± SD	
	1h	**4h**
Tumor	**0,47± 0,02**	**0,12 ± 0,04**
Blood	2,29 ± 0,01	0,24 ± 0,01
Liver	44,1 ± 1,5	35,5 ± 6,4
Intestine	9,6 ± 0,3	12,6 ± 1,0
Spleen	2,77 ± 0,20	0,11 ± 0,02
Heart	0,75 ± 0,27	0,07 ± 0,01
Lung	0,93± 0,21	0,14 ± 0,04
Kidney	1,81 ± 0,06	0,54 ± 0,04
Muscle	0,50 ± 0,06	0,05 ± 0,01
Bone	0,55 ± 0,01	0,06 ± 0,01
Stomach	1,83 ± 0,49	1,34 ± 0,39
Pancreas	0,37± 0,13	0,07 ± 0,00
Total excretion	**0,47 ± 0,99**	**18,0 ± 2,4**

The compound **62** was moderately cleared from the bloodstream and major organs (0.24±0.01 %IA/g, 4h p.i.), except the excretory organs. The slow overall excretion (only 18 % after 4h p.i.) and the very high levels of activity in liver and intestine (about 78 % of the activity at 4h p.i) indicate the hepatobiliar route as the principal path for the elimination of **62**. This is in accordance with the lypophilic character of the radioconjugate (log $P_{o/w}$=1.7). More unfavorable pharmacokinetic profile was observed for the radioconjugate **61**. The blood clearance and whole-body excretion of **61** was very slow with a negligible fraction of the radioactivity excreted via renal (urinary) route at 4h p.i. (about 4 %). The accumulation of **61** in the hepatobiliary tract was again very high, indicating the importance of this path for the elimination of these radioconjugates and again correlating well with the log $P_{o/w}$ value of 2.3. A significant non-specific accumulation was also observed for other non-excretory

organs such as spleen, stomach and lungs. The stomach uptake could be an indication for some in vivo oxidation of the complex to $[^{99m}TcO_4]^-$.

Tumor uptake was minimal (negligible) for both complexes. However, tumor-to-blood ratios slightly increased as a function of time (**61**: 0.2 and 0.5; **62**: 0.03 and 0.05, at 1h and 4h p.i., respectively). Western blotting analysis was performed to confirm the expression levels of CAIX in the tumors.

CAIX Expression in Tumor Xenografts of Human Carcinoma Cell Lines

While HT29 cells showed intermediate expression levels of CAIX under normoxia, tumors showed elevated levels of expression indicating hypoxia conditions (Figure 34).

Considering the encouraging results obtained during the in vitro affinity studies using Re-complexes **52** and **53** for CAIX (K_i: 5.2 and 7 nM, respectively), the negligible uptake of the respective ^{99m}Tc-labeled compounds in CAIX-expressing HT-29 tumors was unexpected. The low accumulation of **61** and **62** in tumors could be due to low expression levels of the active form of CAIX in the tumor. It has been shown, that for efficient binding of sulfonamides to CAIX not only its expression but also its activation is required.[119] Furthermore, tumor biology in vivo with its complexity of microenvironments and with dynamic changes of oxygen gradients at variable episodes resulting in an imbalance in hypoxia, can differ from the in vitro conditions.

In summary, these results show the increasing but low uptake of ^{99m}Tc-complexes **61** and **62** in the tumor, despite of the remarkably low Ki values and significant expression of CAIX in HT29 tumors.

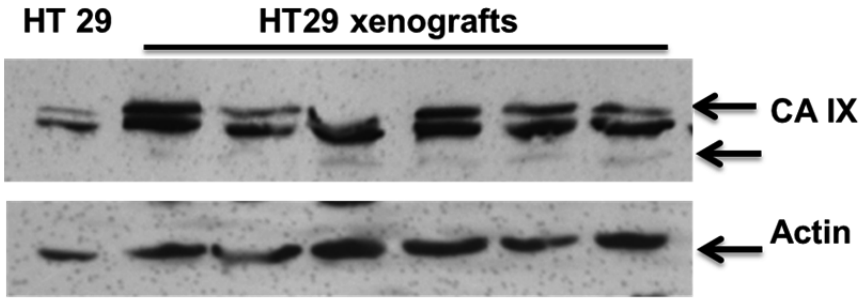

Figure 34: Western blot analysis of CA IX expression in tumor xenografts of HT29 carcinoma cells using a polyclonal CA IX antibody. Actin was used as loading control.

In conclusion, six new piano-stool Re-complexes with pendent arylsulfonamides, -sulfamides or –sulfamates were synthesized. They inhibit CAs with nanomolar affinities. Particularly strong inhibition was found for the pharmaceutically relevant isozymes hCA IX and hCA XII. Compound **46** exhibited superior CA isoform selectivity than the AZA standard. Enhanced receptor selectivity due to better 3-D space occupation is one crucial preponderance of bioorganometallic compounds. For molecular imaging purposes, the ^{99m}Tc homologues of **52** and **53** were synthesized. Inert bioorganometallic ^{99m}Tc and Re compounds behave biologically identical, thus, these potent CAIs can be applied in combination with each other, macroscopic amounts of Re for therapy and microscopic amounts of the ^{99m}Tc analogues for diagnosis, according to the theragnostic concept.

In order to assess the binding mode of the Re-based CAIs with proteins, crystals of hCA II were grown and soaked with inhibitor **53**. The electron density of the complete complex **53** could be traced, confirming its localization in the binding pocket of hCA II and showing hydrophobic interaction between the [(Cp)Re(CO)$_3$]-moiety and the hydrophobic part of Phe131, Leu198 and Pro202.

In vivo accumulation of the ^{99m}Tc-compounds **61** and **62** in BaLb/C nude mice with human HT-29 colon carcinoma was evaluated at 1h and 4h *post* injection. Slow overall excretion and high levels of activity in liver and intestine indicate the hepatobiliar route as the principal path for the elimination of the two CAIs. This is in accordance with the lypophilic character of the radioconjugates (log $P_{o/w}$=1.7 for 62 or 2.3 for **61** respectively). Tumor uptake was negligible for both complexes. However, tumor-to-blood ratios slightly increased as a function of time (**61**: 0.2 and 0.5; **62**: 0.03 and 0.05, at 1h and 4h p.i., respectively).

The stomach uptake could be an indication for some in vivo oxidation of the complex to [^{99m}TcO$_4$]$^-$. Apart from this, the compounds were found intact in the urine and in the blood, pointing out the stability of the complexes.

The high lipophilicity of the compounds caused a relatively high uptake of the compounds into red blood cells. Designing the inhibitors more hydrophilically might therefore improve tumor uptake.[111]

2.3.3 Organometallic Antibiotics

Besides the carbonic anhydrase inhibitors, sulfonamides are an important class of agents, which have pioneered the antimicrobial therapy. Nowadays, these compounds are often applied in combination with other antibiotics, in order to decrease the development of resistance and in order to increase the potency of therapies.[120] Their mechanism of action is related to the inhibition of the bacterial dihydropteroate synthase, catalysing the folic acid synthesis.[121] Structurally, many of these molecules are based on a *p*-amino-benzol-sulfonamide scaffold, which can contain different substituents bound to the sulfonamide moiety (Figure 35). Organometallic analogs of known antibiotics might cause decreased resistance development properties in bacteria. The corresponding ^{99m}Tc-complexes could serve as imaging agents for bacterial infections.

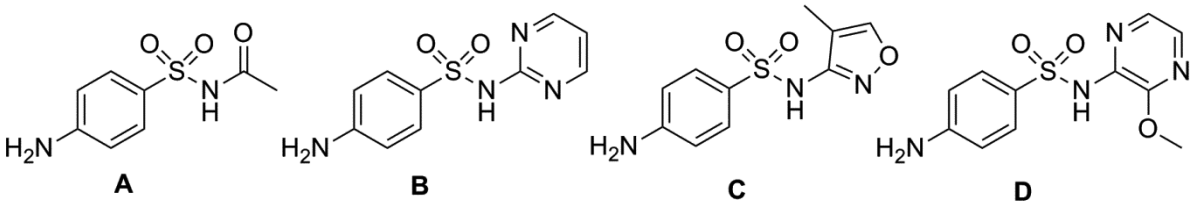

Figure 35: Lewis structures of selected commercialized antibiotics. A) Sulfacetamide, B) Sulfadiazine, C) Sulfamethoxazol, D) Sulfalen.

The Rhenium Complexes I

Depending on the position where the metal complex is introduced, two different approaches were followed for the investigation of organometallic antibiotics with internal sulfonamide moiety. Starting from the sulfonyl-Cp-complex **4**, the replacement of the *p*-amino-benzene-moiety in sulfadiazine and in sulfamethoxazol by the organometallic [(Cp)Re(CO)$_3$]-complex was intended (Figure 36).

As shown with a few examples in figure 35, for sulfonamide antibiotics numberous derivatives can be introduced while keeping the *p*-amino-benzol-sulfonamide scaffold intact. Therefore, another possibility to incorporate the Re-complex is to replace this substituent which is bound opposite to the *p*-amino-benzol-sulfonamide. Following the later strategy, intermediate **45**, which was described in section 2.2.2, was investigated for this purpose (Figure 36).

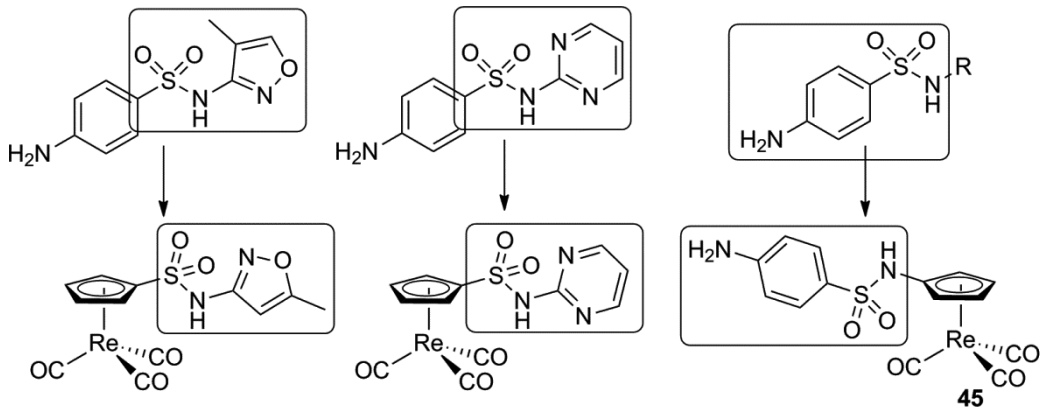

Figure 36: Lewis structure of possible organometallic antibiotics with internal sulfonamide moiety. Either the *p*-amino-benzene-moiety or the R group can be replaced by the metal complex.

A THF-solution of **5** was mixed with 3-amino-5-methylisoxazole or with 2-aminopyrimidine respectively. The mixture was gently heated to 40 °C over night. The main products were purified by silica gel column chromatography to form colourless solids. They were analysed by ^{1}H-NMR, IR (KBr) and crystal structure determination. Crystals were grown by slow diffusion of hexane into a solution of the corresponding compound dissolved in a minimum of CH_2Cl_2. Unfortunately, the condensation of 3-amino-5-methylisoxazole or of 2-aminopyrimidine, with the sulfonyl chloride **5** did not lead to the anticipated products (Scheme 41 and 42). During the reaction the η^5-Cp-complex is degraded and complexes **63** or **65** respectively are formed. Interestingly, as a side product, the free HCp-ligand **64** was also isolated after silica gel column chromatography.

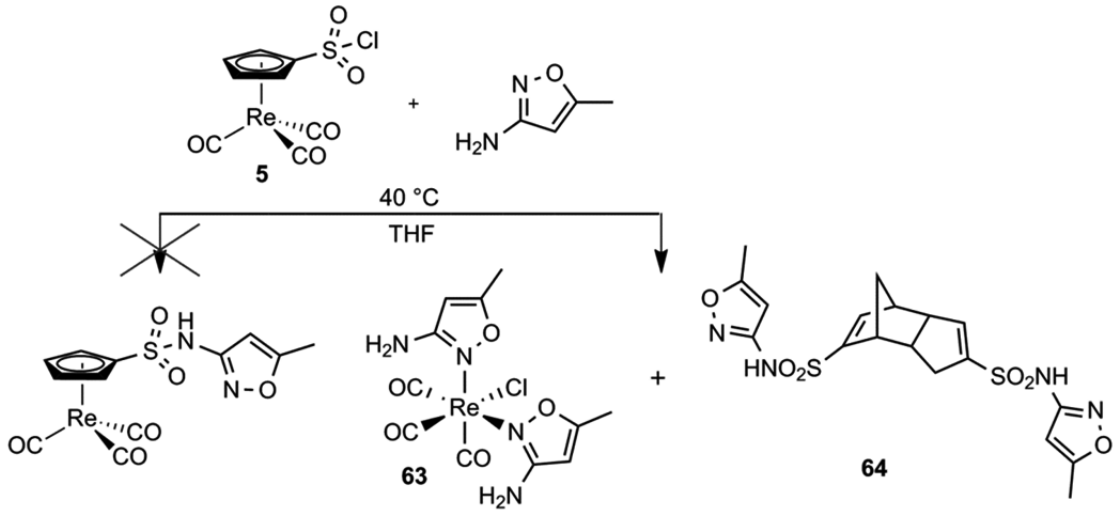

Scheme 41: Decomplexation of **5** upon treatment with 3-amino-5-methylisoxazole. The ligand with the sulfonamide group on the HCp was isolated as a dimer.

The crystallization solution of **63** contained a small amount of DMSO, therefore one DMSO molecule was found in the asymmetric unit. **63** crystallized as colourless plates and in the triclinic crystal system with space group P-1. The geometry around the metal center is slightly distorted octahedral, with angles between neighbouring ligands close to 90°. The M-C (CO) bond lengths range from 1.908(3) to 1.920(3). The C-O bond distances of the carbonyl ligands of **63** (1.147(3)-1.155(3) Å) compare very well to those found for the η^5-Cp-complexes discussed in other sections of this thesis. The bond length between the central rhenium to the coordinating nitrogen of the 3-amino-5-methylisoxazole is 2.1758(17) Å in average and to the chloride 2.5060(6) Å.

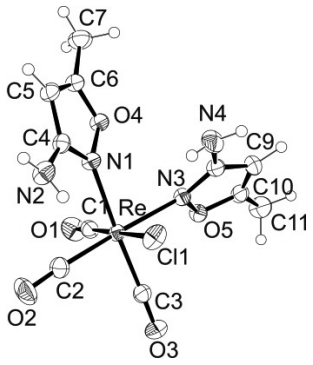

Figure 37: ORTEP plot of **63**: Important bond lengths (Å) and angles (°): Re(1)-C(1) 1.899(2), Re(1)-C(3) 1.913(2), Re(1)-C(2) 1.915(2), Re(1)-N(1) 2.1696(17), Re(1)-N(3) 2.1820(18), Re(1)-Cl(1) 2.5060(6), C(1)-O(1) 1.155(3), C(2)-O(2) 1.147(3), C(3)-O(3) 1.150(3), C(1)-Re(1)-C(3) 87.45(10), C(1)-Re(1)-C(2) 87.96(10), C(3)-Re(1)-C(2) 86.80(10), C(1)-Re(1)-N(1) 95.36(8), C(3)-Re(1)-N(1) 176.67(8), C(2)-Re(1)-N(1) 95.06(9), C(1)-Re(1)-N(3) 93.81(8), C(3)-Re(1)-N(3) 91.34(8), C(2)-Re(1)-N(3) 177.37(8), N(1)-Re(1)-N(3) 86.71(7), C(1)-Re(1)-Cl(1) 178.16(7), C(3)-Re(1)-Cl(1) 93.76(7), C(2)-Re(1)-Cl(1) 90.72(8), N(1)-Re(1)-Cl(1) 83.47(5), N(3)-Re(1)-Cl(1) 87.55(5).

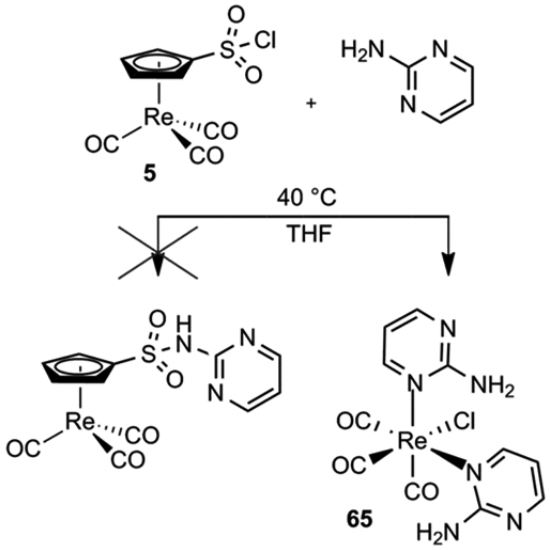

Scheme 42: Decomplexation of **5** upon treatment with 2-aminopyrimidine. The corresponding ligand was not isolated in this case.

64 crystallized as orange plates and in the monoclinic crystal system P21/c. The geometry around the metal center is distorted octahedral, with angles between neighbouring ligands close to 90°. The chloride Cl1 is disordered with the carbonyl ligand C3B-O3B. The M-C (CO) bond lengths are almost identical to those in compound **63** and range from 1.902(3) to 1.920(6). The C-O bond distances of the carbonyl ligands of **64** are within 1.132(6) and 1.150(4) Å. The bond length between the central rhenium to the coordinating nitrogen of the 2-aminopyrimidine is 2.232(2) Å in average and to the chloride 2.4747(16) Å.

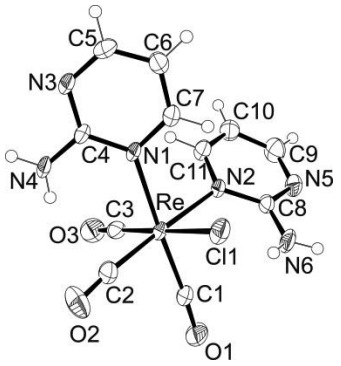

Figure 38: ORTEP plot of **65**: Important bond lengths (Å) and angles (°): Re(1)-C(2) 1.902(3), Re(1)-C(1) 1.918(3), Re(1)-C(3) 1.920(6), Re(1)-C(3B) 1.926(19), Re(1)-N(1) 2.228(2), Re(1)-N(2) 2.235(2), Re(1)-Cl(1B) 2.372(10), Re(1)-Cl(1) 2.4747(16), C(3)-O(3) 1.132(6), O(3B)-C(3B) 1.23(3), C(1)-O(1) 1.144(4), C(2)-O(2) 1.150(4), C(2)-Re(1)-C(1) 84.98(13), C(2)-Re(1)-C(3) 88.97(18), C(1)-Re(1)-C(3) 87.59(18), C(2)-Re(1)-C(3B) 89.3(15), C(1)-Re(1)-C(3B) 91.1(14), C(3)-Re(1)-C(3B) 177.9(15), C(2)-Re(1)-N(1) 97.26(11), C(1)-Re(1)-N(1) 177.30(11), C(3)-Re(1)-N(1) 93.94(15), C(3B)-Re(1)-N(1) 87.4(14), C(2)-Re(1)-N(2) 177.30(11), C(1)-Re(1)-N(2) 92.35(11), C(3)-Re(1)-N(2) 90.57(16), C(3B)-Re(1)-N(2) 91.1(15), N(1)-Re(1)-N(2) 85.43(9), C(2)-Re(1)-Cl(1B) 94.0(3), C(1)-Re(1)-Cl(1B) 88.5(3), C(3)-Re(1)-Cl(1B) 5.0(3), C(3B)-Re(1)-Cl(1B) 176.7(15), N(1)-Re(1)-Cl(1B) 92.9(2), N(2)-Re(1)-Cl(1B) 85.6(2), C(2)-Re(1)-Cl(1) 90.10(11), C(1)-Re(1)-Cl(1) 93.63(11), C(3)-Re(1)-Cl(1) 178.40(14), C(3B)-Re(1)-Cl(1) 2.6(14), N(1)-Re(1)-Cl(1) 84.88(7), N(2)-Re(1)-Cl(1) 90.42(7), Cl(1B)-Re(1)-Cl(1) 175.6(2).

Even though the homologous ligand from the degradation with 2-aminopyrimidine was not isolated, it was concluded from this observation, that in both reactions the desired product might have been formed in a first step. 3-Amino-5-methylisoxazole and 2-aminopyrimidine both contain a tertiary nitrogen atom in the hetero cycle, which is placed in δ-position relative to the Cp-ring, after the condensation reaction (Figure 39). From this position, its lone pairs can interact with the large orbitals of the rhenium metal and compete therefore with the Cp^- as a donor and finally lead to decomplexation (Figure 39). The sulfone, as an electron withdrawing group, supports this decomplexation by destabilizing the complex. The naked *fac*-{$Re(CO)_3$} core is then rapidly trapped by free donors like 3-Amino-5-methylisoxazole or 2-aminopyrimidine respectively. This assumption is supported by the fact that the

chlorine was substituted from the sulfone during the reaction and is found coordinated to the Re-center.

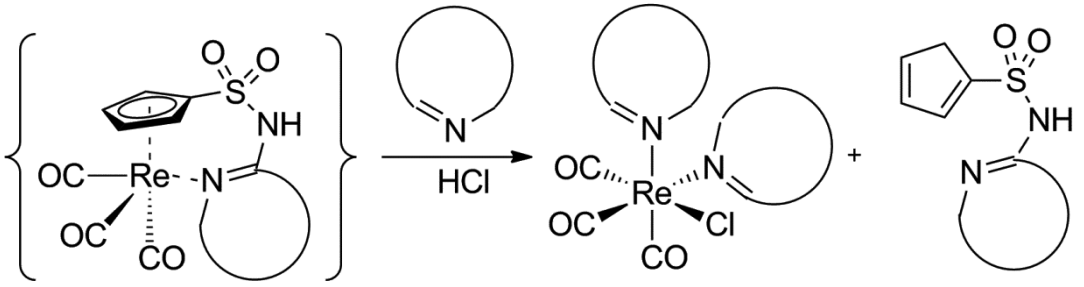

Figure 39: Decomplexation of the sulfonyl-Cp-complexes.

The two complexes showed the IR-υCO-frequencies at 2023 and 1915 cm^{-1} (for **63**) or at 2025 and 1916 cm^{-1} (for **65**) respectively. Comparing with $[Re(Br)_3(CO)_3]$ (1999 and 1868 cm^{-1}), these values indicate much shorter C-O bond lengths. This can be expected, as $[Re(Br)_3(CO)_3]$ has three negatively charged ligands in the coordination sphere. The bromides can transfer more electron density to the metal and stimulate π-backbonding to the carbonyls, whereas **63** and **65** both have only one Cl^- coordinated. The two heterocycles complete the coordination sphere in each complex.

The ^{1}H-NMR of **63** (DMSO) shows a singlet at 6.30 ppm for the isochrone amine protons. Another singlet at 5.85 ppm indicates the olefinic protons. The methyl groups are detected as a singlet at 2.27 ppm. In the ^{1}H-NMR of **65** (DMSO) the aromatic protons are observed in three sets of a doublet times doublet patterns at 8.17 ppm, at 6.84 ppm and at 6.71 ppm respectively. It can be assumed from the pattern of the ^{1}H-NMR, that both heterocycles in both compounds are equivalent.

The isolated ligand **64** revealed in the ^{1}H-NMR (CD_3CN) olefinic multiplets at 6.42 ppm, at 6.18 ppm, 6.05 ppm, 6.04 – 6.02 ppm and at 5.71 ppm respectively, clearly indicating the presence of an isomeric mixture.

The synthesis of compound **45** was discussed in section 2.2.2. This compound was assessed in a simple test for antibiotic activity on escheria coli bacteria. For this purpose, agar solutions were prepared in presence of 0, 50, 100 or 250 μg/ml of complex **45** and filled into petri dishes. The plates were charged with escheria coli bacteria, incubated at 37 °C for 24 to 48 h, and the number of colonies per plate was counted. The results clearly show a decreasing number of colonies with

increasing concentration of the compound **45** and indicate therefore a moderate antibiotic activity (Figure 40). No reference compounds were used for comparison with these results.

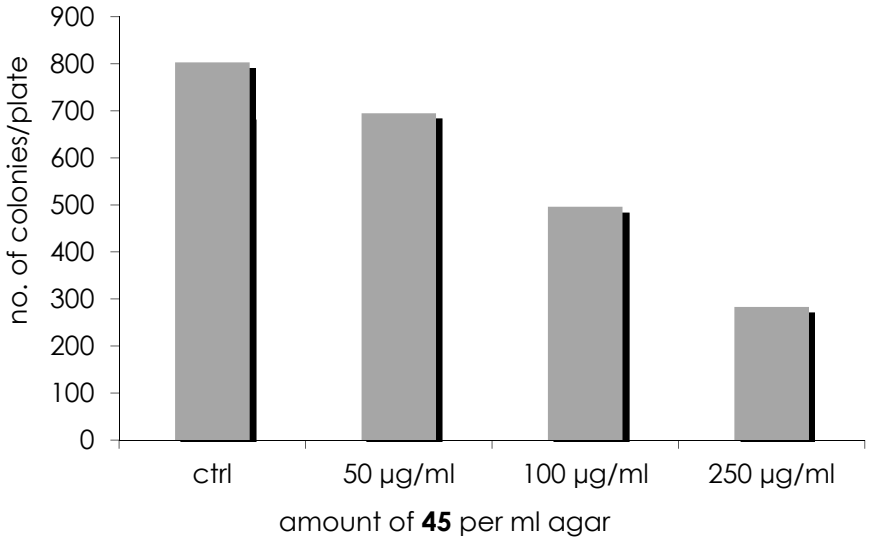

Figure 40: Antibiotic effect of compound 45 on escheria coli.

Another class of well-known antibiotics are penicillins, which are derivatives of the 6-aminopenicillanic acid (6-APA).[120] Their mechanism of action is referred to the inhibition of the bacterial transpeptidase. Structurally, penicillins usually differ in the substituents at the amino group of 6-APA, which influences their antibiotic effects by swaying their receptor binding affinity or cell membrane penetration ability. Penicillin-G for example contains a methylene spacer between the phenyl ring and the carbonyl, which is coupled via amide bond to 6'-aminopenicillanic acid (Figure 41).

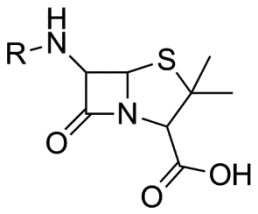

Figure 41: General structure of penicillins. Depending on R, different groups of penicillins are differentiated: benzyl- or phenoxypenicillins, aminopenicillins, acylaminopenicillins, isoxazolylpenicillins.

Organometallic ferrocene-containing analogues have been studied for therapeutic applications.[122-125] Using the three different Cp-moieties that were introduced in section 2.1, carboxylic acids **2**, **24a** and **27** were coupled to the ethyl ester of 6-APA. Therefore, the compounds **66**-**68** differ in the methylene spacers between the Cp^--chelator and the carbonyl group. With one methylene spacer, **67** represents the exact structural analog of penicillin-G.

The Rhenium Complexes II

The three penicillins were prepared by activation of the carboxylic acid with oxalyl chloride and coupling to the previously prepared ethyl ester of 6-APA (Scheme 43).[126] The esterification of the 6-aminopenicillanic acid was necessary, because of solubility issues. Attempts, to use the unprotected 6-APA in aqueous acetone failed, due to the low solubility of the rhenium complexes. Owing to the insolubility of 6-APA in other solvents like CH_2Cl_2 or THF, the ester of 6-APA was used. However, harsh basic or acidic conditions, which are needed for ester hydrolysis, lead to decomposition of the β-lactam ring of the amino penicillanic acid derivative. Therefore, the deprotection of the pharmacologically inactive compounds **66**-**68** to form the active species was not achieved.

Compounds **66**-**68** were characterized by ESI-MS and NMR. All three compounds revealed in their ESI-MS spectrum (MeOD) the $[M+H_3O]^+$ and the $[M+OH]^-$. The shift of the α-proton of the penicillanic acid next to the amide nitrogen and also the Cp^--signals in the ^{1}H-NMR (MeOD) are indicative for the compounds. The α-proton of 6-APA-OEt shifted upon binding to the carboxylic acid for all compounds by approximately 0.5 ppm towards lower field. The Cp^--signals were observed as multiplets, instead of the often found *pseudo* triplets due to the adjacent stereo center at the derivative.

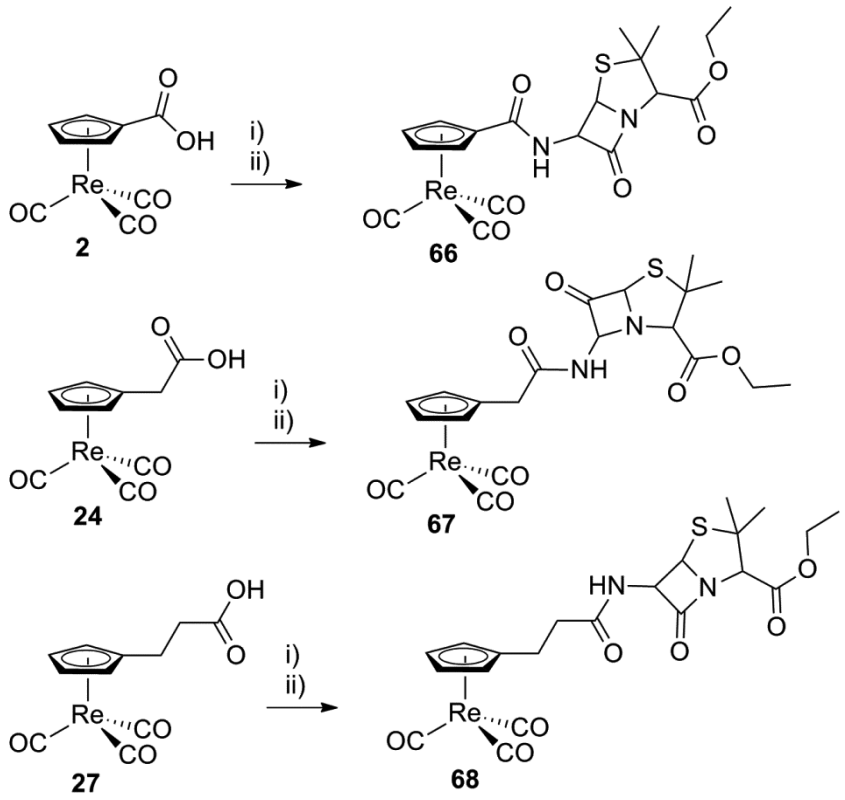

Scheme 43: Synthetic conditions: i) oxalyl chloride, CH_2Cl_2. ii) 6-aminopenicillanic acid ethyl ester, THF, 66-71 %.

The Ligands

In order to prepare the homologous ^{99m}Tc-compounds, the uncoordinated ligand of **68**, namely **69** was synthesized. Starting from acid **20**, the analogous synthetic procedure to the Re-compounds lead to the formation of **69** (Scheme 44).

The compound was analysed by ESI-MS (CH_3OH) and NMR. Similar to the Re-complexes, the $[M+H_3O]^+$-adduct was detected in the ESI-MS. In the ^{1}H-NMR, also similar to the Re-complexes, the signal for the α-proton of 6-APA-OEt shifted upon binding to the carboxylic acid by approximately 0.5 ppm towards lower field and can be found at 4.55 ppm.

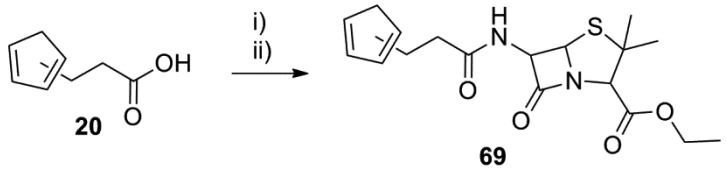

Scheme 44: Synthetic conditions: i) oxalyl chloride, CH_2Cl_2. ii) 6-aminopenicillanic acid ethyl ester, THF, 64 %.

The Technetium Complexes

As mentioned above, harsh basic or acidic conditions lead to decomposition of the β-lactam ring of the amino penicillanic acid derivative. The same was observed when standard labeling conditions were applied with **69**. The high temperatures lead to the formation of a multitude of products. The desired ^{99m}Tc-analog of **68** was therefore not obtained.

Recapitulatory, the synthesis of organometallic antibiotics with an internal sulfonamide group, as a structural analogue of Sulfadiazine or of Sulfamethoxazol respectively, failed. Mechanistically, a degradation of the Re-complex during the coupling reaction is supposed (Figure 39). However, complex **45** was described in section 2.2.2 and contains the ***p***-amino-benzol-sulfonamide scaffold, which is generally found in this class of antibiotics. **45** was assessed in a simple test for antibiotic activity and shows moderate activity against escheria coli.

Furthermore, three different organometallic derivatives of 6-APA-ethyl ester were prepared. Decomposition of the β-lactam ring occurred during ester hydrolysis, therefore the active antibiotics were not isolated. For the same reasons, the corresponding ^{99m}Tc-complexes were not obtained.

2.3.4 Catecholamines

Epinephrine (adrenaline), dopamine and norepinephrine (noradrenaline) structurally belong to the class of catecholamines (Figure 42). Physiologically they have several functions. Binding to adrenergic receptors, they have an impact on the cardiovascular system or act as hormones and as neurotransmitters.[127]

Dopamine-like receptors or noradrenaline transporters on presynaptic terminals have been used as targets for PET-imaging.[128] Using ^{99m}Tc-labeled derivatives of catecholes, the imaging of adrenergic receptors in brain and in the cardiovascular system using SPECT (Single Photon Emission Computed Tomography) is aimed.

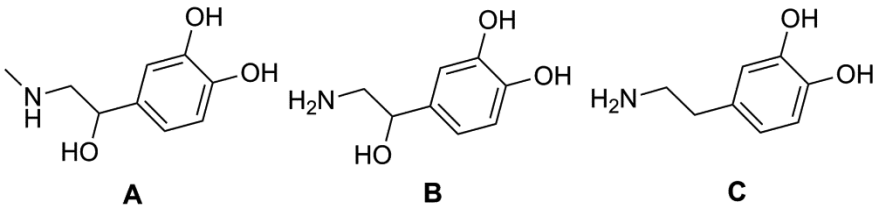

Figure 42: Different catecholamines. A) Epinephrine. B) Norepinephrine. C) Dopamine.

The Rhenium Complexes I

A number of lipid-soluble molecules can diffuse though the BBB and enter the brain in a passive manner.[129] As a very lipophilic and small fragment, the [(Cp)Re(CO)$_3$] is therefore a promising candidate to cross the BBB. Therefore, **2** was derivatized with norepinephrine to form compound **70**. Coupling was performed by activation of **2** with PFPTFA,[63] followed by addition of L-epinephrine in DMF (Scheme 47).

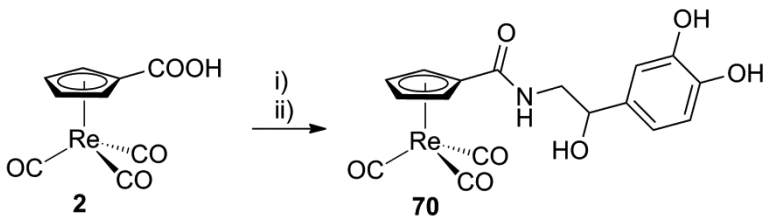

Scheme 45: Synthetic conditions: i) Pentafluorophenyl trifluoroacetate, DMF, 88 %. ii) L-noradrenaline, NEt$_3$, DMF, 76 %.

Similar to **66**-**68**, the aromatic Cp$^-$-signals in the ^{1}H-NMR (DMSO) were observed as multiplets from 6.34 to 5.64 ppm, due to the stereo center in close proximity at the derivative. The amide proton was detected as a triplet at 8.29 ppm and the phenyl signals as a multiplet from 6.75 to 6.52 ppm.

The Ligands

Thilele's Acid was activated with PFPTFA in DMF in quantitative yield.[63] The addition of two equivalents of L-noradrenaline together with an excess of NEt$_3$ led to the formation of compound **71** (Scheme 46).

Two multiplets from 6.65 – 6.60 and from 6.36 – 6.33 ppm respectively for the olefinic protons in the ^{1}H-NMR spectrum of **71** (MeOD) indicated the formation of the product. Like the Re-compound above, the signals show a complicated multiplet pattern, due to the stereocenter, which is introduced next to the olefinic protons.

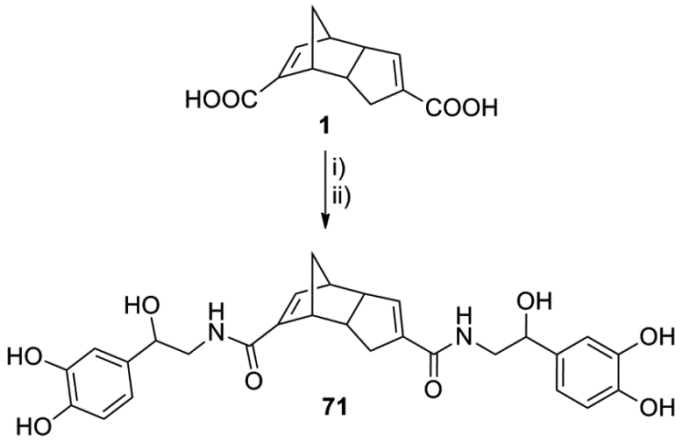

Scheme 46: Synthetic conditions: i) Pentafluorophenyl trifluoroacetate, DMF, 88 %. ii) L-noradrenaline, NEt_3, DMF, 21 %.

The Technetium Complexes

As shown in section 2.2.1 with pendent hydroxamic acids, chemically labile functional groups, that are able to coordinate to the *fac*-{$^{99m}Tc(CO)_3$}-core compete with Thiele's Acid derivatives for complex formation. They represent therefore limitations to this synthetic approach. Comprising an aromatic diol-moiety, the labeling of **71** with [$^{99m}Tc(OH_2)_3(CO)_3$], therefore lead to the formation of a multitude of undefined products. Similar to the hydroxamic acids, coordination to the ^{99m}Tc-core and formation of a polymeric structure or metal oxidations is assumed.

In summary, catecholamine derivative **70** was synthesized as a model compound for adrenergic receptor targeting molecules. The corresponding Thiele's Acid derivative **71** was prepared analogously. ^{99m}Tc-labeling was not successful due to competing coordination via the pendend diol of the catechol.

Further investigations on this topic should therefore include the protection of the pendent diol group before ^{99m}Tc-labeling and the biological investigation of the corresponding Re-compound.

2.3.5 Asymmetric Thiele's Acid-Derivatives

Labeling of bioactive functionalized ligands with the *fac*-{$^{99m}Tc(CO)_3$}$^+$-core was significantly simplified with the introduction of the Isolink Kit, allowing the fast formation of the [$^{99m}Tc(OH_2)_3(CO)_3$]$^+$ precursor.[27, 28] [(Cp-R)$^{99m}Tc(CO)_3$]-type complexes are accessible via metal mediated *retro* Diels-Alder reaction from amide

coupled Thiele's Acid derivatives and $[^{99m}Tc(OH_2)_3(CO)_3]^+$ or $[^{99m}TcO_4]^-$ in water.[61, 63] This reaction allowed to transfer the biological advantages of these complexes to ^{99m}Tc-labelled compounds and therefore paved the way for diagnostic applications. Introducing suitable biologically active residues R, this approach can be regarded as an applicable easy-to-use protocol for routine applications in nuclear medicine.[5, 46, 64]

So far, HCp-R-dimers always contained two identical substituents R, which led to the generation of one imaging agent $[(Cp\text{-}R)^{99m}Tc(CO)_3]$. Mechanistically, it was supposed the carbonyl oxygens to serve as a preliminary anchoring group for the metal core, which is followed by a *retro* Diels-Alder reaction, deprotonation and η^5-coordination of the Cp-ring (see also section 2.1.1).[61] If this mechanism is true, either the bridged or the non-bridged Cp of the dimer could in principle be preferred for metal coordination, unless both parts are considered as equivalent, in the transition state.[93] To gain deeper insights into the mechanism of the metal mediated *retro* Diels-Alder reaction, the asymmetric derivatives of Thiele's Acid **73**-**75** were synthesized and adapted to the usual labeling conditions for type of compounds.[93]

The Ligands

Compounds **73**-**75** were prepared from one single isomer of Thiele's Acid (Scheme 47). [93] Products were obtained after activation of both carboxylic acids with PFPTFA and coupling to the appropriate amines. Depending on the amount of amine that was used and if a base was present or not, single- or di-substituted products were obtained. Mono substituted derivatives were mainly observed as their pentafluorophenyl-esters (PFP) at the bridged side of the HCp-dimer which could be isolated by silica gel column chromatography (**72**). Side products that were formed during the synthesis were not isolated or characterized. However, HPLC-analysis during the reaction showed the formation of two minor products, which were assumed to be the double substituted and as the inverted mono substituted derivative. This observation indicated that the unbridged side of the PFP-ester of Thiele's Acid reacts faster with primary alkyl-amines than the bridged side. This effect was exclusively observed with the PFP-activated Acid. Stronger activation methods did not show this differentiated reaction pattern. Subsequent addition of the second substituent along with triethylamine led to the final products **73**-**75** (Scheme 47).

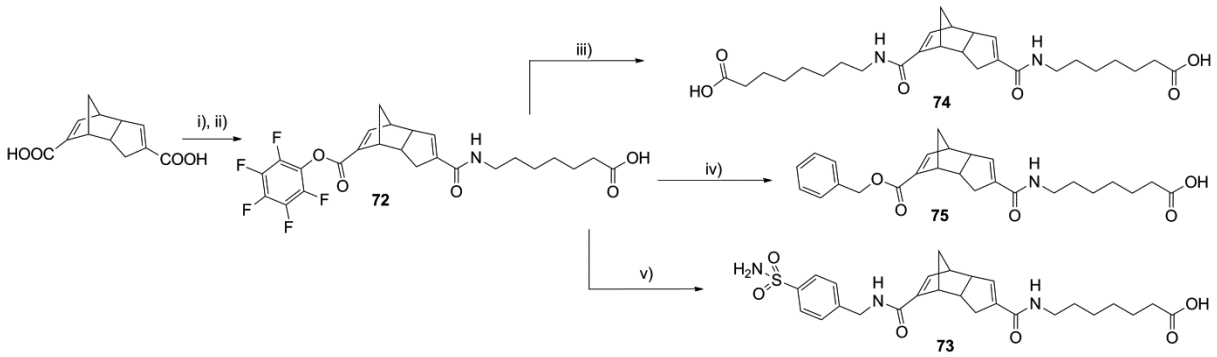

Scheme 47: Synthetic conditions: i) Pentafluorophenyl trifluoroacetate, DMF. ii) 7-aminoheptanoic acid, DMF, 34 %. iii) 8-aminocaprylic acid, triethylamine, DMF, 32 %. iv) benzyl alcohol, triethylamine, DMF, 9 %. v) 4-Aminomethylbenzensulfonamide, triethylamine, DMF, 80 %.

The signals for the olefinic protons in the ^{1}H-NMR spectrum of **72** (MeOD) were observed at 7.35 and at 6.38 ppm. Comparing these values with the ones for starting compound Thiele's Acid (6.86 and 6.51 ppm) or with other derivatives, the signal for the proton next to the electron withdrawing PFP-ester is strongly shifted towards lower field.

The Technetium Complexes.

In extension to the labeling strategy of symmetric HCp-R-dimers, the asymmetric derivatives of Thiele's Acid, **73**-**75** were treated accordingly.[93] All compounds showed the formation of two main peaks in the HPLC trace when reacted with $[^{99m}Tc(OH_2)_3(CO)_3]^+$. Proving, that no site preference for metal coordination of the Cp fragments in HCp-R-dimer is present, the $[(Cp\text{-}R)^{99m}Tc(CO)_3]$-products were formed nearly in a 50:50 ratio. Demonstrating the versatile possibilities of these kind of complexes for medicinal inorganic chemistry and extending the labeling strategy of metal mediated *retro* Diels-Alder reaction, this observation allows now for the synthesis of two different imaging agents with one single substrate and in one pot.

Again, the ligand concentrations were millimolar and reactions were performed at 90 °C in aqueous saline. Besides the two main products **43** and **62**, the labeling of **73** generated a small portion (7 %) of $[^{99m}TcO_4]^-$ (Scheme 48). Compounds **43** and **62** gave a product ratio of 45:55 (**62**:**43**), indicating no clear preference of complex formation concerning localization of the derivatives at the unbridged or at the bridged side of the HCp-dimer. Coinjection of the Re-congeners **32** and **53** respectively clearly confirmed the nature of the products.

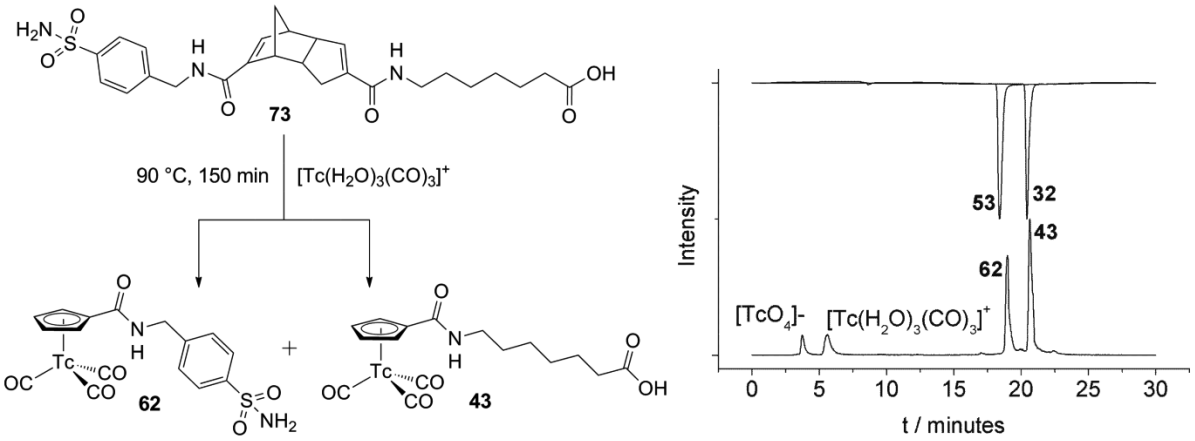

Scheme 48: Bottom-up trace: γ-trace of the two-step labeling of **73** with $[^{99m}Tc(OH_2)_3(CO)_3]^+$. Top-down trace: the UV-trace of Re-compounds **32** and **53**.

A very similar result was observed with **74**, containing two different aliphatic chain lengths but the same conjugation to Cp (Scheme 49). Two products in a similar ratio of 45:55 (**43**:**76**) were obtained as before, confirming the lack of preference for one of the sides in the Thiele's acid dimers.

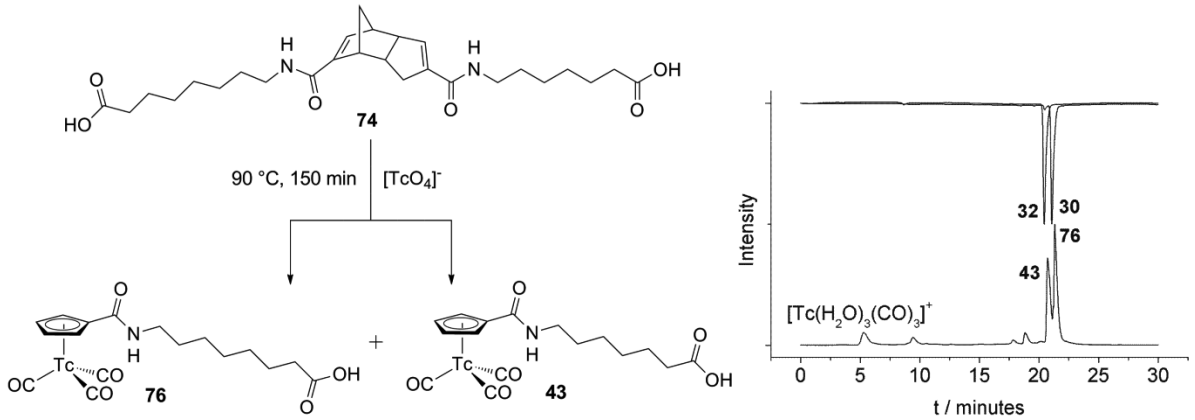

Scheme 49: Bottom-up trace: γ-trace of the one-pot labeling of **74** with $[^{99m}TcO_4]^-$. Top-down trace: the UV-trace of Re-compounds **30** and **32**.

Compound **75** contains an amide bound substituent on one side and an ester group on the other. Even though the labeling of **75**, similar to **73** and **74**, revealed two products, the benzyl ester $[(Cp\text{-}COOCH_2C_6H_5)^{99m}Tc(CO)_3]$ was not obtained but hydrolyzed during the process. One of the products was identified as the acid $[(CpCOOH)^{99m}Tc(CO)_3]$ **3**.[70] The second peak proved to be **43**, the ^{99m}Tc-analogue **32**. The product ratio was nearly 50:50 (Scheme 50).

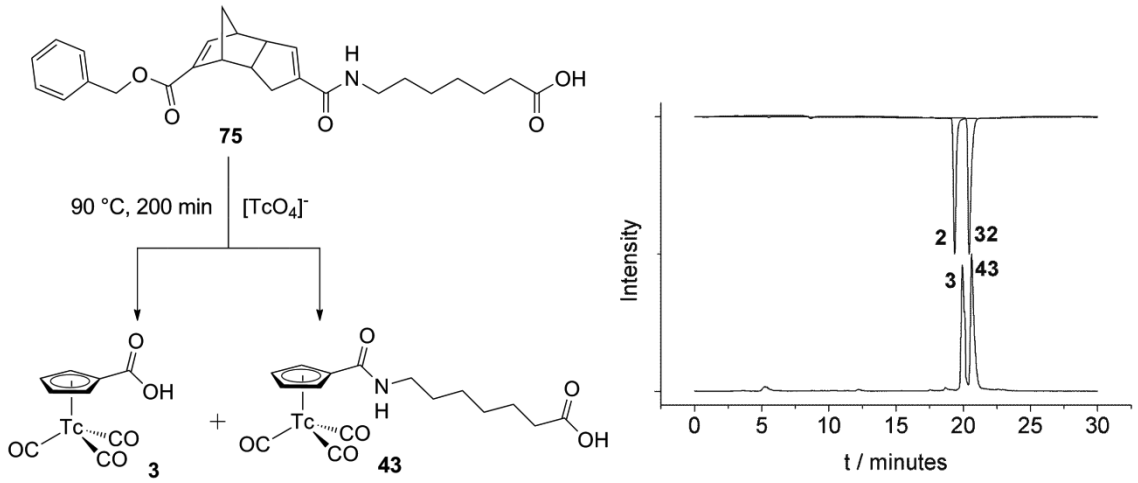

Scheme 50: Top-down trace: γ-trace of the one-pot labeling of **75** with $[^{99m}TcO_4]^-$. Bottom-up trace: the UV-trace of Re-compounds **2** and **32**.

Reactivities of the carboxylic acid groups in Thiele's Acid are not equivalent at the bridged and at the unbridged side. By activation with PFPTFA and addition of aliphatic primary amines like 7-aminoheptanoic acid, the monosubstituted product **72** can be isolated, when no base is used during the reaction. Mono substituted derivatives are mainly observed as their pentafluorophenyl-esters (PFP) at the bridged side of the HCp-dimer. This observation indicates that the unbridged side of the PFP-ester of Thiele's Acid reacts faster with primary alkyl-amines than the bridged side. Subsequent addition of the second substituent along with triethylamine led to asymmetrically derivatized Thiele's Acid.

Using these derivatives, two different imaging agents of $[(Cp\text{-}R)^{99m}Tc(CO)_3]$ (R = potential targeting vector) can be generated in one-pot and from one substrate. Introducing appropriate vectors, combined imaging of two targets from one substrate is now possible.

2.4 Conclusions & Outlook

Structurally, a bifunctional chelator (BFC) can be regarded as consisting of three building blocks:

- a chelator is the part that binds to the metal core, the actual ligand.
- a linker, which consists of a functional group, that enables the coupling of a spacer.
- a targeting vector, which is bound to the spacer and contains a biologically active function.

In the course of the present thesis, the linker, the spacer and the targeting vector were varied and investigated chemically as well as biologically.

Carboxylic acid derived Cp-compounds have been described in literature in the form of the uncoordinated ligand and as η^5-coordinated Re- or ^{99m}Tc tricarbonyl complexes (**1**, **2** and **3**).[61, 70, 72-74] The compounds allow a wide range of synthetic manipulations at the carboxylic acid portion, even in aqueous solvents.
A variety of organic and inorganic amide coupled derivatives like arylsulfonamides, -sulfamides and -sulfamates for the targeting of human carbonic anhydrase IX, hydroxamic acids acting as HDAC-inhibitors, organometallic antibiotics or catechol amine derivatives have been prepared.

The sulfonic acid of the [CpRe(CO)$_3$]-complex and some limited derivatives are available according to literature procedure.[71, 80] The protonated uncoordinated HCp-sulfonic acid, which was also described in literature,[80] was not obtained. Therefore, the corresponding ^{99m}Tc complexes were also not synthesized in the course of this thesis.
The aryl-sulfone-dimer **8** was prepared and its labeling behaviour with ^{99m}Tc was studied. Product formation was only observed in a microwave synthesis at 130 °C. However, the authenticity of the product must still be confirmed by comparison with the corresponding rhenium complex.
No biological active derivatives of the form Cp-SO$_2$-R have been prepared and will be part of further investigations.

The nitro-derivatized Cp-compound **10** was prepared along literature procedure and is readily soluble and stable in water.[65, 73] However, the complexation of **10** with the ^{99m}Tc-core was not observed and needs further improvement.

The organometallic aniline analogue [(CpNH$_2$)Re(CO)$_3$] (**11**) was prepared according to literature.[69] Synthetically, it can be treated like aniline and nucleophilic coupling reactions are suitable methods for derivatization. Coupling to suitable targeting vectors, organometallic antibiotics, HDAC-inhibitors or carbonic anhydrase inhibitors were prepared.
In situ derivatized HCp-amines in their dimeric form were prepared from Thiele's Acid applying the Curtius Rearrangement. The reaction progress was investigated by time resolved IR-measurement and by ^{1}H-NMR. The ^{99m}Tc-labeling behaviour of **16a**-**b** is subject of ongoing investigations.

With the synthesis of the uncoordinated and protonated HCp-compounds **17** and **19**, containing methylene groups between the HCp and the carboxylic acid, a new way of altering the spacer in a BFC has been introduced; before ***and*** after the coupling function. **17** undergoes slow Diels-Alder dimerization at room temperature. Keeping **17** at -20 °C, beside the dimer **23**, the rearrangement product **22** is formed. The dimerization behaviour of **19** was not investigated. Derivatisation of the carboxylic acid **18** by amide coupling with primary amines leads to rearrangement of the double bonds and the formation of a cyclopentene ring, as observed with comounds **21a/b**. Therefore cyclopentadienyl amides of **18** were not accessible.
Labelling experiments of **18** and **20** with [^{99m}Tc(H$_2$O)$_3$(CO)$_3$]$^+$ proved that the carboxylic acid function in β- or in γ-position, with respect to the HCp-ring are still close enough, to allow anchoring of the metal center by the carboxylic acid portion. Therefore, bringing the metal in close proximity, η^5-coordination of the HCp-portion is simplified. However, conversion rates of the ^{99m}Tc starting compounds were very different for the ligand **18** compared to **20**, which is in accordance with the increasing distance of the anchoring group to the HCp-moiety. Similar to Thiele's Acid, the dimer **23** can undergo metal mediated *retro* Diels-Alder reaction and form the same product as obtained with the monomer **18**. The mechanism however is unclear.

24a was synthesized similar to the ^{99m}Tc-compound **28** using ligand **18** with $[Re(Br)_3(CO)_3]^{2-}$ in water. The Re-complex **27** was synthesized along Horner-Wardsworth-Emmons olefination.

3. Experimental

3.1 General Remarks

Reactions were carried out in dried glassware under nitrogen atmosphere. Solvents were dried using standard techniques and stored over molecular sieves. Human Carbonic Anhydrase II (hCAII) and all chemicals were obtained from commercial sources and used without further purification. **2**,[70] **11**,[69] sulfamoyl chloride,[130] **4**, **5**, **6**,[71] **7** and **8**[68] were prepared according to literature procedures. **10**,[65] **18**[66] and **20**[67] were prepared according to literature procedures with slight modifications. ^{1}H-NMR and ^{13}C-NMR spectra were recorded on a Bruker Advance 400 MHz or 500 MHz spectrometer. Mass spectra were measured on a Bruker Esquire HCT (ESI) instrument. IR spectra were recorded as KBr pellets on a Perkin-Elmer BX II IR spectrometer. RP-HPLC was performed on a Merck Hitachi LaChrom L7200 tunable UV detector and a radiodetector, separated by a Teflon tube, which causes about a 0.4 – 1.0 min delay compared to UV/vis detection. UV/vis detection was performed at 250 nm. The detection of radioactive ^{99m}Tc complexes was performed with a Berthold LB 507 radiodetector equipped with a NaI(Tl) scintillation detector. The traces shown in this section are crude and unpurified samples directly taken from the reaction mixture. Analytical separations were performed on a Nucleosil C-18 column (100 Å, 5 □m, 250×4 mm) and were eluted with a flow rate of 0.5 ml min^{-1} using 0.1 % TFA in H_2O (solvent A) and methanol (solvent B) as eluents with a variable gradient (0–3 min, 100 % A; 3–3.1 min, 0 to 25 % B; 3.1–9 min, 25 % B; 9–9.1 min, 25 % B to 34 % B; 9.1–20 min, 34 % B to 100 % B; 20–25 min, 100 % B; 25–25.1 min 100 % B to 100 % A; 25.1–30 min 100 % A).

For carbonic anhydrase inhibitors, absorbance of the DMSO solution of formazan in the cytotoxicity study was determined using a plate spectrophotometer (Power Wave Xs; Bio-Tek). Statistical analysis of the pH-studies were performed with Graph Pad Prism version 5.01 for windows (Graph pad software 2007, CA, USA). For all tests, $P < 0.05$ was considered significant. Antibodies for western blot were purchased from Novus Biologicals for CA IX, Sigma for actin and, secondary antibodies from Biorad. Membranes were developed using the SuperSignal WetsPico Substrate kit from Pierce, Rockford according to the manufacturer's instructions.

For biological studies of the HDAC inhibitors, Dulbecco's Modified Eagle Medium (DMEM) with GlutaMax-I, fetal bovine serum (FBS), penicillin/streptomycin antibiotic solution, phosphate-buffered saline (PBS), and trypsin were purchased from Gibco Invitrogen Co. (Alfagene, Portugal). Methanol, DMSO, 3-(4,5-dimethylthiazol-2-yl)-2,5-diphenyltetrazolium bromide (MTT), and trypan blue were bought from SigmaChemical Co. (Sigma, Portugal). Suberoylanilide hydroxamic acid (SAHA) was purchased from Cayman Corporation. For the determination of the IC_{50}-values, absorbance at 570 nm was measured using a microplate spectrophotometer (PowerWave Xs, Bio-Tek Instruments, Winooski, VT, USA).

Crystallographic data were collected at 183(2) K with Mo K_α radiation (λ = 0.7107 Å) that was graphite-monochromated on a Stoe IPDS diffractometer or an Oxford Diffraction CCD Xcalibur system with a Ruby detector respectively. Suitable crystals were covered with oil (Infineum V8512, formerly known as Paratone N), mounted on top of a glass fibre or a CryoLoop™ (Hampton Research) and immediately transferred to the diffractometer. In the case of the IPDS, a maximum of eight thousand reflections distributed over the whole limiting sphere were selected by the program SELECT and used for unit cell parameter refinement with the program CELL.[131] Data were corrected for Lorentz and polarisation effects as well as for absorption (numerical). In case of the Oxford system, the program suite CrysAlis^{Pro} was used for data collection, multi-scan absorption correction and data reduction.[132] Structures were solved with direct methods using SIR97[133] and were refined by full-matrix least-squares methods on F^2 with SHELXL-97.[134] The hydrogen atoms of the NH_2 units were localized and their positions freely refined. All other hydrogen atoms were placed on calculated positions. The structures were checked for higher symmetry with help of the program Platon.[135]

3.2 Biological Evaluation

3.2.1 Carbonic Anhydrase Inhibitors

In vitro: cells and culture conditions

The human cervical adenocarcinoma HeLa and human breast adenocarcinoma MDA MB 231 cell lines were maintained in DMEM (Invitrogen) supplemented with 10 % fetal calf serum (FBS) in a humidified atmosphere of 5 % CO_2 at 37 °C. The human

colon adenocarcinoma cell line HT29 was maintained in McCoy´s (Invitrogen) supplemented with 10 % FBS in a humidified atmosphere of 5 % CO_2 at 37 ºC.

In vitro: cytotoxicity assays

Cytotoxicity of rhenium complexes **52** and **53** was evaluated using a colorimetric method based on the tetrazolium salt MTT ([3-(4,5-dimethylthiazol-2-yl)-2,5-diphenyltetrazolium bromide), which was reduced by viable cells to yield purple formazan crystals. Cells were seeded in 96-well plates at a density of 15 to 50 x 10^4 cells per well, were allowed to attach overnight and then incubated for 24 h in the presence of various concentrations of the complexes. At the end of the incubation period the media was removed and the cells were incubated with MTT (0.5 mg/mL) for 3h at 37 ºC and 5 % CO_2. The purple formazan crystals formed inside the cells were then dissolved in DMSO by thorough shaking, and the absorbance was measured at 570 nm. Each test was performed with at least six replicates and repeated at least 2 times. The result was expressed as percentage of the surviving cells in relation with the control.

In vitro: pH studies

Cells were platted in 24 well plates at a density of 1 x 10^5 cells per well, one day before the start of the experiment. Cells were then incubated 24 h at 37ºC with 1mM and 500 μM of the sulfonamides or metal complexes under normoxia (air with 5 % CO_2) or hypoxia (1 % O_2, 5 % CO_2 and residual N_2 in a sealed hypoxic culture chamber).

The extracellular acidification of cell lines was measured by inserting a pH probe into the culture medium, at the beginning and at the end of each experiment. Each test was performed with 4 replicates and repeated at least 2 times.

In vitro: western blot

Western blot experiments were performed to evaluate the levels of expression of CA IX. Hela, HT29 and MDA MB231 cells were lysed in Laemmli sample buffer (1.5 % SDS, 10 % glycerol, 0.5 mM dithiothreitol, 31.25 mM Tris, pH 6.8 and 0.001 % bromophenol blue). The total protein content was determined by using the RCDC Protein Assay Kit (Biorad) and aliquots of protein (50 μg) from each sample were analysed using standard western blot procedures. Briefly, protein extracts were subjected to

electrophoresis on a 10 % SDS-polyacrylamide gel and transferred electrophoretically onto nitrocellulose membranes. The blots were blocked with PBS-T containing 5 % nonfat dry milk for 1 h. Then, the blotting membranes were incubated with primary antibodies against CA IX (1:2000, rabbit polyclonal, Novus Biologicals) and actin (1:8000, mouse monoclonal, Sigma) overnight. Membranes were washed with PBS-T and incubated for 1 h with secondary antibodies (goat anti-mouse and goat anti-rabbit IgG-HRP, Biorad) diluted 1:3000. Finally, membranes were developed using the SuperSignal WetsPico Substrate kit (Pierce, Rockford, IL) according to the manufacturer's instructions.

In vitro: hCA inhibition

An Applied Photophysics stopped-flow instrument was used for assaying the CA catalysed CO_2 hydration activity.15 Phenol red (0.2 mM) was used as indicator, working at the absorbance maximum of 557 nm, with 20 mM Hepes (pH 7.4) and 20 mM $NaBF_4$ (in order to keep the ionic strength constant), following the initial rates of the CA-catalyzed CO_2 hydration reaction for a period of 10-100 s. The CO_2 concentrations ranged from 1.7 to 17 mM for the determination of the kinetic parameters and inhibition constants. For each inhibitor, at least six traces of the initial 5-10 % of the reaction have been used for determining the initial velocity. The uncatalyzed rates were determined in the same manner and subtracted from the total observed rates. Stock solutions of inhibitor (10 mM) were prepared in distilled-deionized water and dilutions up to 0.01 nM were done thereafter with distilled-deionized water. Inhibitor and enzyme solutions were preincubated together for 15 min at room temperature prior to assay, in order to allow formation of the E-I complex. The inhibition constants were obtained by non-linear least-squares methods using PRISM 3, whereas the kinetic parameters for the uninhibited enzymes were obtained from Lineweaver-Burk plots and represent the mean from at least three different determinations. All CAs were recombinant proteins obtained as reported earlier by these groups.[136-141]

In vivo: cell culture, animals and tumor model

Biodistribution of the radiolabeled compounds **61** and **62** at 1h and 4h p.i. was evaluated in HT-29 xenograft mice bearing CAIX-expressing tumors.

Exponentially growing colorectal HT-29 adenocarcinoma cells were cultured in McCoy´s medium (Invitrogen) supplemented with 10 % fetal bovine serum as described above.[5]

Animal experiments were performed using adult BaLB/c (nu/nu) female mice with an average body weight of 30 g (6-8 weeks). The animal facilities and experiments were in accordance with Portuguese and European regulations. The animals were housed in a temperature- and humidity-controlled room with a 12h light/12h dark schedule.

HT-29 cells were resuspended with 50 % Basement Membrane Matrix (Matrigel™ BD Biosciences, ref 356234) in PBS and were subcutaneously injected into the lateral flank of the animal (10^7 cells per animal).

When tumors reached an average volume of 500 mm^3 (9 and 14 days after inoculation for 1h and 4h biodistribution of **61** and **62**, respectively), the isoflurane-anesthetised animals were intravenously injected with purified ^{99m}Tc-labelled compounds (**61** or **62**) into their retro-orbital sinus.

Mice were killed by cervical dislocation at 1 and 4h respectively after injection. The injected activity and the activity in the killed animals were measured using a dose calibrator (Curiemeter IGC-3, Aloka, Tokyo, Japan). The difference between the injected radioactivity and the activity that was measured in the killed animals was assumed to be excretied by the mice. Tumors and normal tissues of interest were dissected, rinsed to remove excess blood, weighed, and their radioactivity was measured using a γ-counter (LB2111, Berthold, Germany). The uptake in the tumor and in healthy tissues of interest was calculated and expressed as a percentage of the injected activity per gram of tissue (%IA/g). For blood, bone, muscle, and skin, total activity was estimated assuming that these organs constitute 6, 10, 40, and 15 % of the total body weight, respectively.

In vivo: stability

The stability of the complexes was assessed by urine, and murine serum RP-HPLC analysis. The samples were taken 1 h *post* injection. The urine collected at the time of sacrifice was filtered through a Millex GV filter (0.22 μm) before RP-HPLC analysis. Blood collected from mice was centrifuged at 3000 rpm for 15 min at 4 °C, and the serum was separated. The serum was treated with ethanol in a 2:1 (v/v) ratio to

precipitate the proteins. After centrifugation at 3000 rpm for 15 min at 4 °C, the supernatant was collected and analysed by RP-HPLC.

In vivo: western blot analysis of tumor samples

Quantification of CAIX expression in BaLB/c nude mice bearing HT-29 tumors was also carried by western blot experiments. Tumors were excised, rinsed in PBS and homogenized with ice cold Cell Lytic-MT Extraction reagent (Sigma) supplemented with Complete protease inhibitor cocktail tablets (Roche Applied Science) using a Dounce glass apparatus. Lysates were transferred to microcentrifuge tubes and centrifuged at 14000g for 10 min at 4 °C to pellet the cellular debris and the supernatants removed for further use.

The total protein concentration was determined by the DC Protein Assay Kit (BioRad) with bovine serum albumin as standard. Aliquots of protein (50 µg) from each sample were analysed using standard western blot procedures.[5] Protein extracts were subjected to electrophoresis on a 10 % SDS-polyacrylamide gel and transferred electrophoretically onto nitrocellulose membranes. The blots were blocked with PBS-T containing 5 % nonfat dry milk for 1 h. Then, the blotting membranes were incubated with primary antibodies against CA IX (1:2000, rabbit polyclonal, Novus Biologicals) and actin (1:8000, mouse monoclonal, Sigma) overnight. Membranes were washed with PBS-T and incubated for 1 h with secondary antibodies (goat antimouse and goat anti-rabbit IgG-HRP, Biorad) diluted 1:3000. Finally, membranes were developed using the SuperSignal West Pico Substrate kit (Pierce, Rockford, IL) according to the manufacturer's instructions.

3.2.2 HDAC Inhibitors

Tumor cell lines

The human breast carcinoma MCF-7, prostate carcinoma PC3, cervical carcinoma HeLa, vulva epidermal carcinoma A43 and melanoma A375 cell lines as well as the murine melanoma B16F1cell line used in this study were grown in Dulbecco's Modified Eagle Medium (DMEM) containing GlutaMax-I supplemented with 10 % heat-inactivated foetal bovine serum (FBS) and 1 % penicillin/streptomycin antibiotic solution (all from Gibco, Alfagene, Lisbon). Cells were cultured in a humidified atmosphere of 95 % air and 5 % CO_2 at 37 °C (Heraeus, Germany), with the medium

changed every other day. The cells were adherent in monolayers and, when confluent, were harvested from the cell culture flasks with trypsin EDTA (Gibco, Alfagene, Lisbon) and seeded farther apart.

Cytotoxic activity

The antiproliferative activity on tumor cells was evaluated using a colorimetric method based on the tetrazolium salt MTT ([3-(4,5-dimethylthiazol-2-yl)-2,5-diphenyltetrazolium bromide]), which is reduced in viable cells to yield purple formazan crystals. The optimal plating density of each cell line, which ensures exponential growth throughout all of the experimental period, was first optimized. MCF-7 (15× 10^3 cells), HeLa (9 × 10^3 cells), A431 (7.5 × 10^3 cells), A375 (7 × 10^3 cells), PC3 (6 × 10^3 cells) and B16F1 (6 × 10^3 cells) cells were plated in 96-well sterile plates in 150 µL of culture medium per well and incubated for 24 h at 37 ºC/5 % CO_2 for seeding. Then the cells were incubated with various concentrations of the compounds **31, 33, 36, 38, 40** and SAHA for 72 h at 37 °C/5 % CO_2, dissolved in methanol and diluted in the culture medium (methanol final concentration 0.025 % and 0.1 % respectively). The effect of the vehicle solvent (methanol) on the growth of these cell lines was evaluated in all experiments by exposing untreated control cells to both concentrations of methanol used (0.025 % and 0.1 %).

At the end of the incubation period, the compounds were removed and cells were washed with 200 µL of PBS. Cell viability was then determined by incubating cells with 200 µL of MTT solution (0.5 mg mL^{-1} in PBS). After 3 h at 37 °C/5 % CO_2, the solution was removed and the purple formazan crystals formed inside the cells were dissolved in 200 µL DMSO by thorough shaking. For each test compound and for each cell line, a dose−response curve was obtained. The cytotoxic effects of ligands and Re-complexes were quantified by calculating the compound concentration inhibiting tumor cell growth by 50 % (IC_{50}), based on non-linear regression analysis of dose–response data (GraphPad Prisma 5 software). For comparison suberoylanilide hydroxamic acid (SAHA), was evaluated under the same experimental conditions. All compounds were tested in at least two independent studies with eight replicates for each concentration.

3.3 hCAII Crystallization

Applying similar conditions as Behnke et al,[142] crystals were grown with the hanging drop vapor diffusion method. 1 µl of protein solution and 1 µl of precipitant (2.4 M $(NH_4)_2SO_4$, 0.1 M Tris-HCl at pH 7.5, 1 mM 4-(hydroxymercuri) benzoic acid sodium salt and 5.1 % vol. DMSO) were mixed. The protein solution consisted of hCA II dissolved in unbuffered water at 20 mg/ml. Good crystals were obtained after four weeks at 298 K, two weeks at 277 K then again four weeks at 298 K. The obtained crystals were soaked for four weeks at 298 K with 0.25 mg of solid inhibitor.

One crystal was covered with oil (Infineum V8512, formerly known as Paratone N) and the mother liquid was removed as gently as possible by moving the crystal through the oil. The crystal was frozen by dropping into liquid nitrogen. Single crystal diffraction data till 1.2 Å resolution were recorded at 100 K at the Swiss Light Source (Paul Scherrer Institute, Villigen, Switzerland) using the X06DA beamline (λ = 1 Å) equipped with a mar225 mosaic CCD detector. The data sets were indexed and integrated with XDS.[143] The structure was solved by molecular replacement with Phaser[144] using the GUI of CCP4i[145] and pdb entry 3IQK.[146] Refinement of the structure was done with SHELXL[134] and inspection of the model and electron densities with COOT.[147] The restraints for the rhenium complexes were taken from the corresponding small molecule structures. Atomic coordinates and diffraction data have been deposited in the RCSB Protein Data Bank under accession code 3RJ7. Pictures were drawn with the help of ccp4mg [148] and Pymol.[149]

The electron density of complex **53** could be traced till the terminal carbonyl units. Additionally, two high residual electron densities were found nearby and assigned to minor disordered rhenium positions. The ratio of the three conformations was refined as 6:2:2, summing up to full occupancy. The benzyl-sulfonamide part of the complex is not disordered. One of the minor conformations is near PHE131 with a closest distance of the found rhenium position to PHE131, CZ, of 1.21 Å. For this conformation of the complex, the phenyl ring of PHE131 must be oriented away from the complex. For both minor conformations, it was impossible to locate the electron density of the light elements.

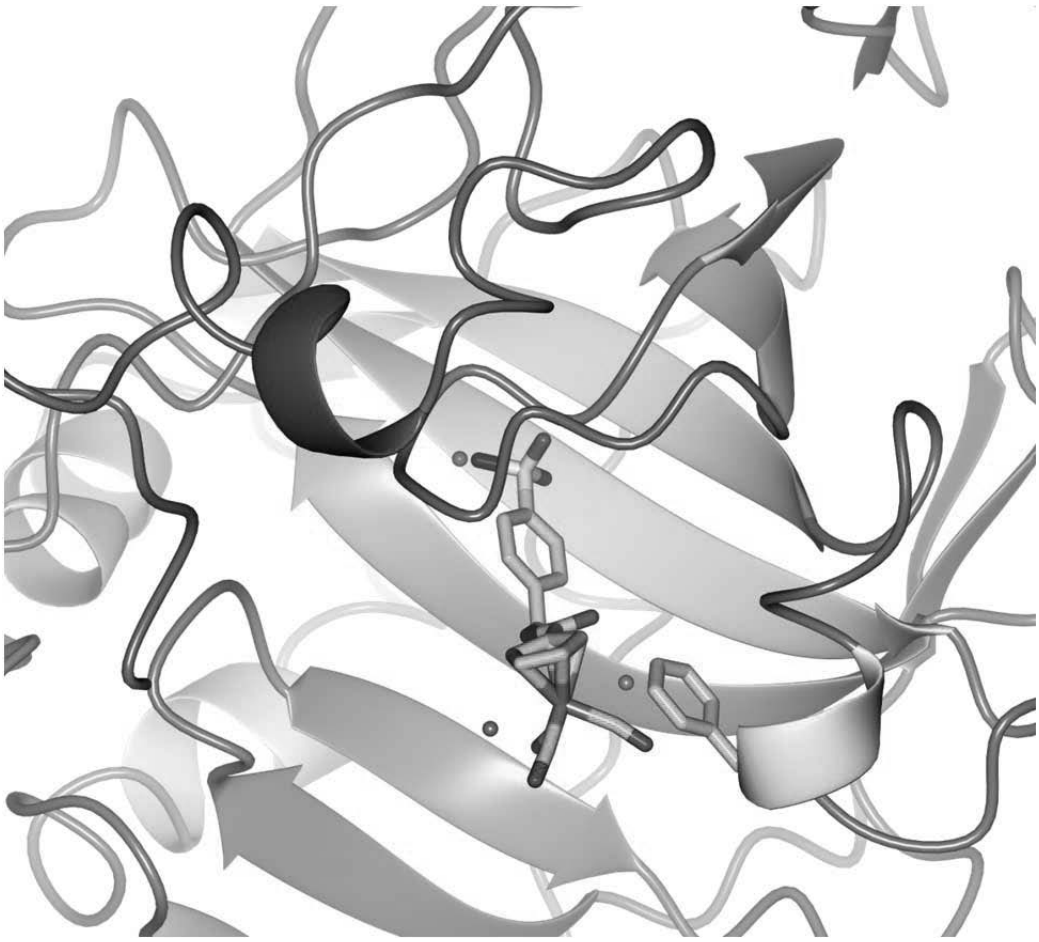

Figure 43: Ribbon presentation of hCAII with bound **53** to the zinc center (zinc in magenta). The minor conformations of **53** with their found two disordered Rhenium centers (in grey, 20 % probability each) and the side chain group of PHE131 are also shown.

3.4 The Re-complexes

3.4.1 [Re(CO)$_3$Cp-NHSO$_2$R]

(12)

[(Cp-NH$_2$)Re(CO)$_3$] (50 mg, 0.142 mmol) was dissolved in 10 ml of dry CH_2Cl_2 containing pyridine (11.5 µl, 0.142 mmol). Benzenesulfonyl chloride (23.8 µl, 0.186 mmol) was added and the solution was stirred for 10h at room temperature. Water was added and the mixture was extracted three times with fresh CH_2Cl_2. The combined organic layers were dried over Na_2SO_4 and evaporated under reduced pressure to give **12** (95 %). No further purification was necessary.

Calc. for Mr ($C_{14}H_{10}NO_5ReS$) 490.5; ESI-MS [m/z] (CH_3OH): 489.9 $[M-H]^-$; ^{1}H NMR (500 MHz, $CDCl_3$, δ in ppm): 7.78 (m, 2H, Ar), 7.58 (m, 2H, Ar), 6.17 (s, 1H, N*H*), 5.23 (m, 2H, Cp), 5.03 (m, 2H, Cp).

(13)

[(Cp-NH$_2$)Re(CO)$_3$] (50 mg, 0.142 mmol) was dissolved in 10 ml of dry CH_2Cl_2 containing pyridine (11.5 µl, 0.142 mmol). *p*-Toluenesulfonyl chloride (35.4 mg, 0.1855 mmol) was added and the solution was refluxed for 10h. After cooling to room temperature, water was added and the mixture was extracted three times with fresh CH_2Cl_2. The combined organic layers were dried over Na_2SO_4 and evaporated under reduced pressure. Recrystallization from CH_2Cl_2/Hexane afforded coloreless needles of **13** (95 %). Crystals suitable for X-Ray analyses were grown from CH_2Cl_2/hexane.

Calc. for Mr ($C_{15}H_{12}NO_5ReS$) 504.5; ESI-MS [m/z] (CH_3OH): 506.0 $[M+H]^+$; ^{1}H NMR (500 MHz, $CDCl_3$, δ in ppm): 7.75 (m, 2H, Ar), 7.37 (m, 2H, Ar), 6.28 (s, 1H, N*H*), 5.32 (m, 2H, Cp), 5.11 (m, 2H, Cp), 2.47 (s, 3H, C*H$_3$*).

(44)

[(Cp-NH$_2$)Re(CO)$_3$] (200 mg, 0.57 mmol) was dissolved in 10 ml of dry CH_2Cl_2 containing pyridine (46.1 µl, 0.57 mmol). 4-Acetylsulfanilyl chloride (133.3 mg, 0.57 mmol) was added and the suspension was refluxed for 8 h. After cooling to r.t., the colorless precipitate was filtered off and washed with a small portion of CH_2Cl_2. Silica gel column chromatography using EtOAc/Hexane 1:1 afforded **44** in 80 % yield.

IR (cm^{-1} KBr): 2020, 1915, 1678, 1594, 1492, 1399, 1325, 1157; Calc. for Mr ($C_{16}H_{13}N_2O_6ReS$) 547.6; ESI-MS [m/z] (CH_3OH): 546.8 $[M-H]^-$; ^1H NMR (400 MHz, MeOD, δ in ppm): 7.82 (s, 4H, Ar), 5.43 (m, 2H, Cp), 5.27 (m, 2H, Cp), 2.19 (s, 3H, C***H***$_3$). ^{13}C NMR (125 MHz, DMSO-***d***$_6$, δ in ppm): 194.8 (***C***O), 169.2 (***C***OCH_3), 143.8 (Ar1), 131.0 (Ar4), 128.5 (Ar2), 118.6 (Ar3), 117.6 (Cp1), 81.3 (Cp2), 73.1 (Cp3), 24.2 (***C***H_3); Calc. C, 35.10; H, 2.39; N, 5.12; Found. C, 35.21; H, 2.46; N, 5.08.

(45)

44 (50 mg, 0.091 mmol) was dissolved in 10 ml of absolute EtOH. Conc. HCl (1 ml) was added and the solution was refluxed at 90 °C for 1 h. After cooling to room temperature, the mixture was neutralized with conc. $NaHCO_3$. The solvent was removed under reduced pressure to give **45** in quantitative yield. Crystals suitable for X-Ray analysis were grown from Hexane/CH_2Cl_2.

IR (cm^{-1} KBr): 2021, 1914, 1595, 1494, 1316, 1157, 1093; Calc. for Mr. ($C_{14}H_{11}N_2O_5ReS$) 505.5; ESI-MS [m/z] (CH_3OH): 505.0 $[M-H]^-$; ^1H NMR (400 MHz, MeOD, δ in ppm): 7.55 (m, 2H, Ar), 6.72 (m, 2H, Ar), 5.37 (m, 2H, Cp), 5.25 (m, 2H, Cp), ^{13}C NMR (125 MHz, DMSO-***d***$_6$, δ in ppm): 195.02 (***C***O), 153.45 (Ar1), 129.3 (Ar4), 122.2 (Ar2), 119.3 (Cp1), 112.7 (Ar3), 81.0 (Cp2), 72.3 (Cp3); Calc. C, 33.26; H, 2.19; N, 5.54; Found C, 33.01; H, 2.28; N, 5.35.

(46)

45 (100 mg, 0.2 mmol) was dissolved in 3 ml of dry DMA and freshly prepared sulfamoyl chloride was added dropwise until no more starting material was observed (TLC monitoring). The reaction mixture was quenched with H_2O and extracted with EtOAc (3 x 15 ml). The combined organic layers were washed with brine (3 x 15 ml) and H_2O (3 x 15 ml), dried over Na_2SO_4, filtered and concentrated in ***vacuo*** to give a yellow oil. Silica gel column chromatography eluting with 10 % MeOH in CH_2Cl_2 followed by recrystallization from H_2O/EtOH afforded the desired product as a yellow solid in 68 % yield.

IR (cm^{-1} KBr): 2014, 1934, 1915, 1593, 1490, 1342, 1313, 1149; Calc. for Mr. ($C_{14}H_{12}N_3O_7ReS_2$) 584.6; ESI-MS [m/z] (CH_3OH): 584.1 $[M-H]^-$; ^1H NMR (400 MHz, DMSO-***d***$_6$, δ in ppm): 10.44 (s, 1H, Ar-N***H***), 10.28 (s, 1H, Cp-N***H***), 7.75 (m, 2H, Ar), 7.43 (s, 2H, SO_2-N***H***$_2$), 7.31 (m, 2H, Ar), 5.46 (m, 2H, Cp), 5.42 (m, 2H, Cp); ^{13}C NMR (100 MHz, DMSO-***d***$_6$, δ in ppm): 195.7 (***C***O), 145.0 (Ar1), 130.9 (Ar4), 129.4 (Ar2), 119.0 (Ar3), 117.5

(Cp1), 82.3 (Cp2), 74.1 (Cp3); Calc. C, 28.76; H, 2.07; N, 7.19; Found. C, 28.91; H, 2.04; N, 7.07.

3.4.2 [Re(CO)$_3$Cp-CONHR]

(47a/b)

[(Cp-COOH)Re(CO)$_3$] was activated with pentafluorophenyl trifluoroacetate according to literature procedure.[63] *p*-Aminophenol (11.2 mg, 0.10 mmol) was dissolved in 5 ml of THF and the activated acid (56 mg, 0.10 mmol) was added. The mixture was heated at 60 °C for 16 h, then the solvent was evaporated and the residue was extracted with CH_2Cl_2 and 0.1 M HCl. The combined organic fractions were dried over Na_2SO_4, evaporated to dryness and purified by silica gel chromatography using a gradient from pure CH_2Cl_2 to EtOAc/Hex 1:1. Two fractions were isolated, revealing the amide bound product **47a** as a coloreless oil (39 %) and the ester **47b** as a yellow powder (24 %).

47a: Calc. for Mr. ($C_{15}H_{10}NO_5Re$) 470.5; ESI-MS [m/z] (CH_3OH): 470.8 $[M+H]^-$, 506.1 $[M+H_3O_2]^-$; ^{1}H NMR (400 MHz, DMSO-d_6, δ in ppm): 9,69 (s, 1H, Ar-N*H*), 9.31 (s, 1H, Ar-O*H*), 7.37 (m, 2H, Ar), 6.74 (m, 2H, Ar), 6.44 (m, 2H, Cp), 5.79 (m, 2H, Cp).

47b: ^{1}H NMR (400 MHz, DMSO-d_6, δ in ppm): 6.78 (m, 2H, Ar), 6.59 (m, 2H, Ar), 6.48 (m, 2H, Cp), 5.87 (m, 2H, Cp), 5.12 (s, 2H, NH_2).

(48)

$NaHCO_3$ (167 mg, 2 mmol) was dissolved in 5 ml of Water and added to a suspension of 4-Aminophenol (218.3 mg, 2 mmol) in 10 ml of CH_2Cl_2. Boc_2O (433.7 mg, 2 mmol) was added and the mixture was strirred under reflux for 3 h and for another 12 h at room temperature. The organic layer was separated and washed with brine (3 x 10 ml) and H_2O (3 x 10 ml), dried over Na_2SO_4, filtered and concentrated in *vacuo* to give a slightly yellow oil which was not further purified (78 %).

Calc. for Mr. ($C_{11}H_{15}NO_3$) 209.2; ESI-MS [m/z] (CH_3OH): 232.1 $[M+Na]^+$; ^{1}H NMR (400 MHz, DMSO-d_6, δ in ppm): 9,00 (s, 1H, Ar-N*H*), 8.95 (s, 1H, Ar-O*H*), 7.20 (m, 2H, Ar), 6.63 (m, 2H, Ar), 1.45 (s, 9H, *t*Bu).

(49)

48 (1 g, 4.8 mmol) was dissolved in 5 ml of dry DMA and freshly prepared sulfamoylchloride was added drop-wise until no more starting material was observed (HPLC monitoring). The reaction mixture was quenched with H_2O and extracted with ethyl acetate (3 x 15 ml). The combined organic layers were washed with brine (3 x 15 ml) and H_2O (3 x 15 ml), dried over Na_2SO_4, filtered and concentrated in *vacuo* to give a brown oil, which was used without further purification (85 %).

Calc. for Mr. ($C_{11}H_{16}N_2O_5S$) 288.3; ESI-MS [m/z] (CH_3OH): 287.4 $[M-H]^-$, 311.3 $[M+Na]^+$; ^1H NMR (400 MHz, DMSO-d_6, δ in ppm): 9,43 (s, 1H, Ar-N*H*), 7.86 (s, 2H, SO_2-NH_2), 7.48 (m, 2H, Ar), 7.16 (m, 2H, Ar), 1.47 (s, 9H, *t*Bu).

(50)

49 (450 mg, 1.6 mmol) was dissolved in 10 ml of CH_2Cl_2 and 1 ml of trifluoroacetic acid was added dropwise. The mixture was stirred for 3 h at room temperature and then concentrated in *vacuo* to give a brown oil. The product was not further purified.

Calc. for Mr. ($C_6H_8N_2O_3S$) 188.2; ESI-MS [m/z] (CH_3OH): 189.8 $[M+H]^+$; ^1H NMR (400 MHz, DMSO-d_6, δ in ppm): 7.97 (s, 2H, SO_2-NH_2), 7.23 (m, 2H, Ar), 7.13 (m, 2H, Ar).

(51)

[(Cp-COOH)Re(CO)$_3$] (30 mg, 0.08 mmol) was dissolved in 1 ml of dry DMF. N-Methylmorpholine (13.2 µl, 0.12 mmol) and O-(7-Azabenzotriazol-1-yl)-N,N,N',N'-tetramethyluronium hexafluorophosphate (45.6 mg, 0.12 mmol) was added. After 30 min of strirring **50** (30 mg, 0.16 mmol) was added and the mixture was stirred for 15 h at room temperature. The solvent was evaporated in *vacuo* and the residue was purified by silica gel column chromatography using EtOAc/Hexane 1:1, which afforded **51** in 66 % yield. Crystals were grown from a concentrated methanol solution of **51** by slow evaporation while standing in the air.

IR (cm^{-1} KBr): 2030, 1941, 1907, 1655, 1605, 1527, 1502, 1381, 1314, 1161; Calc. for Mr ($C_{15}H_{11}N_2O_7ReS$) 549.5; ESI-MS [m/z] (CH_3OH): 573.5 $[M+Na]^+$; ^1H NMR (400 MHz, DMSO-d_6, δ in ppm): 9.97 (s, 1H, Ar-*NH*), 7.94 (s, 2H, SO_2N-H_2), 7.68 (m, 2H, Ar), 7.26 (m, 2H, Ar), 6.49 (m, 2H, Cp), 5.81 (m, 2H, Cp); ^{13}C NMR (125 MHz, DMSO-d_6, δ in ppm): 193.9 (*C*O), 160.4 (*C*ONH), 146.0 (Ar1), 136.7 (Ar4), 122.7 (Ar2), 121.5 (Ar3), 95.2 (Cp1), 88.0 (Cp2), 86.7 (Cp3); Calc. C, 32.78; H, 2.02; N, 5.10; Found. C, 32.97; H, 2.11; N, 5.01

(52)

Using 1.5 eq. of 4-Aminobenzensulfonamide, **52** was obtained in an analogueous procedure to **51**. The reaction time was 6 h and the crude product was purified by silica column chromatography eluting with CH_2Cl_2/Hexane/EtOAc (3:2:3) yielding a pale yellow solid (80 %). Crystals were grown from a concentrated methanol solution of **52** by slow evaporation while standing in the air.

IR (cm^{-1} KBr): 2034, 1941, 1914, 1667, 1594, 1535, 1327, 1153; Calc. for Mr ($C_{15}H_{11}N_2O_6ReS$) 533.5; ESI-MS [m/z] (CH_3OH): 557.0 $[M+Na]^+$; ^1H NMR (400 MHz, DMSO-d_6, δ in ppm): 10.14 (s, 1H, Ar-*NH*), 7.80 (s, 4H, Ar), 7.27 (s, 2H, SO_2N-H_2), 6.51 (m, 2H, Cp), 5.82 (m, 2H, Cp); ^{13}C NMR (125 MHz, DMSO-d_6, δ in ppm): 193.8 (*C*O), 160.8 (*C*ONH), 141.3 (Ar1), 130.1 (Ar4), 126.7 (Ar2), 120.0 (Ar3), 94.7 (Cp1), 88.2 (Cp2), 86.8 (Cp3); Calc. C, 33.77; H, 2.08; N, 5.25; Found. C, 33.57; H, 2.00; N, 5.19.

(53)

[(Cp-COOH)Re(CO)$_3$] was activated with pentafluorophenyl trifluoroacetate according to literature procedure.[63] 4-(Aminomethyl)benzene-sulfonamid hydrochloride (81.7 mg, 0.37 mmol) was suspended in 1 ml of DMF. Triethylamine (51.2 µl, 0.37 mmol) was added and the mixture was stirred for 10 min before it was added to a solution of [(Cp-COOPFP)Re(CO)$_3$] (100 mg, 0.18 mmol) in 1 ml DMF. After stirring for 4 h at room temperature, the solvent was evaporated in *vacuo*. The crude product was dissolved in EtOAc and washed with brine (3 x 10 ml) and H_2O (3 x 10 ml), dried over Na_2SO_4, filtered and concentrated in *vacuo*. Silica gel chromatography using EtOAc/Hex 3:1 yielded **53** in 78 % as a colorless powder.

IR (cm^{-1} KBr): 2025, 1918, 1642, 1542, 1325, 1158; Calc. for Mr ($C_{16}H_{13}N_2O_6ReS$) 547.6; ESI-MS [m/z] (CH_3OH): 571.0 $[M+Na]^+$; ^1H NMR (400 MHz, DMSO-d_6, δ in ppm): 8.88 (t, *J*=5.90 Hz, 1H, CH_2-*NH*), 7.76 (m, 2H, Ar), 7.41 (m, 2H, Ar), 7.31 (s, 2H, SO_2N-H_2), 6.34 (m, 2H, Cp), 5.75 (m, 2H, Cp), 4.45 (d, *J*=5.8 Hz, 2H, CH_2); ^{13}C NMR (125 MHz, DMSO-d_6, δ in ppm): 194.1 (*C*O), 161.1 (*C*ONH), 143.4 (Ar1), 142.7 (Ar4), 127.2 (Ar2), 125.7 (Ar3), 94.9 (Cp1), 87.9 (Cp2), 86.4 (Cp3), 41.8 (*C*H_2); Calc. C, 35.10; H, 2.39; N, 5.12; Found. C, 34.89; H, 2.45; N, 5.09.

(30)

[(Cp-COOH)Re(CO)$_3$] was activated with pentafluorophenyl trifluoroacetate according to literature procedure.[63] PFP-activated acid (360.4 mg, 0.53 mmol) was

dissolved in 5 ml DMF and cooled to 0 °C. A solution of 8-aminocaprylic acid (100 mg, 0.63 mmol) and $NaHCO_3$ (53 mg, 0.63 mmol) in 5 ml H_2O was slowly added. A thick cream colored precipitate formed instantly. The mixture was allowed to reach room temperature and was stirred for 18 h whereon the precipitate was consumed. Removal of the solvent under reduced pressure and silica gel chromatography using CH_2Cl_2/MeOH/AcOH 100:1:1 afforded **30** in 88 % yield.

IR (cm^{-1} KBr): 2022, 1907, 1706, 1621, 1551; Calc. for Mr ($C_{16}H_{13}N_2O_6ReS$) 547.6; ESI-MS [m/z] (CH_3OH): 519.8 $[M-H]^-$; ^{1}H-NMR (400 MHz, DMSO-d_6, δ in ppm): 8.16 (t, *J*=5.7 Hz, 1H, NH), 6.26 (m, 2H, Cp), 5.70 (m, 2H, Cp), 3.13 (m, 2H, CH_2), 2.17 (m, 2H, CH_2), 1.45 (m, 4H, CH_2), 1.25 (m, 6H, CH_2); ^{13}C-NMR (125 MHz, DMSO-d_6, δ in ppm): 194.2 (***C***O), 174.5 (***C***OOH), 161.2 (NH***C***O), 96.0 (Cp1), 87.2 (Cp2), 86.2 (Cp3), 38.7 (CH_2), 33.7 (CH_2), 29.0 (CH_2), 28.6 (CH_2), 28.5 (CH_2), 26.2 (CH_2), 24.5 (CH_2); Calc. C, 39.07 H, 4.24; N, 2.68; Found: C, 38.19; H, 3.97; N, 2.86.

(32)

32 was prepared as described for **30** using 7-aminoheptanoic acid. Silica gel chromatography using CH_2Cl_2/MeOH/AcOH 100:1:1 afforded **32** in 86 % yield.

IR (cm^{-1} KBr): 2022, 1909, 1705, 1623, 1551; Calc. for Mr ($C_{16}H_{18}NO_6Re$) 506.5; ESI-MS [m/z] (CH_3OH): 508.0 $[M+H]^+$, 530.0 $[M+Na]^+$, 505.7 $[M-H]^-$; ^{1}H-NMR (400 MHz, DMSO-d_6, δ in ppm): 8.17 (t, *J*=5.7 Hz, 1H, NH), 6.26 (m, 2H, Cp), 5.70 (m, 2H, Cp), 3.13 (m, 2H, CH_2), 2.18 (m, 2H, CH_2), 1.30 (m, 4H, CH_2), 1.26 (m, 4H, CH_2); ^{13}C-NMR (125 MHz, DMSO-d_6, δ in ppm): 194.2 (***C***O), 174.5 (***C***OOH), 161.2 (***C***ONH), 96.0 (Cp1), 87.2 (Cp2), 86.2 (Cp3), 38.6 (CH_2), 33.6 (CH_2), 28.9 (CH_2), 28.3 (CH_2), 26.1 (CH_2), 24.5 (CH_2); Calc. C, 37.94; H, 3.58; N, 2.77; Found: C, 37.74; H, 3.61; N, 2.60.

(31)

To a solution of **31** (318 mg, 0.61 mmol) in 5 ml dry THF, NEt_3 (123 µl, 0.88 mmol) and ClCOOEt (78 µl, 1.0 mmol) were added. After stirring the mixture for 1h at room temperature, a solution of NH_2OH*HCl (141 mg, 2.03 mmol) and NaOMe (30 % in MeOH, 381 µl, 2.03 mmol) in 2 ml MeOH was added and the mixture was stirred at room temperature for 18h. Solvents were evaporated at reduced pressure and the residue was redissolved in THF, filtered and evaporated to dryness. Silica gel chromatography using a gradient from CH_2Cl_2/AcOH 100:5 to CH_2Cl_2/MeOH 100:5 afforded **31** (80 %).

IR (cm^{-1} KBr): 2020, 1905, 1633, 1548, 1367, 1303, 1036; Calc. for Mr ($C_{16}H_{13}N_2O_6ReS$) 535.5; ESI-MS [m/z] (CH_3OH): 559.1 $[M+Na]^+$, 537.2 $[M+H]^+$; ^{1}H-NMR (500 MHz, MeOD, δ in ppm): 8.19 (t, *J*=5.6 Hz, 2H, N*H*CH_2), 6.15 (m, 2H, Cp), 5.56 (m, 2H, Cp), 3.26 (m, 2H, C*H*$_2$), 2.08 (m, 2H, C*H*$_2$), 1.60 (m, 4H, C*H*$_2$), 1.35 (m, 6H, C*H*$_2$); ^{13}C-NMR (125 MHz, MeOD, δ in ppm): 194.3 (*C*O), 173.2 (*C*ONHOH), 164.9 (*C*ONH), 96.2 (Cp1), 87.9 (Cp2), 86.6 (Cp3), 40.7 (CH_2), 33.9 (CH_2), 30.5 (CH_2), 30.2 (CH_2), 30.1 (CH_2), 27.9 (CH_2), 26.8 (CH_2).

(33)

33 was prepared as described for **31** using **32**. Silica gel chromatography using a gradient from CH_2Cl_2/AcOH 100:5 to CH_2Cl_2/MeOH 100:5 afforded **16** (83 %).

IR (cm^{-1} KBr): 2020, 1907, 1633, 1549, 1368, 1303, 1036; Calc. for Mr ($C_{16}H_{19}N_2O_6Re$) 521.5; ESI-MS [m/z] (CH_3OH): 545.1 $[M+Na]^+$; ^{1}H-NMR(400 MHz, DMSO-*d*$_6$, δ in ppm): 10.32 (s, 1H, OH), 8.63 (s, 1H, N*H*OH), 8.20 (t, *J*=5.6 Hz, 2H, N*H*CH_2), 6.27 (m, 2H, Cp), 5.70 (m, 2H, Cp), 3.13 (m, 2H, CH_2), 1.92 (m, 2H, CH_2), 1.45 (m, 4H, CH_2), 1.25 (m, 4H, CH_2); ^{13}C-NMR (125 MHz, DMSO-*d*$_6$, δ in ppm): 194.2 (*C*O), 169.1 (*C*ONHOH), 161.2 (*C*ONH), 96.1 (Cp1), 87.3 (Cp2), 86.2 (Cp3), 38.7 (CH_2), 32.3 (CH_2), 29.0 (CH_2), 28.4 (CH_2), 26.1 (CH_2), 25.1 (CH_2).

(34a/b)

Suberic acid monomethyl ester (309 µl, 1.72 mmol) was dissolved in 10 ml dry THF. Addition of N-methylmorpholine (190 µl, 1.72 mmol) and isobutyl chloroformate (225.5 µl, 1.72 mmol) resulted in formation of a coloreless precipitate. After stirring the suspension for 10 minutes, [(Cp-NH_2)M$(CO)_3$] (a: M = Re, b: M = Mn) [69] (0.86 mmol) was added and the mixture was stirred for another 17 h at room temperature. The solvent was removed at reduced pressure. 30 ml H_2O was added and the residue was extracted three times with 50 ml EtOAc. The combined organic fractions were dried over Na_2SO_4 and evaporated under reduced pressure. Silica gel chromatography with hexane/EtOAc 2:1 afforded **34a/b** in quantitative yield. Crystals of **34b** were grown from CH_2Cl_2/Hexane.

a: IR (cm^{-1} KBr): 2024, 1910, 1719, 1703, 1541, 1487, 1235, 1163; Calc. for Mr ($C_{17}H_{20}NO_6Re$) 520.6; ESI-MS [m/z] (CH_3OH): 544.0 $[M+Na]^+$; ^{1}H-NMR (400 MHz, DMSO-*d*$_6$, δ in ppm): 10.02 (s, 1H, NH), 5.78 (m, 2H, Cp), 5.48 (m, 2H, Cp), 3.57 (s, 3H, CH_3), 2.27 (m, 2H, CH_2), 2.14 (m, 2H, CH_2), 1.25 (m, 4H, CH_2), 1.23 (m, 4H, CH_2); ^{13}C-NMR (125

MHz, DMSO-d_6, δ in ppm): 195.5 (*C*O), 173.3 (*C*OCH$_3$), 171.3 (NH*C*O), 118.7 (Cp1), 81.4 (Cp2), 72.5 (Cp3), 51.2 (CO*C*H$_3$), 35.6 (CH_2), 33.2 (CH_2), 28.1 (CH_2), 28.0 (CH_2), 24.7 (CH_2), 24.2 (CH_2); Calc. C, 39.02; H, 4.09; N, 2.84; Found: C, 38.91; H, 3.95; N, 2.76.
b: ESI-MS [m/z] (CH$_3$OH): 412.0 $[M+Na]^+$

(35)

34a (342 mg, 0.66 mmol) was dissolved in a mixture of 2 ml THF and 4 ml MeOH. LiOH (138 mg, 3.28 mmol) in 2 ml H_2O was added and the mixture was stirred at room temperature for 2h. Solvents were evaporated at reduced pressure to roughly 2 ml and the mixture was acidified with HCl (conc.) to pH 1. Extraction of the aqueous layer with EtOAc afforded 310 mg of **18** (92 %).
Calc. for Mr ($C_{16}H_{18}NO_6Re$) 506.5; ESI-MS [m/z] (CH$_3$OH): 530.0 $[M+Na]^+$, 506.0 $[M-H]^-$; ^{1}H-NMR (400 MHz, DMSO-d_6, δ in ppm): 10.02 (s, 1H, NH), 5.78 (m, 2H, Cp), 5.48 (m, 2H, Cp), 2.17 (m, 4H, CH_2), 1.47 (m, 4H, CH_2), 1.24 (m, 4H, CH_2).

(36)

36 was prepared as described for **31** using **35**. Silica gel chromatography using a gradient from CH_2Cl_2/AcOH 100:5 to CH_2Cl_2/MeOH 100:5 afforded **36** (86 %).
IR (cm^{-1} KBr): 2019, 1913, 1640, 1558, 1487, 1385; Calc. for Mr ($C_{16}H_{19}N_2O_6Re$) 521.5; ESI-MS [m/z] (CH$_3$OH): 545.1 $[M+Na]^+$; ^{1}H-NMR (400 MHz, DMSO-d_6, δ in ppm): 10.30 (s, 1H, OH), 10.02 (s, 1H, NH), 8.63 (s, 1H, *NH*OH), 5.78 (m, 2H, Cp), 5.48 (m, 2H, Cp), 2.14 (m, 2H, CH_2), 1.92 (m, 2H, CH_2), 1.47 (m, 4H, CH_2), 1.22 (m, 4H, CH_2); ^{13}C-NMR (125 MHz, DMSO-d_6, δ in ppm): 195.5 (*C*O), 171.3 (NH*C*O), 169.0 (*C*ONHOH), 118.7 (Cp1), 81.4 (Cp2), 72.5 (Cp3), 35.7 (CH_2), 32.2 (CH_2), 28.3 (CH_2), 28.2 (CH_2), 25.0 (CH_2), 24.8 (CH_2); Calc. C, 39.02; H, 4.09; N, 2.84; Found: C, 38.91; H, 3.95; N, 2.76.

(37)

Benzoic acid (250 mg, 2.05 mmol) was dissolved in 5 ml dry DMF. Pyridine (180.6 □l, 2.24 mmol) and pentafluorophenyl trifluoracetate (386.8 µl, 2.24 mmol) were added and the solution was stirred for 3 h at room temperature. DMF was evaporated at reduced pressure. EtOAc was added and the residue was extracted three times with 0.1 M HCl and three times with 5 % $NaHCO_3$. The organic fraction was washed with fresh H_2O, dried over Na_2SO_4 and evaporated to dryness. The activated acid (151.3 mg, 0.53 mmol) was dissolved in 5 ml DMF and cooled to 0 °C. A solution of 8-

aminocaprylic acid (100 mg, 0.63 mmol) and $NaHCO_3$ (53 mg, 0.63 mmol) in 1 ml H_2O was slowly added. A thick cream colored precipitate formed instantly. The mixture was allowed to reach room temperature and was stirred for 18 h. Silica gel chromatography using EtOAc/Hexane 1:1 afforded **37** (90 %).

Calc. for Mr ($C_{15}H_{21}NO_3$) 263.3; ESI-MS [m/z] (CH_3OH): 286.1 $[M+Na]^+$, 264.0 $[M+H]^+$, 262.0 $[M-H]^-$; ^{1}H-NMR (400 MHz, DMSO-d_6, δ in ppm): 8.41 (t, *J*=5.4 Hz, 1H, NH), 7.81 (m, 2H, Ar), 7.46 (m, 3H, Ar), 3.24 (m, 2H, CH_2), 2.19 (m, 2H, CH_2), 1.50 (m, 4H, CH_2), 1.29 (m, 6H, CH_2); ^{13}C-NMR (125 MHz, MeOD, δ in ppm): 177.9 (***C***OOH), 170.4 (***C***ONH), 136.0 (Ar1), 132.7 (Ar2), 129.7 (Ar3), 128.4 (Ar4), 41.1 (CH_2), 35.1 (CH_2), 30.6 (CH_2), 30.3 (CH_2), 30.2 (CH_2), 28.1 (CH_2), 26.2 (CH_2); Calc. C, 68.42; H, 8.04; N, 5.32; Found: C, 67.99; H, 7.76; N, 5.26.

(39)

39 was prepared as described for **37** using 7-aminoheptanoic acid. Silica gel chromatography using EtOAc/Hexane 1:1 afforded **39** (89 %).

Calc. for Mr ($C_{15}H_{19}NO_3$) 249.3; ESI-MS [m/z] (CH_3OH): 250.0 $[M+H]^+$, 272.0 $[M+Na]^+$, 247.9 $[M-H]^-$; ^{1}H-NMR (400 MHz, DMSO-d_6, δ in ppm): 8.41 (t, *J*=5.3 Hz, 1H, NH), 7.81 (m, 2H, Ar), 7.46 (m, 3H, Ar), 3.24 (m, 2H, CH_2), 2.19 (m, 2H, CH_2), 1.50 (m, 4H, CH_2), 1.30 (***m***, 4H, CH_2); ^{13}C-NMR (125 MHz, MeOD, δ in ppm): 177.9 (***C***OOH), 170.5 (***C***ONH), 136.1 (Ar1), 132.7 (Ar2), 129.7 (Ar3), 128.4 (Ar4), 41.1 (CH_2), 35.1 (CH_2), 30.5 (CH_2), 30.1 (CH_2), 27.9 (CH_2), 26.2 (CH_2); Calc. C, 67.45; H, 7.68; N, 5.62; Found: C, 67.25; H, 7.48; N, 5.46.

(38)

38 was prepared as described for **31** using **37**. Silica gel chromatography using a gradient from CH_2Cl_2/AcOH 100:5 to CH_2Cl_2/MeOH 100:5 afforded **22** (90 %).

Calc. for Mr ($C_{15}H_{22}N_2O_3$) 278.4; ESI-MS [m/z] (CH_3OH): 279.1 $[M+H]^+$, 301.1 $[M+Na]^+$, 277.1 $[M-H]^-$; ^{1}H-NMR (400 MHz, DMSO-d_6, δ in ppm): 10.33 (s, 1H, OH), 8.62 (s, 1H, ***NH***OH), 8.41 (t, *J*=5.5 Hz, 1H, NH), 7.81 (m, 2H, Ar), 7.46 (m, 3H, Ar), 3.24 (m, 2H, CH_2), 1.93 (m, 2H, CH_2), 1.50 (m, 4H, CH_2), 1.15 (m, 6H, CH_2); ^{13}C-NMR (125 MHz, MeOD, δ in ppm): 173.2 (***C***ONHOH), 170.4 (***C***ONH), 136.0 (Ar1), 132.7 (Ar2), 129.7 (Ar3), 128.4 (Ar4), 48.0 (CH_2), 41.1 (CH_2), 33.9 (CH_2), 30.6 (CH_2), 30.2 (CH_2), 28.0 (CH_2), 26.8 (CH_2); Calc. C, 64.73; H, 7.97; N, 10.06; Found: C, 64.32; H, 7.88; N, 9.91.

(40)

40 was prepared as described for **31** using **39**. Silica gel chromatography using a gradient from CH_2Cl_2/AcOH 100:5 to CH_2Cl_2/MeOH 100:5 afforded **23** (92 %).

Calc. for Mr ($C_{14}H_{20}N_2O_3$) 264.3; ESI-MS [m/z] (CH_3OH): 265.2 $[M+H]^+$, 263.2 $[M-H]^-$; ^{1}H-NMR (400 MHz, DMSO-d_6, δ in ppm): 10.33 (s, 1H, OH), 8.64 (s, 1H, *NH*OH), 8.42 (t, *J*=5.5 Hz, 1H, NH), 7.83 (m, 2H, Ar), 7.46 (m, 3H, Ar), 3.24 (m, 2H, CH_2), 1.93 (m, 2H, CH_2), 1.50 (m, 4H, CH_2), 1.15 (m, 4H, CH_2); Calc. (for **23** + 0.5 H_2O) C, 61.52; H, 7.74; N, 10.25; Found: C, 61.14; H, 7.67; N, 9.89.

(66)

[(Cp-COOH)Re(CO)$_3$] (135 mg, 0.36 mmol) was dissolved in 5 ml dry CH_2Cl_2. Oxalylchloride (91.5 µl, 1.07 mmol) and a catalytic amount of DMF was added. The suspension was stirred at 0 °C for 1h and for 4h at room temperature. The solvent was evaporated and the residue was redissolved in dry THF.

In a separate flask 6-aminopenicillanic acid (84.7 mg, 0.39 mmol) was suspended in 1 ml EtOH. Trimethylsilyl chloride (87.3 µl, 0.69 mmol) was added, whereas the mixture turned clear instandly and was stirred for 2h. Solvents and excess of trimethylsilyl chloride were removed under reduced pressure. The colourless residue was redissolved in dry THF and triethylamine (150 µl, 1.08 mmol) was added.

Both solutions were slowly mixed together at 0 °C and stirred for 1h, then the mixture was allowed to reach room temperature and was stirred for another 3h. THF was evaporated and the residue was purified by silica gel column chromatography using CH_2Cl_2/MeOH/AcOH 100:2:1 (70 %).

Calc. for Mr ($C_{19}H_{19}N_2O_7ReS$) 605.5; ESI-MS [m/z] (CH_3OH): 625.0 $[M+H_3O]^+$, 622.9 $[M+OH]^-$; ^{1}H NMR (400 MHz, MeOD, δ in ppm): 6.27 – 6.21 (m, 2H, Cp), 5.66 – 5.55 (m, 2H, Cp), 5.05 (d, *J*=8.3 Hz, 1H, CH), 4.62 (d, *J*=8.3 Hz, 1H, CH), 4.21 (q, J=3x7.0, 2H, CH_2 ester), 3.75 (s, 1H, C*H*COOEt), 1.64 (s, 3H, CH_3), 1.30 (t, *J*=2x7.2, 3H, CH_3 ester), 1.30 (s, 3H, CH_3); ^{13}C NMR (125 MHz, $CDCl_3$, δ in ppm): 194.1 (3xCO), 172.3 (CO), 171.4 (CO), 165.1 (CO), 94.8 (Cp1), 89.1 (Cp2), 88.2 (Cp3), 87.0 (Cp4), 86.2 (Cp5), 73.7 (*C*HCO), 66.9 (CHS), 62.8 (tert. C), 59.8 (CH_2 ester), 59.2 (CHNH), 28.3 (CH_3), 27.6 (CH_3), 14.6 (CH_3).

(70)

[(Cp-COOH)Re(CO)$_3$] was activated with pentafluorophenyl trifluoroacetate according to literature procedure.[63] PFP-activated acid (100.0 mg, 0.18 mmol) was dissolved in 1 ml DMF. L-Noradrenaline (34.2 mg, 0.20 mmol) and triethylamine (28.0 µl, 0.20 mmol) were slowly added. The mixture was stirred for 5 h. Removal of the solvent under reduced pressure and silica gel chromatography using CH_2Cl_2/MeOH/AcOH 100:5:1 afforded **70** in 76 % yield.

Calc. for Mr ($C_{17}H_{14}NO_7Re$) 530.5; ESI-MS [m/z] (CH_3OH): 530.0 [M-H]$^-$; ^{1}H-NMR (400 MHz, DMSO-d_6, δ in ppm): 8.28 (t, *J*=5.8 Hz, 1H, NH), 6.79 – 6.5 (m, 3H, Ar), 6.34 – 6.21 (m, 2H, Cp), 5.73 – 5.64 (m, 2H, Cp), 4.50 – 4.42 (m, 1H, CH).

3.4.3 [Re(CO)$_3$Cp-SO$_2$R]

(4)

[CpRe(CO)$_3$] (1 g, 2.98 mmol) was suspended in 2 ml of acetic anhydride. Over the course of 1h H_2SO_4 (95-97 %, 329 µl) was added, while keeping the temperature between 25 and 30 °C. The dark solution was stirred for another hour and was then refluxed for 1 h at 60 °C. The mixture was chilled to room temperature and was poured over ice and was allowed to stand for 1h. After filtration, the aqueous layer was separated. ***p***-Toluidine (555 mg, 5.13 mmol), dissolved in 2 ml of water containing 0.5 ml conc HCl, was added under vigorous stirring, whereas a cream colored thick precipitate formed instantly. The suspension was stirred for another 30min, then filtered and washed with toluene to give **4** (90 % yield).

IR (cm^{-1} KBr): 2032, 1939, 1920, 1515, 1198; Calc. for Mr ($C_8H_4O_6ReS^-$) 414.9; ESI-MS [m/z] (CH_3OH): 414.9 [M-H]$^-$; ^{1}H NMR (400 MHz, MeOD, δ in ppm): 7.35 (m, 2H, Ar), 7.27 (m, 2H, Ar), 5.91 (m, 2H, Cp), 5.43 (m, 2H, Cp), 2.30 (s, 3H, CH_3); Calc. C, 34.48; H, 2.70; N, 2.68; Found C, 34.29; H, 2.76; N, 2.59.

(5)

A mixture of **28** (250 mg, 0.478 mmol) and phosphorus pentachloride (197 mg, 0.959 mmol) was stirred vigorously for 20min at room temperature until a melt was formed. The mixture was then heated at 45 °C for 1h. After cooling to room temperature, toluene was added. The mixture was stirred well, poured over ice, allowed to stand for 1h and was then filtered. The organic layer was separated, dried over Na_2SO_4,

treated with activated charcoal and evaporated under reduced pressure. The residue was dissolved in a minimum of CH_2Cl_2 and hexane was added. The pale yellow precipitate was collected to afford **5** (70 %). Crystals suitable for X-Ray analysis were grown from CH_2Cl_2/hexane.

IR (cm^{-1} KBr): 2038, 1949, 1508, 1378, 1214; Calc. for Mr ($C_8H_4ClO_5ReS$) 433.9; ESI-MS [m/z] (CH_3OH): 433.1 $[M-H]^-$. ^1H NMR (500 MHz, CD_3CN, δ in ppm): 6.35 (m, 2H, Cp), 5.71 (m, 2H, Cp). Calc. C, 22.15; H, 0.93; Found C, 22.09; H, 0.98

(6)

5 (50 mg, 0.115 mmol) and ***p***-Toluidine (37 mg, 0.345 mmol) were dissolved in 10 ml of absolute EtOH. The solution was refluxed at 90 °C for 5h. After cooling to room temperature, the solvent was evaporated under reduced pressure and the residue was purified by column chromatography using EtOAc/Hexane 2:1 to afford a light brown powder (49 %).

IR (cm^{-1} KBr): 2036, 1957, 1943, 1510, 1334, 1138; Calc. for Mr ($C_{15}H_{12}NO_5ReS$) 505.0; ESI-MS [m/z] (CH_3OH, formic acid): 503.7 $[M-H]^-$. ^1H NMR (500 MHz, MeOD, δ in ppm): 7.12 (m, 2H, Ar), 7.06 (m, 2H, Ar), 5.83 (m, 2H, Cp), 5.48 (m, 2H, Cp), 2.30 (s, 3H, C***H***$_3$).

(63/64)

5 (50 mg, 0.115 mmol) and 3-amino-5-methylisoxazole (33.8 mg, 0.345 mmol) were dissolved in 5 ml of dry THF. The solution was heated under stirring at 40 °C for 10h. After cooling to room temperature, the solvent was evaporated under reduced pressure. The dark residue was purified by silica gel column chromatography using EtOAc/hexane 1:1, to give a coloreless powder (69 %). Crystals suitable for X-Ray analysis were grown from CH_2Cl_2/hexane containing a small amount of DMSO.

NMR analysis and crystal structure showed the unexpected formation of complex **63** instead of the desired sulfonamide. Compound **64** was isolated as a second product of the decomplexation.

63: IR (cm^{-1} KBr): 2023, 1915, 1883, 1626, 1534, 1473; ^1H NMR (400 MHz, DMSO, δ in ppm): 6.30 (s, 4H, N***H***$_2$); 5.85 (s, 2H, CH); 2.27 (s, 6H, C***H***$_3$).

64: Calc. for Mr ($C_{18}H_{20}N_4O_6S_2$) 452.5; ESI-MS [m/z] (CH_3OH): 451.3 $[M-H]^-$. ^1H NMR (500 MHz, CD_3CN, δ in ppm): 6.42 (m, 1H), 6.18 (s, 1H), 6.05 (s, 1H), 6.04 – 6.02 (m, 1H), 5.71 (d, *J*=5.7 Hz, 1H), 3.90 – 3.87 (m, 1H), 3.27 – 3.22 (m, 1H), 3.09 (s, 1H), 1.84-1.72 (m, 2H).

(65)

5 (50 mg, 0.115 mmol) and 2-aminopyrimidine (32.1 mg, 0.345 mmol) were dissolved in 5 ml of dry THF. The solution was heated under stirring at 40 °C for 12h. After cooling to room temperature, the solvent was evaporated under reduced pressure. Crystals were grown from methanol.

Similar to **63**, the crystal structure shows the formation of complex **65** instead of the desired sulfonamide.

IR (cm^{-1} KBr): 2025, 1916, 1890, 1867, 1638, 1555; ^{1}H NMR (400 MHz, DMSO, δ in ppm): 8.17 (dd, *J*=6.0, 4.5 Hz, 2H, Ar); 6.84 (dd, *J*=5.8, 4.7 Hz, 2H, Ar); 6.71 (dd, *J*=6.0, 4.5 Hz, 2H, Ar)

3.4.4 [$Re(CO)_3Cp$-CH_2COR]

(24a)

$(NEt_4)_2[Re(Br)_3(CO)_3]$ (100 mg, 0.13 mmol), **18** (16.1 mg, 0.13 mmol) and Borax (70 mg) were suspended in 10 ml distilled water. The mixture was stirred at 90 °C for 16 h and then concentrated to dryness under reduced pressure. The crude product was purified by silica gel column chromatography using CH_2Cl_2/Hexane 1:2 containing 1.6 % AcOH (20 %).

IR (cm^{-1} KBr): 2020, 1911, 1579, 1394, 1024; Calc. for Mr ($C_{10}H_7O_5Re$) 393.4; ESI-MS [m/z] (CH_3OH): 348.8 $[M\text{-}CO_2]^-$, 321.0 $[M\text{-}C_2O_3]^-$; ^{1}H NMR (400 MHz, $CDCl_3$, δ in ppm): 5.46 (m, 2H, Cp), 5.31 (m, 2H, Cp), 3.5 (s, 2H, CH_2). ^{13}C NMR (125 MHz, $CDCl_3$, δ in ppm): 194.0 (CO), 175.9 (COOH), 99.7 (Cp1), 85.5 (Cp2), 84.2 (Cp3), 34.90 (CH_2); Calc. C, 30.53; H, 1.79; Found. C, 30.18; H, 1.94.

(24b)

$[(Cp)Re(CO)_3]$ (150 mg, 0.40 mmol) was dissolved in 5 ml dry THF. The Solution was cooled to -78 °C and *n*BuLi (2 M, 246 µl, 0.492 mmol) was added tropwise. After stirring for 1h, bromoacetic acid methylester (83.6 µl, 0.88 mmol) was dropped to the mixture was stirred for 3h at room temperature. The solvent was removed under reduced pressure, CH_2Cl_2 was added and the residue was extracted with brine. The product was purified by silica gel column chromatography using CH_2Cl_2/Hexane 2:3. Crystals were grown from CH_2Cl_2/Hexane. X-Ray and NMR analysis revealed the unexpected formation of compound **24b** instead of **24a** (50 % yield).

IR (cm^{-1} KBr): 2018, 1921, 1904, 1639; ^1H NMR (400 MHz, $CDCl_3$, δ in ppm): 5.71 (m, 2H, Cp), 5.56 (m, 2H, Cp), 5.30 (m, 4H, Cp), 3.72 (s, 2H, CH_2), 2.41 (s, 1H, OH).

(67)

24a (50 mg, 0.13 mmol) was dissolved in 2 ml dry CH_2Cl_2. Oxalylchloride (33.6 µl, 0.39 mmol) and a catalytic amount of DMF was added. The suspension was stirred at 0 °C for 1h and for 4h at room temperature. The solvent was evaporated and the residue was redissolved in dry THF.

In a separate flask 6-aminopenicillanic acid (32.6 mg, 0.13 mmol) was suspended in 1 ml EtOH. Trimethylsilyl chloride (29 µl, 0.33 mmol) was added, whereas the mixture turned clear instandly and was stirred for 2h. Solvents and excess of trimethylsilyl chloride were removed under reduced pressure. The colourless residue was redissolved in dry THF and triethylamine (70 µl, 0.504 mmol) was added.

Both solutions were slowly mixed together at 0 °C and stirred for 1h, then the mixture was allowed to reach room temperature and was stirred for another 3h. THF was evaporated and the residue was purified by silica gel column chromatography using CH_2Cl_2/MeOH/AcOH 100:2:1 (66 %).

Calc. for Mr ($C_{20}H_{21}N_2O_7ReS$) 619.1; ESI-MS [m/z] (CH_3OH): 639.0 $[M+H_3O]^+$, 637.0 $[M+OH]^-$; ^1H NMR (400 MHz, MeOD, δ in ppm): 5.68 – 5.60 (m, 2H, Cp), 5.45 – 5.41 (m, 2H, Cp), 5.00 (d, *J*=7.2 Hz, 1H, CH), 4.53 (d, *J*=7.2 Hz, 1H, CH), 4.20 (q, J=3x7.2, 2H, CH_2 ester), 3.75 (s, 1H, C*H*COOEt), 3.42 (s, 1H, CH_2), 3.40 (s, 1H, CH_2), 1.62 (s, 3H, CH_3), 1.29 (t, *J*=2x7.2, 3H, CH_3 ester), 1.28 (s, 3H, CH_3); ^{13}C NMR (125 MHz, $CDCl_3$, δ in ppm): 195.7 (CO), 172.6 (CO), 172.3 (CO), 171.5 (CO), 104.2 (Cp1), 86.8 (2xCp), 85.3 (2xCp), 73.8 (*C*HCO), 67.4 (CHS), 62.7 (tert. C), 60.1 (CH_2 ester), 59.4 (CHNH), 36.2 (CH_2), 28.1 (CH_3), 27.5 (CH_3), 14.6 (CH_3).

(54)

24a (50 mg, 0.13 mmol) was activated with pentafluorophenyl trifluoroacetate in an analogous procedure to the literature procedure for $[(CpCOOH)Re(CO)_3]$.[63]

4-(Aminomethyl)benzene-sulfonamid hydrochloride (57.6 mg, 0.25 mmol) was suspended in 1 ml of DMF. Triethylamine (36.1 µl, 0.25 mmol) was added and the mixture was stirred for 10 min before it was added to a solution of $[(Cp\text{-}CH_2COOPFP)Re(CO)_3]$ (72.7 mg, 0.13 mmol) in 1 ml DMF. After stirring for 16 h at room temperature, the solvent was evaporated in *vacuo*. The crude product was

dissolved in CH_2Cl_2 and extracted first three times with 0.1 M HCl and then three times with 5 % $NaHCO_3$. The Organic layer was dried over Na_2SO_4, filtered and concentrated in *vacuo* (66 %).

IR (cm^{-1} KBr): 2020, 1930, 1899, 1618, 1552; Calc. for Mr ($C_{17}H_{15}N_2O_6ReS$) 561.6; ESI-MS [m/z] (CH_3OH): 1144.8 $[2M+Na]^+$; ^1H NMR (400 MHz, $CDCl_3$, δ in ppm): 7.89 (m, 2H, Ar), 7.43 (m, 2H, Ar), 5.46 (m, 2H, Cp), 5.31 (m, 2H, Cp), 4.52 (d, *J*=5.8 Hz, 2H, C*H*$_2$), 3.39, (s, 2H, C*H*$_2$); ^{13}C NMR (125 MHz, MeOD, δ in ppm): 172.7 (*C*O), 144.6 (Ar1), 144.1 (Ar2), 129.2 (Ar3), 127.6 (Ar4), 104.3 (Cp1), 86.7 (Cp2), 85.3 (Cp3), 44.0 (*C*H_2), 36.3 (*C*H_2); Calc. C, 36.36; H, 2.69; N, 4.99; Found. C, 36.49; H, 2.74; N, 5.06.

3.4.5 [Re(CO)$_3$Cp-CH$_2$CH$_2$COR]

(25)

Sodium metal (25.7 mg, 1.11 mmol) was dissolved in 5 ml of MeOH. When the sodium was consumed, [(CpCOH)Re(CO)$_3$] (271 mg, 0.746 mmol) in 2 ml MeOH and triethyl phosphonoacetate (167.2 mg, 0.746 mmol) in 2 ml MeOH were added dropwise at 0 °C. The mixture was allowed to reach room temperature and was stirred for 2h. The solvent was removed in vacuo and the residue was purified by silica gel column chromatography using Hexane/EtOAc 10:1 (80 %).

IR (cm^{-1} KBr): 2023, 1934, 1909, 1714, 1642, 1428, 1307, 1205; Calc. for Mr ($C_{12}H_9O_5Re$) 420.0; ESI-MS [m/z] (CH_3OH): 443.0 $[M+Na]^+$; ^1H NMR (400 MHz, $CDCl_3$, δ in ppm): 7.30 (d, *J*=15.8 Hz, 1H, CH), 6.12 (d, *J*=15.8 Hz, 1H, CH), 5.68 (m, 2H, Cp), 5.37 (m, 2H, Cp), 3.77 (s, 3H, CH_3); ^{13}C NMR (125 MHz, $CDCl_3$, δ in ppm): 193.0 (CO), 166.6 (*C*OCH_3), 136.6 (CH), 118.7 (CH), 97.6 (Cp1), 85.5 (Cp2), 85.0 (Cp3), 52.1 (CH_3); Calc. C, 34.37; H, 2.16; Found. C, 33.81; H, 2.35.

(26-27)

25 (100 mg, 0.231 mmol) and palladium adsorbed on charcoal (10 %, 20 mg) were dispersed in 10 ml EtOAc. The mixture was first saturated with N_2, then with H_2 and was then stirred for 48h under an atmosphere of H_2 at ambient pressure. Filtration and evaporation of the solvent afforded the reduced product quantitatively (**26**).

Calc. for Mr ($C_{12}H_{11}O_5Re$) 421.4; ESI-MS [m/z] (CH_3OH): 445.0 $[M+Na]^+$; ^1H NMR (400 MHz, $CDCl_3$, δ in ppm): 5.29 (m, 2H, Cp), 5.24 (m, 2H, Cp), 3.70 (s, 3H, CH_3), 2.78 (t, *J*=7.4 Hz, 2H, CH_2), 2.53 (t, *J*=7.4 Hz, 2H, CH_2); ^{13}C NMR (125 MHz, $CDCl_3$, δ in ppm):

194.4 (CO), 172.8 (*C*OCH$_3$), 109.0 (Cp1), 83.8 (Cp2,3), 52.1 (CH$_3$), 36.1 (CH$_2$), 23.48 (CH$_2$).

Hydrolysis of the ester function was performed with LiOH (5 eq.) in a mixture of H$_2$O/MeOH/THF (1:2:2). The solution was stirred for 2h at 0 °C and for another 5h at room temperature. Concentration under reduced pressure and acidification with 1M HCl to pH 3 produced a colourless precipitate. Et$_2$O was added and the aqueous phase was extracted three times. The combined organic fractions were dried with Na$_2$SO$_4$ and evaporated under reduced pressure. **27** was obtained as a pale yellow solid (78 %).

IR (cm^{-1} KBr): 2023, 1912, 1697; Calc. for Mr ($C_{11}H_9O_5Re$) 408.4; ESI-MS [m/z] (CH$_3$OH): 407.0 [M-H]$^-$; ^{1}H NMR (500 MHz, CDCl$_3$, δ in ppm): 5.31 (m, 2H, Cp), 5.26 (m, 2H, Cp), 2.77 (t, *J*=7.3 Hz, 2H, CH$_2$), 2.59 (t, *J*=7.3 Hz, 2H, CH$_2$); ^{13}C NMR (125 MHz, CDCl$_3$, δ in ppm): 194.3 (CO), 177.1 (*C*OCH$_3$), 108.55 (Cp1), 83.9 (Cp2), 83.8 (Cp3), 35.8 (CH$_2$), 23.2 (CH$_2$); Calc. C, 32.43; H, 2.23; Found. C, 32.15; H, 2.42.

(68)

27 (53 mg, 0.13 mmol) was dissolved in 2 ml dry CH$_2$Cl$_2$. Oxalylchloride (33.6 µl, 0.39 mmol) and a catalytic amount of DMF was added. The suspension was stirred at 0 °C for 1h and for 4h at room temperature. The solvent was evaporated and the residue was redissolved in dry THF.

In a separate flask 6-aminopenicillanic acid (32.6 mg, 0.13 mmol) was suspended in 1 ml EtOH. Trimethylsilyl chloride (29 µl, 0.33 mmol) was added, whereas the mixture turned clear instandly and was stirred for 2h. Solvents and excess of trimethylsilyl chloride were removed under reduced pressure. The colourless residue was redissolved in dry THF and triethylamine (70 µl, 0.504 mmol) was added.

Both solutions were slowly mixed together at 0 °C and stirred for 1h, then the mixture was allowed to reach room temperature and was stirred for another 3h. THF was evaporated and the residue was purified by silica gel column chromatography using CH$_2$Cl$_2$/MeOH/AcOH 100:2:1 (71 %).

Calc. for Mr ($C_{21}H_{23}N_2O_7ReS$) 633.7; ESI-MS [m/z] (CH$_3$OH): 653.1 [M+H$_3$O]$^+$, 650.9 [M+OH]$^-$; ^{1}H NMR (400 MHz, MeOD, δ in ppm): 5.55 – 5.52 (m, 1H, Cp), 5.50 – 5.45 (m, 1H, Cp), 5.41 – 5.38 (m, 1H, Cp), 5.38 – 5.34 (m, 1H, Cp), 4.96 (d, *J*=7.8 Hz, 1H, CH), 4.57 (d, *J*=7.8 Hz, 1H, CH), 4.18 (q, J=3x7.0, 2H, CH$_2$ ester), 3.75 (s, 1H, C*H*COOEt), 2.85 –

2.66 (m, 2H, CH_2), 2.49 (t, *J*=7.2 Hz, 2H, CH_2), 1.61 (s, 3H, CH_3), 1.27 (t, *J*=2x7.0, 3H, CH_3 ester), 1.27 (s, 3H, CH_3); ^{13}C NMR (125 MHz, $CDCl_3$, δ in ppm): 196.0 (CO), 174.4 (CO), 172.4 (CO), 171.6 (CO), 111.2 (Cp1), 85.4 (Cp2), 85.3 (Cp3), 85.2 (Cp4), 85.0 (Cp5), 73.8 (*C*HCO), 67.5 (CHS), 62.7 (tert. C), 60.1 (CH_2 ester), 59.2 (CHNH), 38.6 (CH_2), 28.3 (CH_3), 27.6 (CH_3), 25.1 (CH_2), 14.6 (CH_3).

(55)

27 (153 mg, 0.38 mmol) was activated with pentafluorophenyl trifluoroacetate in an analogous procedure to the literature description for [(CpCOOH)Re(CO)$_3$].[63]
4-(Aminomethyl)benzene-sulfonamid hydrochloride (100.4 mg, 0.45 mmol) was suspended in 1 ml of DMF. Triethylamine (62.5 µl, 0.45 mmol) was added and the mixture was stirred for 10 min before it was added to a solution of [(Cp-CH_2 CH_2COOPFP)Re(CO)$_3$] (217.5 mg, 0.38 mmol) in 1 ml DMF. After stirring for 16 h at room temperature, the solvent was evaporated in *vacuo*. The crude product was purified by silica gel column chromatography using a gradient from pure CH_2Cl_2 to a mixture of CH_2Cl_2/MeOH/AcOH 14:1:0.2 (78 %).
IR (cm^{-1} KBr): 2017, 1911, 1636, 1548, 1323; Calc. for Mr ($C_{18}H_{17}N_2O_6ReS$) 575.6; ESI-MS [m/z] (CH_3OH): 689.3 $[M-H]^-$; ^1H NMR (400 MHz, MeOD, δ in ppm): 7.85 (m, 2H, Ar), 7.42 (m, 2H, Ar), 5.42 (m, 2H, Cp), 5.38 (m, 2H, Cp), 4.43 (s, 2H, C*H*$_2$), 2.75 (t, *J*=7.3 Hz, 2H, C*H*$_2$), 2.48 (t, *J*=7.3 Hz, 2H, C*H*$_2$); ^{13}C NMR (125 MHz, MeOD, δ in ppm): 195.9 (*C*O), 174.4 (*C*ONH), 144.8 (Ar1), 144.0 (Ar2), 129.2 (Ar3), 127.5 (Ar4), 110.9 (Cp1), 85.2 (Cp2), 43.8 (*C*H$_2$), 39.0 (*C*H$_2$), 25.3 (*C*H$_2$); Calc. C, 37.56; H, 2.98; N, 4.97; Found. C, 37.89; H, 3.01; N, 4.82.

3.5 Organic Syntheses

3.5.1 Cp-CONHR

(56)

3a,4,7,7a-Tetrahydro-1H-4,7-methanoindene-2,6-dicarboxylic acid (Thiele's acid) (85.4 mg, 0.39 mmol) were suspended in 5 ml of CH_2Cl_2. Oxalyl chloride (100.0 µl, 1.16 mmol) and a catalytic amount of DMF was added. The mixture was stirred until all reactants were dissolved. The solvent was removed in *vacuo* and the activated Thiele's acid was redissolved in 10 ml of THF. 4-aminophenol (85 mg, 0.78 mmol) and triethylamine (110.0 µl, 0.79 mmol) were added and the mixture was stirred for 2 h. Filtration and silica gel column chromatography using THF/Hexane 1:1 afforded pure **56** (63 %).

^{1}H NMR (400 MHz, MeOD, δ in ppm): 7.36-7.20 (m, 4H, Ar), 6.87 (s, 1H, C*H*), 6.78 – 6.56 (m, 4H, Ar), 6.51 (s, 1H, C*H*), 3.65-3.55 (m, 1H, C*H*), 3.54-3.45 (m, 1H, C*H*), 3.25-3.16 (m, 1H, C*H*), 3.11 – 3.00 (m, 1H, C*H*), 2.65-2.53 (m 1H, C*H*), 2.31-2.20 (m, 1H, C*H*), 1.76 – 1.67 (m, 1H, C*H*), 1.55 – 1.46 (m, 1H, C*H*).

(57)

56 (120 mg, 0.30 mmol) was dissolved in 1 ml of dry DMA at 0 °C and freshly prepared sulfamoylchloride was added drop-wise until no more starting material was observed (HPLC monitoring). The reaction mixture was quenched with H_2O and extracted with ethyl acetate (3 x 15 ml). The combined organic layers were washed with brine (3 x 15 ml) and H_2O (3 x 15 ml), dried over Na_2SO_4, filtered and concentrated in *vacuo* to give a brown oil, which was not further purified (89 %).

^{1}H NMR (400 MHz, MeOD, δ in ppm): 7.59-7.47 (m, 4H, Ar), 7.05 – 6.99 (m, 4H, Ar), 6.91 – 6.88 (m, 1H, C*H*), 6.55 – 6.50 (m, 1H, C*H*), 3.65-3.55 (m, 1H, C*H*), 3.54-3.49 (m, 1H, C*H*), 3.27-3.19 (m, 1H, C*H*), 3.11 – 3.00 (m, 1H, C*H*), 2.67-2.54 (m 1H, C*H*), 2.34-2.23 (m, 1H, C*H*), 1.77 – 1.70 (m, 1H, C*H*), 1.56 – 1.48 (m, 1H, C*H*).

(58)

3a,4,7,7a-Tetrahydro-1H-4,7-methanoindene-2,6-dicarboxylic acid (Thiele's acid) (100 mg, 0.46 mmol) were suspended in 5 ml of CH_2Cl_2. Oxalyl chloride (98 µl, 1.35 mmol) and a catalytic amount of DMF was added. The mixture was stirred until all reactants

were dissolved. The solvent was removed in *vacuo* and the activated Thiele's acid was redissolved in 10 ml of THF. 4-aminobenzensulfonamide (172 mg, 0.99 mmol) and triethylamine (138.5 µl, 0.99 mmol) were added and the mixture was stirred for 15 h. Filtration and washing with fresh THF and a small portion of MeOH yielded the product as yellow solid (43 %).

Calc. for Mr ($C_{24}H_{24}N_4O_6S_2$) 528.6; ESI-MS [m/z] (CH_3OH): 529.5 $[M+H]^+$; ^1H NMR (400 MHz, DMSO-d_6, δ in ppm): 9.88 (s, 1H, Ar-*NH*), 9.77 (s, 1H, Ar-*NH*), 7.92-7.67 (m, 8H, Ar), 7.20 (s, 4H, SO_2N-H_2), 6.95 (d, *J*=3.26 Hz, 1H, C*H*), 6.59 (d, *J*=2.01 Hz, 1H, C*H*), 3.62-3.53 (m, 1H, C*H*), 3.48-3.40 (m, 1H, C*H*), 3.26-3.20 (m, 1H, C*H*), 3.02-2.90 (m, 1H, C*H*), 2.71-2.63 (m 1H, C*H*), 2.46-2.43 (m, 1H, C*H*), 2.22-2.12 (m, 1H, C*H*), 1.65-1.58 (m, 1H, C*H*), 1.48-1.40 (m, 1H, C*H*); Calc. C, 54.53; H, 4.58; N, 10.60; Found. C, 54.19; H, 4.71; N, 10.60.

(59)

Thiele's acid was activated with pentafluorophenyl trifluoroacetate as described earlier.[63] 4-(Aminomethyl)benzene-sulfonamide hydrochloride (151.6 mg, 0.68 mmol) was suspended in 1 ml of DMF. Triethylamine (190 µl, 1.36 mmol) was added and the mixture was stirred for 10 minutes The activated Thiele's acid (188 mg, 0.34 mmol) was added and the reaction mixture was stirred for 15 h. The solvent was evaporated in *vacuo* and the residue was extracted with EtOAc and H_2O (3 x 10 ml), dried over Na_2SO_4, filtered and concentrated in *vacuo*. Silica gel chromatography using 10 % MeOH in EtOAc yielded **59** as a cream colored powder (90 %).

Calc. for Mr ($C_{26}H_{28}N_4O_6S_2$) 556.7; ESI-MS [m/z] (CH_3OH): 555.1 $[M-H]^-$; ^1H NMR (400 MHz, MeOD, δ in ppm): 8.51 (t, *J*=6.02 Hz, 1H, CH_2-*NH*), 8.23 (t, *J*=6.02 Hz, 1H, CH_2-*NH*), 7.88-7.79 (m, 4H, Ar), 7.47-7.36 (m, 4H, Ar), 6.78 (d, *J*=3.01 Hz, 1H, C*H*), 6.42 (d, *J*=1.00 Hz, 1H, C*H*), 4.57-4.40 (m, 4H, CH_2), 3.63-3.54 (m, 1H, C*H*), 3.46-3.40 (m, 1H, C*H*), 3.23-3.16 (m, 1H, C*H*), 3.09-2.99 (m, 1H, C*H*), 2.62-2.49 (m, 1H, C*H*), 2.23-2.11 (m, 1H, C*H*), 1.74-1.65 (m, 1H, C*H*), 1.54 -1.45 (m, 1H, C*H*); Calc. C, 56.10; H, 5.07; N, 10.06; Found. C, 55.94; H, 5.18; N, 9.73.

(71)

Thiele's acid was activated with pentafluorophenyl trifluoroacetate as described earlier.[63] L-Noradrenaline (745.0 mg, 4.4 mmol) and triethylamine (1.16 ml, 8.8 mmol) were suspended in 1 ml DMF. The activated acid (200 mg, 0.36 mmol) was added in

one portion and the dark reaction mixture was stirred for 48 h at room temperature. The solvent was evaporated in *vacuo* and the residue was purified by flash silica gel chromatography using a gradient from pure CH_2Cl_2 to CH_2Cl_2/MeOH/AcOH 7:1:0.01 (21 %).

Calc. for Mr ($C_{28}H_{30}N_2O_8$) 522.2; ESI-MS [m/z] (CH_3OH): 521.1 $[M-H]^-$, 545.2 $[M+Na]^+$; ^{1}H-NMR (400 MHz, MeOD, δ in ppm): 6.88 – 6.65 (m, 6H, Ar), 6.65 – 6.60 (m, 1H, CH), 6.36 – 6.33 (m, 1H, CH), 4.70 – 4.58 (m, 2H, C*H*OH), 3.56 – 3.48 (m, 1H, CH), 3.17 – 3.09 (m, 1H, CH), 3.06 – 2.93 (m, 1H, CH), 2.53 – 2.41 (m, 1H, CH), 2.21 – 2.11 (m, 1H, CH), 1.70 – 1.63 (m, 1H, CH), 1.49 – 1.43 (m, 1H, CH).

(72)

Thiele's acid was activated with pentafluorophenyl trifluoroacetate as described earlier.[63] 7-aminoheptanoic acid (1.2 eq, 60.3 mg, 0.42 mmol) was dissolved in 1 ml of DMF. The activated acid (191 mg, 0.34 mmol) was added in one portion and the reaction mixture was stirred for 20 h at room temperature. The solvent was evaporated in *vacuo* and the residue was purified by silica gel chromatography using CH_2Cl_2/MeOH/AcOH 100:1:1 (34 %).

Calc. for Mr ($C_{25}H_{24}F_5NO_5$) 513.5; ESI-MS [m/z] (CH_3OH): 536.1 $[M+Na]^+$; ^{1}H-NMR (400 MHz, MeOD, δ in ppm): 7.67 (t, *J*=5.5 Hz, 1H, NH), 7.35 (m, 1H, CH), 6.38 (m, 1H, CH), 3.67 (m, 1H, CH), 3.47 (m, 1H, CH), 3.22 (m, 3H, CH_2 superimposed with CH), 3.11 (m, 1H, CH), 2.58 (m, 1H, CH), 2.29 (t, *J*=7.4 Hz, 2H, CH_2), 2.08 (m, 1H, CH), 1.81 (m, 1H, CH), 1.57 (m, 5H, CH_2 superimposed with CH), 1.35 (m, 4H, CH_2).

(73)

4-(Aminomethyl)benzene-sulfonamide hydrochloride (1.2 eq, 92.4 mg, 0.42 mmol) was dissolved in 1 ml DMF. Triethylamine (5 eq, 235.6 µl, 1.7 mmol) and **72** (174.6 mg, 0.34 mmol) was added. The reaction progress was monitored by HPLC. When the starting compound was consumed, the solvent was evaporated in *vacuo* and the residue was purified by silica gel chromatography using CH_2Cl_2/MeOH/AcOH 100:5:5 (80 %).

Calc. for Mr ($C_{26}H_{33}N_3O_6S$) 515.6; ESI-MS [m/z] (CH_3OH): 514.1 $[M-H]^-$, 538.2 $[M+Na]^+$; ^{1}H-NMR (400 MHz, MeOD, δ in ppm): 7.86 (m, 2H, Ar), 7.61 (t, *J*=5.9 Hz, 1H, NH), 7.41 (m, 2H, Ar), 6.77 (m, 1H, CH), 6.35 (m, 1H, CH), 3.56 (m, 1H, CH), 4.52 (m, 2H, CH_2) 3.41 (m, 1H, CH), 3.22 (m, 3H, CH_2 superimposed with CH), 3.03 (m, 1H, CH), 2.51 (m, 1H,

CH), 2.27 (t, *J*=7.4 Hz, 2H, CH_2), 2.11 (m, 1H, CH), 1.69 (m, 1H, CH), 1.56 (m, 5H, CH_2 superimposed with CH), 1.35 (m, 4H, CH_2).

(74)

74 was synthesized as described for **73** using 8-aminocaprylic acid. The crude product was purified by flash chromatography on silica gel (eluent gradient from CH_2Cl_2 to CH_2Cl_2/MeOH/AcOH 20 : 1 : 1), from which the pure product were obtained (32 %).

Calc. for Mr ($C_{27}H_{40}N_2O_6$) 488.3; ESI-MS [m/z] (CH_3OH): 527.3 $[M+K]^+$, 511.3 $[M+Na]^+$, 489.3 $[M+H]^+$; ^{1}H-NMR (500 MHz, MeOD, δ in ppm): 7.83 (t, *J*=5.7 Hz, 1H, NH), 7.54 (t, *J*=5.7 Hz, 1H, NH), 6.66 (m, 1H, CH), 6.33 (m, 1H, CH), 3.52 (m, 1H, CH), 3.37 (m, 1H, CH), 3.17 (m, 4H, CH_2), 3.13 (m, 1H, CH), 3.01 (m, 1H, CH), 2.48 (m, 1H, CH), 2.30 (m, 4H, CH_2), 2.06 (m, 1H, CH), 1.65 (m, 5H, CH_2 superimposed with CH), 1.51 (m, 5H, CH_2 superimposed with CH), 1.35 (m, 10H, CH_2).

(75)

To a solution of **72** (934.5 mg, 1.82 mmol) in 3 ml DMF benzyl alcohol (4 eq, 754 µl, 7.28 mmol) and triethylamine (4 eq, 1.01 ml, 7.28 mmol) were added, and the mixture was stirred at room temperature under nitrogen. Reaction control by NMR still showed incomplete coupling after seven days. Hence, more benzyl alcohol (4 eq, 754 µl, 7.28 mmol) and triethylamine (2 eq, 500 µl, 3.64 mmol) were added, and the mixture was stirred during additional 24 hours at 50 °C. The solvent was evaporated at reduced pressure. The residue was suspended in 4 ml saturated $NaHCO_3$ solution diluted 20fold by water and extracted with 100 ml EtOAc. The aqueous phase was then acidified by 1 M HCl to pH 1, and extracted three times with 100 ml EtOAc. The combined organic phases were dried with Na_2SO_4, and the solvent was removed *in vacuo*, yielding 700 mg crude product. The crude product was purified by flash chromatography on silica gel (eluent gradient from CH_2Cl_2 to CH_2Cl_2/MeOH 9 : 1), from which 70 mg (9 %) pure product were obtained.

Calc. for Mr ($C_{26}H_{31}NO_5$) 473.2; ESI-MS [m/z] (CH_3OH): 460.1 $[M+Na]^+$, 438.1 $[M+H]^+$, 436.1 $[M-H]^-$; ^{1}H-NMR (500 MHz, MeOD, δ in ppm): 7.64 (t, *J*=5.5 Hz, 1H, NH) 7.35 (m, 5H, Ar), 6.95 (m, 1H, CH), 6.32 (m, 1H, CH), 3.55 (m, 1H, CH), 3.36 (m, 1H, CH), 3.20 (m, 3H, CH_2 superimposed with CH), 3.01 (m, 1H, CH), 2.49 (m, 1H, CH), 2.28 (t, *J*=7.4 Hz, 2H,

CH_2), 2.02 (m, 1H, CH), 1.67 (m, 1H, CH), 1.60 (m, 1H, CH), 1.48 (m, 4H, CH_2), 1.33 (m, 4H, CH_2).

(41)

Thiele's acid was activated with pentafluorophenyl trifluoroacetate as described earlier.[63] 7-aminoheptanoic acid (2.2 eq, 115.7 mg, 0.80 mmol) was dissolved in 1 ml of DMF and triethylamine (4.4 eq, 220.8 µl, 1.59 mmol) was added. The activated acid (200 mg, 0.36 mmol) was added in one portion and the reaction mixture was stirred for 20 h at room temperature. The solvent was evaporated in *vacuo* and the residue was purified by silica gel chromatography using CH_2Cl_2/MeOH/AcOH 100:0.5:0.1 (54 %).

Calc. for Mr ($C_{26}H_{38}N_2O_6$) 474.6; ESI-MS [m/z] (CH_3OH): 497.2 $[M+Na]^+$, 475.3 $[M+H]^+$; ^{1}H-NMR (400 MHz, MeOD, δ in ppm): 7.81 (t, *J*=5.7 Hz, 1H, NH), 7.52 (t, *J*=5.7 Hz, 1H, NH), 6.63 (m, 1H, CH), 6.30 (m, 1H, CH), 3.48 (m, 1H, CH), 3.34 (m, 1H, CH), 3.18 (m, 4H, CH_2), 3.10 (m, 1H, CH), 2.97 (m, 1H, CH), 2.45 (m, 1H, CH), 2.27 (m, 4H, CH_2), 2.00 (m, 1H, CH), 1.60 (m, 5H, CH_2 superimposed with CH), 1.47 (m, 5H, CH_2 superimposed with CH), 1.33 (m, 8H, CH_2).

(42)

42 (50 mg, 0.11 mmol) was dissolved in 1 ml DMF and N-methylmorpholine (3 eq, 35.1 µl, 0.32 mmol) and O-(7-Azabenzotriazol-1-yl)-N,N,N',N'-tetramethyluronium hexafluorophosphate (3 eq, 121.1 mg, 0.32 mmol) was added. The solution was stirred for 30 minutes at room temperature. O-(*tert*-Butyldimethylsilyl)hydroxylamine (3 eq, 47 mg, 0.32 mmol) dissolved in 1 ml DMF was added and the reaction mixture was stirred for 5 h at room temperature. The solvent was evaporated in *vacuo.* The residue was suspended in distilled water and extracted three times with 20 ml EtOAc. The aqueous phase was evaporated and the residue was purified by silica gel chromatography using CH_2Cl_2/MeOH/AcOH 10:1:0.1 (70 %).

Calc. for Mr ($C_{26}H_{40}N_4O_6$) 504.6; ESI-MS [m/z] (CH_3OH): 527.3 $[M+Na]^+$; ^{1}H-NMR (400 MHz, MeOD, δ in ppm): 7.86 (t, *J*=5.7 Hz, 1H, NH), 7.59 (t, *J*=5.6 Hz, 1H, NH), 6.68 (m, 1H, CH), 6.33 (m, 1H, CH), 3.53 (m, 1H, CH), 3.38 (m, 1H, CH), 3.21 (m, 5H, CH_2 superimposed with CH), 3.02 (m, 1H, CH), 2.49 (m, 1H, CH), 2.12 (m, 4H, CH_2), 2.06 (m, 1H, CH), 1.65 (m, 5H, CH_2 superimposed with CH), 1.51 (m, 5H, CH_2 superimposed with CH), 1.36 (m, 8H, CH_2).

3.5.2 Cp-SO_2R

(7)

Bis-phenylsulfonyl-methane (296.0 mg, 1.0 mmol) was dissolved in 15 ml toluene. 50 % aqueous NaOH (3 ml), a catalytic amound of TBAF (1 mol %) and cis-1,4-dichloro-2-butene (162.5 mg, 1.3 mmol) were added. The mixture was stirred vigorously for 24h at room temperature. The two layers were separated and the aqueous layer was extracted with MTBE. The combined organic layers were washed with brine, dried over Na_2SO_4 and evaporated under reduced pressure. The residue was recrystallized from CH_2Cl_2/hexane to yield **7** (90 %).

Calc. for Mr ($C_{17}H_{16}O_4S_2$) 348.4; ESI-MS [m/z] (CH_3OH): 387.0 $[M+K]^+$. ^1H NMR (500 MHz, $CDCl_3$, δ in ppm): 8.06 – 7.60 (m, 10H, Ar), 5.43 (s, 2H, CH), 3.39 (s, 4H, CH_2). Calc. C, 58.60; H, 4.63; Found C, 58.39; H, 4.74.

3.5.3 Cp-NO_2

(9)

Phenylsulfonyl-nitromethane (100 mg, 0.5 mmol) was dissolved in 6 ml DMF. The solution was cooled to 0 °C and NaH (60 %, 50 mg, 1.25 mmol) was added. After 1.5h cis-1,4-dichloro-2-butene (60.5 µl, 0.575 mmol) was added and the mixture was stirred at room temperature for 5 days. The reaction was quenched with aqueous NH_4Cl. The aqueous layer was removed and the organic layer was diluted with CH_2Cl_2 and extracted two times with water and two times with brine. After drying over Na_2SO_4, solvents were removed under reduced pressure and the residue was purified by silica gel column chromatography using CH_2Cl_2/hexane 1:1 to yield **9** as a coloreless powder (80 %). Crystals suitable for X-Ray analysis were grown from CH_2Cl_2/hexane.

Calc. for Mr. ($C_{11}H_{11}NO_4S$) 253.3; ESI-MS [m/z] (CH_3OH): 276.1 $[M+Na]^+$. ^1H NMR (500 MHz, $CDCl_3$, δ in ppm): 7.80 – 7.50 (m, 5H, Ar), 5.63 (s, 2H, CH), 3.43 (s, 4H, CH_2). Calc. C, 52.16; H, 4.38; N, 5.53; Found C, 52.29; H, 4.43; N, 5.60.

(8)

7 or **9** was dissolved in 5 ml THF and cooled to -78 °C. Saturated KtBuO (1 ml) in THF was added and the mixture was stirred for 1h, before it was allowed to reach -20 °C and after 30min 0 °C. At this point, the reaction was quenched by adding a

saturated aqueous solution of NH_4Cl. The product was extracted two times with CH_2Cl_2 and brine and dried. Concentration under reduced pressure and column chromatography with CH_2Cl_2 with EtOAc gradient afforded dimer **8** (65-70 %).
Calc. for Mr. ($C_{22}H_{20}O_4S_2$) 412.08; ESI-MS [m/z] (CH_3OH): Dimer: 435.1 $[M+Na]^+$; Monomer: 229.1 $[M+Na]^+$. ^1H NMR (500 MHz, $CDCl_3$, δ in ppm): 7.83 – 7.43 (m, 8H, Ar), 6.45 (d, 1H, CH), 5.90 – 5.79 (m, 2H, CH), 3.86 – 3.83 (m, 1H, CH), 3.04 – 2.99 (m, 2H, CH), 2.89 (s, 1H, CH), 2.40 – 2.34 (m, 1H, CH), 1.81 – 1.76 (m, 2H, CH_2). Calc. C, 52.16; H, 4.38; N, 5.53; Found C, 52.29; H, 4.43; N, 5.60.

(10)

Sodium (1g, cutt in small pieces) was dissolved in 20 ml of EtOH and cooled to 0 °C. Freshly distilled cyclopentadiene (2.91 g, 44 mmol) and isopropyl nitrate (4.46 ml, 0.44 mmol) were added and the mixture was stirred for one hour and was then allowed to warm to room temperature. After stirring for another two hours, the orange precipitate was collected by filtration and was washed with toluene on the filter (15 % yield).
^1H NMR (400 MHz, D_2O, δ in ppm): 6.49 – 6.47 (m, 2H, Cp), 6.23 – 6.21 (m, 2H, Cp).

3.5.4 Cp-NHR

(14)

Thiele's Acid (50 mg, 0.22 mmol) was suspended in Toluene (1 ml). Triethylamine (72.3 μl, 0.48 mmol) and diphenylphosphoryl azide (107.8 μl, 0.50 mmol) were added. The mixture was stirred until the solution became clear and then one more hour. The solvent was evaporated under reduced pressure and the residue was purified by silica gel column chromatography, using CH_2Cl_2/hexane 2:3 (80 %).
IR (cm^{-1} KBr): 2030, 1681, 1618, 1487, 1175; Calc. for Mr ($C_{12}H_{10}N_6O_2$) 270.3; ESI-MS [m/z] (CH_3OH): 269.3 $[M-H]^-$; ^1H NMR (400 MHz, $CDCl_3$, δ in ppm): 6.96 – 6.93 (m, 1H, CH), 6.62 – 6.59 (m, 1H, CH), 3.60 – 3.53 (m, 1H, CH), 3.45 – 3.41 (m, 1H, CH), 3.23 - 3.18 (m, 1H, CH), 3.05 - 2.96 (m, 1H, CH), 2.56 - 2.47 (m, 1H, CH), 2.06 - 1.98 (m, 1H, CH), 1.74 - 1.69 (m, 1H, CH), 1.49 - 1.44 (m, 1H, CH).

(15-16a/b)

14 (50 mg, 0.19 mmol) was dissolved in 5 ml toluene. The solution was stirred at 80°C for 1 h, then an 10 fold excess (or more) of nucleophile **a**-**f** was added and the mixture was stirred for another hour at 80°C. Solvents were removed under reduced pressure and the crude products were analysed.

15: IR (cm^{-1} KBr): 2267

16a: IR (cm^{-1} KBr): 1744, 1726, 1715; Calc. for Mr ($C_{14}H_{18}N_2O_4$) 278.3; ESI-MS [m/z] (CH_3OH): 279.1 $[M+H]^+$; ^1H NMR (400 MHz, $CDCl_3$, δ in ppm): 6.10 – 5.97 (m, 1H, CH), 5.60 – 5.36 (m, 1H, CH), 3.76 (s, 3H, CH_3), 3.71 (s, 3H, CH_3), 3.38 – 3.29 (m, 1H, CH), 2.87 – 2.77 (m, 1H, CH), 2.62 - 2.56 (m, 1H, CH), 2.43 - 2.38 (m, 1H, CH), 2.34 - 2.26 (m, 1H, CH), 2.12 - 2.02 (m, 1H, CH), 1.83 - 1.76 (m, 1H, CH), 1.76 - 1.68 (m, 1H, CH).

16b: Calc. for Mr ($C_{26}H_{28}N_4O_2$) 428.5; ESI-MS [m/z] (CH_3OH): 429.2 $[M+H]^+$; ^1H NMR (400 MHz, $CDCl_3$, δ in ppm): 7.38 - 7.10 (m, 10H, Ar), 6.60 – 6.44 (m, 1H, CH), 5.20 – 5.05 (m, 1H, CH), 4.41 - 4.06 (m, 4H, CH_2), 3.27 – 3.16 (m, 1H, CH), 2.81 – 2.71 (m, 1H, CH), 2.60 - 2.48 (m, 2H, CH), 2.33 - 2.21 (m, 1H, CH), 2.12 - 2.01 (m, 1H, CH), 1.79 - 1.62 (m, 1H, CH).

3.5.5 Cp-CH_2COR

(17-18)

NaCp (2M in THF, 4 ml, 8.0 mmol) was cooled with a water/Ice-bath to 0 °C. Bromoacetic acid methylester (836 µl, 8.8 mmol) was added dropwise via syringe over 10minutes A cream colored precipitate formed instantly and the dark red colour gradually diminished. The suspension was stirred for 1h at 0 °C and for 3h at room temperature. The solid salts were removed by filtration and the filtrate was concentrated under flushing nitrogen. The liquid residue was purified by distillation at 60 °C (0.4 mbar) (**17**, 30 – 50 %, isomeric mixture).

^1H NMR (400 MHz, $CDCl_3$, δ in ppm): 6.54 – 6.48 (m, 1H, CH), 6.48 – 6.40 (m, 2H, CH), 6.37 – 6.32 (m, 2H, CH) 6.24 – 6.19 (m, 1H, CH), 3.70 (s, 3H, CH_3), 3.69 (s, 3H, CH_3), 3.47 – 3.44 (m, 2H, CH_2), 3.44 – 3.40 (m, 2H, CH_2), 3.05 – 2.97 (m, 4H, CH_2); ^{13}C NMR (125 MHz, $CDCl_3$, δ in ppm): 172.1 (CO), 172.0 (CO), 148.4 (olefinic Cp), 140.2 (olefinic Cp), 138.8 (olefinic Cp), 134.8 (olefinic Cp), 134.4 (olefinic Cp), 134.3 (olefinic Cp), 132.8 (olefinic Cp), 132.4 (olefinic Cp), 130.6 (olefinic Cp), 130.1 (olefinic Cp), 108.4 (olefinic Cp),

52.0 (2xCH_3), 51.0 (CH_3), 43.8 (CH_2), 41.7 (CH_2), 36.4 (CH_2), 35.7 (CH_2), 33.5 (CH_2), 30.0 (CH_2).

Hydrolysis of the ester function was performed with LiOH (5 eq.) in a mixture of H_2O/MeOH/THF (1:2:2). The solution was stirred for 2h at 0 °C and for another 5h at room temperature. Concentration under reduced pressure and acidification with 1M HCl to pH 3 produced a cream colored precipitate. EtOAc was added and the aqueous phase was extracted three times. The combined organic fractions were dried over Na_2SO_4 and evaporated under reduced pressure. **18** was obtained as a yellowish cream (74 % isomeric mixture).
^{1}H NMR (400 MHz, $CDCl_3$, δ in ppm): 6.51 – 6.49 (m, 1H, CH), 6.48 – 6.40 (m, 2H, CH), 6.37 – 6.32 (m, 2H, CH) 6.24 – 6.19 (m, 1H, CH), 3.49 – 3.40 (m, 4H, CH_2), 3.05 – 2.97 (m, 4H, CH_2); ^{13}C NMR (125 MHz, $CDCl_3$, δ in ppm): 178.3 (CO), 178.2 (CO), 139.3 (olefinic Cp), 138.1 (olefinic Cp), 134.6 (olefinic Cp), 134.2 (olefinic Cp), 133.1 (olefinic Cp), 132.3 (olefinic Cp), 131.1 (olefinic Cp), 130.7 (olefinic Cp), 43.7 (CH_2), 41.6 (CH_2), 36.2 (CH_2), 35.5 (CH_2).

(21a/b)

18 (103 mg, 0.81 mmol) was dissolved in 2 ml dry DMF and N-methylmorpholine (132 µl, 1.20 mmol) and O-(7-Azabenzotriazol-1-yl)-N,N,N',N'-tetramethyluronium hexa-fluorophosphate (456 mg, 1.20 mmol) were added. The mixture was stirred for 45 min, then triethylamine (111.5 µl, 0.81 mmol) and the appropriate amine (0.81 mmol) was added. After stirring for 16 h, the solvent was removed under reduced pressure and the crude product was purified by silica gel column chromatography using CH_2Cl_2 (**a**) or CH_2Cl_2/MeOH 100:5 (**b**) respectively (20-55 %). Crystals were grown from CH_2Cl_2/Hexane. Analyses revealed a rearrangement of the double bonds in the cyclopentadienyl-ring for both amide substituted compounds **66a** and **b**. The "true" cyclopentadienyl form was not obtained.
21a: Calc. for Mr ($C_{14}H_{15}NO$) 213.3; ESI-MS [m/z] (CH_3OH): 235.9 $[M+Na]^+$, 449.1 $[2M+Na]^+$; ^{1}H NMR (400 MHz, $CDCl_3$, δ in ppm): 7.40 – 7.30 (m, 5H, Ar), 6.54 (m, 1H, Cp), 6.25 (m, 1H, Cp), 5.68 (m, 1H, CH), 3.11 (m, 2H, CH_2), 2.62 (m, 2H, CH_2).
21b: Calc. for Mr ($C_{10}H_{13}NO_3$) 195.2; ESI-MS [m/z] (CH_3OH): 217.9 $[M+Na]^+$, 413.0 $[2M+Na]^+$; ^{1}H NMR (500 MHz, $CDCl_3$, δ in ppm): 6.56 (m, 1H, CH), 6.26 (m, 1H, CH), 5.74

(m, 1H, CH), 4.11 (d, *J*=5.4 Hz, 2H, CH_2), 3.77 (s, 3H, CH_3), 3.07 (m, 2H, CH_2), 2.61 (m, 2H, CH_2).

3.5.6 Cp-CH_2CH_2COR

(19-20)

NaCp (4 ml, 8.0 mmol) was cooled with a water/Ice-bath to 0 °C. Methyl-3-brompropionate (960 µl, 8.8 mmol) was added dropwise via syringe over 10minutes A cream colored precipitate formed instantly and the dark red colour gradually dininished.The suspension was stirred for 1h at 0 °C and for 3h at room temperature. The solid salts were removed by filtration and the filtrate was concentrated under a stream of nitrogen. The liquid brown residue was purified by distillation at 70 °C (0.4 mbar) (**19**, 30 – 50 %, isomeric mixture).

^{1}H NMR (400 MHz, $CDCl_3$, δ in ppm): 6.44 – 6.40 (m, 3H, CH), 6.30 – 6.26 (m, 1H, CH), 6.21 – 6.17 (m, 1H, CH) 6.06 – 6.02 (m, 1H, CH), 3.68 (s, 6H, CH_3), 2.99 – 2.93 (m, 2H, CH_2), 2.93 – 2.88 (m, 2H, CH_2), 2.80 – 2.67 (m, 4H, CH_2), 2.62 – 2.54 (m, 4H, CH_2); ^{13}C NMR (125 MHz, $CDCl_3$, δ in ppm): 173.9 (2x CO), 147.7 (olefinic Cp), 145.5 (olefinic Cp), 134.5 (2x olefinic Cp), 132.5 (olefinic Cp), 131.3 (olefinic Cp), 127.1 (olefinic Cp), 126.6 (olefinic Cp), 51.8 (2x CH_3), 43.5 (CH_2), 41.6 (CH_2), 34.2 (CH_2), 33.6 (CH_2), 26.1 (CH_2), 25.3 (CH_2).

Hydrolysis of the ester function was performed with LiOH (5 eq.) in a mixture of H_2O/MeOH/THF (1:2:2). The solution was stirred for 2h at 0 °C and for another 5h at room temperature. Concentration under reduced pressure and acidification with 1M HCl to pH 3 produced a cream colored precipitate. EtOAc was added and the aqueous phase was extracted three times. The combined organic fractions were dried over Na_2SO_4 and evaporated under reduced pressure. **20** was obtained as a yellowish cream (69 %, isomeric mixture).

Calc. for Mr ($C_8H_{10}O_2$) 138.2; ESI-MS [m/z] (CH_3OH): 139.0 $[M+H]^+$, 277.0 $[2M+H]^+$; ^{1}H NMR (400 MHz, $CDCl_3$, δ in ppm): 6.48 – 6.40 (m, 3H, CH), 6.32 – 6.27 (m, 1H, CH), 6.24 – 6.19 (m, 1H, CH) 6.10 – 6.05 (m, 1H, CH), 3.00 – 2.95 (m, 2H, CH_2), 2.95 – 2.90 (m, 2H, CH_2), 2.82 – 2.59 (m, 8H, CH_2).

(69)

20 (40 mg, 0.29 mmol) was dissolved in 3 ml dry CH_2Cl_2. Oxalylchloride (75 µl, 0.87 mmol) and a catalytic amount of DMF was added. The suspension was stirred at 0 °C for 1h and at room temperature for another 5h. The solvent was evaporated and the residue was redissolved in dry THF.

In a separate flask 6-aminopenicillanic acid (94.1 mg, 0.435 mmol) was suspended in 2 ml EtOH. Trimethylsilyl chloride (138.3 µl, 1.09 mmol) was added, whereas the mixture turned clear instandly and was stirred for 2h. Solvents and excess of trimethylsilyl chloride were removed under reduced pressure. The colourless residue was redissolved in dry THF and triethylamine (120.6 µl, 0.87 mmol) was added.

Both solutions were slowly mixed together at 0 °C and stirred for 1h, then the mixture was allowed to reach room temperature and was stirred for another 2h. THF was evaporated under reduced pressure and the residue was purified by silica gel column chromatography using CH_2Cl_2/MeOH/AcOH 100:2:1 (64 %).

Calc. for Mr ($C_{18}H_{24}N_2O_4S$) 364.5; ESI-MS [m/z] (CH_3OH): 383.2 $[M+H_3O]^+$; ^1H NMR (400 MHz, MeOD, δ in ppm): 6.56 – 6.07 (m, 3H, Cp), 5.00 (d, *J*=7.5 Hz, 1H, CH), 4.55 (d, *J*=7.5 Hz, 1H, CH), 4.21 (q, *J*=3x7.2 Hz, 2H, CH_2 ester), 3.75 (s, 1H, C*H*COOEt), 2.98 – 2.90 (m, 2H, CH_2), 2.80 – 2.65 (m, 2H, CH_2), 2.58 – 2.50 (m, 2H, CH_2), 1.63 (s, 3H, CH_3), 1.30 (t, *J*=2x7.2, 3H, CH_3 ester), 1.30 (s, 3H, CH_3); ^{13}C NMR (125 MHz, $CDCl_3$, δ in ppm): 175.7 (CO), 172.4 (CO), 171.7 (CO), 149.2 (Cp), 147.0 (Cp), 135.4 (Cp), 135.0 (Cp), 133.3 (Cp), 132.0 (Cp), 128.2 (Cp), 127.6 (Cp), 73.9 (*C*HCO), 67.4 (CHS), 62.6 (tert. C), 60.0 (CH_2 ester), 59.2 (CHNH), 44.3 (CH_2), 42.2 (CH_2), 36.9 (CH_2), 36.3 (CH_2), 28.2 (CH_3), 27.6 (CH_3), 26.9 ($CpCH_2CH_2$), 15.6 (CH_3 ester).

3.6 Labeling with ^{99m}Tc

(61/62)

A vial was charged with [H_3BCOOH] (4 mg), $Na_2[C_4H_4O_6]*2H_2O$ (7 mg), $Na_2B_4O_7*10H_2O$ (7 mg) and the ligand **58** or **59** respectively (1-1.5 mg). The vial was sealed and flushed with nitrogen for 5 minutes Freshly eluted $Na[TcO_4]$ (1 ml) was injected into the vial and the mixture was heated at 85-90 °C. After cooling to room temperature and filtering, the products were analysed by HPLC. Quantitative conversion of $[TcO_4]^-$ to the desired product was observed after 60 or 90 minutes

respectively. The nature of the product was identified by coinjection of the corresponding Re-complex.

(60)

A vial was charged with [H_3BCOOH] (4 mg), $Na_2[C_4H_4O_6]*2H_2O$ (7 mg), $Na_2B_4O_7*10H_2O$ (7 mg) and the ligand **56** (5 mg). The vial was sealed and flushed with nitrogen for 5 minutes Freshly eluted $Na[TcO_4]$ (1 ml) was injected into the vial and the mixture was heated at 85-90 °C. After cooling to room temperature and filtering, the products were analysed by HPLC. 72 % conversion of $[TcO_4]^-$ to the desired product was observed after 90 minutes. 27 % of the activity was observed as unreacted $[Tc(CO)_3(OH_2)_3]$ and 1 % as $[TcO_4]^-$.The nature of the product was identified by coinjection of the corresponding Re-complex.

(43)

A vial was charged with [H_3BCOOH] (4 mg), $Na_2[C_4H_4O_6]*2H_2O$ (7 mg), $Na_2B_4O_7*10H_2O$ (7 mg) and the ligand **41** (5 mg). The vial was sealed and flushed with nitrogen for 5 minutes Freshly eluted $Na[^{99m}TcO_4]$ (1 ml) was injected and the mixture was heated at 85-90 °C. After cooling to room temperature and filtering, the products were analysed by HPLC. 87 % conversion of $[^{99m}TcO_4]^-$ was observed after 80 minutes. 12 % of the activity was observed as unreacted $[Tc(CO)_3(OH_2)_3]$. Coinjection of the corresponding Re-complex confirmed the nature of the product.

(43/76)

A vial was charged with [H_3BCOOH] (4 mg), $Na_2[C_4H_4O_6]*2H_2O$ (7 mg), $Na_2B_4O_7*10H_2O$ (7 mg) and the ligand **74** (8 mg). The vial was sealed and flushed with nitrogen for 5 minutes Freshly eluted $Na[^{99m}TcO_4]$ (1 ml) was injected and the mixture was heated at 85-90 °C. After cooling to room temperature and filtering, the products were analysed by HPLC. 80 % conversion of $[^{99m}TcO_4]^-$ was observed after 150 minutes. 10 % of the activity was observed as unreacted $[Tc(CO)_3(OH_2)_3]$ and 10 % as undefined sideproducts. The product radio (**43**:**76**) was 45:55. The nature of the products was confirmed by coinjection of the corresponding Re-complex.

(43/3)

A vial was charged with [H_3BCOOH] (4 mg), $Na_2[C_4H_4O_6]*2H_2O$ (7 mg), $Na_2B_4O_7*10H_2O$ (7 mg) and the ligand **73** (3-4 mg). The vial was sealed and flushed with nitrogen for 5 minutes Freshly eluted $Na[^{99m}TcO_4]$ (1 ml) was injected and the mixture was heated at 85-90 °C. After cooling to room temperature and filtering, the products were analysed by HPLC. Quantitative conversion of $[^{99m}TcO_4]^-$ was observed after 200 minutes. The product radio (**43**:**3**) was nearly 50:50. The nature of the products was confirmed by coinjection of the corresponding Re-complex.

(43/62)

To a commercially available Isolink-kit freshly eluted $Na[^{99m}TcO_4]$ (1 ml) was injected and the mixture was heated at 85-90 °C. The full conversion of $[^{99m}TcO_4]^-$ to $[^{99m}Tc(OH_2)_3(CO)_3]^+$ was confirmed by HPLC after 30 minutes. A new vial was charged with **71** (3-5 mg), sealed and flushed with nitrogen for 5 minutes $[^{99m}Tc(OH_2)_3(CO)_3]^+$-solution (1 ml) was injected into the vial and the mixture was heated at 85 – 90 °C. After cooling to room temperature and filtering, the products were analysed by HPLC. 81 % conversion of $[^{99m}Tc(OH_2)_3(CO)_3]^+$ to the products was observed after 150 minutes. 7 % of $[^{99m}TcO_4]^-$ was formed as a side product. The product radio (**43**:**62**) was 45:55. The nature of the products was confirmed by coinjection of the corresponding Re-complexes.

(28)

A vial was charged with [H_3BCOOH] (4 mg), $Na_2[C_4H_4O_6]*2H_2O$ (7 mg), $Na_2B_4O_7*10H_2O$ (7 mg) and the ligand **18** (4-6 mg). The vial was sealed and flushed with nitrogen for 5 minutes Freshly eluted $Na[TcO_4]$ (1 ml) was injected and the mixture was heated at 85-90 °C. After cooling to room temperature, the products were analysed by HPLC. Quantitative conversion of $[TcO_4]^-$ to the desired product was observed after 30 minutes. The nature of the product was identified by coinjection of the corresponding Re-complex.

(29)

A vial was charged with [H_3BCOOH] (4 mg), $Na_2[C_4H_4O_6]*2H_2O$ (7 mg), $Na_2B_4O_7*10H_2O$ (7 mg) and the ligand **20** (4-6 mg). The vial was sealed and flushed with nitrogen for 5 minutes Freshly eluted $Na[TcO_4]$ (1 ml) was injected and the

mixture was heated at 85-90 °C in a heating block. After cooling to room temperature, the products were analysed by HPLC. 65 % conversion of $[TcO_4]^-$ to the desired product was observed after 5h. Microwave heating at 130 °C results in the same yield after 30 minutes The nature of the product was identified by coinjection of the corresponding Re-complex.

4. Crystallographic Data

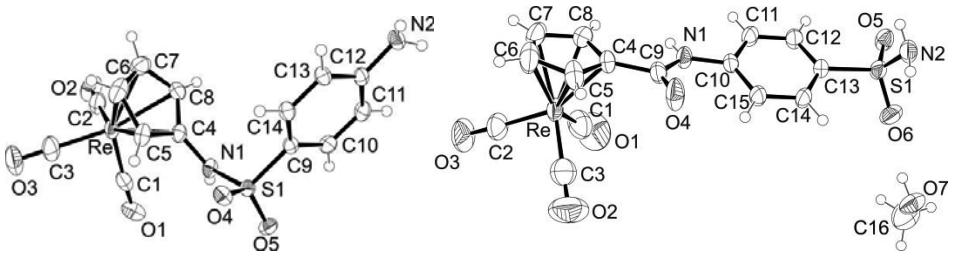

	45	**52**
Empirical formula	$C_{14}H_{11}N_2O_5ReS$	$C_{16}H_{15}N_2O_7ReS$
Formula weight	505.51	565.56
Crystal system	Orthorhombic	Triclinic
Space group	Pbcn	P-1
a [Å]	33.1611(3)	10.0414(17)
b [Å]	6.8940(8)	10.7314(16)
c [Å]	13.7984(16)	10.7480(16)
α [°]	90	65.930(14)
β [°]	90	65.719(15)
γ [°]	90	88.243(13)
Volume [Å^3]	3154.5(6)	950.8(3)
Z	8	2
Crystal size [mm^3]	0.20 x 0.19 x 0.14	0.33 x 0.25 x 0.11
Crystal description	orange block	colourless plate
Reflections collected	46378	10267
Independent refl. [R(int)]	4808 [0.0307]	5791 [0.0203]
Refl. observed [I>2σ (I)]	3748	4320
Completeness to Θ	100.0 % to 30.51°	99.7 % to 30.51°
Goodness-of-fit on F^2	1.038	0.875
Final R indices [I>2σ (I)]	R1 = 0.0223 wR2 = 0.0479	R1 = 0.0263 wR2 = 0.0430
Diff. peak and hole [e/Å^3]	1.023 and -0.729	0.898 and -0.849

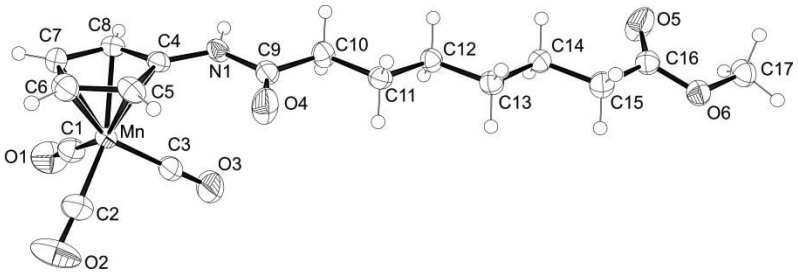

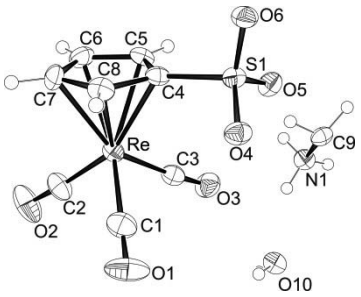

	34b	**4**
Empirical formula	$C_{17}H_{20}MnNO_6$	$C_{18}H_{22}N_2O_{14}Re_2S_2$
Formula weight	398.28	926.90
Crystal system	Monoclinic	Monoclinic
Space group	P21/c	P21/c
a [Å]	12.2182(4)	16.3126(6)
b [Å]	19.1058(7)	8.4958(6)
c [Å]	7.5939(3)	9.4921(11)
α [°]	90	90
β [°]	90.240(3)	101.248(8)
γ [°]	90	90
Volume [Å^3]	1772.69(11)	1290.23(18)
Z	4	2
Crystal size [mm^3]	0.35 x 0.23 x 0.17	0.23 x 0.21 x 0.14
Crystal description	colourless block	colourless block
Reflections collected	12863	13140
Independent refl. [R(int)]	5402 [0.0334]	2490 [0.0901]
Refl. observed [I>2σ (I)]	4080	2137
Completeness to Θ	99.7 % to 30.51°	94.7 % to 26.36°
Goodness-of-fit on F^2	1.066	0.982
Final R indices [I>2σ (I)]	R1 = 0.0460	R1 = 0.0305
	wR2 = 0.1119	wR2 = 0.0748
Diff. peak and hole [e/Å^3]	0.400 and -0.914	1.783 and -1.654

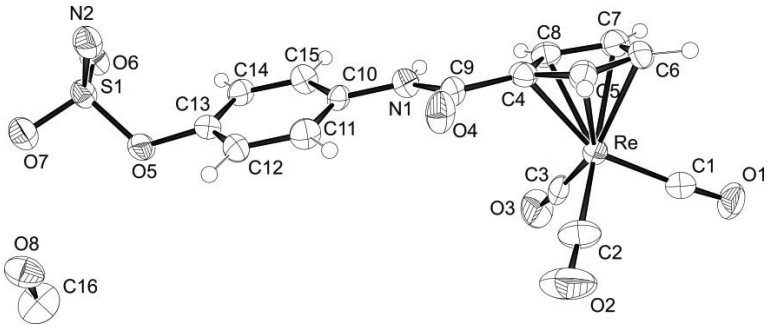

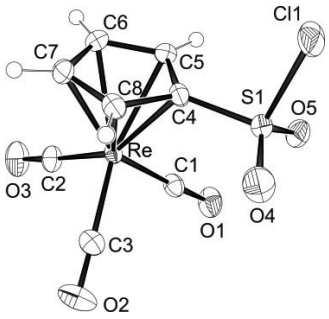

	51	**5**
Empirical formula	$C_{16}H_{15}N_2O_8ReS$	$C_8H_4ClO_5ReS$
Formula weight	581.56	433.82
Crystal system	Triclinic	Triclinic
Space group	P-1	P-1
a [Å]	10.1572(13)	6.8766(2)
b [Å]	10.5517(13)	7.0479(3)
c [Å]	10.6043(13)	12.0274(3)
α [°]	107.528(14)	83.440(3)
β [°]	90.995(15)	75.831(2)
γ [°]	115.459(14)	72.196(3)
Volume [Å^3]	964.2(2)	537.62(3)
Z	2	2
Crystal size [mm^3]	0.67 x 0.60 x 0.20	0.34 x 0.25 x 0.12
Crystal description	yellow plate	light yellow plate
Reflections collected	11737	12712
Independent refl. [R(int)]	4326 [0.1676]	5445 [0.0261]
Refl. observed [I>2σ (I)]	3691	4797
Completeness to Θ	90.6 % to 28.23°	99.9 % to 30.44°
Goodness-of-fit on F^2	1.050	0.994
Final R indices [I>2σ (I)]	R1 = 0.0566	R1 = 0.0263
	wR2 = 0.1355	wR2 = 0.0559
Diff. peak and hole [e/Å^3]	3.213 and -3.236	1.218 and -3.291

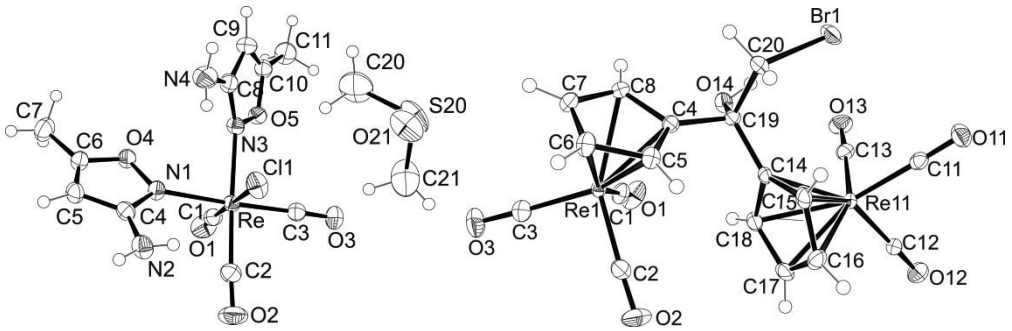

	63	**24b**
Empirical formula	$C_{13}H_{18}ClN_4O_6ReS$	$C_{18}H_{11}BrO_7Re_2$
Formula weight	580.02	791.58
Crystal system	Triclinic	Monoclinic
Space group	P-1	P21/c
a [Å]	9.20508(12)	13.62640(17)
b [Å]	9.54693(11)	10.26800(13)
c [Å]	11.51214(15)	13.47480(17)
α [°]	84.3940(10)	90
β [°]	76.6940(10)	93.9328(12)
γ [°]	87.2470(10)	90
Volume [Å^3]	979.48(2)	1880.90(4)
Z	2	4
Crystal size [mm^3]	0.42 x 0.27 x 0.08	0.24 x 0.20 x 0.13
Crystal description	colourless plate	colourless plate
Reflections collected	56216	13876
Independent refl. [R(int)]	6868 [0.0281]	6271 [0.0251]
Refl. observed [I>2σ (I)]	6397	5633
Completeness to Θ	99.9 % to 30.44°	99.9 % to 30.44°
Goodness-of-fit on F^2	1.048	1.112
Final R indices [I>2σ (I)]	R1 = 0.0190	R1 = 0.0309
	wR2 = 0.0490	wR2 = 0.0536
Diff. peak and hole [e/Å^3]	1.918 and -1.327	1.056 and -1.783

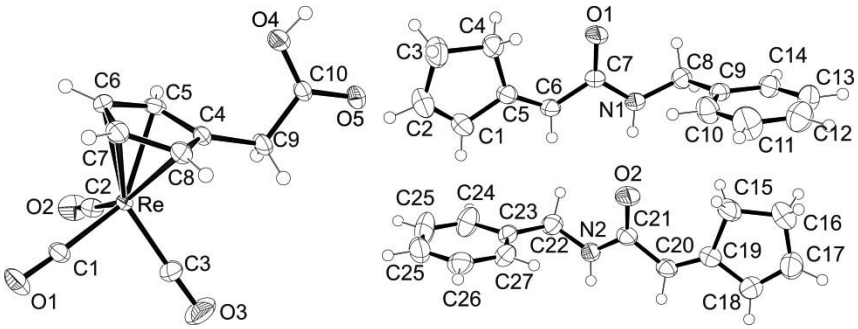

	24a	**21a**
Empirical formula	$C_{10}H_7O_5Re$	$C_{14}H_{15}NO$
Formula weight	393.36	213.27
Crystal system	Triclinic	Triclinic
Space group	P-1	P-1
a [Å]	6.59246(9)	9.5988(3)
b [Å]	6.91029(13)	9.8084(3)
c [Å]	13.1124(2)	13.3768(3)
α [°]	91.7016(15)	106.403(2)
β [°]	97.9610(13)	90.368(2)
γ [°]	116.1410(16)	94.364(2)
Volume [Å^3]	528.305(15)	1204.14(6)
Z	2	4
Crystal size [mm^3]	0.35 x 0.22 x 0.21	0.70 x 0.55 x 0.28
Crystal description	colourless block	brown block
Reflections collected	50233	30310
Independent refl. [R(int)]	5609 [0.0336]	7327 [0.0247]
Refl. observed [I>2σ (I)]	5411	5948
Completeness to Θ	99.2 % to 36.23°	99.8 % to 30.51°
Goodness-of-fit on F^2	1.237	0.937
Final R indices [I>2σ (I)]	R1 = 0.0191	R1 = 0.0577
	wR2 = 0.0457	wR2 = 0.1561
Diff. peak and hole [e/Å^3]	0.800 and -2.107	0.299 and -0.194

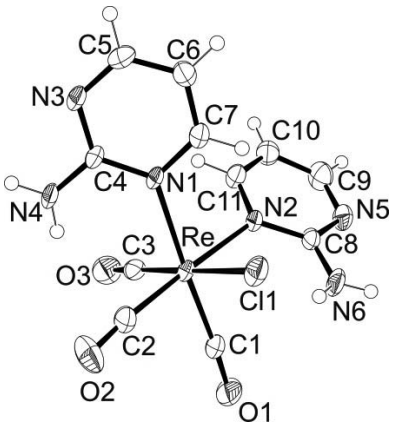

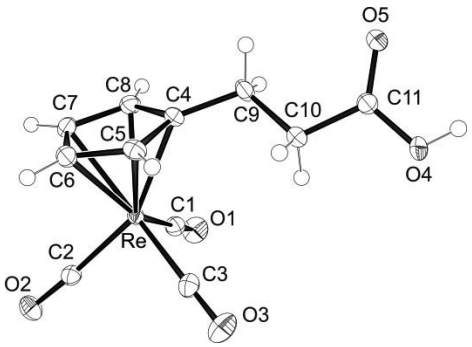

	65	**27**
Empirical formula	$C_{11}H_{10}ClN_6O_3Re$	$C_{11}H_9O_5Re$
Formula weight	495.90	407.38
Crystal system	Monoclinic	Triclinic
Space group	P21/c	P-1
a [Å]	14.8937(3)	7.0099(3)
b [Å]	7.76476(15)	7.3494(2)
c [Å]	13.4271(3)	11.5145(3)
α [°]	90	102.217(2)
β [°]	100.284(2)	94.765(2)
γ [°]	90	104.059(3)
Volume [Å^3]	1527.84(5)	556.72(3)
Z	4	2
Crystal size [mm^3]	0.22 x 0.19 x 0.08	0.55 x 0.42 x 0.32
Crystal description	orange plate	colourless block
Reflections collected	20160	19486
Independent refl. [R(int)]	5302 [0.0310]	5352 [0.0664]
Refl. observed [I>2σ (I)]	4139	5104
Completeness to Θ	99.9 % to 30.44°	99.1 % to 36.23°
Goodness-of-fit on F^2	1.071	1.141
Final R indices [I>2σ (I)]	R1 = 0.0272	R1 = 0.0252
	wR2 = 0.0501	wR2 = 0.0626
Diff. peak and hole [e/Å^3]	1.692 and -0.968	1.509 and -3.642

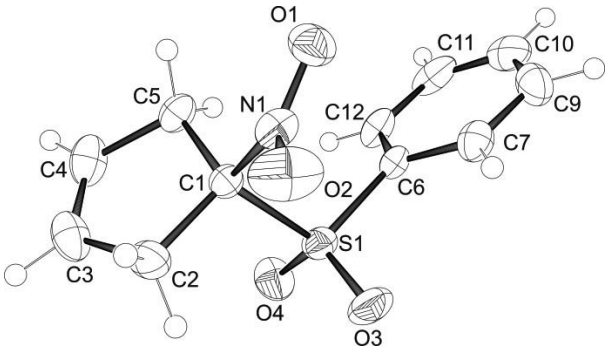

	9
Empirical formula	$C_{11}H_{11}NO_4S$
Formula weight	253.27
Crystal system	Monoclinic
Space group	P21/n
a [Å]	15.4647(3)
b [Å]	6.35360(10)
c [Å]	22.8489(4)
α [°]	90
β [°]	91.2560(15)
γ [°]	90
Volume [Å^3]	2244.51(7)
Z	8
Crystal size [mm^3]	0.26 x 0.24 x 0.05
Crystal description	colourless plate
Reflections collected	31636
Independent refl. [R(int)]	6832 [0.0449]
Refl. observed [I>2σ (I)]	4198
Completeness to Θ	99.9 % to 30.44°
Goodness-of-fit on F^2	0.954
Final R indices [I>2σ (I)]	R1 = 0.0454
	wR2 = 0.0891
Diff. peak and hole [e/Å^3]	0.337 and -0.376

5. References

[1] R. Alberto, in *Bioinorganic Medicinal Chemistry* (Ed.: E. Alessio), Wiley-VCH, Weinheim, **2011**, pp. 253-282.
[2] J. R. Dilworth, S. J. Parrott, *Chem. Soc. Rev.* **1998**, *27*, 43-55.
[3] V. Ozdemir, B. Williams-Jones, *Nat. Biotechnol.* **2006**, *24*, 1324-1326.
[4] F. Pene, E. Courtine, A. Cariou, J. P. Mira, *Crit. Care Med.* **2009**, *37*, S50-S58.
[5] D. Can, B. Spingler, P. Schmutz, F. Mendes, P. Raposinho, C. Fernandes, F. Carta, A. Innocenti, I. Santos, C. T. Supuran, R. Alberto, *Angew. Chem., Int. Ed.* **2012**, *51*, 3354-3357.
[6] R. Alberto, *J. Organomet. Chem.* **2007**, *692*, 1179-1186.
[7] N. J. Farrer, P. J. Sadler, in *Bioinorg. Med. Chem.* (Ed.: E. Alessio), Wiley-VCH, Weinheim, **2011**, pp. 1-8.
[8] G. Gasser, N. Metzler-Nolte, *Curr. Opin. Chem. Biol.* **2012**, *16*, 84-91.
[9] C. Biot, G. Glorian, L. A. Maciejewski, J. S. Brocard, *J. Med. Chem.* **1997**, *40*, 3715-3718.
[10] L. Delhaes, C. Biot, L. Berry, P. Delcourt, L. A. Maciejewski, D. Camus, J. S. Brocard, D. Dive, *Chembiochem* **2002**, *3*, 418-423.
[11] G. Jaouen, S. Top, A. Vessières, P. Pigeon, G. Leclercq, I. Laios, *Chem. Commun.* **2001**, 383-384.
[12] M. Patra, G. Gasser, A. Pinto, K. Merz, I. Ott, J. E. Bandow, N. Metzler-Nolte, *ChemMedChem* **2009**, *4*, 1930-1938.
[13] C. Bolzati, D. Carta, N. Salvarese, F. Refosco, *Anti-Cancer Agents Med. Chem.* **2012**, *12*, 428-461.
[14] R. Alberto, H. Braband, in *Comprehensive Inorganic Chemistry II, 2nd Edition, in press, Vol. 3* (Ed.: Reedijk), Eds. ELSEVIER, **2013**.
[15] N. S. Loktionova, D. V. Filosofov, M. Pruszynski, A. Majkowska, F. Rosch, *Nucl. Med. Biol.* **2010**, *37*, 718-718.
[16] D. V. Filosofov, N. S. Loktionova, F. Rosch, *Radiochim. Acta* **2010**, *98*, 149-156.
[17] G. B. Saha, N. T. Porile, L. Yaffe, *Phys. Rev.* **1966**, *144*, 962-971.
[18] B. T. Christian, R. J. Nickles, C. K. Stone, *J. Nucl. Med.* **1993**, *34*, P248-P248.
[19] R. Alberto, in *Bioinorg. Med. Chem.* (Ed.: E. Alessio), Wiley-VCH, Weinheim, **2011**, pp. 253-282.
[20] K. Schwochau, *Angew. Chem., Int. Ed.* **1994**, *33*, 2258-2267.
[21] M. Bartholoma, J. Valliant, K. P. Maresca, J. Babich, J. Zubieta, *Chem. Commun.* **2009**, 493-512.
[22] S. Liu, *Adv. Drug Delivery Rev.* **2008**, *60*, 1347-1370.
[23] S. Kasina, T. N. Rao, A. Srinivasan, J. A. Sanderson, J. N. Fitzner, J. M. Reno, P. L. Beaumier, A. R. Fritzberg, *J. Nucl. Med.* **1991**, *32*, 1445-1451.
[24] C. Bolzati, F. Refosco, A. Cagnolini, F. Tisato, A. Boschi, A. Duatti, L. Uccelli, A. Dolmella, E. Marotta, M. Tubaro, *Eur. J. Inorg. Chem.* **2004**, 1902-1913.
[25] C. Bolzati, A. Boschi, L. Uccelli, F. Tisato, F. Refosco, A. Cagnolini, A. Duatti, S. Prakash, G. Bandoli, A. Vittadini, *J. Am. Chem. Soc.* **2002**, *124*, 11468-11479.
[26] A. Boschi, L. Uccelli, A. Duatti, C. Bolzati, F. Refosco, F. Tisato, R. Romagnoli, P. G. Baraldi, K. Varani, P. A. Borea, *Bioconjugate Chem.* **2003**, *14*, 1279-1288.
[27] R. Alberto, K. Ortner, N. Wheatley, R. Schibli, A. P. Schubiger, *J. Am. Chem. Soc.* **2001**, *123*, 3135-3136.
[28] R. Alberto, R. Schibli, A. Egli, A. P. Schubiger, U. Abram, T. A. Kaden, *J. Am. Chem. Soc.* **1998**, *120*, 7987-7988.

[29] R. Alberto, J. K. Pak, D. van Staveren, S. Mundwiler, P. Benny, *Biopolymers* **2004**, *76*, 324-333.
[30] Y. Liu, B. L. Oliveira, J. D. G. Correia, I. C. Santos, I. Santos, B. Spingler, R. Alberto, *Org. Biomol. Chem.* **2010**, *8*, 2829-2839.
[31] K. P. Maresca, J. C. Marquis, S. M. Hillier, G. L. Lu, F. J. Femia, C. N. Zimmerman, W. C. Eckelman, J. L. Joyal, J. W. Babich, *Bioconjugate Chem.* **2010**, *21*, 1032-1042.
[32] M. Walther, C. M. Jung, R. Bergmann, J. Pietzsch, K. Rode, K. Fahmy, P. Mirtschink, S. Stehr, A. Heintz, G. Wunderlich, W. Kraus, H. J. Pietzsch, J. Kropp, A. Deussen, H. Spies, *Bioconjugate Chem.* **2007**, *18*, 216-230.
[33] H. Spies, M. Glaser, H. J. Pietzsch, F. E. Hahn, T. Lugger, *Inorg. Chim. Acta* **1995**, *240*, 465-478.
[34] J. U. Kunstler, R. Bergmann, E. Gniazdowska, P. Kozminski, M. Walther, H. J. Pietzsch, *J. Inorg. Biochem.* **2011**, *105*, 1383-1390.
[35] J. U. Kunstler, G. Seidel, R. Bergmann, E. Gniazdowska, M. Walther, E. Schiller, C. Decristoforo, H. Stephan, R. Haubner, J. Steinbach, H. J. Pietzsch, *Eur. J. Med. Chem.* **2010**, *45*, 3645-3655.
[36] P. Mirtschink, S. N. Stehr, M. Walther, J. Pietzsch, R. Bergmann, H. J. Pietzsch, J. Weichsel, A. Pexa, P. Dieterich, G. Wunderlich, B. Binas, J. Kropp, A. Deussen, *Nucl. Med. Biol.* **2009**, *36*, 833-843.
[37] H. Braband, Y. Tooyama, T. Fox, R. Alberto, *Chem. Eur. J.* **2009**, *15*, 633-638.
[38] H. Braband, *Chimia* **2011**, *65*, 776-781.
[39] S. M. Bentzen, *Lancet Oncol.* **2005**, *6*, 112-117.
[40] V. Ozdemir, B. Williams-Jones, S. J. Glatt, M. T. Tsuang, J. B. Lohr, C. Reist, *Nat. Biotechnol.* **2006**, *24*, 942-947.
[41] S. V. Frye, *Nat. Chem. Biol.* **2010**, *6*, 159-161.
[42] E. Meggers, G. E. Atilla-Gokcumen, H. Bregman, J. Maksimoska, S. P. Mulcahy, N. Pagano, D. S. Williams, *Synlett* **2007**, *2007*, 1177,1189.
[43] E. Meggers, *Angew. Chem., Int. Ed.* **2011**, *50*, 2442-2448.
[44] E. Meggers, *Curr. Opin. Chem. Biol.* **2007**, *11*, 287-292.
[45] L. Feng, Y. Geisselbrecht, S. Blanck, A. Wilbuer, G. E. Atilla-Gokcumen, P. Filippakopoulos, K. Krailing, M. A. Celik, K. Harms, J. Maksimoska, R. Marmorstein, G. Frenking, S. Knapp, L.-O. Essen, E. Meggers, *J. Am. Chem. Soc.* **2011**, *133*, 5976-5986.
[46] N. Metzler-Nolte, *Angew. Chem., Int. Ed.* **2001**, *40*, 1040-1042.
[47] U. Schatzschneider, N. Metzler-Nolte, *Angew. Chem., Int. Ed.* **2006**, *45*, 1504-1507.
[48] G. Gasser, I. Ott, N. Metzler-Nolte, *J. Med. Chem.* **2011**, *54*, 3-25.
[49] R. P. Hanzlik, P. Soine, W. H. Soine, *J. Med. Chem.* **1979**, *22*, 424-428.
[50] R. E. Mewis, S. J. Archibald, *Coord. Chem. Rev.* **2010**, *254*, 1686-1712.
[51] N. Metzler-Nolte, *Top. Organometal. Chem.* **2010**, *32*, 195-217.
[52] K. H. Thompson, C. Orvig, *J. Chem. Soc., Dalton Trans.* **2006**, 761-764.
[53] S. J. Dougan, P. J. Sadler, *Chimia* **2007**, *61*, 704-715.
[54] P. J. Dyson, G. Sava, *Dalton Trans.* **2006**, 1929-1933.
[55] L. Feng, Y. Geisselbrecht, S. Blanck, A. Wilbuer, G. E. Atilla-Gokcumen, P. Filippakopoulos, K. Kraling, M. A. Celik, K. Harms, J. Maksimoska, R. Marmorstein, G. Frenking, S. Knapp, L. O. Essen, E. Meggers, *J. Am. Chem. Soc.* **2011**, *133*, 5976-5986.
[56] M. Wenzel, *J. Labelled Compd. Radiopharm.* **1992**, *31*, 641-650.
[57] T. W. Spradau, J. A. Katzenellenhogen, *Organometallics* **1998**, *17*, 2009-2017.

[58] T. W. Spradau, W. B. Edwards, C. J. Anderson, M. J. Welch, J. A. Katzenellenbogen, *Nucl. Med. Biol.* **1999**, *26*, 1-7.
[59] F. Minutolo, J. A. Katzenellenbogen, *J. Am. Chem. Soc.* **1998**, *120*, 13264-13265.
[60] J. Wald, R. Alberto, K. Ortner, L. Candreia, *Angew. Chem., Int. Ed.* **2001**, *40*, 3062-3066.
[61] Y. Liu, B. Spingler, P. Schmutz, R. Alberto, *J. Am. Chem. Soc.* **2008**, *130*, 1554-1556.
[62] T. Okuyama, Y. Ikenouchi, T. Fueno, *J. Am. Chem. Soc.* **1978**, *100*, 6162-6166.
[63] H. W. P. N'Dongo, Y. Liu, D. Can, P. Schmutz, B. Spingler, R. Alberto, *J. Organomet. Chem.* **2009**, *694*, 981-987.
[64] H. W. P. N'Dongo, P. D. Raposinho, C. Fernandes, I. Santos, D. Can, P. Schmutz, B. Spingler, R. Alberto, *Nucl. Med. Biol.* **2010**, *37*, 255-264.
[65] R. C. Kerber, M. J. Chick, *J. Org. Chem.* **1967**, *32*, 1329-1332.
[66] D. Scapens, H. Adams, T. R. Johnson, B. E. Mann, P. Sawle, R. Aqil, T. Perrior, R. Motterlini, *Dalton Trans.* **2007**, 4962-4973.
[67] J. Boonsompat, A. Padwa, *J. Org. Chem.* **2011**, *76*, 2753-2761.
[68] M. H. Nantz, X. Radisson, P. L. Fuchs, *Synth. Commun.* **1987**, *17*, 55-69.
[69] D. Chong, D. R. Laws, A. Nafady, P. J. Costa, A. L. Rheingold, M. J. Calhorda, W. E. Geiger, *J. Am. Chem. Soc.* **2008**, *130*, 2692-2703.
[70] S. Top, J.-S. Lehn, P. Morel, G. Jaouen, *J. Organomet. Chem.* **1999**, *583*, 63-68.
[71] M. Cais, J. Kozikowski, *J. Am. Chem. Soc.* **1960**, *82*, 5667-5670.
[72] A. P. Marchand, I. N. N. Namboothiri, S. B. Lewis, W. H. Watson, M. Krawiec, *Tetrahedron* **1998**, *54*, 12691-12698.
[73] J. Thiele, *Chem. Ber.* **1900**, *33*, 666-673.
[74] J. Thiele, *Chem. Ber.* **1901**, *34*, 68-71.
[75] F. Zobi, B. Spingler, R. Alberto, *Eur. J. Inorg. Chem.* **2008**, 4205-4214.
[76] C. M. Nunn, A. H. Cowley, S. W. Lee, M. G. Richmond, *Inorg. Chem.* **1990**, *29*, 2105-2112.
[77] G. K. Yang, R. G. Bergman, *Organometallics* **1985**, *4*, 129-138.
[78] A. C. Filippou, B. Lungwitz, G. KociokKohn, I. Hinz, *J. Organomet. Chem.* **1996**, *524*, 133-146.
[79] F. H. Allen, O. Kennard, D. G. Watson, L. Brammer, A. G. Orpen, R. Taylor, *J. Chem. Soc. Perkin Trans. 2* **1987**, S1-S19.
[80] A. P. Terentev, A. V. Dombrovskii, *Zhurnal Obshchei Khimii* **1951**, *21*, 278-280.
[81] CambridgeSoft, 12.0.2.1076 ed., CambridgeSoft, **2010**.
[82] E. ter Meer, *Liebigs Ann. Chem.* **1876**, *181*, 1-22.
[83] T. Curtius, *J. Prakt. Chem.* **1894**, *50*, 275-294.
[84] H. Lebel, O. Leogane, *Org. Lett.* **2006**, *8*, 5717-5720.
[85] I. Jaafar, G. Francis, R. Danionbougot, D. Danion, *Synthesis* **1994**, 56-60.
[86] I. S. Blagbrough, N. E. Mackenzie, C. Ortiz, A. I. Scott, *Tetrahedron Lett.* **1986**, *27*, 1251-1254.
[87] P. W. Manley, U. Quast, H. Andres, K. Bray, *J. Med. Chem.* **1993**, *36*, 2004-2010.
[88] K. Ninomiya, T. Shioiri, S. Yamada, *Tetrahedron* **1974**, *30*, 2151-2157.
[89] R. L. Schaaf, C. T. Lenk, *J. Org. Chem.* **1964**, *29*, 3430-&.
[90] A. Egli, K. Hegetschweiler, R. Alberto, U. Abram, R. Schibli, R. Hedinger, V. Gramlich, R. Kissner, P. A. Schubiger, *Organometallics* **1997**, *16*, 1833-1840.
[91] E. Metay, M. C. Duclos, S. Pellet-Rostaing, M. Lemaire, R. Kannappan, C. Bucher, E. Saint-Aman, C. Chaix, *Tetrahedron* **2009**, *65*, 672-676.
[92] J. M. Heldt, N. Fischer-Durand, M. Salmain, A. Vessieres, G. Jaouen, *J. Organomet. Chem.* **2004**, *689*, 4775-4782.

[93] D. Can, H. W. Peindy N'Dongo, B. Spingler, P. Schmutz, P. Raposinho, I. Santos, R. Alberto, *Chem. Biodiv.* **2012**, *9*, 1849-1866.
[94] C. Choudhary, C. Kumar, F. Gnad, M. L. Nielsen, M. Rehman, T. C. Walther, J. V. Olsen, M. Mann, *Science* **2009**, *325*, 834-840.
[95] W. S. Xu, R. B. Parmigiani, P. A. Marks, *Oncogene* **2007**, *26*, 5541-5552.
[96] W. Xu, L. Ngo, G. Perez, M. Dokmanovic, P. A. Marks, *Proc. Natl. Acad. Sci. U. S. A.* **2006**, *103*, 15540-15545.
[97] D. Griffith, M. P. Morgan, C. J. Marmion, *Chem. Commun.* **2009**.
[98] J. Spencer, J. Amin, M. H. Wang, G. Packham, S. S. S. Alwi, G. J. Tizzard, S. J. Coles, R. M. Paranal, J. E. Bradner, T. D. Heightman, *ACS Med. Chem. Lett.* **2011**, *2*, 358-362.
[99] J. Spencer, J. Amin, R. Boddiboyena, G. Packham, B. E. Cavell, S. S. S. Alwi, R. M. Paranal, T. D. Heightman, M. H. Wang, B. Marsden, P. Coxhead, M. Guille, G. J. Tizzard, S. J. Coles, J. E. Bradner, *Medchemcomm* **2012**, *3*, 61-64.
[100] T. Beckers, C. Burkhardt, H. Wieland, P. Gimmnich, T. Ciossek, T. Maier, K. Sanders, *Int. J. Cancer* **2007**, *121*, 1138-1148.
[101] C. T. Supuran, *Nat. Rev. Drug Discovery* **2008**, *7*, 168-181.
[102] C. T. Supuran, *Bioorg. Med. Chem. Lett.* **2010**, *20*, 3467-3474.
[103] C. P. S. Potter, A. L. Harris, *Br. J. Cancer* **2003**, *89*, 2-7.
[104] F. L. Sung, E. P. Hui, Q. Tao, H. Li, N. B. Y. Tsui, Y. M. Dennis Lo, B. B. Y. Ma, K. F. To, A. L. Harris, A. T. C. Chan, *Cancer Lett.* **2007**, *253*, 74-88.
[105] P. H. Maxwell, M. S. Wiesener, G.-W. Chang, S. C. Clifford, E. C. Vaux, M. E. Cockman, C. C. Wykoff, C. W. Pugh, E. R. Maher, P. J. Ratcliffe, *Nature* **1999**, *399*, 271-275.
[106] G. Gasser, N. Metzler-Nolte, in *Bioinorganic Medicinal Chemistry* (Ed.: E. Alessio), Wiley-VCH, Weinheim, **2011**, pp. 351-382.
[107] L. Dubois, N. G. Lieuwes, A. Maresca, A. Thiry, C. T. Supuran, A. Scozzafava, B. G. Wouters, P. Lambin, *Radiother. Oncol.* **2009**, *92*, 423-428.
[108] C. T. Supuran, *BJU International* **2008**, *101*, 39-40.
[109] J.-Y. Winum, M. Rami, A. Scozzafava, J.-L. Montero, C. Supuran, *Med. Res. Rev.* **2008**, *28*, 445-463.
[110] A. Chrastina, J. Závada, S. Parkkila, Š. Kaluz, M. Kaluzová, J. Rajčáni, J. Pastorek, S. Pastoreková, *Int. J. Cancer* **2003**, *105*, 873-881.
[111] V. Akurathi, L. Dubois, N. G. Lieuwes, S. K. Chitneni, B. J. Cleynhens, D. Vullo, C. T. Supuran, A. M. Verbruggen, P. Lambin, G. M. Bormans, *Nucl. Med. Biol.* **2010**, *37*, 557-564.
[112] F. W. Monnard, T. Heinisch, E. S. Nogueira, T. Schirmer, T. R. Ward, *Chem. Commun.* **2011**, *47*, 8238-8240.
[113] K. M. Jude, A. L. Banerjee, M. K. Haldar, S. Manokaran, B. Roy, S. Mallik, D. K. Srivastava, D. W. Christianson, *J. Am. Chem. Soc.* **2006**, *128*, 3011-3018.
[114] E. Svastova, A. Hulikova, M. Rafajova, M. Zatovicova, A. Gibadulinova, A. Casini, A. Cecchi, A. Scozzafava, C. T. Supuran, J. Pastorek, S. Pastorekova, *FEBS letters* **2004**, *577*, 439-445.
[115] D. Neri, C. T. Supuran, *Nat. Rev. Drug Discovery* **2011**, *10*, 767-777.
[116] A. Thiry, B. Masereel, J. M. Dogne, C. T. Supuran, J. Wouters, C. Michaux, *ChemMedChem* **2007**, *2*, 1273-1280.
[117] C. Temperini, A. Cecchi, A. Scozzafava, C. T. Supuran, *Bioorg. Med. Chem. Lett.* **2008**, *18*, 2567-2573.
[118] B. S. Avvaru, J. M. Wagner, A. Maresca, A. Scozzafava, A. H. Robbins, C. T. Supuran, R. McKenna, *Bioorg. Med. Chem. Lett.* **2010**, *20*, 4376-4381.

[119] L. Dubois, K. Douma, C. T. Supuran, R. K. Chiu, M. A. M. J. van Zandvoort, S. Pastorekova, A. Scozzafava, B. G. Wouters, P. Lambin, *Radiother. Oncol.* **2007**, *83*, 367-373.
[120] W. Stille, H.-R. Brodt, A. H. Groll, G. Just-Nübling, in *Antibiotika-Therapie*, *Vol. 11*, Schattauer, Stuttgart, **2005**.
[121] Mccullou.Jl, T. H. Maren, *Antimicrob. Agents Chemother.* **1973**, *3*, 665-669.
[122] E. I. Edwards, R. Epton, G. Marr, *J. Organomet. Chem.* **1975**, *85*, C23-C25.
[123] E. I. Edwards, R. Epton, G. Marr, *J. Organomet. Chem.* **1979**, *168*, 259-272.
[124] E. I. Edwards, R. Epton, G. Marr, *J. Organomet. Chem.* **1976**, *107*, 351-357.
[125] E. I. Edwards, R. Epton, G. Marr, *J. Oranomet. Chem.* **1976**, *122*, C49-C53.
[126] M. A. Brook, T. H. Chan, *Synthesis* **1983**, 201-203.
[127] R. W. Fuller, *Annu. Rev. Pharmacol. Toxicol.* **1982**, *22*, 31-55.
[128] S. Jakobsen, K. Pedersen, D. F. Smith, S. B. Jensen, O. L. Munk, P. Cumming, *J. Nucl. Med.* **2006**, *47*, 2008-2015.
[129] N. J. Abbott, A. A. K. Patabendige, D. E. M. Dolman, S. R. Yusof, D. J. Begley, *Neurobiol. Dis.* **2010**, *37*, 13-25.
[130] S. R. Hanson, L. J. Whalen, C.-H. Wong, *Bioorg. Med. Chem.* **2006**, *14*, 8386-8395.
[131] STOE & Cie, GmbH, Darmstadt, Germany, **1999**.
[132] Oxford Diffraction Ltd., 171.32 ed., Oxford, UK, **2007**, p. Xcalibur CCD system.
[133] A. Altomare, M. C. Burla, M. Camalli, G. L. Cascarano, C. Giacovazzo, A. Guagliardi, A. G. G. Moliterni, G. Polidori, R. Spagna, *J. Appl. Cryst.* **1999**, *32*, 115-119.
[134] G. M. Sheldrick, *Acta Cryst.* **2008**, *A64*, 112-122.
[135] A. L. Spek, *J. Appl. Cryst.* **2003**, *36*, 7-13.
[136] D. Vullo, A. Innocenti, I. Nishimori, J. Pastorek, A. Scozzafava, S. Pastoreková, C. T. Supuran, *Bioorg. Med. Chem. Lett.* **2005**, *15*, 963-969.
[137] I. Nishimori, D. Vullo, A. Innocenti, A. Scozzafava, A. Mastrolorenzo, C. T. Supuran, *Bioorg. Med. Chem. Lett.* **2005**, *15*, 3828-3833.
[138] R. G. Khalifah, *J. Biol. Chem.* **1971**, *246*, 2561-2573.
[139] K. D'Ambrosio, R.-M. Vitale, J.-M. Dognelì , B. Masereel, A. Innocenti, A. Scozzafava, G. De Simone, C. T. Supuran, *J. Med. Chem.* **2008**, *51*, 3230-3237.
[140] C. Temperini, A. Cecchi, N. A. Boyle, A. Scozzafava, J. E. Cabeza, P. Wentworth Jr, G. M. Blackburn, C. T. Supuran, *Bioorg. Med. Chem. Lett.* **2008**, *18*, 999-1005.
[141] J. R. Casey, P. E. Morgan, D. Vullo, A. Scozzafava, A. Mastrolorenzo, C. T. Supuran, *J. Med. Chem.* **2004**, *47*, 2337-2347.
[142] C. A. Behnke, I. Le Trong, J. W. Godden, E. A. Merritt, D. C. Teller, J. Bajorath, R. E. Stenkamp, *Acta Crystallogr., Sect. D: Biol. Crystallogr.* **2010**, *66*, 616-627.
[143] W. Kabsch, *Acta Cryst.* **2010**, *D66*, 125-132.
[144] L. C. Storoni, A. J. McCoy, R. J. Read, *Acta Cryst.* **2004**, *D60*, 432-438.
[145] E. Potterton, P. Briggs, M. Turkenburg, E. Dodson, *Acta Cryst.* **2003**, *D59*, 1131-1137.
[146] K. H. Sippel, C. Genis, L. Govindasamy, M. Agbandje-McKenna, J. J. Kiddle, B. C. Tripp, R. McKenna, *J. Phys. Chem. Lett.* **2010**, *1*, 2898-2902.
[147] P. Emsley, B. Lohkamp, W. G. Scott, K. Cowtan, *Acta Cryst.* **2010**, *D66*, 486-501.
[148] S. McNicholas, E. Potterton, K. S. Wilson, M. E. M. Noble, *Acta Cryst.* **2011**, *D67*, 386-394.
[149] Schrödinger LLC, 1.2r1 ed., **2009**.

6. Curriculum Vitae

Personal Information

Name	Can
Surname	Daniel
Date of Birth	2nd of July 1983
Place of Origin	Auw AG
Nationality	swiss
Martial Status	married

Education/Work Experience

Since 10/2012	**Wissenschaftlicher Mitarbeiter & Stv. Laborleiter** Parcopharm SA, Baar
01/2009 - 09/2012	**PHD in Chemistry** PHD thesis on the evaluation and synthesis of ^{99m}Tc labeled radiopharmaceuticals, University of Zurich
02/2008 - 12/2008	**Master of Science in Chemistry** • Master thesis in medicinal inorganic chemistry about tumor targeting with ^{99m}Tc labeled molecules, University of Zurich • Received the award of the Alfred Werner-Legacy for good accomplishment in graduate studies
10/2008	**Apprenticeship as a Radioprotection Officier** Radioprotection Officier for open and closed radioactive sources, theory and practice, PSI Villigen
09/2004 – 10/2007	**Bachelor of Science in Chemistry** • Major in organic and inorganic chemistry • Minor in biochemistry University of Zurich
07/2004 – 09/2004	**Military Service** Rekrutenschule, infantry combat vehicle driver, Aarau (AG)
08/2000 – 06/2004	**Secondary School, Kantonsschule** • Bilingual graduation (German and French) • Major in chemistry, biology and sports • Matura thesis in physics: a depth profile of a part of the Hallwilersee Kantonsschule Wohlen (AG)

Publications

- S. Sulieman, D. Can, J. Mertens, H. W. Peindy N'Dongo, Y. Liu, P. Schmutz, M. Bauwens, B. Spingler, R. Alberto, *Organometallics*, **2012**, 31 (19), 6880-6886
- D. Can, H. W. Peindy N'Dongo, B. Spingler, P. Schmutz, P. Raposinho, I. Santos, R. Alberto, *Special Issue of Chemistry & Biodiversity*, **2012**, 9, 1849-1866
- D. Can, B. Spingler, P. Schmutz, F. Mendes, P. Raposinho, C. Fernandes, F. Carta, A. Innocenti, I. Santos, C. T. Supuran, R. Alberto, *Angew. Chem., Int. Ed.*, **2012**, 51, 3354-3357
- H. W. Peindy N'Dongo, P. Raposinho, C. Fernandes, D. Can, P. Schmutz, B. Spingler, I. Santos, R. Alberto, *Nuc. Med. and Biol.*, **2010**; 37(3), 255-264
- H. W. Peindy N'Dongo, Y. Liu, D. Can, P. Schmutz, B. Spingler, R. Alberto, *J. Organomet. Chem.*, **2009**, 694(6), 981-987

7. Acknowledgment

My PhD thesis started with Prof. Dr. Roger Alberto's words: "I want you to become the worlds leading Cp-chemist". This statement is, without any doubt, representative for the enthusiastic way, of how Prof. Alberto guided me into this challenging field of research. And without any doubt, it was this attitude, that made me feel the respect and the confidence he was putting in me, teaching me more than just how to practise research.

The greatest success is often achieved, when people work together. Therefore I would like to thank our collaboration partners; the group Prof. Dr. Claudiu Supuran for inhibition studies on human carbonic anhydrases, the group of Prof. Dr. Isabel Santos for cell- and animal studies, PD. Dr. Bernhard Spingler for a lot of effort in any crystallizing issues and Dr. Henrik Braband for his support in the radiolaboratory.

In the same sense, I want to thank Dr. Paul Schmutz. During my PhD thesis he was intensively involved in my work and some important synthetic stages would not have been possible, without his support.

I would like to thank Dr. Henrik Braband, Miguel Guttentag, Nando Gartmann, Michael Felber, Sebastian Imstepf, Miri Oberholzer, Michael Benz and Dr. Fabio Zobi for not just being members of the same working group, but for being good friends, that accompanied me during a nice period of my life.

In terms of organic synthesis, Dr. Karel Zelenka teached me a lot of his (almost infinite) knowledge in the time, when he was my lab mate.

At the end of the year I was privileged to be part of the traditional Christmas Lecture, together with Heinz Spring and several professors. I would like to thank Heinz for the great time we spent, while working meticulously on fascinating experiments.

Non of this would have been possible without my family. My parents, my brothers and my wife support me and guide me, whenever I need them and make my life complete. You represent the "happy-place" I will always belong to, thank you!